Universidade de Aveiro Departamento de Biologia
2016

MARIA CRISTINA MONTEIRO

CITOGENOTOXICIDADE DO CRÓMIO E CÁDMIO EM PLANTAS E EM CÉLULAS HUMANAS

CYTOGENOTOXICITY OF CHROMIUM AND CADMIUM IN PLANTS AND IN HUMAN CELLS

Universidade de Aveiro Departamento de Biologia
2016

MARIA CRISTINA MONTEIRO

CITOGENOTOXICIDADE DO CRÓMIO E CÁDMIO EM PLANTAS E EM CÉLULAS HUMANAS

CYTOGENOTOXICITY OF CHROMIUM AND CADMIUM IN PLANTS AND IN HUMAN CELLS

Tese apresentada à Universidade de Aveiro para cumprimento dos requisitos necessários à obtenção do grau de Doutor em Biologia, realizada sob a orientação científica da Professora Doutora Maria da Conceição Vieira Lopes dos Santos, Professora Catedrática da Faculdade de Ciências da Universidade do Porto, e co-orientação da Doutora Helena Cristina Correia de Oliveira, Estagiária de Pós-Doutoramento do Departamento de Biologia da Universidade de Aveiro e do Professor Doutor Francisco Manuel Pereira Peixoto, Professor Associado com Agregação da Universidade de Trás-os-Montes e Alto Douro.

Apoio financeiro da FCT e do FSE no âmbito do III Quadro Comunitário de Apoio (SFRH/BD/48204/2008). FEDER/COMPETE (Projeto FCT/PTDC/AAC-AMB/112804/2009, BioREM: Integrating multiple toxicological BIOmarkers in a phytoREMediation assay of Pb and Cd contaminated sites).

À minha mãe Fernanda Façanha e ao meu namorado Francisco Pinho, por todo o amor e porque sempre desejei a vossa felicidade.

“One, remember to look up at the stars and not down at your feet.
Two, never give up work. Work gives you meaning and purpose and life is empty without it.
Three, if you are lucky enough to find love, remember it is there and don't throw it away.”

Stephen Hawking

In life and science...

“The important thing is to not stop questioning. Curiosity has its own reason for existence. One cannot help but be in awe when he contemplates the mysteries of eternity, of life, of the marvellous structure of reality. It is enough if one tries merely to comprehend a little of this mystery each day.”

Albert Einstein

The mystery will always be present...

“Somewhere, something incredible is waiting to be known.”

Carl Sagan

o júri

presidente

Prof. Doutor Artur da Rosa Pires
Professor Catedrático, Departamento de Ciências Sociais, Políticas e do Território, Universidade de Aveiro

Prof. Doutor Carlos Manuel Marques Palmeira
Professor Catedrático, Departamento de Ciências da Vida, Faculdade de Ciências e Tecnologia, Universidade de Coimbra

Prof. Doutor Francisco Manuel Pereira Peixoto
Professor Associado com Agregação, Departamento de Biologia e Ambiente, Escola de Ciências da Vida e do Ambiente, Universidade de Trás-os-Montes e Alto Douro (co-orientador)

Prof. Doutora Maria da Conceição Lopes Vieira dos Santos
Professora Catedrática, Departamento de Biologia, Faculdade de Ciências, Universidade do Porto (orientadora)

Prof. Doutor José Joaquim Saraiva Pissarra
Professor Associado, Departamento de Biologia, Faculdade de Ciências, Universidade do Porto

Prof. Doutor Romeu António Videira
Professor Investigador, Departamento de Química, Escola de Ciências da Vida e do Ambiente, Universidade de Trás-os-Montes e Alto Douro

Doutor José Miguel Pimenta de Oliveira
Estagiário de Pós-Doutoramento, Departamento de Biologia, Universidade de Aveiro

Doutora Maria Celeste Pereira Dias
Estagiária de Pós-Doutoramento, Departamento de Ciências da Vida, Faculdade de Ciências e Tecnologia, Universidade de Coimbra

agradecimentos

Gostaria de agradecer a todos os que me apoiaram e contribuíram para a realização deste trabalho. Agradeço à FCT pelos financiamentos da bolsa de doutoramento e do projeto BioREM sem os quais este trabalho não seria possível.
Agradeço à minha orientadora principal da tese, Professora Doutora Conceição Santos, por me ter acolhido no seu laboratório, por me ter escolhido para fazer parte da equipa e ter acreditado no meu potencial para desenvolver este trabalho. Agradeço-lhe todo o esforço para que eu seguisse o desenvolvimento de trabalhos numa das minhas áreas de sonho, trabalhar em cultura de células humanas. Toda a orientação com demonstração de conhecimento, críticas, sugestões e com persistência, grande apoio e compreensão foram essenciais para chegar a esta data com todo este trabalho desenvolvido. Agradeço à minha orientadora Doutora Helena Oliveira pelo acompanhamento diário no laboratório, pela discussão de ideias e planos que me fizeram crescer e ser capaz, em cada dia, de tomar decisões que conduziram ao seguimento da investigação. Agradeço ao meu orientador Professor Doutor Francisco Peixoto a orientação exemplar e dedicada, a sua capacidade de motivação constante e demonstração de conhecimento, abertura e generosidade. Agradeço-lhe ainda a simpatia e pronta disponibilidade para me acolher na Universidade de Trás-os-Montes e Alto Douro, onde me senti feliz e mais confiante numa nova equipa de investigação, onde também tive a oportunidade de receber conselhos e ajuda de outros professores e colegas de investigação, a todos muito obrigada! Agradeço aos meus orientadores o grande apoio, motivação e compreensão, principalmente na fase de escrita desta tese.
Aos meus colegas do Laboratório de Biotecnologia e Citómica agradeço a sua colaboração, orientação nos trabalhos e o acompanhamento e amizade que se tornou crescente e fundamental no dia-a-dia. À Doutora Glória Pinto e à Doutora Celeste Dias agradeço os ensinamentos de biologia vegetal que me proporcionaram e ao Doutor Miguel Oliveira pela orientação nos ensaios de expressão génica. Agradeço de modo especial à Ana Vasques e Sónia Pinho por me incentivarem e encorajarem sempre, por me acompanharem bem de perto, quer com os pés assentes na terra, quer com o coração. Obrigada pela interajuda, discussão de resultados e conselhos, assim como estou muito grata pelos momentos de conforto, alegria e amizade! Agradeço à Cátia Guerra pela colaboração, enorme força e entusiasmo que irradiava no seu sorriso, bem como à Susana Barros e Andreia Ascenso pela alegria, presença de espírito, dinamismo e amizade. Aos colegas Fernanda Rosário, Jenny Costa, Bruno Ladeiro, Catarina Remédios, Pedro Pinto, Tiago Pedrosa e Verónica Bastos por contribuírem para um grupo unido e solidário. À Alexandra Fernandes pela simpatia e companheirismo.
Aos meus amigos Jorge Ferreira, Joana Machado, Helena Silva, Cláudia Machado, Lúcia Noronha, Raquel Ferreira, mana Rosarinho Andrade, Armanda Fernandes e Madalena Conceição agradeço a força que me têm dado ao longo dos anos com a sua presença em diversos momentos, mesmo que às vezes longe geograficamente.
Ao Francisco, o meu pilar nesta longa caminhada, por todo o incentivo, presença, paciência, compreensão e por toda a força que me foi dando para que superasse cada obstáculo. Obrigada por acreditares em mim, por seres a pessoa que se preocupa, que me acompanha na vida, por também teres sido um ótimo colega e que partilha a sua sabedoria com entusiasmo. A tua preciosa ajuda no laboratório foi uma enorme motivação para mim, assim como o teu bom humor e simpatia que contagia e alarga fronteiras de amizade. Obrigada pela tua dedicação e amor, que foram essenciais nesta etapa. Agradeço ainda à D. Matilde Pinho toda a compreensão, carinho e ajuda que me deu nesta fase. Agradeço à minha família…à minha mãe Fernanda Façanha, à Florinda Oliveira, à Guida Sousa, e ao Virgílio Silva, pelo amor incondicional, por me acompanharem ao longo da vida e me incentivarem todos os dias neste desafio concreto, para que eu superasse medos, hesitações e dificuldades, contribuindo para a conquista deste objetivo.

palavras-chave

Cádmio, crómio, citotoxicidade, genotoxicidade, osteoblastos humanos, *Lactuca sativa* L.

resumo

Os metais têm sido alvo de preocupação devido à sua persistência no ambiente e potencial toxicidade para os seres vivos, após a atividade humana desmensurada. Nesta tese é dada relevância ao Cr e ao Cd, considerados metais poluentes prioritários. Assim, o objetivo do trabalho foi avaliar e compreender os efeitos cito- e genotóxicos putativamente induzidos por sais de Cr e Cd em plantas e células humanas. O Capítulo 1 expõe as fontes de poluição de Cr e Cd, os seus efeitos tóxicos para os seres vivos e mecanismos de absorção a nível celular em plantas e humanos. Os biomarcadores mais usados na avaliação de exposição e toxicidade de metais foram brevemente discutidos, assim como a possibilidade de realização de ensaios *in vivo* e *in vitro*. Dois modelos biológicos foram escolhidos para avaliação da toxicidade do Cr e Cd: a alface (*Lactuca sativa* L.) e osteoblastos humanos, considerados alvos de acumulação e toxicidade destes metais. Além disso, os efeitos cito- e genotóxicos do Cr e Cd não estavam esclarecidos nos modelos biológicos utilizados. Assim, no Capítulo 2 foram avaliados os efeitos cito- e genotóxicos do Cr e Cd em alface *in vivo*, enquanto o Capítulo 3 abordou as mesmas questões em osteoblastos humanos *in vitro*. Cada estudo envolveu a compreensão e integração dos mecanismos de cito- e genotoxicidade em ambos os modelos biológicos em resposta à exposição aos metais. Finalmente, na última secção – Capítulo 4, é apresentada uma conclusão geral, considerando os resultados obtidos para ambos os metais e modelos biológicos e trabalhos futuros relativos aos efeitos e níveis de toxicidade descritos ao longo do trabalho.

keywords

Cadmium, chromium, cytotoxicity, genotoxicity, human osteoblasts, *Lactuca sativa* L.

abstract

Metals have been a major concern regarding their persistence in the environment and potential toxicity to living organisms, after immoderate human activity. In this thesis, it is given relevance to Cr and Cd which are among the priority metal pollutants. Therefore, the aim of this work was to evaluate and understand putative cyto- and genotoxic effects induced by Cr and Cd salts in plants and human cells. In Chapter 1, it is described the source of Cr and Cd pollution, toxic effects to living organisms, and mechanisms of metal uptake at the cellular level, in plants and humans. Briefly, the most used biomarkers in metal exposure and toxicity assessment were discussed as well as *in vivo* and *in vitro* testing. Two biological models were chosen for toxicity assessment of Cr and Cd: lettuce (*Lactuca sativa* L.) and human osteoblasts, both considered targets of these metals accumulation and toxicity. Moreover, the cyto- and genotoxic effects of Cr and Cd had not yet been clarified in both biological models used. Therefore, Chapter 2 begins to address the cyto- and genotoxic effects of Cr and Cd in lettuce *in vivo*, while Chapter 3 takes over these issues in human osteoblasts *in vitro*. Each of these studies involved an understanding and integration of the mechanisms of cyto- and genotoxicity in both biological models in response to metal exposure. Finally, over the last section – Chapter 4, a global conclusion is raised considering the results obtained for both metals and biological models, and future work on the effects and levels of toxicity presented along this work are also included in these final remarks.

Index

Abbreviations and acronyms

ABC – ATP-binding cassette

ABTS – 2,2'-azino-bis(3-ethylbenzthiazoline-6-sulfonic acid)

ADHP – 10-Acetyl-3,7-dihydrophenoxazine

ADP – Adenosine diphosphate

AFLP – Amplified fragment length polymorphism

AMP – Adenosine monophosphate

ANOVA – Analysis of variance

APX – Ascorbate peroxidase

Asc – Ascorbate

ATM – Ataxia telangiectasia mutated

ATM – Ataxia telangiectasia mutated coding gene

ATP – Adenosine triphosphate

BER – Base excision repair

BSA – Bovine serum albumin

CAT – Catalase

CAX – Cation exchanger

CBMN – Cytokinesis-block micronucleus

CCNB1 – Cyclin B1

CCNB1 – Cyclin B1 coding gene

CCNE1 – Cyclin E1

CCNE1 – Cyclin E1 coding gene

CDC25A – Cell division cycle 25A coding gene

CDF – Cation diffusion facilitator

CDK2 – Cyclin-dependent kinase 2

CDK2 – Cyclin-dependent kinase 2 coding gene

CHEK1 – Checkpoint kinase 1

CHEK1 – Checkpoint kinase 1 coding gene

CHEK2 – Checkpoint kinase 2

CHEK2 – Checkpoint kinase 2 coding gene

CoA – Coenzyme A

Cys – Cysteine

DCF – 2',7'-Dichlorofluorescin

$DCFH_2$ – 2',7'-Dichlorodihydrofluorescin

$DCFH_2$-DA – 2',7'-Dichlorodihydrofluorescin diacetate

DHA – Dehydroascorbate

DHAR – Dehydroascorbate reductase

DMEM – Dubelcco's modified eagle medium

DMSO – Dimethyl sulfoxide

DMT1 – Divalent metal transporter 1

DNPH – Dinitrophenylhydrazine

DSB – Double strand breaks

DTNB – 5,5'-Dithiobis-(2-nitrobenzoic acid)

DTT – Dithiothreitol

DW – Dry weight

EDTA – Ethylenediaminetetraacetic acid

EGTA – Ethyleneglycoltetraacetic acid

ER – Endoplasmic reticulum

F-actin – Filamentous actin

FBS – Fetal bovine serum

FCM – Flow cytometry

FITC – Fluorescein isothiocyanate

FL – Fluorescence intensity

FPCV – Full peak coefficient of variation

FS – Forward scatter

GAPDH – Glyceraldehyde 3-phosphate dehydrogenase coding gene

GPx – Glutathione peroxidase

GR – Glutathione reductase

GSH – Glutathione, reduced form

GSSG – Glutathione, oxidized form

HEPES – 2-(4-(2-hydroxyethyl)piperazin-1-yl)ethanesulfonic acid

HPCV – Half peak coefficient of variation

HPLC – High-performance liquid chromatography

HRP – Horseradish peroxidase

IC – Inhibition concentration

ICP-AES – Inductively coupled plasma atomic emission spectrometry

ICP-OES – Inductively coupled plasma optical emission spectrometry

ISO – International Organization for Standardization

LC – Lethal concentration

LMPA – Low melting point agarose

MDA – Malondialdehyde

MDHA – Monodehydroascorbate

MDHAR – Monodehydroascorbate reductase

MEM-α – Minimum essential medium alpha

MFI – Median fluorescence intensity

MMR – Mismatch repair

MMS – Methyl methanosulfonate

MN – Micronucleus/micronuclei

MoM – Metal-on-metal

MT(s) – Metallothionein(s)

MTF1 – Metal-responsive transcription factor 1

MTP – Metal tolerance protein

MTT – 3-(4,5-Dimethylthiazol-2-yl)-2,5-diphenyltetrazolium bromide

NAD(P)H – Reduced nicotinamide adenine dinucleotide (phosphate)

NDI – Nuclear division index

NER – Nucleotide excision repair

NHEJ – Non- homologous end-joining

NMPA – Normal melting point agarose

NPBs – Nucleoplasmic bridges

NRAMP – Natural resistance associated macrophage protein

$^1O_2$ – Singlet oxygen

$O_2^{\bullet -}$ – Superoxide anion

$^{\bullet}OH$ – Hydroxyl radical

8-OHdG – 8-oxo-2'-deoxyguanosine

PBS – Phosphate buffer saline

PC(s) – Phytochelatin(s)

PCS – Phytochelatin synthases

PCR – Polymerase chain reaction

PDA – Photodiode array detector

PI – Propidium iodide

PMSF – Phenylmethylsulfonyl fluoride

POX – Guaiacol peroxidase

PRI – “Post-R point” index

PVP – Polyvinylpyrrolidone

qPCR – Quantitative polymerase chain reaction

RBCs – Red blood cells

RER – Rough endoplasmic reticulum

Rho123 – Rhodamine 123

RNase – Ribonuclease

RNS – Reactive nitrogen species

ROS – Reactive oxygen species

RT – Room temperature

SD –Standard deviation

SDS – Sodium dodecyl sulphate

SE – Standard error

SNP – Single nucleotide polymorphism

SOD – Superoxide dismutase

SS – Side scatter

SSB – Single stranded breaks

TAA – Total antioxidant activity

TBA – Thiobarbituric acid

TBARS – Thiobarbituric acid reactive substances

TCA – Tricarboxilic acid

TNB – 5-Thio-2-nitrobenzoic acid

TRITC – Tetramethylrhodamine

Tris-HCl – Tris(hydroxymethyl)aminomethane hydrochloride

UV – Ultra violet

WPB – Woody plant buffer

WST1 – 2-(4-Iodophenyl)-3-(4-nitrophenyl)-5-(2,4-disulfophenyl)-2H-tetrazolium, monosodium salt

ZIP – Zinc-related iron-related protein

$\Delta\Psi m$ – Mitochondrial membrane potential

ε – Extinction coefficient

CHAPTER 1 – GENERAL INTRODUCTION

Metal environmental pollution

Metals occur naturally in Earth's crust but episodes of environmental metal contamination are increasing mostly due to anthropogenic activities including agriculture (e.g., liming, sewage sludge, irrigation waters, pesticides and fertilizers) or municipal/industrial and mining effluents and wastes (Nagajyoti et al. 2010). Despite most dramatic increases of environmental contamination with metals had been occurring since the industrial revolution (18^{th}-19^{th} centuries), some examples of metal contamination and/or intoxication were already reported in ancient Roman and Greece (Gilbert 2012). Also, the increasing use of metals over the last centuries "*has significantly altered the natural distribution of metals in the environment*" (Gilbert 2012). These contaminants are, therefore, spread through the soils, water and air, where they become available and may be accumulated in living organisms (Nagajyoti et al. 2010).

Metals have been classified as essential metals or micronutrients (e.g., Cu, Zn, Fe, Mn), and non-essential metals (e.g., Cd, As, Pb, Hg) to living organisms. Metals from both groups may be toxic to plants or animals (Nagajyoti et al. 2010). The form/association of metals may differ in the environment, which alters their bioavailability and consequently their level of toxicity. This evidence is particularly significant in studies of (eco)toxicology and of environmental fate of metals, and their transport/accumulation through the food chain (Gilbert 2012). Thus, metals' pollution and their persistence in the environment, as well as their toxicity to living organisms have been considered by international/governments agencies, like the Environmental Protection Agency (2013), the Agency for Toxic Substances and Disease Registry (2014), and European Comission (2001). For example, the Agency for Toxic Substances and Disease Registry has launched a substance priority list (of 275 substances) ranking Cd in the 7^{th} place, and Cr^{6+}, Cr^{6+} trioxide, and Cr in the 17^{th}, 66^{th} and 78^{th} positions, respectively (Agency for Toxic Substances and Disease Registry 2014).

Chromium and cadmium contamination and toxicity – a general approach

Data published by the British Geologic Survey (2012) showed that from 2008-2012 China has been the major producer of Cd (and metals in general), and that the world's total production of this metal over these years had remained overall constant. On the other hand, South Africa was the major producer of Cr (44% of world total Cr production). Also the

demand for Cr has dramatically increased these last decades, as Cr use increased from less than 2 million (in the early 20th century) to around 25 million tonnes in 2012 (British Geologic Survey 2012).

Supporting the scientific and public concern on metals' pollution, it should also be highlighted that among different types of contaminants (e.g., chlorinated hydrocarbons, mineral oil, polycyclic aromatic hydrocarbons) affecting Europe, metals are the main category, with average values of contamination reaching 34.8% and 30.8% in soil and groundwater, respectively (Panagos et al. 2013).

Contaminations with Cr and Cd have been found in several Portuguese areas mostly associated to mining and industrial activities. The map below (Figure 1) summarizes the existing sources of mineral extraction (metallic and energetic), where some of the reported Cr and Cd-contaminated regions were identified. For example, in an active mine located in Coval da Mó high contamination levels with Pb, Zn and Cd were reported (Ferreira da Silva et al. 2009). Abandoned mines are still sources of metal contamination, like the Lousal mine where water and sediments contain high concentrations of Cd and other metals (Luís et al. 2011). In sampling sites of Ave River, water and sediments presented contamination with Cd and other metals, with the highest levels being found in areas near industries and highways (Pinto et al. 2011).

Since 1999 the Portuguese Environment Agency has been performing regular analyses of hazardous substances in monitoring stations of water sources (interior, estuary and coastal waters). The most recent report (Portuguese Environment Agency 2012) shows that Cd is among the most detected metals in sediments of these waters in the period of 1999-2004. The highest levels of Cd were found in monitoring stations near mines (e.g., Dornelas do Zêzere near Panasqueira mine (the major W mine of Europe) and in areas with a great urban and industrial impact (e.g., Lisbon and Setubal areas) (Figure 1).

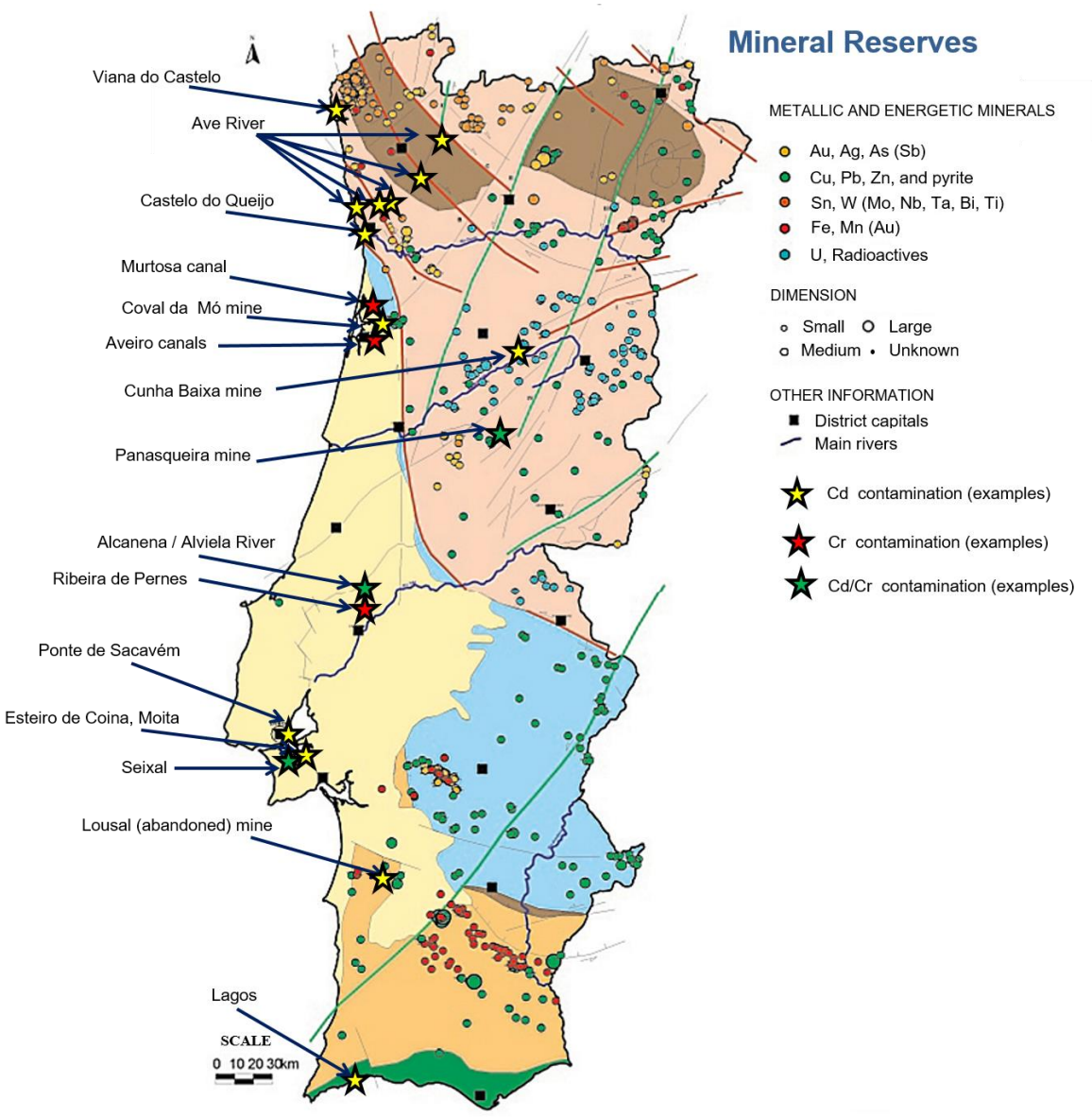

Figure 1. Reserves of metallic and radioactive minerals in Portugal, and several regions contaminated with Cd, Cr or both metals. In general, in contaminated sites that are not located near mineral reserves, the main source of Cd and/or Cd presence/contamination is due to industrial and urban activity (adapted from Direcção Geral de Energia e Geologia (2013)).

In addition to the detection of contaminating metals in water, aquatic organisms such as barbel (*Barbus* sp.), harvested in the rivers Vouga, Douro, Mondego, Tejo, Sado, and Guadiana, showed contamination with Cd in their liver, with the highest levels observed in fishes from Sado River. Moreover, in all monitoring stations of estuary or coastal waters Cd was detected being the highest values found in Viana do Castelo, Castelo do Queijo, and

Lagos. Also in all stations of estuary or coastal waters Cd was found to accumulate in mussels and plankton (Portuguese Environment Agency 2012). The same report showed that Cr was also detected in some monitoring stations (e.g., Ribeira de Pernes) in water, and in the liver of fishes captured in Sado River (Portuguese Environment Agency 2012).

Environmental contamination with Cr in Portugal is mostly linked to industrial activities, and the Portuguese Environment Agency (2012) also identified the main and most recent national areas having Cr soil contamination (excluding mining areas), or where Cr and/or Cd represent a concern (including other contaminants). The national agency has approved investments for environmental recovery of soils contaminated with Cr and/or Cd. For example, investments were approved to recover soils of a former steel industry in Seixal (Cr and Cd contamination), and to recover the treatment plant of the tannery industry of Alcanena contaminated with Cr (Branco et al. 2005) (Figure 1).

More watercourses in other regions of the country had sediments contaminated with Cr (among other metals). Particularly relevant are the Aveiro canals, near former industries of ceramic and metallurgy, and the Murtosa canal that receives wastewater discharges from the Chemical Complex of Estarreja (Martins et al. 2013) (Figure 1).

In addition to environmental contamination, occupational exposure has also been identified as a main way of human contamination. As an example of these two ways of contamination, individuals working in Panasqueira mine, and populations living nearby, had higher concentrations of As, Cr, Mg, Mn, Mo, Ni, Pb, S, Se, and Zn compared to individuals living in non-contaminated areas (Coelho et al. 2014). Curiously, the populations environmentally exposed (and mainly women compared to men) showed higher levels of these metals (Coelho et al. 2014) and DNA damage (Coelho et al. 2013) than a similar population that was occupationally exposed. The higher frequency of MN (only in females) and chromosome aberrations was proposed by the authors to be related to environmental exposure (Coelho et al. 2013). Also, in a U mine area (in Cunha Baixa, Mangualde) contaminated with several metals (including Cd), local wild animals (mice and earthworms) accumulated high levels of Cd (Lourenço et al. 2012, 2013).

Chromium

Plants contamination by Cr: environmental contamination with Cr and its toxicity depend on multiple conditions (e.g., Cr oxidation state, soil/water pH and model organism) (Peralta-Videa et al. 2009). Particularly, the oxidation state (Cr, Cr^{2+}, Cr^{3+}, Cr^{4+}, Cr^{5+}, and Cr^{6+}) is crucial, being Cr^{3+} and Cr^{6+} the most stable forms (Zayed and Terry 2003), and Cr^{6+} the valence most widely studied concerning toxicity. The oxidative state of Cr affects Cr solubility and bioavailability in the environment, as well as its absorption, accumulation and toxicity in living organisms (Panda and Choudhury 2005). Contamination of crops with Cr may occur through contaminated irrigation water, soil and air/aerosols.

Contrarily to Cr^{6+}, the effects of Cr^{3+} in plants are rather unknown (e.g., Song et al. 2014), and it has been widely assumed that Cr^{3+} is not necessary to plants and presents low toxicity or even may stimulate growth at low doses. For example, in bean plants, Cr^{3+} at low concentrations (0.25-1 µM) enhanced plant growth (Bonet et al. 1991). In another study, the response of seedlings of sorghum exposed to 50 and 100 µM Cr^{6+} or Cr^{3+} for 10 days was compared (Shanker and Pathmanabhan 2004). The results showed that Cr^{3+} led to lower accumulation of Cr in plant organs than Cr^{6+}, and in both conditions the highest level of Cr was found in roots, followed by leaves and stems. Furthermore, 50 µM Cr^{3+} did not induce plant growth inhibition, neither increased ROS content in leaves, while Cr^{6+} reduced plant growth and was more cytotoxic (Shanker and Pathmanabhan 2004). Compared to the effects of Cr^{3+}, Cr^{6+} induced higher levels of ROS, and lipid peroxidation, and stimulated antioxidant enzymes (SOD, DHAR, GR, CAT, and APX), but decreased GSH. Therefore, at the cellular level, Cr^{6+} induced an unbalance between ROS production and antioxidant defenses, i.e. Cr^{6+} induced oxidative stress (Shanker and Pathmanabhan 2004). More recently, Song et al. (2014) demonstrated in barley (*Hordeum vulgare*) that the Cr^{3+} toxicity, measured by the metal effects on root elongation, decreased with increasing activity of Ca^{2+} and Mg^{2+} (but not with K^{+} or Na^{+}). The effect of pH was also explained by the H^{+} competition with Cr^{3+} and the concomitant toxicity of $CrOH^{2+}$ in solution.

Induction of growth inhibition by Cr^{6+} was reported in maize (Sharma et al. 2003), citrillus (Dube et al. 2003), and alfalfa (in particular, root and shoot growth inhibition) (Peralta et al. 2001). In these studies, maize also presented chlorosis together with decrease of chlorophyll a and b contents and CAT inhibition (Sharma et al. 2003); citrillus showed

necrotic leaves and alterations in minerals content (Dube et al. 2003); and alfalfa had decreased seed germination (Peralta et al. 2001).

Our laboratory has extensively studied the toxic effects of Cr^{6+} in crops, particularly in *Phaseolus vulgaris*: in addition to root growth inhibition (Rodriguez et al. 2011), our group showed that Cr^{6+} negatively affected photosynthesis in pea plants after 28 days of exposure, e.g., by changing the morphology of chloroplasts, decreasing photosynthetic pigments content, the rate of CO_2 assimilation, as well as Rubisco activity (Rodriguez et al. 2012). Furthermore, genotoxic effects of Cr^{6+} were also observed in these plants, i.e., Cr^{6+} induced DNA damage, polyploidization, and mutations, associated with cell cycle arrest at G_2 phase (Rodriguez et al. 2011, 2013).

***Human contamination by Cr*:** Despite the consensus that Cr^{6+} is toxic for both plants and animals (O'Brien et al. 2013; see Chapters 2.1 and 3.1), Cr^{3+} is essential to animal diet, contributing to the normal metabolism of proteins, carbohydrates and lipids (Peralta-Videa et al. 2009). Some *in vivo* (mouse, rat and fruit fly) and *in vitro* (mouse and human cell lines) studies showed that Cr^{3+} used in nutritional supplements was not significantly toxic, while other studies showed that Cr^{3+} induced DNA damage, mutations, decrease of cell viability, or increase of cancer rates in offspring in mice (Levina and Lay 2008). Cr^{3+} supplements are freely available in the market, e.g., Cr^{3+} picolinate that was approved and considered safe by Food and Drug Administration (USA) and by Food Standards Agency (UK). But both agencies and the Agency for Toxic Substances and Disease Registry have been following published scientific data about toxicity of Cr^{3+} compounds used as dietary supplements. Considering this followed data the Agency for Toxic Substances and Disease Registry alerts for supplement consumption that should be taken with care, mainly at excessive doses (Wilbur et al. 2012).

Human/animal contamination with Cr may occur by several ways, including ingestion of contaminated water or food (*via* the food chain), occupational exposure (Keegan et al. 2008), and use of Cr-containing medical devices (e.g., dental (Eliasson et al. 2007), hip or other joint orthopedic prostheses (Sampson and Hart 2012)) often made of stainless steel or Co-Cr alloys (Gunaratnam and Grant 2008; Sampson and Hart 2012). During the use of some of these Cr-containing prostheses metal debris are released in the form of particles or ions (Cr^{6+} (Eiselstein et al. 2007)) and spread to many tissues (Gunaratnam and Grant 2008;

Campbell and Estey 2013) where they can lead to cyto- and genotoxicity (see more details in Chapter 3.1).

An experimental study demonstrated that mice exposed to Cr^{6+} suffered from oxidative stress leading to an increase of lipid and protein oxidation (Ben Hamida et al. 2013). The authors also demonstrated that the levels of nonenzymatic antioxidants (GSH, nonprotein thiol, vitamin C) as well as antioxidant enzyme activities (GPx and SOD) decreased despite of an increase of CAT activity. Also several biomarkers of liver injury (e.g., aspartate transaminase, alanine transaminase and lactate dehydrogenase activities, bilirubin, and albumin levels) increased (Ben Hamida et al. 2013).

The toxic effects of Cr^{6+} in chrome electroplating workers were evaluated in a research. For that, blood Cr levels and biomarkers of oxidative stress such as lipid peroxidation, thiol groups and antioxidant capacity of plasma were analyzed (Zendehdel et al. 2014), demonstrating Cr^{6+} induced biochemical toxicity. Another study demonstrated that chronic exposure to Cr^{6+} could disrupt blood element homeostasis (Song et al. (2012) *vide* Song et al. (2014)). These authors demonstrated in Sprague-Dawley rats that among blood, serum, and RBCs, the latest is the most sensitive to Cr^{6+} exposure. Song et al. (2014) also found dose-response relationships among rats exposed to Cr^{6+}: Ca, Mg, and Mn in blood, Fe, Mg, and Se in serum, and Mg and Zn in lung tissue decreased with exposure. However, Ca, Co, Cr, Mg, Mn, and Se in RBCs, and Ca, Co and Mo increased in lung after Cr^{6+} exposure (Song et al. 2014).

In general, it has been demonstrated that absorbed Cr in mammalians distributes to nearly all tissues and it mostly accumulates in kidney and liver. Moreover, bone is also a major target, thus contributing to long-term persistence of Cr in the organism (Wilbur et al. 2012).

Cadmium

Crops contamination by Cd: As stated above Cd is used in industry (e.g., mines, production of batteries, coatings and plating, pigments, plastic stabilizers, and also alloys (Faroon et al. 2012)). The improper disposal of wastes in the environment has led to Cd spread and contamination, accumulating in plants that are grown in contaminated soils. For example, high levels of Cd accumulated in edible parts of 20 plant species (e.g., lettuce, tomato, bean, carrot, and spinach plants) harvested from several sites around a Zn plant in Huludao, in China (Zheng et al. 2007). Also other wild organisms like mushrooms living in contaminated areas accumulate Cd (Petkovšek and Pokorny 2013).

Humans are generally exposed to Cd by ingestion of contaminated food (e.g., crops, mollusks, and crustaceans). In particular, cereals such as rice and wheat, green leafy vegetables, potato, carrot and celeriac may contain higher Cd levels than other edible plants and even more than fish and meat (Järup and Akesson 2009). Many urban gardens, like some from the urban area of Porto, have been found to contain soil contaminated with Cd, other metals and other toxic compounds at levels exceeding maximum values allowed by governmental laws, and at higher levels than those quantified in rural areas (Rodrigues et al. 2013). Therefore, plants harvested in urban areas are at risk of being contaminated with metals. This occured in harvested plants from home gardens of the municipality of Celje in Slovenia. Among these plants root and leafy vegetables accumulated more Cd compared to grain vegetables (Bešter et al. 2013).

Concerning Cd accumulation and its effect on plant growth, a research study showed that four plant species, *Zea mays* (sweet corn), *Triticum aestivum* (wheat), *Cucumis sativus* (cucumber), and *Sorghum bicolor* (sorghum) that were grown for 5 days in an artificial soil contaminated with increasing Cd concentrations, accumulated this metal in their tissues, mostly in roots (An 2004). Although seed germination was insignificantly affected by Cd, the growth of seedlings decreased in a dose-dependent manner. Moreover, between root and shoot growth evaluation, root growth was the most sensitive endpoint of Cd toxicity in these plant species. In particular, sorghum was the species accumulating the highest levels of Cd and the most sensitive to Cd, followed by cucumber, wheat, and sweet corn (An 2004). Similarly to Cr^{6+}, in most species, Cd is also able to decrease the levels of chlorophyll pigments by substituting Mg^{2+} (Mysliwa-Kurdziel and Strzałka 2002), thereby inducing

chlorosis (Sanità di Toppi and Gabbrielli 1999). Cd may cause necrotic lesions in plant organs (Sanità di Toppi and Gabbrielli 1999) and may affect photosynthesis (e.g. in lettuce (Monteiro et al. 2009b; Dias et al. 2012)). Cd also induces oxidative stress by increasing ROS levels and changing the activity of antioxidant enzymes e.g. in lettuce (Monteiro et al. 2009b; Chapter 2.2). Cd is genotoxic to plants, as this metal induced DNA damage detected by comet assay in species like *Allium cepa*, and *Nicotiana tabacum* (Bandyopadhyay et al. 2011), or MN formation in *Vicia faba* (Souguir et al. 2010) (), and microsatellite mutations in lettuce, which were dependent on plant age and exposure conditions (Monteiro et al. 2007, 2009a).

Tobacco plants accumulate high levels of Cd in their leaves, and because of that, inhalation of tobacco smoke is an important source of Cd exposure in humans (Järup and Akesson 2009).

Human contamination by Cd: Cd has a long biological half-life in humans/animals, particularly in kidneys and liver. Chronic ingestion of Cd might lead to different pathologies, like neurological diseases, infertility, diabetes, cancer, or renal and bone injuries like osteoporosis and osteomalacia (Oliveira et al. 2009; Nair et al. 2013).

Cadmium is known to cause a disease called "Itai Itai disease", characterized by loss of bone tissue and failure of the kidneys. This disease was first mentioned in the early 20th century, when the population living near the Jinzu river basin in Toyama, Japan, was exposed to Cd by drinking contaminated water and by ingesting contaminated rice grown in that area (Nordberg 2009). More recently, a study involving a population living in an industrial complex in Korea showed high levels of Cd in urine associated with osteopenia and osteoporosis in adults, being the older people and female the groups presenting lower bone mineral density (Shin et al. 2011).

Cadmium is classified as carcinogenic to humans based on animal studies and occupational exposure to workers (IARC 1993). For example, wild mice living in a Cd-contaminated mine in Cunha Baixa, showed accumulation of Cd in bones, kidney and liver. These mice also showed altered gene expression of tumor suppressing genes (Lourenço et al. 2013). In addition, these mice and earthworms showed DNA damage (Lourenço et al. 2012, 2013).

Chromium and cadmium in the trophic chain: some case studies

As reported above, a way of human contamination by Cr and Cd includes ingestion of contaminated water and food (including contaminated crops). Some ecotoxicological studies have been done to evaluate the potential of metal transfer/biomagnification through different levels of the trophic chain. But compared with toxicological studies in isolated organisms, the consequences and fate of metals from plants/producers through terrestrial food chain has been less studied. Most research involved studies of metal transfer in the trophic chain in aquatic environments. Some authors (Wallace and Luoma 2003; Seebaugh and Wallace 2004) suggested that trophically available metal [i.e., metal associated with heat shock proteins such as MT, high density proteins (such as enzymes), and organelles] could support the bioenhancement of Cd transfer along aquatic food chains.

Some of the biological models used to assess metal bioaccumulation *in situ* or in lab conditions include crops such as pea (Rodriguez et al. 2011) and lettuce (Monteiro et al. 2009b), and other species (Zheng et al. 2007) including the hyperaccumulator plant species like *Thlaspi* spp. (Monteiro et al. 2010). Regarding animals/consumers, models as earthworms (e.g., *Eisenia fetida* (Alonso et al. 2009)), aquatic organisms like isopods (e.g., *Porcellio dilatatus* (Monteiro et al. 2008)), mollusks (e.g., oyster (Kurochkin et al. 2011)), crustaceans (e.g., *Daphnia magna* (Regaldo et al. 2009), crayfish (Kuklina et al. 2014)) and foraminiferal species (Martins et al. 2013); snails (e.g., Scheifler et al. 2002; Ebenso et al. 2013); rodents (Lourenço et al. 2012, 2013; Tête et al. 2014) and birds (Coeurdassier et al. 2012) were used. Also, microalgae (e.g., *Chlorella vulgaris* (Regaldo et al. 2009), diatoms (Ferreira da Silva et al. 2009)), bacteria (e.g., Megharaj et al. 2003; Khan et al. 2010; Kumar et al. 2012), and fungi as edible mushrooms (e.g., Kalač 2010) were also used. These organisms are considered bioindicators of metal contamination in ecosystems because they can be used for monitoring purposes in contaminated sites by evaluating metal bioaccumulation and toxicity in these living organisms.

The availability of a metal does not only depend on the total metal concentration in soil/water by itself, but it also depends on the pH of soil/water, metal form, organic matter content, chelating agents, as well as the species of living organism and the route of exposure (Rogival et al. 2007; Peralta-Videa et al. 2009). Thus, the bioconcentration factor (ratio between the metal concentration accumulated in the organism and the metal concentration

in the environment) is consequently different (Peralta-Videa et al. 2009). In a study of Marchese et al. (2008) the bioconcentration factor of Cr was calculated in several aquatic organisms from different levels of the food chain following 28 days of exposure to Cr-contaminated sediments. Plants (*Ceratophyllum demersum*) presented the highest value, 718.66 ± 272.91, followed by worm (*Limnodrillus udekemianus*) with 172.55 ± 80.8, the crab (*Zilchiopsis collastinensis*) with 67.72 ± 35.4, and the fish (*Cnesterodon decemmaculatus*) with 23.11 ± 12.82 (Marchese et al. 2008). Moreover, through the food chain, metals can be assimilated at different rates. For example, Calhôa et al. (2006) showed that Cd was more efficiently assimilated by isopods fed with lettuce contaminated superficially with 100 µM $Cd(NO_3)_2$ than by isopods fed with biologically contaminated lettuce (i.e., lettuce grown and exposed to 100 µM Cd for 7 days). This fact was related to the form of Cd present in lettuce: in biologically exposed lettuce, Cd was bound to thiol groups forming complexes of e.g., Cd-GSH, or Cd-Cys, reducing Cd availability; on the other hand, in lettuce superficially exposed to Cd, the metal was more available, leading to a high level of accumulation in isopods (Calhôa et al. 2006). Another study showed that Cd bioavailability to isopods was dependent on the subcellular partitioning of the metal in lettuce and two species of *Thlaspi* spp. (*T. caerulescens*, a hyperaccumulator species, and *T. arvense*, a nonaccumulator species) (Monteiro et al. 2008). Also Ding et al. (2013) used *Amaranthus hypochondriacus L*. and the insect *Prodenia litura* to characterize Cd allocation along these trophic levels and corresponding detoxification strategies. When exposed to contaminated soil, *A. hypochondriacus* leaves accumulated high levels of Cd and the concentration in *P. litura* larvae increased with increasing Cd concentrations in the leaves used as food supply. The authors found high Cd transfer coefficients from soil to leaf and from larvae to feces. *A. hypochondriacus* leaves showed the highest contents of Cd in pectates and in protein-integrated forms (Ding et al. 2013). On the other hand, cell fractions of *P. litura* larva showed that the type of proteins dominant for metal-binding compartmenting Cd were those obtained in the heat-stable protein fraction. These data supported that the way Cd is retained/accumulated at subcellular level is crucial for the mechanisms of Cd sequestration and excretion by *P. litura* larva feeding (Ding et al. 2013). Also in the worm species *Limnodrilu hoffmeisteri*, Cd showed different levels of bioavailability depending on its association with molecules or organelles. Cd associated with high density proteins and heat shock proteins was fully available to the consumer

Palaemonetes pugio, while Cd bound to organelles was less (70%) trophically available, and Cd bound to metal-rich granules was unavailable (Wallace and Lopez 1997).

Many ecotoxicological assays involve monitoring of contaminated areas, and organisms living there to assess metal bioaccumulation. For example, in several metal-contaminated sites near an active non-ferrous metallurgic factory in south of Antwerp, in Belgium, the metals As, Cd, Cu, Pb and Zn were found in soil (Rogival et al. 2007). In that study, two foods of the diet of wood mice – acorns (seeds of *Quercus robur*) and earthworms – were collected. Regarding Cd, the metal concentration in soil was positively correlated with Cd concentration in acorns and earthworms. Moreover, wood mice also living near the factory accumulated Cd in liver and kidneys, in a dose dependent manner related to the Cd concentration present in mouse diet (Rogival et al. 2007), supporting Cd transfer and bioaccumulation.

Juvenile snails (*Helix aspersa*), fed for 4 weeks with rape plants previously contaminated with Cd, showed Cd accumulation (Scheifler et al. 2002). In another study, other snail species (*Limicolaria aurora*) was fed for 4 weeks with edible mushrooms that were harvested in three contaminated (Cd, Cr, and other metals) farm sites in Niger Delta (Nigeria) (Ebenso et al. 2013). However, the metal uptake by the snails was low and bioaccumulation was not enough to consider the snails improper for human consumption (< 1 mg Kg^{-1} Cr or Cd, (FAO/WHO 2001 *vide* Ebenso et al. 2013)).

Compared to Cd, less ecotoxicological assays have been done regarding Cr contamination of the environment and its transfer through the trophic chain. Some studies show the possibility of Cr accumulation and toxicity in organisms. For example, Kuykendall et al. (2006) exposed two species of fish, fathead minnows and largemouth bass (*Micropterus salmoides*) (predator), to 2 ppm Cr^{6+} in water for 4 days. Cr^{6+} led to DNA-protein crosslink formation in erythrocytes of both species (higher levels in fathead minnows). When largemouth bass individuals were fed with fathead exposed to Cr^{6+} DNA-protein crosslinks also increased. Thus, both water and diet intake with Cr^{6+} led to DNA-protein crosslink formation in a predator fish (Kuykendall et al. 2006).

In Nord-Pas-de-Calais, France, where a former Pb and Zn smelter is located, some vegetables produced in agricultural soils and home gardens contained high concentrations

of Cd and Pb at levels higher than permissible values for human consumption (Douay et al. 2013). In other polluted areas, in Zhejiang Province, China, there are agricultural fields located near local industries (e.g., metal smelting and battery making) where high levels of Pb, Cd, Cr, Hg, and As were found (Liu et al. 2013). Almost 300 vegetable species were sampled from these soils and depending on the plants species metals accumulated at different levels: e.g., celery accumulated the highest Cr concentration and tomato the lowest, and asparagus and lettuce plants accumulated higher Cd and Cr concentrations compared to rape. According to the model of risk assessment applied in this study, Cd is the metal causing the greatest cancer risk (Liu et al. 2013).

Mechanisms of chromium and cadmium uptake in plants and humans

Chromium

Uptake of Cr by plants and translocation from roots to shoots depends on the metal oxidation state, which in turn depends on soil pH, organic matter, chelating compounds, and microorganisms present in the rhizosphere (Manara 2012). In particular, in acidic soils Cr^{6+} compounds are more mobile and also more easily reduced to Cr^{3+}. Moreover, the organic matter, Fe^{2+}, and sulfites can readily reduce them to Cr^{3+}, whereas manganese oxides can oxidize Cr^{3+} to Cr^{6+} (Becquer et al. 2003). In addition, some compounds from root exudates, like organic acids may reduce Cr^{6+} and/or form complexes, increasing the solubility and mobility of Cr through the root xylem (Bluskov et al. 2005).

In the current proposed model of Cr uptake and toxicity in plant roots (Figure 2), both Cr^{6+} and Cr^{3+} are taken up *via* symplast (Shanker et al. 2005) and plants may be capable of reducing Cr^{6+} to Cr^{5+}, Cr^{4+} and Cr^{3+}, contributing to detoxification of Cr^{6+} (Santos and Rodriguez 2012). Uptake of Cr^{6+} by root cells occurs by active transport through carriers of sulphate, phosphate and iron ions, while Cr^{3+} is taken up by passive transport (Shanker et al. 2005).

Figure 2 also shows that Cr^{6+} may be immobilized in vacuoles of root cells and possibly reduced to Cr^{3+} as a way of detoxification and prevention of Cr^{6+} translocation from roots to leaves (Shanker et al. 2005). In fact, Cr content is frequently very much higher in roots than in other parts of the plant. For example, it was evaluated the uptake of Cr^{3+} and Cr^{6+} in water

hyacinth, and it was found that both Cr states accumulated preferably in the root and that Cr^{6+} was more translocated (Paiva et al. 2009). In tumbleweed, the same pattern of Cr^{3+} and Cr^{6+} uptake was observed (Gardea-Torresdey et al. 2005). Unlike other metals (e.g., Cd), Cr is unable to induce PCs in plants (Shanker et al. 2005), and it is thought that Cr may induce the synthesis of MT, although the mechanisms involved are not yet clear (Shanker and Pathmanabhan 2004).

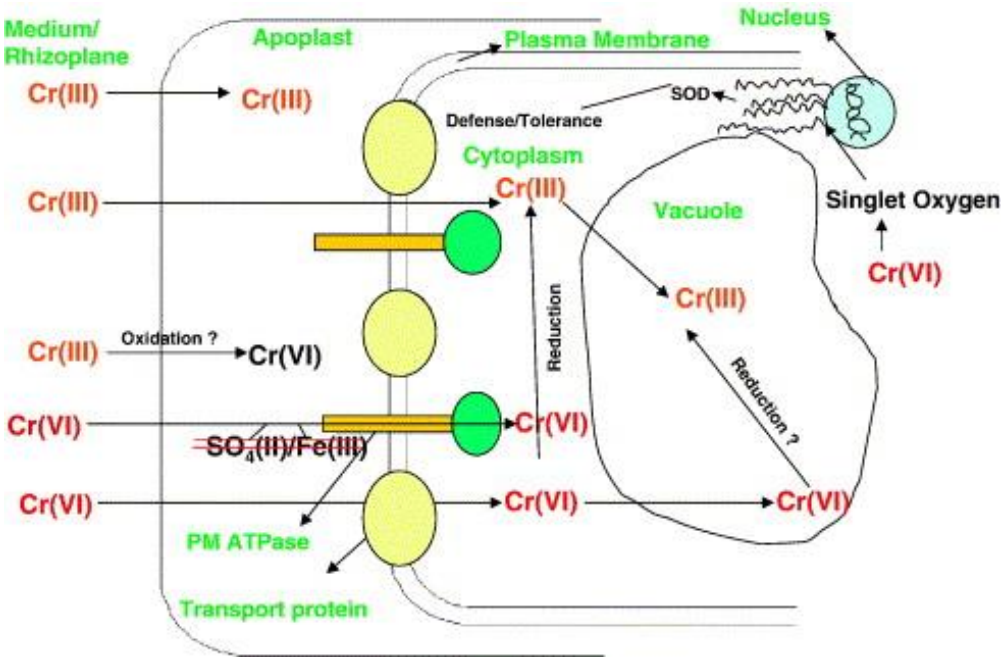

Figure 2. Model of Cr uptake and toxicity in plant roots proposed by Shanker et al. (2005).

In animal cells Cr^{6+} (e.g., CrO_4^{2-}) uptake (Figure 3A) occurs *via* anion channels (sulphate and phosphate) (Beyersmann and Hartwig 2008), like in plant root cells. In the extracellular environment Cr^{6+} may be reduced to Cr^{3+} as a way of prevention of toxicity, and the existent Cr^{3+} ions enter slowly into the cell by diffusion or phagocytosis (Collins et al. 2010; Zhitkovich 2011). According to Beyersmann and Hartwig (2008) and as shown in Figure 3A, Cr^{3+} can form complexes with hydrophobic ligands (e.g., 1,10-phenanthroline, 2,2'-bipyridine, picolinic acid) that permeate by diffusion through plasma membrane. Moreover, Cr_2O_3 particles can be taken up by phagocytosis, and then solubilized in lysosomes and Cr^{3+} is released. Cr^{3+} can also bind to transferrin (competing with Fe^{2+}) and enter the cell by endocytosis (Figure 3A).

Figure 3B shows that once in cells, Cr^{6+} is rapidly reduced to Cr^{5+}, Cr^{4+} and Cr^{3+} by reducing enzymes (e.g., NADPH cytochrome c reductase, GR) and non-enzymatic reducers like Asc, GSH, and Cys (Afolaranmi et al. 2008). As Cr^{6+} is being reduced, ROS are generated in Fenton or Haber-Weiss reactions (Raghunathan et al. 2009). These ROS and intermediate forms of Cr can induce genetic damages, including Cr-DNA adducts, Cr-DNA crosslinks, Cr-DNA-protein crosslinks, DNA interstrand crosslinks, oxidative DNA damage, DNA DSB/SSB and abasic sites (O'Brien et al. 2003).

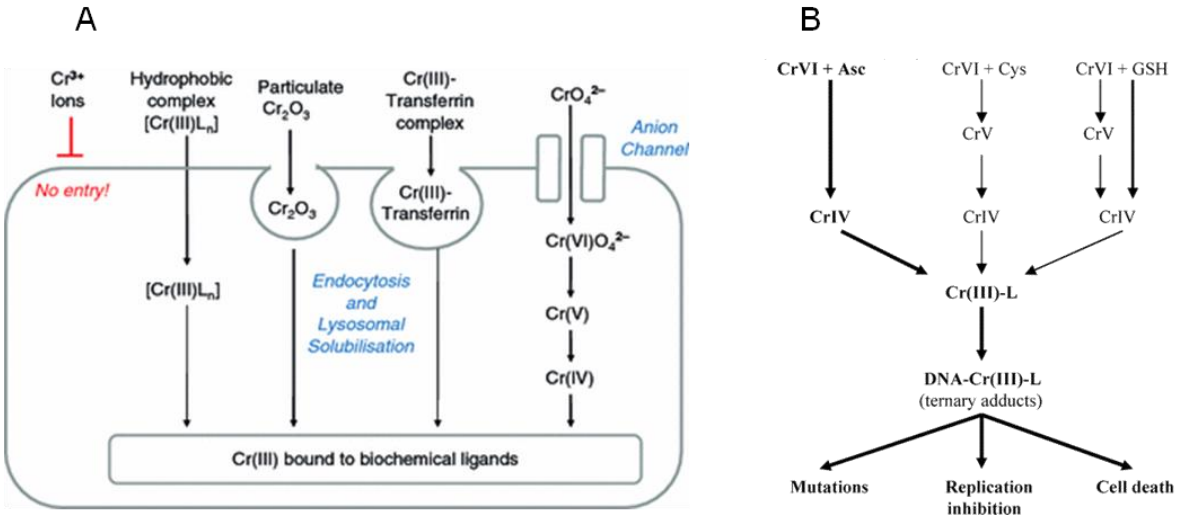

Figure 3. (A) Model of Cr uptake in animal cells, proposed by Beyersmann and Hartwig (2008). (B) Reduction of Cr^{6+} by Asc, Cys, and GSH, and formation of Cr-DNA adducts that may lead to cyto- and genotoxic effects. L – ligand (Asc, GSH, Cys, or histidine) (Adapted from Zhitkovich (2005)).

Cadmium

Uptake of Cr in plants depends on the rhizosphere factors, as previously mentioned for Cr. When Cd ions come in contact with root cells, they can be retained in the cell wall containing pectic sites, hystidyl groups, and extracellular carbohydrates (e.g., callose and mucilage) (Manara 2012). Yang and Chu (2011) presented the mechanism of Cd uptake in plant root cells that is shown in Figure 4.

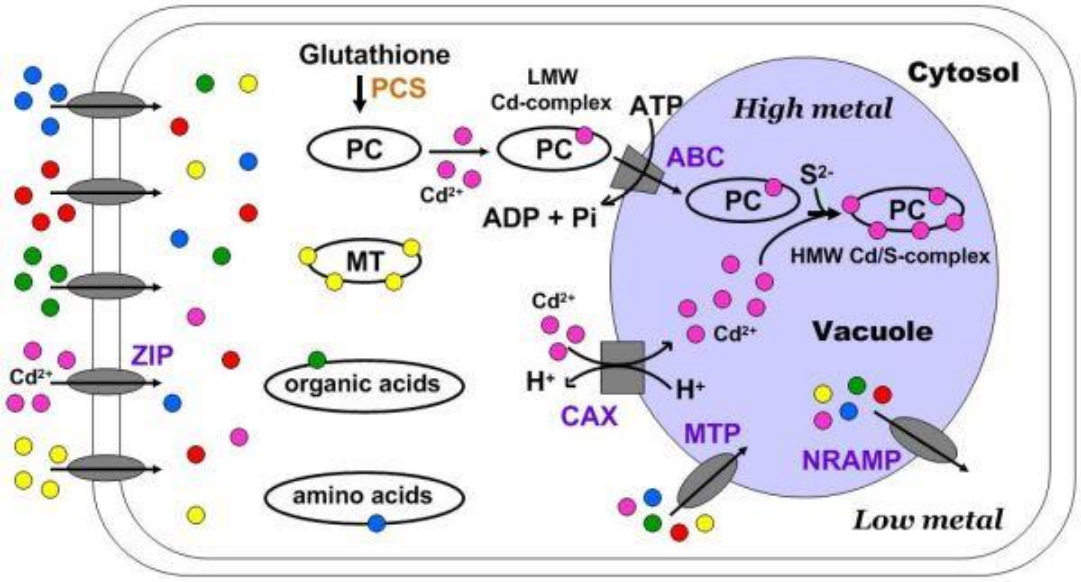

Figure 4. Cd uptake and sequestration in vacuoles of plant cells (Yang and Chu 2011).

Similarly to Cr, Cd enters the root cell via symplast (Clemens et al. 2002). The cell membrane of a root cell has several families of transporters (also observed in other living organisms) involved in metal uptake and homeostasis, and some of them like the ZIP family (carrier of e.g., Fe^{2+}, Mn^{2+}, Zn^{2+}), has been associated with Cd^{2+} carriage into the cytoplasm (Yang and Chu 2011). In addition, Cd uptake can be reduced by membrane efflux transporters (CDF family) that pump Cd ions outside the cell, and these transporters can also carry Cd into the xylem (Manara 2012). The increase of Cd ions in cytoplasm increases the generation of Cys-rich metal binding peptides – PCs, which were identified in plants, fungi and diatoms, and apparently may also exist in some animals (Clemens et al. 2001). These are synthesized from GSH by PCS. Cd is then complexed with PC (due to thiol and carboxyl groups), originating a low molecular weight complex that is sequestered into the vacuole through an ABC transporter. Other Cd ions that enter into the vacuole via CAX transporters

(Ca^{2+}/H^{+} antiports) and sulfide bind to low molecular weight complexes to produce the high molecular weight complex (Yang and Chu 2011). The vacuole is, therefore, the main storage compartment of Cd (Manara 2012), but when necessary, MTP and NRAMP transporters regulate the flux of metal ions (Yang and Chu 2011). Also in response to high Cd levels in cytoplasm, MTs (Cys-rich metal binding polypeptides (Cobbett and Goldsbrough 2002)), organic acids (e.g., malate, citrate and oxalate), amino acids (e.g., hystidine, and proline), GSH, and phytate (a main storage of phosphorous in plants) are able to chelate Cd (Yang and Chu 2011; Manara 2012), decreasing Cd availability to induce ROS formation and cause cellular damages. Besides being a chelating agent, MT is able to eliminate $^{\bullet}O_2^{-}$ and $^{\bullet}OH$ by reaction of Cys residues, thus it can reduce the levels of ROS induced by Cd in cells (Yang and Chu 2011). Cd is translocated from roots to shoots as complexes and via xylem(Hossain et al. 2012).

Uptake of Cd in animal cells may occur by different ways. Complexes of Cd with MT, albumin or other proteins enter the cell by endocytosis. Moreover, when Cd is free (Cd^{2+}) or complexed with Cys, GSH, it can bind to active sites of carrier proteins and channels of substrates as amino acids, oligopeptides, organic anions or organic cations (e.g., the organic anion transporters Oat-1, Oat-3) to enter the cell (Bridges and Zalups 2005; Sabolić et al. 2010). Cd ions can also be transported by carrier proteins and channels (mainly DMT1, voltage gated Ca^{2+} channels and ZIP8) involved in the uptake of divalent cations like Ca^{2+}, Fe^{2+}, and Zn^{2+}. Figure 5 shows Cd entering the animal cell (according to Sarkar et al. (2013)) by these ion transporters and, when inside the cell Cd may take different pathways: (1) Cd competes with Fe^{2+}, Mn^{2+}, Cu^{2+}, Zn^{2+}, for active sites of MT either leading to misfolding of the protein or production of ROS/RNS that contribute to oxidative damage and, ultimately, to cell death; (2) Cd can also bind to MT displacing Zn^{2+} which in turn binds to MTF1 transcription factor that encodes a transcription factor that induces the expression of MT and other genes involved in metal homeostasis; (3) Cd ions can also bind to ER membrane leading to release of Ca^{2+}, which in turn can lead to apoptosis by caspases activation, or Ca^{2+} can activate some kinases and phosphatases resulting in transcription of cell cycle genes (e.g., related with cell cycle progression, therefore influencing cell proliferation); binding of Ca^{2+} may also lead to proteasomal degradation of proteins. When in the cell, (4) Cd also induces apoptosis by mitochondrial pathway (Sarkar et al. 2013).

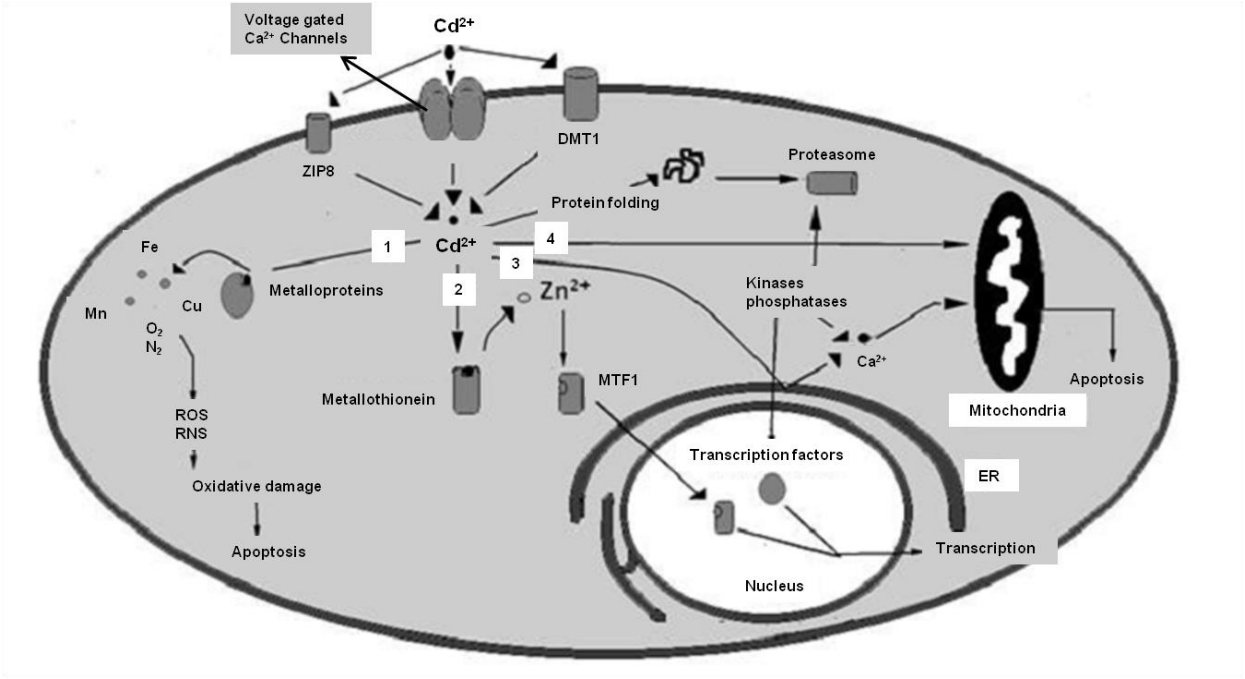

Figure 5. Cd uptake and some cytotoxic effects in animal cells (Adapted from Sarkar et al. (2013)).

Chronic exposure to low Cd doses is highly correlated with Cd accumulation and cellular damages in kidneys, and Cd concentration in urine has been used as biomarker of long-term Cd exposure. However in acute exposure with high Cd doses, Cd mainly accumulates in liver, and Cd concentration in blood has been used as biomarker of a recent exposure to Cd (Godt et al. 2006). Besides bones, liver and kidneys, Cd can also accumulate in testis, spleen, heart, lungs, thymus, salivary glands, epididymis, prostate, pancreas, and central nervous system (Sarkar et al. 2013).

Most current biomarkers used in metal exposure and toxicity assessment

In the assessment of metal exposure and toxicity, different biomarkers have been used at all levels of biological organization (from molecules to cells, individuals, populations, communities and ecosystems) (Mussali-Galante et al. 2013). Figure 6 explains how biomarkers can be classified. The use of biomarkers allows the assessment of exposure level – *biomarkers of exposure* – and the extent of toxic response, including changes in the structure, function/performance of the cell/tissue/organism – *biomarkers of effect* (Bearer

2001; Mussali-Galante et al. 2013). For example, concerning biomarkers of exposure, one can consider the measurement of a contaminant or related metabolites (e.g., Cd, Cd-MT, Cr, Cr-GSH) in target organs/tissues or in body fluids. The set of biomarkers (of exposure and effect) are considered *biomarkers of susceptibility* allowing prediction of individual's susceptibility to a particular compound/xenobiotic (Mussali-Galante et al. 2013). Biomarkers of susceptibility are therefore valuable tools for diagnostics providing insight into the mechanisms of action and the pathways and targets of the compound/xenobiotic. A set of biomarkers can also be used in biomonitoring, and risk assessment involving predictive evaluations in non-intentionally exposed organisms, populations, or ecosystems.

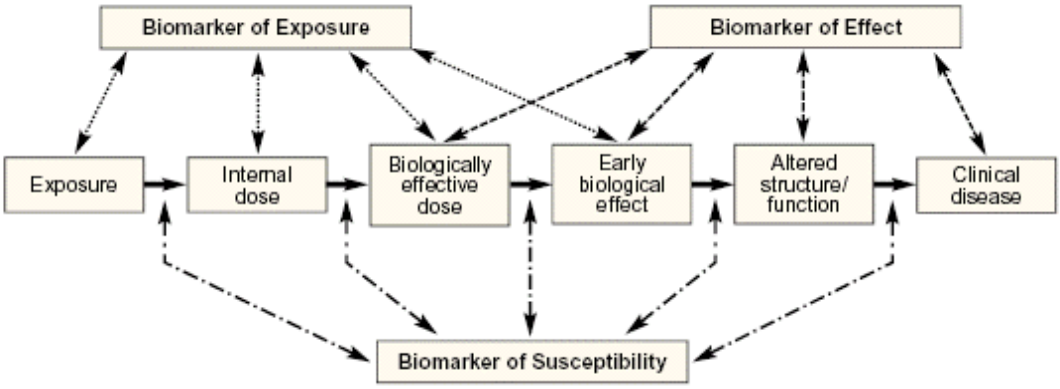

Figure 6. Biomarkers of exposure, effect and susceptibility in an individual under xenobiotic exposure (Bearer 2001).

Therefore, the ideal combination of biomarkers should combine different types of biomarkers, and consider all levels of biological organization, including molecules, cell, organism, population, community and ecosystem (Mussali-Galante et al. 2013). Moreover, this ideal combination of biomarkers should allow a distinction between reversible and irreversible effects, by identifying the most sensitive changes occurring within the shortest period of time, and using minimally invasive techniques to the living being under study.

At cellular level (in both plants and animals), metal biomarkers are frequently classified according to the cell's ability for metal uptake and cytotoxic effects (Aziz et al. 2014). Cytotoxicity is usually evaluated by measuring changes in cell viability, oxidative stress, cell cycle progression, mitochondrial dysfunction, and cell death. In particular, these

biomarkers have been largely used in human cell lines (AshaRani et al. 2009; Aziz et al. 2014). Other biomarkers are focused on measuring genotoxic effects. We highlight here DNA damage measured by comet assay – i.e., DNA DSB/SSB and alkali-labile sites; presence of MN in e.g., *Allium sepa* L. (Seth et al. 2008) and human cell lines (AshaRani et al. 2009); DNA-ploidy changes, which were identified, for example, by FCM in *Pisum sativum* (Rodriguez et al. 2011); and microsatellite instability, which was found in *Lactuca sativa* L. (Monteiro et al. 2009a) and in *P. sativum* (Rodriguez et al. 2013), exposed to Cd and Pb, respectively. These data support that at the cellular level one should combine cytotoxic with genotoxic biomarkers.

The combination of multiple biomarkers of cytotoxicity and genotoxicity has been exhaustively investigated in animals and less in plants. Some of the cytotoxic and genotoxic biomarkers used to assess metal toxicity are commonly used in animals and plant models (e.g., oxidative stress, loss of membrane integrity, DNA damage, mutations, MN) (Monteiro et al. 2007, 2009b; Rodríguez-Serrano et al. 2009; Wu et al. 2010; Rodriguez et al. 2011; Patnaik et al. 2013).

Brief notes on biological models used in metal toxicity assays

In vivo vs in vitro assays

Toxicological research usually involves *in vivo* assays with exposure of animals to chemicals, or *in vitro* assays using cell/tissue culture, or isolated organs. *In vivo* assays are closer to real exposure conditions because the response of an organism to a chemical is influenced by the function of organs, circulatory and lymphatic systems in superior animals, or vascular system in plants. Moreover, assays with living organisms imply different perspectives of exposure, i.e. acute exposure, or chronic exposure throughout their life cycle, where effects on reproduction may be observed. While *in vivo* assays using plants do not raise ethical issues (however it requires some logistic requirements), *in vivo* assays using animals have, nowadays, many restrictions. Regarding the value of animal welfare (without suffer, pain and discomfort) it is considered that an "*animal is any vertebrate animal non human and cephalopods (as it was proved they suffer pain), including autonomous larval and/or reproduction forms"* (European Commission 2010). In general, *in vivo* assays follow guidelines of good practices when using animals, following the principle of 3Rs firstly

advocated by William Russell and Rex Burch (Russell and Burch 1959), and actually into force by the European Commission (2010). This principle incites for *Reduction* of the number of animals used *per* treatment condition, *Refinement* of protocol methodologies providing the best possible welfare conditions, and *Replacement* of *in vivo* assays by *in vitro*, or *in silico* assays, or the use of lower organisms and/or at early stages of development (i.e. with or without incomplete development of neuronal system) (European Commission 2010)). In the European directive it is stated that "*An experiment shall not be performed on an animal, if another scientifically satisfactory method of obtaining the result…, is reasonably and practicably available"* (European Commission 2010).

Why lettuce and human bone cells as models?

Toxicity assays on the effects of metals in humans cannot be done directly (only biomonitoring, risk assessment, and *in silico* evaluations) clearly due to ethical issues, thus *in vivo* assays using e.g., rats, mice, pigs, or *in vitro* assays have been performed. But using animal models not always reflects the human response to the same chemical. Therefore, *in vitro* assays using human cells are promising alternatives, providing preliminary data that may help in planning future trials *in vivo*. Other alternatives are the reduction of the number of animals and analyses of the necessary biomarkers only to avoid or at least reduce animal suffering.

In this thesis, metal (Cr and Cd) toxicity is assessed in two biological models, plants *in vivo* (Chapters 2.1 and 2.2.), and human cells *in vitro* (Chapters 3.1-3.3.). Some plant species, including crops like lettuce (*L. sativa* L.) are recommended by OECD for standard ISO toxicity tests (OECD 2006). Lettuce was also chosen because it is a widely commercialized crop and able to accumulate metals (e.g., accumulation of Cd, Cr, Ni, Pb, among others, in edible parts (Peris et al. 2007)), and several toxicity effects have previously been observed in lettuce exposed to Cd (Monteiro et al. 2007, 2009a, 2009b, 2010). However, most of these studies provided non systematized data (e.g., focusing only some particular aspects of plant cellular response to Cd), being mostly focused on e.g., oxidative stress (e.g., Monteiro et al. 2009b). Besides, data provided by Monteiro et al. (2009b) only used one dose, 100 µM, currently acknowledged as too high. Therefore, to decipher the mechanisms underlying Cd cyto- and genotoxicity and the cell responses, it is crucial to study, in a more systematic and

interdependent way, the cyto- and genotoxicity of lower doses 0, 1, 10, and 50 µM Cd. For that we will use the largest set of cytotoxic and genotoxic biomarkers ever used (to our knowledge): seed germination rates, plant survival and growth, Cd accumulation, oxidative stress (ROS, antioxidant enzyme activities), lipid peroxidation, protein oxidation, membrane integrity (membrane permeability), DNA damage (by comet assay), MN, and changes in cell cycle. With these data and other data available in the group (e.g., nutrient disorders, photosynthetic performance (Monteiro et al. 2009b; Dias et al. 2012)), or found in the literature, we can propose here a more mechanistic model on the action of Cd in the plant cell (Chapter 2.2).

For *in vitro* assessment of Cr and Cd toxicity human osteoblasts (involved in bone formation) were used, due primarily to the accumulation of these metals in bones and their toxic effects in humans and other mammalians, including e.g., osteoporosis, as previously described, and in more detail afterwards in Chapter 3. Thus, a human osteoblast cell line, MG-63, was chosen for this work. This cell line (available in the American Type Culture Collection center) is derived from an osteosarcoma, a malignant bone tumor of a 14 years old Caucasian male and maintains some characteristics of the osteoblast phenotype, like growing in an adherent monolayer and expressing alkaline phosphatase and osteocalcin immunocytochemical markers (Pautke et al. 2004). These cells in culture present fibroblast morphology and are moderately differentiated and non-mineralizing (Schwartz et al. 1999; Hattar et al. 2002). Being a continuous cell line, MG-63 cell line, the cell growth for a long period of time is a major advantage compared to primary cell lines that can only replicate few times (Freshney 2005). There are many toxicity assays using osteoblast cell lines like Saos-2, U2-OS or MG-63, however they focus only on a single or few approaches of cytotoxicity or genotoxicity. For example, regarding the assessment of Cd cytotoxicity, some authors only evaluated cell viability and metal uptake (MG-63 cells were exposed to ≤ 100 µM Cd for 3-24 h), or apoptosis (Saos-2 cells were exposed to 10, 100, 200 µM Cd for 3-48 h (Romero et al. 2005; Coonse et al. 2007)). In our group, the evaluation of cyto- and genotoxicity of Cd (20, and 50 µM for 24, and 48 h) in MG-63 cell line have started with analysis of cell viability (Pinto 2011), DNA damage and cell cycle progression (Pinho 2011), in Chapter 3.2. However, in order to contribute for a larger and more integrative analysis of Cd cyto- and genotoxicity in MG-63 cell line we decided to add useful biomarkers (in Chapters 3.2 and 3.3), and an additional Cd concentration (65 µM) (in Chapter 3.3). Thus,

the new biomarkers included are: MN, NPBs, apoptosis and necrosis (using CBMN assay), cytoskeletal organization, expression of genes encoding for proteins involved in cell cycle regulation and DNA damage checkpoints, and Cd uptake (Chapter 3.2); expression of genes encoding for antioxidant enzymes (CAT, SOD, GR, GPx), ROS quantification, TAA, protein oxidation and lipid peroxidation, $\Delta\Psi m$, mitochondrial morphology, mitochondrial respiratory chain complexes (I and IV) and citrate synthase activities, and cellular energetic status (Chapter 3.3). To enable an easier integrative analysis of the results and an enrichment of the overall discussion on cyto- and genotoxicity of Cd on MG-63 cells, the past presented results of our group and the new ones are unified in this thesis with the main purpose of publishing the results in two papers (one corresponding to Chapter 3.2 and other corresponding to Chapter 3.3).

Objectives

The main objective of this thesis is to evaluate and understand the mechanisms of putative cyto- and genotoxic effects induced by Cr and Cd salts, in plants and human cells. To fulfill this objective, lettuce plants (**Chapter 2**: **Chapters 2.1** and **2.2**) were exposed to Cr^{3+}/Cr^{6+} or Cd, and human osteoblasts (**Chapter 3: Chapters 3.1-3.3**) were exposed to Cr^{6+} or Cd. Several biomarkers of susceptibility related to metal uptake and cyto- and genotoxicity were used.

To achieve this main goal, specific aims were defined and are distributed in Chapters, being the following:

1. To evaluate putative cyto- and genotoxic effects of Cr^{3+}/Cr^{6+} in lettuce, concerning biomarkers of general toxicity (e.g., plant growth), oxidative stress, cell cycle progression, and genotoxicity (DNA damage, MN formation, mitotic aberrations), addressed in **Chapter 2.1**.
2. To evaluate putative cyto- and genotoxic effects of Cd in lettuce, concerning biomarkers of general toxicity, the state of membrane permeability, cell cycle progression, oxidative stress, protein oxidation, lipid peroxidation, and genotoxicity (DNA damage and MN formation), addressed in **Chapter 2.2**.
3. To evaluate putative cyto- and genotoxic effects of Cr^{6+} in human osteoblast cell line MG-63, concerning biomarkers of cell viability, cell cycle progression, and genotoxicity (DNA damage, MN, and NPBs formation), addressed in **Chapter 3.1**.
4. To evaluate putative cyto- and genotoxic effects of Cd in human osteoblast cell line MG-63, concerning biomarkers of cell viability, cell death, cell cycle progression, genotoxicity (DNA damage, MN, and NPBs formation), and changes in gene expression, addressed in **Chapter 3.2**. Moreover, this objective is completed in **Chapter 3.3**, where biomarkers of oxidative stress, changes in gene expression, protein oxidation, lipid peroxidation, and mitochondrial function are assessed.

In the final section of the thesis, **Chapter 4**, a global discussion with relevant conclusions of this work, and future perspectives are presented.

References

Afolaranmi, G. A., Tettey, J., Meek, R. M. D., and Grant, M. H. (2008) Release of chromium from orthopaedic arthroplasties. *Open Orthop. J.* 2, 10–18.

Agency for Toxic Substances and Disease Registry. (2014) The priority list of hazardous substances that will be the subject of toxicological profiles. Available from: http://www.atsdr.cdc.gov/spl/ (accessed Jun, 2014)

Alonso, E., González-Núñez, M., Carbonell, G., Fernández, C., and Tarazona, J. V. (2009) Bioaccumulation assessment via an adapted multi-species soil system (MS.3) and its application using cadmium. *Ecotoxicol. Environ. Saf.* 72 (4), 1038–1044.

An, Y.-J. (2004) Soil ecotoxicity assessment using cadmium sensitive plants. *Environ. Pollut.* 127 (1), 21–26.

AshaRani, P. V., Low Kah Mun, G., Hande, M. P., and Valiyaveettil, S. (2009) Cytotoxicity and genotoxicity of silver nanoparticles in human cells. *ACS Nano.* 3 (2), 279–290.

Aziz, R., Rafiq, M. T., Yang, J., Liu, D., Lu, L., He, Z., Daud, M. K., Li, T., and Yang, X. (2014) Impact assessment of cadmium toxicity and its bioavailability in human cell lines (Caco-2 and HL-7702). *Biomed. Res. Int.* 2014:839538, pp 8.

Bandyopadhyay, A., and Mukherjee, A. (2011) Sensitivity of Allium and Nicotiana in cellular and acellular comet assays to assess differential genotoxicity of direct and indirect acting mutagens. *Ecotoxicol. Environ. Saf.* 74 (4), 860-865.

Bearer, C. F. (2001) Markers to detect drinking during pregnancy. *Alcohol Res. Health.* 25 (3), 210–218.

Becquer, T., Quantin, C., Sicot, M., and Boudot, J. P. (2003) Chromium availability in ultramafic soils from New Caledonia. *Sci. Total Environ.* 301 (1-3), 251–261.

Ben Hamida, F., Troudi, A., Sefi, M., Boudawara, T., and Zeghal, N. (2013) The protective effect of propylthiouracil against hepatotoxicity induced by chromium in adult mice. *Toxicol. Ind. Health.* [Epub ahead of print].

Bešter, P. K., Lobnik, F., Eržen, I., Kastelec, D., and Zupan, M. (2013) Prediction of cadmium concentration in selected home-produced vegetables. *Ecotoxicol. Environ. Saf.* 96, 182–190.

Beyersmann, D., and Hartwig, A. (2008) Carcinogenic metal compounds: recent insight into molecular and cellular mechanisms. *Arch. Toxicol.* 82 (8), 493–512.

Bluskov, S., Arocena, J. M., Omotoso, O. O., and Young, J. P. (2005) Uptake, distribution, and speciation of chromium in *Brassica juncea*. *Int. J. Phytoremediation.* 7 (2), 153–165.

Bonet, A., Poschenrieder, Ch., and Barcelo, J. (1991) Chromium III-iron interaction in Fe-deficient and Fe-sufficient bean plants. I. Growth and nutrient content. *J. Plant Nutr.* 14 (4), 403–414.

Branco, R., Chung, A.-P., Veríssimo, A., and Morais, P. V. (2005) Impact of chromium-contaminated wastewaters on the microbial community of a river. *FEMS Microbiol. Ecol.* 54 (1), 35–46.

Bridges, C. C., and Zalups, R. K. (2005) Molecular and ionic mimicry and the transport of toxic metals. *Toxicol. Appl. Pharmacol.* 204 (3), 274–308.

British Geologic Survey. (2012) World Mineral Production 2008-2012. Keyworth, Nottingham: British Geological Survey: NERC.

Calhôa, C. F., Soares, A. M. V. M., and Mann, R. M. (2006) Cadmium assimilation in the terrestrial isopod, *Porcellio dilatatus* – is trophic transfer important? *Sci. Total Environ.* 371 (1-3), 206–213.

Campbell, J. R., and Estey, M. P. (2013) Metal release from hip prostheses: cobalt and chromium toxicity and the role of the clinical laboratory. *Clin. Chem. Lab. Med.* 51 (1), 213–220.

Clemens, S., Palmgren, M. G., and Krämer, U. (2002) A long way ahead: understanding and engineering plant metal accumulation. *Trends Plant Sci*. 7 (7), 309–315.

Clemens, S., Schroeder, J. I., and Degenkolb, T. (2001) *Caenorhabditis elegans* expresses a functional phytochelatin synthase. *Eur. J. Biochem.* 268 (13), 3640–3643.

Cobbett, C., and Goldsbrough, P. (2002) Phytochelatins and metallothioneins: roles in heavy metal detoxification and homeostasis. *Annu. Rev. Plant Biol.* 53, 159–182.

Coelho, P., Costa, S., Costa, C., Silva, S., Walter, A., Ranville, J., Pastorinho, M. R., Harrington, C., Taylor, A., Dall'Armi, V., Zoffoli, R., Candeias, C., Ferreira da Silva, E., Bonassi, S., Laffon, B., and Teixeira, J. P. (2014) Biomonitoring of several toxic metal(loid)s in different biological matrices from environmentally and occupationally exposed populations from Panasqueira mine area, Portugal. *Environ. Geochem. Health.* 36 (2), 255–269.

Coelho, P., García-Lestón, J., Costa, S., Costa, C., Silva, S., Dall, V., Zoffoli, R., Bonassi, S., Pereira de Lima, J., Gaspar, J. F., Pásaro, E., Laffon, B., and Teixeira, J. P. (2013) Genotoxic effect of exposure to metal(loid)s. A molecular epidemiology survey of populations living and working in Panasqueira mine area, Portugal. *Environ. Int.* 60, 163–170.

Coeurdassier, M., Fritsch, C., Faivre, B., Crini, N., and Scheifler, R. (2012) Partitioning of Cd and Pb in the blood of European blackbirds (*Turdus merula*) from a smelter contaminated site and use for biomonitoring. *Chemosphere.* 87 (11), 1368–1373.

Collins, B. J., Stout, M. D., Levine, K. E., Kissling, G. E., Melnick, R. L., Fennell, T. R., Walden, R., Abdo, K., Pritchard, J. B., Fernando, R. A., Burka, L. T., and Hooth, M. J. (2010) Exposure to hexavalent chromium resulted in significantly higher tissue chromium burden compared with trivalent chromium following similar oral doses to male F344/N rats and female B6C3F1 mice. *Toxicol. Sci.* 118 (2), 368–379.

Coonse, K. G., Coonts, A. J., Morrison, E. V., and Heggland, S. J. (2007) Cadmium induces apoptosis in the human osteoblast-like cell line Saos-2. J. *Toxicol. Environ. Health A.* 70 (7), 575–581.

Dias, M. C., Monteiro, C., Moutinho-Pereira, J., Correia, C., Gonçalves, B., and Santos, C. (2012) Cadmium toxicity affects photosynthesis and plant growth at different levels. *Acta Physiol. Plant.* 35 (4), 1281–1289.

Ding, P., Zhuang, P., Li, Z., Xia, H., and Lu, H. (2013) Accumulation and detoxification of cadmium by larvae of *Prodenia litura* (Lepidoptera: Noctuidae) feeding on Cd-enriched amaranth leaves. *Chemosphere*. 91 (1), 28–34.

Direcção Geral de Energia e Geologia. (2013) Boletim de minas. 41 (1).

Douay, F., Pelfrêne, A., Planque, J., Fourrier, H., Richard, A., Roussel, H., and Girondelot, B. (2013) Assessment of potential health risk for inhabitants living near a former lead smelter. Part 1: metal concentrations in soils, agricultural crops, and homegrown vegetables. *Environ. Monit. Assess.* 185 (5), 3665–3680.

Dube, B. K., Tewari, K., Chatterjee, J., and Chatterjee, C. (2003) Excess chromium alters uptake and translocation of certain nutrients in citrullus. *Chemosphere.* 53 (9), 1147–1153.

Ebenso, I. E., Solomon, I. P., Akoje, C. C., Akpan, I. P., Eko, P. M., Akpan, E. A., and Omole, A. J. (2013) Bioaccumulation of iron, zinc, cadmium and chromium by juvenile snail *Limicolaria aurora* J., fed edible mushroom *Pleurotus spp* from Niger Delta, Nigeria. *Bull. Environ. Contam. Toxicol.* 90 (3), 314–317.

Eiselstein, L. E., Proctor, D. M., and Flowers, T. C. (2007) Trivalent and hexavalent chromium issues in medical implants. *Mater. Sci. Forum.* 539-543, 698–703.

Eliasson, A., Arnelund, C. F., Johansson, A. (2007) A clinical evaluation of cobalt-chromium metal-ceramic fixed partial dentures and crowns: A three- to seven-year retrospective study. *J. Prosthet. Dent.* 98 (1), 6-16.

Environmental Protection Agency (2013) Priority Pollutants. Available from: http://water.epa.gov/scitech/methods/cwa/pollutants.cfm (accessed Jan, 2014).

European Comission (2001) Decision 2455/2001/EC of the European Parliament and of the Council of 20 November 2001, establishing the list of priority substances in the field of water policy and amending Directive 2000/60/EC. *Off. J. Eur. Union.* O.J. L 331/4.

European Commission (2010) Directive 2010/63/EU of the European Parliament and of the Council of 22 September 2010 on the protection of animals used for scientific purposes. *Off. J. Eur. Union.* O.J. L 33–79.

FAO/WHO (Food and Agriculture Organization of the United Nations/World Heath Organization) (2001) List of maximum levels recommended for contaminants/food standard by joint FAO/WHO Codex Alimentarius Commision. The Netherlands: Joint Office.

Faroon, O., Ashizawa, A., Wright, S., Tucker, P., Jenkins, K., Ingerman, L., and Rudisill, C. (2012) Toxicological profile for cadmium. Atlanta (GA). Agency for Toxic Substances and Disease Registry (US). Available from: http://www.ncbi.nlm.nih.gov/books/NBK158838/ (accessed Jan, 2014)

Ferreira da Silva, E., Almeida, S. F. P., Nunes, M. L., Luís, A. T., Borg, F., Hedlund, M., Marques de Sá, C., Patinha, C., and Teixeira, P. (2009) Heavy metal pollution downstream the abandoned Coval da Mó mine (Portugal) and associated effects on epilithic diatom communities. *Sci. Total Environ.* 407 (21), 5620–5636.

Freshney, R. I. (2005) Culture of animal cells: a manual of basic technique. 5th edition. John Wiley & Sons, Inc., Hoboken, New Jersey. pp 580.

Gardea-Torresdey, J. L., de la Rosa, G., Peralta-Videa, J. R., Montes, M., Cruz-Jimenez, G., and Cano-Aguilera, I. (2005) Differential uptake and transport of trivalent and hexavalent chromium by tumbleweed (*Salsola kali*). *Arch. Environ. Contam. Toxicol.* 48 (2), 225–232.

Gilbert, S. G. (2012) A small dose of toxicology – The health effects of common chemicals. 2nd Edition. Seattle: Healthy World Press; p 129.

Godt, J., Scheidig, F., Grosse-Siestrup, C., Esche, V., Brandenburg, P., Reich, A., and Groneberg, D. A. (2006) The toxicity of cadmium and resulting hazards for human health. *J. Occup. Med. Toxicol.* 1:22, pp 6.

Gunaratnam, M., and Grant, M. H. (2008) Cr (VI) inhibits DNA, RNA and protein syntheses in hepatocytes: involvement of glutathione reductase, reduced glutathione and DT-diaphorase. *Toxicol. In Vitro*. 22 (4), 879–886.

Hattar, S., Berdal, A, Asselin, A., Loty, S., Greenspan, D. C., and Sautier, J.-M. (2002) Behaviour of moderately differentiated osteoblast-like cells cultured in contact with bioactive glasses. *Eur. Cell Mater*. 4 (1), 61–69.

Hossain, M. A., Piyatida, P., Teixeira da Silva, J. A., and Fujita, M. (2012) Molecular mechanism of heavy metal toxicity and tolerance in plants: central role of glutathione in detoxification of reactive oxygen species and methylglyoxal and in heavy metal chelation. *J. Bot.* 2012, 1–37.

IARC (International Agency for Research on Cancer) (1993) Beryllium, cadmium, mercury and exposures in the glass manufacturing industry, *IARC Monographs on the Evaluation of Carcinogenic Risk of Chemicals to Humans*, Vol. 58, pp. 119–146, International Agency for Research on Cancer, Lyon, France.

Järup, L., and Akesson, A. (2009) Current status of cadmium as an environmental health problem. *Toxicol. Appl. Pharmacol.* 238 (3), 201–208.

Kalač, P. (2010) Trace element contents in European species of wild growing edible mushrooms: A review for the period 2000-2009. *Food Chem.* 122 (1), 2–15.

Keegan, G. M., Learmonth, I. D., and Case, C. P. (2008) A systematic comparison of the actual, potential, and theoretical health effects of cobalt and chromium exposures from industry and surgical implants. *Crit. Rev. Toxicol.* 38 (8), 645–674.

Khan, S., Hesham, A. E.-L., Qiao, M., Rehman, S., and He, J.-Z. (2010) Effects of Cd and Pb on soil microbial community structure and activities. *Environ. Sci. Pollut. Res. Int.* 17 (2), 288–296.

Kuklina, I., Kouba, A., Buřič, M., Horká, I., Duriš, Z., and Kozák, P. (2014) Accumulation of heavy metals in crayfish and fish from selected Czech reservoirs. *Biomed. Res. Int.* 2014:306103, pp 9.

Kumar, A., Cameotra, S. S., and Gupta, S. (2012) Screening and characterization of potential cadmium biosorbent *Alcaligenes* strain from industrial effluent. *J. Basic Microbiol.* 52 (2), 160–166.

Kurochkin, I. O., Etzkorn, M., Buchwalter, D., Leamy, L., and Sokolova, I. M. (2011) Top-down control analysis of the cadmium effects on molluscan mitochondria and the mechanisms of cadmium-induced mitochondrial dysfunction. *Am. J. Physiol. Regul. Integr. Comp. Physiol.* 300 (1), R21–R31.

Kuykendall, J. R., Miller, K. L., Mellinger, K. N., and Cain, A. V. (2006) Waterborne and dietary hexavalent chromium exposure causes DNA-protein crosslink (DPX) formation in erythrocytes of largemouth bass (*Micropterus salmoides*). *Aquat. Toxicol.* 78 (1), 27–31.

Levina, A., and Lay, P. A. (2008) Chemical properties and toxicity of chromium(III) nutritional supplements. *Chem. Res. Toxicol.* 21 (3), 563–571.

Liu, X., Song, Q., Tang, Y., Li, W., Xu, J., Wu, J., Wang, F., and Brookes, P. C. (2013) Human health risk assessment of heavy metals in soil – vegetable system: a multi-medium analysis. *Sci. Total Environ.* 463-464, 530–540.

Lourenço, J., Pereira, R., Gonçalves, F., and Mendo, S. (2013) Metal bioaccumulation, genotoxicity and gene expression in the European wood mouse (*Apodemus sylvaticus*) inhabiting an abandoned uranium mining area. *Sci. Total Environ.* 443, 673–680.

Lourenço, J., Pereira, R., Silva, A., Carvalho, F., Oliveira, J., Malta, M., Paiva, A., Gonçalves, F., and Mendo, S. (2012) Evaluation of the sensitivity of genotoxicity and cytotoxicity endpoints in earthworms exposed in situ to uranium mining wastes. *Ecotoxicol. Environ. Saf.* 75 (1), 46–54.

Luís, A. T., Teixeira, P., Almeida, S. F. P., Matos, J. X., and Ferreira da Silva, E. (2011) Environmental impact of mining activities in the Lousal area (Portugal): chemical and diatom characterization of metal-contaminated stream sediments and surface water of Corona stream. *Sci. Total Environ.* 409 (20), 4312–4325.

Manara, A. (2012), Plant responses to heavy metal toxicity, Chapter 2. In Furini, A., editor. Plants and Heavy Metals. *SpringerBriefs Molec. Sci.* Dordrecht: Springer Netherlands; pp 27–54.

Marchese, M., Gagneten, A. M., Parma, M. J., and Pavé, P. J. (2008) Accumulation and elimination of chromium by freshwater species exposed to spiked sediments. *Arch. Environ. Contam. Toxicol.* 55 (4), 603–609.

Martins, V. A., Frontalini, F., Tramonte, K. M., Figueira, R. C. L., Miranda, P., Sequeira, C., Fernández-Fernández, S., Dias, J. A., Yamashita, C., Renó, R., Laut, L. L. M., Silva, F. S., Rodrigues, M. A. da C., Bernardes, C., Nagai, R., Sousa, S. H. M., Mahiques, M., Rubio, B., Bernabeu, A., Rey, D., and Rocha, F. (2013) Assessment of the health quality of Ria de Aveiro (Portugal): heavy metals and benthic foraminifera. *Mar. Pollut. Bull.* 70 (1-2), 18–33.

Megharaj, M, Avudainayagam, S, and Naidu, R. (2003) Toxicity of hexavalent chromium and its reduction by bacteria isolated from soil contaminated with tannery waste. *Curr. Microbiol.* 47 (1), 51–54.

Monteiro, M., Santos, C., Mann, R. M., Soares, A. M. V. M., and Lopes, T. (2007) Evaluation of cadmium genotoxicity in *Lactuca sativa* L. using nuclear microsatellites. *Environ. Exp. Bot.* 60 (3), 421–427.

Monteiro, M. S., Lopes, T., Mann, R. M., Paiva, C., Soares, A. M. V. M., and Santos, C. (2009a) Microsatellite instability in *Lactuca sativa* chronically exposed to cadmium. *Mutat. Res.* 672 (2), 90–94.

Monteiro, M. S., Rodriguez, E., Loureiro, J., Mann, R. M., Soares, A. M. V. M., and Santos, C. (2010) Flow cytometric assessment of Cd genotoxicity in three plants with different metal accumulation and detoxification capacities. *Ecotoxicol. Environ. Saf.* 73 (6), 1231–1237.

Monteiro, M. S., Santos, C., Soares, A. M. V. M., and Mann, R. M. (2008) Does subcellular distribution in plants dictate the trophic bioavailability of cadmium to *Porcellio dilatatus* (Crustacea, Isopoda)? *Environ. Toxicol.* 27 (12), 2548–2556.

Monteiro, M. S., Santos, C., Soares, A. M. V. M., and Mann, R. M. (2009b). Assessment of biomarkers of cadmium stress in lettuce. *Ecotoxicol. Environ. Saf.* 72 (3), 811–818.

Mussali-Galante, P., Tovar-Sánchez, E., Valverde, M., and Rojas del Castillo, E. (2013) Biomarkers of exposure for assessing environmental metal pollution: from molecules to ecosystems. *Rev. Int. Contam. Ambie.* 29 (1), 117–140.

Mysliwa-Kurdziel, B., and Strzałka, K. (2002) Influence of metal on biosynthesis of photosynthetic pigments. In: Prasad, M. N. V., Strzałka, K., editors. *Physiol. Biochem. Met. Toxic. Toler. plants.* Dordrecht, Netherlands: Kluwer Academic Publishers. pp 201–227.

Nagajyoti, P. C., Lee, K. D., and Sreekanth, T. V. M. (2010) Heavy metals, occurrence and toxicity for plants: a review. *Environ. Chem. Lett.* 8 (3), 199–216.

Nair, A. R., Degheselle, O., Smeets, K., Van Kerkhove, E., and Cuypers, A. (2013) Cadmium-induced pathologies: where is the oxidative balance lost (or not)? *Int. J. Mol. Sci.* 14 (3), 6116–6143.

Nordberg, G. F. (2009) Historical perspectives on cadmium toxicology. *Toxicol. Appl. Pharmacol.* 238 (3), 192–200.

O'Brien, T. R., Ceryak, S., and Patierno, S. R. (2003) Complexities of chromium carcinogenesis: role of cellular response, repair and recovery mechanisms. *Mutat. Res.-Fund. Mol. M.* 533 (1-2), 3–36.

OECD (Organization for Economic Cooperation and Development). (2006) OECD guidelines for the teseting ofchemicals. Terrestrial Plant Test: Seedling Emergence and Seedling Growth Test. pp 208−221, OECD, Paris.

Oliveira, H., Spanò, M., Santos, C., and Pereira, M. de L. (2009) Adverse effects of cadmium exposure on mouse sperm. *Reprod. Toxicol.* 28 (4), 550–555.

Paiva, L. B., Gonçalves de Oliveira, J., Azevedo, R. A., Ribeiro, D. R., Gomes da Silva, M., and Vitória, A. P. (2009) Ecophysiological responses of water hyacinth exposed to Cr^{3+} and Cr^{6+}. *Environ. Exp. Bot.* 65 (2-3), 403–409.

Panagos, P., Van Liedekerke, M., Yigini, Y., and Montanarella, L. (2013) Contaminated sites in Europe: review of the current situation based on data collected through a European network. *J. Environ. Public Health.* 2013:158764, pp 11.

Panda, S. K., and Choudhury, S. (2005) Chromium stress in plants. *Braz. J. Plant Physiol.* 17 (1), 95–102.

Patnaik, A. R., Achary, V. M. M., and Panda, B.B. (2013) Chromium (VI)-induced hormesis and genotoxicity are mediated through oxidative stress in root cells of *Allium cepa* L. *Plant Growth Regul.* 71 (2), 157–170.

Pautke, C., Schieker, M., Tischer, T., Kolk, A., Neth, P., Mutschler, W., and Milz, S. (2004) Characterization of osteosarcoma cell lines MG-63, Saos-2 and U-2 OS in comparison to human osteoblasts. *Anticancer Res.* 24 (6), 3743–3748.

Peralta, J. R., Gardea-Torresdey, J. L., Tiemann, K. J., Gomez, E., Arteaga, S., Rascon, E., and Parsons, J. G. (2001) Uptake and effects of five heavy metals on seed germination and

plant growth in alfalfa (*Medicago sativa* L.). *Bull. Environ. Contam. Toxicol.* 66 (6), 727–734.

Peralta-Videa, J. R., Lopez, M. L., Narayan, M., Saupe, G., and Gardea-Torresdey, J. (2009) The biochemistry of environmental heavy metal uptake by plants: implications for the food chain. *Int. J. Biochem. Cell Biol.* 41 (8-9), 1665–1677.

Peris, M., Micó, C., Recatalá, L., Sánchez, R., and Sánchez, J. (2007) Heavy metal contents in horticultural crops of a representative area of the European Mediterranean region. *Sci. Total Environ.* 378 (1-2), 42–48.

Petkovšek, S. A. S., and Pokorny, B. (2013) Lead and cadmium in mushrooms from the vicinity of two large emission sources in Slovenia. *Sci. Total Environ.* 443, 944–954.

Pinho F. (2011) Cytotoxic and genotoxic effects of cadmium in human osteoblasts. Master thesis, Master of Applied Biology, University of Aveiro. Available from: ria.ua.pt/handle/10773/8061 (accessed Jun, 2014)

Pinto, D., Fernandes, A., Fernandes, R., Mendes I, Pereira S, Vinha, A., Herdeiro, T., Santos, E., and Machado, M. (2011) Determination of heavy metals and other indicators in waters, soils and medicinal plants from Ave valley, in Portugal, and its correlation to urban and industrial pollution. In: Méndez-Vilas A, editor. Science against microbial pathogens: communicating current research and technological advances. Badajoz, Spain: FORMATEX. pp 303–309.

Pinto T. (2011) Evaluation of cadmium induced cytotoxicity in osteosarcoma cell line. Master thesis, Master of Applied Biology, University of Aveiro. Available from: ria.ua.pt/handle/10773/8040 (accessed Jun, 2014)

Portuguese Environment Agency. (2012) Relatório de actividades da EP Solo e Sedimentos 2009-2011. Lisbon. pp 120.

Raghunathan, V.K., Tettey, J. N. A., Ellis, E. M., and Grant, M. H. (2009) Comparative chronic *in vitro* toxicity of hexavalent chromium to osteoblasts and monocytes. *J. Biomed. Mater. Res. A.* 88 (2), 543–550.

Regaldo, L., Gagneten, A. M., and Troiani, H. (2009) Accumulation of chromium and interaction with other elements in *Chlorella vulgaris* (Cloroficeae) and *Daphnia magna* (Crustacea, Cladocera). *J. Environ. Biol.* 30 (2), 213–216.

Rodrigues, S. M., Cruz, N., Coelho, C., Henriques, B., Carvalho, L., Duarte, A.C., Pereira, E., and Römkens, P. F. A. M. (2013) Risk assessment for Cd, Cu, Pb and Zn in urban soils: chemical availability as the central concept. *Environ. Pollut.* 183, 234–242.

Rodriguez, E., Azevedo, R., Fernandes, P., and Santos, C. (2011) Cr(VI) induces DNA damage, cell cycle arrest and polyploidization: a flow cytometric and comet assay study in *Pisum sativum*. *Chem. Res. Toxicol.* 24 (7):1040–1047.

Rodriguez, E., Azevedo, R., Remédios, C., Almeida, T., Fernandes, P., and Santos, C. (2013) Exposure to Cr(VI) induces organ dependent MSI in two loci related with photophosphorylation and with glutamine metabolism. *J. Plant Physiol.* 170 (5), 534–538.

Rodriguez, E., Santos, C., Azevedo, R., Moutinho-Pereira, J., Correia, C., and Dias, M. C. (2012) Chromium (VI) induces toxicity at different photosynthetic levels in pea. *Plant Physiol. Biochem.* 53, 94–100.

Rodríguez-Serrano, M., Romero-Puertas, M. C., Pazmiño, D. M., Testillano, P. S., Risueño, M. C., del Río, L. A., and Sandalio, L. M. (2009) Cellular response of pea plants to cadmium toxicity: cross talk between reactive oxygen species, nitric oxide, and calcium. *Plant Physiol.* 150 (1), 229–243.

Rogival, D., Scheirs, J., and Blust, R. (2007) Transfer and accumulation of metals in a soil-diet-wood mouse food chain along a metal pollution gradient. *Environ. Pollut.* 145 (2), 516–528.

Romero, K. D., Coonse, K. G., Coonts, A. J., Morrison, E. V., and Heggland, S. J. (2005) The effects of cadmium on apoptosis in cultured human osteosarcoma cells. *J. Idaho Academy Sci.* Idaho Academy of Science, publisher. Available from: www.freepatentsonline.com/article/Journal-Idaho-Academy-Science/138949204.html (accessed Sep, 2013)

Russell, W. M. S., and Burch, R. L. (1959) The principles of humane experimental technique. London UK: Methuen, publisher.

Sabolić, I., Breljak, D., Skarica, M., and Herak-Kramberger, C. M. (2010) Role of metallothionein in cadmium traffic and toxicity in kidneys and other mammalian organs. *Biometals.* 23 (5), 897–926.

Sampson, B., and Hart, A. (2012) Clinical usefulness of blood metal measurements to assess the failure of metal-on-metal hip implants. *Ann. Clin. Biochem.* 49 (Pt2), 118-131.

Sanità di Toppi, L., and Gabbrielli, R. (1999) Response to cadmium in higher plants. *Environ. Exp. Bot.* 41 (2), 105–130.

Santos, C., and Rodriguez, E. (2012) Review on some emerging endpoints of chromium (VI) and lead phytotoxicity. Chapter 3. In: Mworia, J. K., editor. Botany. InTech, publisher. pp 61–82.

Sarkar, A., Ravindran, G., and Krishnamurthy, V. (2013) A brief review on the effect of cadmium toxicity: from cellular to organ level. *Int. J. Bio-Technology Res.* 3 (1), 17–36.

Scheifler, R., Gomot-de Vaufleury, A., and Badot, P. M. (2002) Transfer of cadmium from plant leaves and vegetable flour to the snail *Helix aspersa*: bioaccumulation and effects. *Ecotoxicol. Environ. Saf.* 53 (1), 148–153.

Schwartz, Z., Lohmann, C. H., Oefinger, J., Bonewald, L. F., Dean, D. D., and Boyan, B. D. (1999) Implant surface characteristics modulate differentiation behavior of cells in the osteoblastic lineage. *Adv. Dent. Res.* 13 (1), 38–48.

Seebaugh, D. R., and Wallace, W. G. (2004) Importance of metal-binding proteins in the partitioning of Cd and Zn as trophically available metal (TAM) in the brine shrimp *Artemia franciscana*. *Mar. Ecol. Prog. Ser.* 272, 215–230.

Seth, C. S., Misra, V., Chauhan, L. K. S., and Singh, R. R. (2008) Genotoxicity of cadmium on root meristem cells of *Allium cepa*: cytogenetic and Comet assay approach. *Ecotoxicol. Environ. Saf.* 71 (3), 711–716.

Shanker, A. K., Cervantes, C., Loza-Tavera, H., and Avudainayagam, S. (2005) Chromium toxicity in plants. *Environ. Int.* 31 (5), 739–753.

Shanker, A. K., and Pathmanabhan, G. (2004) Speciation dependant antioxidative response in roots and leaves of sorghum (*Sorghum bicolor* (L.) Moench cv CO 27) under Cr (III) and Cr (VI) stress. *Plant Soil.* 265 (1), 141–151.

Sharma, D. C., Sharma, C. P., and Tripathi, R. D. (2003) Phytotoxic lesions of chromium in maize. *Chemosphere*. 51 (1), 63–68.

Shin, M., Paek, D., and Yoon, C. (2011) The relationship between the bone mineral density and urinary cadmium concentration of residents in an industrial complex. *Environ. Res.* 111 (1), 101–109.

Song, Y., Wang, T., Pu, J., Guo, J., Chen, Z., Wang, Y., and Jia, G. (2014) Multi-element distribution profile in Sprague-Dawley rats: effects of intratracheal instillation of Cr(VI) and Zn intervention. *Toxicol. Lett.* 226 (2), 198–205.

Song, Y., Zhang, J., Yu, S., Wang, T., Cui, X., Du, X., and Jia, G. (2012) Effects of chronic chromium(VI) exposure on blood element homeostasis: an epidemiological study. *Metallomics.* 4 (5), 463–472.

Souguir, D., Ferjani, E., Ledoigt, G., and Goupil, P. (2010) Sequential effects of cadmium on genotoxicity and lipoperoxidation in *Vicia faba* roots. *Ecotoxicology.* 20 (2), 329–336.

Tête, N., Durfort, M., Rieffel, D., Scheifler, R., and Sánchez-Chardi, A. (2014) Histopathology related to cadmium and lead bioaccumulation in chronically exposed wood mice, *Apodemus sylvaticus*, around a former smelter. *Sci. Total Environ.* 481, 167–177.

Wallace, W. G., and Luoma, S. N. (2003) Subcellular compartmentalization of Cd and Zn in two bivalves. II. Significance of trophically available metal (TAM). *Mar. Ecol. Prog. Ser.* 257, 125–137.

Wallace, W. G., and Lopez, G. R. (1997) Bioavailability of biologically sequestered cadmium and the implications of metal detoxification. *Mar. Ecol. Prog. Ser.* 147 (1-3), 149–157.

Wilbur, S., Abadin, H., Fay, M., Yu, D., Tencza, B., Ingerman, L., Klotzbach, J., and James, S. (2012) Toxicological profile for chromium. Atlanta (GA). Agency for Toxic Substances and Disease Registry (US). Available from: http://www.ncbi.nlm.nih.gov/books/NBK158855/ (accessed Jan, 2014).

Wu, L., Yi, H., and Yi, M. (2010) Assessment of arsenic toxicity using *Allium*/*Vicia* root tip micronucleus assays. *J. Hazard. Mater.* 176 (1-3), 952–956.

Yang, Z., and Chu, C. (2011) Towards understanding plant response to heavy metal stress. Chapter 4. In: Shanker, A., editor. Abiotic stress plants – mechanisms and adaptations. InTech, publisher. pp 59–78.

Zayed, A. M., and Terry, N. (2003) Chromium in the environment: factors affecting biological remediation. *Plant Soil.* 249 (1), 139–156.

Zendehdel, R., Shetab-Boushehri, S. V., Azari, M. R., Hosseini, V., and Mohammadi, H. (2014) Chemometrics models for assessment of oxidative stress risk in chrome-electroplating workers. *Drug Chem. Toxicol.* 1–6. [Epub ahead of print].

Zheng, N., Wang, Q., and Zheng, D. (2007) Health risk of Hg, Pb, Cd, Zn, and Cu to the inhabitants around Huludao Zinc Plant in China via consumption of vegetables. *Sci. Total Environ.* 383 (1-3), 81–89.

Zhitkovich, A. (2005) Importance of chromium-DNA adducts in mutagenicity and toxicity of chromium(VI). *Chem. Res. Toxicol.* 18 (1), 3–11.

Zhitkovich, A. (2011) Chromium in drinking water: sources, metabolism, and cancer risks. *Chem. Res. Toxicol.* 24 (10), 1617–1629.

CHAPTER 2 – CHROMIUM AND CADMIUM CYTO- AND GENOTOXICITY IN PLANTS

Chapter 2.1 – Chromium-induced cyto- and genotoxicity in lettuce

Cristina Monteiro, Maria Celeste Dias, Helena Oliveira, Conceição Santos

Department of Biology and CESAM, Laboratory of Biotechnology and Cytomics, University of Aveiro

Results presented in this chapter integrate papers submitted/published to international journal(s).

Abstract

The extensive use of Cr compounds in industry and its unregulated disposal in soil and ground water result in significant adverse biological and ecological effects for the environment. Little is known about Cr^{3+} effects in plants, but Cr^{6+} even at very low concentrations can be toxic. This work aims to compare the effects of Cr^{3+} and Cr^{6+} (up to 300 ppm) in lettuce after 30 days of exposure, regarding plant growth and cytogenotoxicity (cell cycle, MN, and mitotic aberrations). The results showed that both Cr forms led to Cr accumulation in a dose-dependent manner. Plant growth decreased in plants exposed to Cr^{6+}. Moreover, neither Cr^{3+} nor Cr^{6+} concentrations disturbed cell cycle progression in lettuce. However, 300 ppm Cr^{6+} induced cytogenotoxic effects in roots including formation of MN and mitotic aberrations. As the high levels of toxicity were observed on Cr^{6+}-exposed plants comparatively to Cr^{3+} that showed to be nontoxic, DNA damage and oxidative stress biomarkers were assessed in Cr^{6+}-exposed plants. An increase of DNA damage with increasing Cr^{6+} concentrations was observed only in leaves. Antioxidant enzyme (APX, POX, CAT, GR, and SOD) activities showed different profiles dependent on the concentration of Cr^{6+} and on the organ of lettuce. In this comparative study, we demonstrate that Cr^{6+} was the toxic valence of Cr to lettuce, and it led to higher levels of Cr accumulation compared to Cr^{3+}. Finally, Cr^{6+} showed cyto- and genotoxic effects that were not observed in Cr^{3+}-exposed plants.

Keywords

Chromium, DNA damage, lettuce, micronuclei, mitotic aberrations, oxidative stress

Introduction

Heavy metal contamination of soil caused by anthropogenic activities has become a worldwide problem due to the potential health impacts of consuming contaminated products (Schützendübel and Polle 2002). Besides its natural occurrence, in particular the extensive use of Cr compounds in industries such as pigment textile, leather tanning, stainless steel production, wood preservation, Cr chemicals production, pulp and paper production, mines, and its unregulated disposal in soil and ground water results in significant adverse biological and ecological effects for the environment (Zayed and Terry 2003; Brien et al. 2005; Shanker et al. 2005). Chromium occurs in various oxidation states (Cr, Cr^{2+}, Cr^{3+}, Cr^{4+}, Cr^{5+} and Cr^{6+}), but the most stable forms are Cr^{3+} and Cr^{6+} (Zayed and Terry 2003). These forms differ in terms of their mobility, bioavailability and toxicity (Panda and Choudhury 2005). Cr^{3+} is essential in human and animal diet, and insufficient human dietary intake has been largely reported (reviewed by Pechova and Pavlata (2007)). In plants it was demonstrated that low Cr^{3+} concentrations enhanced growth (Zayed and Terry 2003; Peralta-Videa et al. 2009), however there is still doubt about an essential role of Cr in plant metabolism (Sharma et al. 2003; Zayed and Terry 2003). At high concentrations, Cr^{3+} may inhibit plant growth, and in humans it may decrease immune system activity (Gardea-Torresdey et al. 2005). Cr^{6+} usually occurs associated with oxygen as chromate (CrO_4^{2-}) or dichromate ($Cr_2O_7^{2-}$) oxyanions (Shanker et al. 2005). The hexavalent form is mutagenic (Zhitkovich 2011) and is classified as a highly toxic/and human carcinogenic by the International Agency for Research on Cancer (IARC 1990), even at very low concentrations (Zhitkovich 2011). However, its effects are highly dependent on the type/solubility of Cr compound (eg., $PbCr(O_4)$, $ZnCr(O_4)$, $CaCr(O_4)$ or $K_2Cr(O_4)$), probably because the most soluble forms hardly reach high local concentrations in tissues/cells (O'Brien 2003).

In plants, differential toxicity of Cr has been reported (e.g., Gardea-Torresdey et al. 2005), wherein the hexavalent chromium has been found to be more toxic, more soluble and more mobile than the trivalent form (Panda and Choudhury 2005). Consequently, some hypotheses were proposed to justify the higher toxicity of Cr^{6+} in plants: it penetrates better the cell wall, it has better capacity of competing with other nutrients, it induces a stronger oxidative stress response, and it induces more damages in cell membrane (Zayed and Terry 2003; Shanker et al. 2005). However, these hypotheses are based on isolated studies involving different Cr compounds. The exposure of plants to Cr interferes with several

metabolic processes, causing toxicity, which results in a reduction and inhibition of plant growth, foliar chlorosis, impaired photosynthesis, wilting, root injury and finally plant death (e.g., Vajpayee et al. 2000; Vernay et al. 2007; Yu et al. 2007; Scoccianti et al. 2008; Oliveira 2012; Rodriguez et al. 2012; Singh et al. 2013). Chromium is an oxidant agent and is responsible for production of ROS: O_2^-, $^1O_2$, OH^-, H_2O_2 (Zayed and Terry 2003). Consequently, this metal causes oxidative stress which damages biomolecules such as lipids, proteins, pigments and nucleic acids (e.g., Vernay et al. 2007; Zou et al. 2009; Ozdener et al. 2001; Rodriguez et al. 2011; Adki et al. 2013; Patnaik et al. 2013), it changes the activities of antioxidant enzymes and others enzymes such as nitrate reductase and RNase (e.g., Sharma et al. 2003; Rai 2004; Shanker and Pathmanaabhan 2004; Maiti et al. 2012; Adki et al. 2013), and may alter plant water status (Vernay et al. 2007; Singh et al. 2013).

In addition, an adequate antioxidant defense system requires efficient scavenging of ROS. Among these mechanisms of defense, there are antioxidant metabolites (e.g., Asc, GSH, tocopherol) and antioxidant enzymes capable of neutralizing free radicals and may reduce or even help to prevent some of the potential damage (Shanker et al. 2005). SOD is an antioxidant enzyme that converts the strong oxidant O_2^- radicals into H_2O_2 and water, and the accumulation of H_2O_2 is prevented in the cell by reduction to water through the actions of either CAT, POX using guaiacol as substrate, or APX (Apel and Hirt, 2004; Singh et al. 2013). Several enzymes are involved in the reduction and oxidation of antioxidant biomolecules, such as Asc and GSH. Among these enzymes, APX catalyses Asc oxidation to DHA while GR reduces GSSG with help of NAD(P)H (Smirnoff 1996; Smirnoff 2000; Singh et al. 2013).

The present study focuses on the comparative effects of Cr^{3+} *vs* Cr^{6+} on plant growth, cell cycle disturbances and presence of MN, and mitotic aberrations of lettuce (*L. sativa* L. cv. Povoa). As data support that Cr^{6+} was more toxic, then the effects of Cr^{6+} on the antioxidant capacity (i.e., SOD, POX, APX, CAT and GR activities) of Cr^{6+}-exposed plants were analyzed. These analyses were done in both roots and leaves as Cr^{6+} may accumulate differently in roots and leaves, therefore it could lead to different organ responses (Zayed et al. 1998; Oliveira 2012; Singh et al. 2013). Lettuce was chosen for this study since it is a recommended plant for standard toxicity tests (OECD 2006), and because it is one of the most consumed leafy vegetables in the human dietary.

Materials and methods

Plant culture and growth conditions

L. sativa L. cv. Povoa seeds were germinated in H_2O in the dark, and seedlings were then grown in plastic pots (350 cm^3) filled with a soil mixture of peat and vermiculite [1:3 (v/v)]. The greenhouse conditions were photon flux density of 430 $\mu molm^{-2}s^{-1}$, photoperiod of 16h/8h (light/dark), and a temperature of 23 ± 2 ºC. During the first 15 days of the assay normal growth conditions were applied, watering plants twice a week with 15 mL of ½ strength Hoagland's nutrient solution (pH 5.8). During the following 30 days, plants were watered twice a week with 15 mL of ½ strength Hoagland's nutrient solution (pH 5.8), and once a week with 50, 150, 200 and 300 mg/L Cr^{6+} solution (K_2CrO_4), or with 50, and 300 mg/L Cr^{3+} solution ($CrCl_3.6H_2O$). Plants without addition of Cr solution served as control.

Before all subsequent procedures, plant roots were washed in a 5% $Ca(NO_3)_2$ solution to remove Cr adsorbed to the surface, and then washed in distilled water. Fresh leaves and roots were used for the analyses, with the exception of the measurement of antioxidant enzyme activities, where fresh roots and leaves were immersed in liquid nitrogen and kept at -80 ºC until further analyzes.

General toxicity and measurement of plant growth

At the end of Cr exposure, visible symptoms of toxicity like presence or absence of e.g., chlorosis, red color of leaves, necrotic spots and plant death, were recorded.

The length of plants was used as a measure of plant growth.

Total Cr content

For total Cr quantification, fresh roots and leaves of plants exposed to Cr^{6+} or Cr^{3+} were dried at 60 ºC, and then treated according to Evers and Bücking (1976) for Cr content analyzis by ICP-AES (Jobin Ivon JY70 Plus).

Flow cytometric analysis

Changes in cell cycle progression were evaluated in both roots and leaves by FCM, according to Rodriguez et al. (2011). Briefly, nuclei suspensions were obtained by fine chopping in WPB, containing 0.2 M Tris-HCl, 4 mM $MgCl_2$, 2 mM EDTA, 86 mM NaCl, 10 mM sodium metabisulfite, 1% PVP-10, 1% (v/v) Triton X-100, pH 7.5 (Loureiro et al. 2007), and then filtered through a 55 µm nylon mesh. To the nucleus suspensions, 50 µg mL^{-1} PI and 50 µg mL^{-1} RNase were added. At least 5000 nuclei were analyzed per sample in a flow cytometer (EPICS-XL Coulter Electronics, USA) equipped with an argon laser (15 mW, 488 nm). The results were acquired using the SYSTEM II software (v. 3.0, Beckman Coulter®). The G_0/G_1 fluorescence peak of sample nuclei was adjusted to channel 200. The nucleus populations in the phases G_0/G_1, S, and G_2 and changes in cell cycle progression were analyzed to assess putative Cr mitogenic/cytostatic effects.

Micronuclei

The procedure of MN assay was done according to the previous work of our group (Monteiro et al. 2012, see Chapter 2.2). Meristematic tissues from roots of control, and Cr^{3+} or Cr^{6+}-exposed (50, and 300 ppm) plants were collected and stained with PI. Slide preparations were observed under 1000x magnification using a fluorescence microscope (Nikon Eclipse 80i) with an excitation filter of 510-560 nm and a barrier filter of 590 nm. To calculate the frequency of MN, a total of 200 cells were scored from three plants, per Cr concentration. The criteria of Fenech (2006) for identifying MN were followed. Images were captured with NIS-Elements F 3.00, SP7 software.

Mitotic aberrations

Meristematic tissues from roots of control, and Cr^{3+} or Cr^{6+}-exposed (50, and 300 ppm) plants were collected and stained with a solution containing 2% acetic orcein with 2 N HCl. Samples were then fixed by heat, and observed under light microscopy (Nikon Eclipse 80i). Images were captured with NIS-Elements F 3.00, SP7 software.

Comet assay

As Cr^{6+} showed to be more toxic than Cr^{3+} in the previous analyses, the procedure for DNA damage assessment was done only for this Cr valence.

DNA damage was measured performing the comet assay as described by Gichner et al. (2004) with slight modifications. Leaves and roots from control, and Cr^{6+}-exposed (50, 150, and 300 ppm) plants were sliced in cold 0.4 M Tris buffer (pH 7.5), and the isolated nucleoids were collected in the buffer. A mixture of 50 µL of the nucleoids suspension and 50 µL of 1% LMPA was spread on each slide covered with a layer of 1% NMPA. The slides were immersed in an alkaline buffer (0.30 M NaOH and 1 mM EDTA, pH>13) for DNA unwinding (15 min) and electrophoresis at 0.74 V cm^{-1} and 300 mA for 30 min at 4 ºC. Slides were then neutralized with 0.4 M Tris buffer (pH 7.5) and washed with water. Nucleoids were stained with ethidium bromide and examined using a fluorescence microscope (Nikon Eclipse 80i) equipped with an excitation filter of 510-560 nm and a barrier filter of 590 nm. Images were captured with NIS-Elements F 3.00, SP7 software. The parameter % tail DNA was calculated using image analysis software (CASPLAB v1.2.2).

Antioxidant enzyme activities

As Cr^{6+} showed to be toxic and Cr^{3+} non toxic in the previous analyses, further assays to assess antioxidant enzyme activities were done only with hexavalent Cr form.

Antioxidant enzyme activities were estimated after 30 days of plant exposure to the Cr^{6+} concentrations (50, 150, 200, and 300 ppm). Frozen samples of leaves and roots were ground to a powder in a mortar and pestle using liquid nitrogen. The powder was homogenized according to Ali et al. (2005) with slight modifications. The following procedure was carried out at 4 ºC. The homogenization occurred in 0.1 M potassium phosphate buffer (pH 7.8) containing 5 mM Na_2EDTA, 1% PVP and 0.2% (v/v) Triton X-100. Homogenates were squeezed through four layers of muslin and centrifuged in a refrigerated centrifuge at 8000*g* for 15 min. Supernatants obtained were used for enzyme assays (POX, CAT, APX, SOD and GR) and total soluble protein quantification. Protein concentration was determined according to the method of Bradford (1976) using the Total Protein Kit, Micro (Sigma-Aldrich, USA).

APX activity was determined at 25 ºC by recording the decrease in absorbance at 290 nm due to Asc ($\varepsilon = 2.8\ mM^{-1}cm^{-1}$) oxidation to DHA by H_2O_2, according to the method of Nakano and Asada (1981). The reaction mixture contained 100 mM potassium phosphate buffer (pH 7.0), 0.5 mM Asc, and an aliquot of enzyme extract and 0.5 mM H_2O_2 were added to start the reaction. One unit of APX activity was expressed as mmol Asc oxidized per minute.

POX activity was determined at 25 ºC following the Bergmeyer (1983) method, where the reaction mixture contained 96.5 mM potassium phosphate (pH 7.0), 0.3 mM guaiacol and enzyme extract. After starting the reaction with 0.12 mM H_2O_2, it was monitored the increase in absorbance at 436 nm resulting from the decomposition of H_2O_2 using guaiacol as hydrogen donor, leading to tetraguaiacol ($\varepsilon = 25.5\ mM^{-1}cm^{-1}$).

CAT activity was assayed at 25 ºC as described by Beers and Sizer (1952). Assay mixture contained 0.1 M potassium phosphate buffer (pH 7.0) and enzyme extract. To start the reaction, 20 mM H_2O_2 ($\varepsilon = 39.4\ mM^{-1}cm^{-1}$) was added and decrease of absorbance at 240 nm was recorded.

SOD activity was assayed at 25 ºC by monitoring the decrease of absorbance at 560 nm generated by the inhibition of the reduction of NBT following the method of Agarwal et al. (2005). The reaction mixture contained 13.3 mM methionine, 63 µM NBT, 0.1 mM EDTA, 50 mM potassium phosphate buffer (pH 7.8), 50 mM Na_2CO_3 and an aliquot of extract. Reaction was started by adding 2 µM riboflavin and placing the tubes under a fluorescent lamp (15 W) for 15 min. As control it was used a reaction mixture without the extract. To stop the reaction, the light was switched off and the tubes were maintained in the dark. For enzymatic and control assays a non-irradiated correspondent reaction mixture, with or without extract respectively, was used as blank. One unit of SOD activity was defined as the amount of enzyme required to cause 50 % inhibition of the reduction of NBT in comparison with control.

GR activity was determined at 30 ºC according to Sgherri et al. (1994). The reaction mixture contained 0.2 M potassium phosphate (pH 7.5), 0.2 mM Na_2EDTA, 1.5 mM $MgCl_2$, 0.25 mM GSSH, and enzyme extract. The reaction was started with 25 µM NADPH, and the

decrease in absorbance at 340 nm was monitored. The GR activity was calculated using the ε of NADPH (6.22 $mM^{-1}cm^{-1}$).

Statistical analysis

Results were expressed as the mean ± SD. Data were analyzed by one-way ANOVA ($p < 0.05$), followed by a Holm-Sidak test ($p < 0.05$) to evaluate the significance of differences in the parameters. When necessary, data were transformed to achieve normality and equality of variances. When these criteria were not verified, the non parametric test, Kruskal–Wallis one-way ANOVA by ranks, was done. All statistical analyses were performed using Sigma Plot 11.0 software (Systat Software Inc., Germany). The number of replicates (individuals) used for each parameter is provided in the corresponding figure.

Results and discussion

General toxicity and plant growth

At the end of exposure, some plants treated with 300 ppm Cr^{6+} presented leaves with reddish colored regions. This effect was not observed in plants exposed to lower Cr^{6+} concentrations nor in plants exposed to any Cr^{3+} concentrations nor in control plants. Also, it is noteworthy that none of the tested Cr conditions induced plant death.

Figure 7 shows how Cr^{3+} and Cr^{6+} affected plant growth, in terms of the length of roots and shoots. Overall roots had much higher length than shoots, independently of the condition. Also, Cr^{3+} did not induce significant difference in length of roots or shoots compared to the control (Figure 7A). Contrarily, Cr^{6+} decreased the length of both shoots and roots of all Cr^{6+}-exposed plants (Figure 7B). This effect was particularly significant to doses above 150 ppm, i.e. the toxic effects measured as the reduction of growth (length) were observed in both organs at the same doses of Cr^{6+}(≥ 200 ppm). Similar results were shown in other research comparing the effects of Cr^{3+} with Cr^{6+} in sorghum plants, although much higher Cr doses were applied (50 and 100 µM) and for 10 days: 50 µM Cr^{3+} did not induce plant growth inhibition nor oxidative stress, while the tested Cr^{6+} concentrations reduced plant growth and led to more cytotoxic effects, including increase of H_2O_2, activation of antioxidant enzymes (SOD, APX, GR, DHAR, MDHAR), occurrence of lipid peroxidation, and depletion of GSH (Shanker and Pathmanabhan 2004).

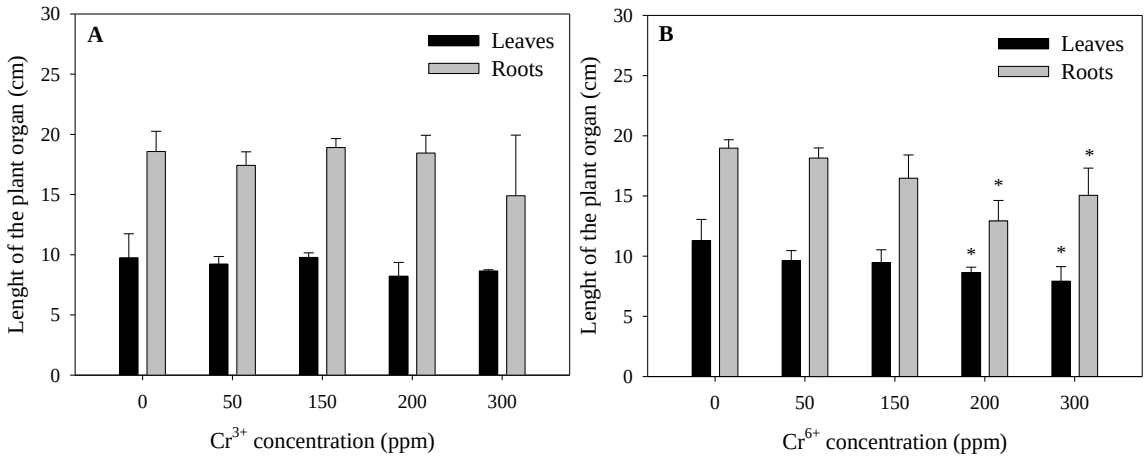

Figure 7. Cr^{3+} and Cr^{6+} effect on lettuce growth, in terms of the length of shoots and roots (n = 4). (A) Cr^{3+}. (B) Cr^{6+}. Symbol * represents significant difference relative to the control (roots: 200 ppm – $p < 0.05$, 300 ppm – $p < 0.001$; shoots: 2000 ppm – $p < 0.001$, 300 ppm – $p < 0.05$).

Contrarily to the absence of growth inhibition with Cr^{3+} in our study with lettuce, Shanker and Pathmanabhan (2004) observed that Cr^{3+} inhibited the root growth of sorghum at the dose of 100 µM (i.e., 26.6 ppm $CrCl_3.6H_2O$), a lower concentration than those used in our study and for only 10 days of exposure. Therefore, lettuce of our work was tolerant to Cr^{3+}, while sorghum of the assay performed by Shanker and Pathmanabhan (2004) showed

to be sensitive to this metal that caused toxicity effects, even at lower Cr^{3+} concentrations and less time of exposure.

These overall growth and morphological data indicate that, in terms of survival, both Cr valences at the concentrations tested were tolerated by the used lettuce cultivar.

Total Cr content

Figure 8 shows that Cr^{3+} and Cr^{6+} were absorbed by lettuce and accumulated in plant organs in a dose-dependent manner. The level of Cr^{3+} accumulation (Figure 8A), in both roots and shoots, was much lower than that observed in plants exposed to Cr^{6+} (Figure 8B).

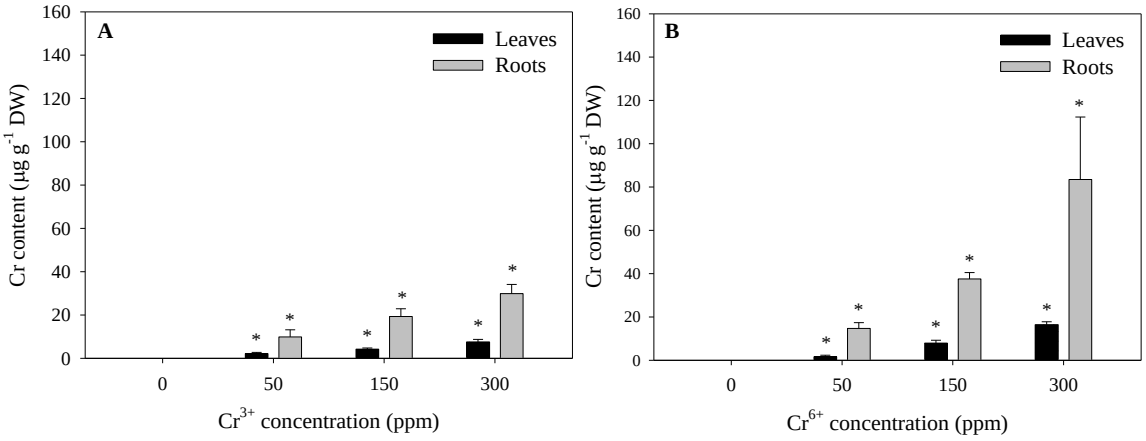

Figure 8. Cr accumulation in roots and leaves of lettuce exposed to Cr^{3+} (A), or Cr^{6+} (B) (n = 3). Symbol * represents significant difference relative to the control (roots: $p < 0.05$; leaves: $p < 0.001$).

All conditions of Cr exposure led to higher Cr content in roots than in leaves. This result was also observed by Paiva et al. (2009) who showed that the uptake of both Cr^{3+} and Cr^{6+} in water hyacinth, led to Cr accumulation preferably in roots. In the same work the authors found that Cr^{6+} was more translocated to leaves compared to Cr^{3+} (Paiva et al. 2009). In our research, similar levels of metal translocation from roots to leaves were obtained (translocation factor = 0.2) in plants exposed to Cr^{3+} or Cr^{6+}, with the exception of plants exposed to 50 ppm Cr^{6+} that had lower translocation rates of Cr to leaves (translocation factor = 0.1). From data, it is inferred that, as expected, Cr mostly accumulated in roots, though, as seen in other studies, the higher doses of Cr^{6+} affected photosynthetic activity (Dias et al.

2015, personal communication). Less translocation from roots to shoots may be due to a possible increased synthesis of MT that can bind to Cr (Shanker and Pathmanabhan 2004), and/or due to Cr^{6+} sequestration in vacuoles of root cells, where the ions are reduced to Cr^{3+} (Shanker et al. 2005), preventing higher levels of Cr^{6+} translocation from roots to leaves.

Flow cytometric analysis

Flow cytometric analysis showed typical cell cycle phases distributions, for control organs, compared with our previous studies with this species (e.g., Monteiro et al. 2012; see Chapter 2.2): there is a predominance of cells in G_0/G_1, and due to the preferential use of apical regions in the root samples, often root histograms presented higher frequency of cells in S and/or G_2 than leaves, as observed in our study (Figure 9). In general, Cr^{3+} and Cr^{6+}-exposed leaves and roots showed a similar profile between each other and between the exposed plants and the respective controls, supporting that none of the tested Cr valences induced changes in the dynamics of the cell cycle (no cytostatic nor mitogenic effects were observed, because no significant changes were observed in the percentage of cells in each phase). Also, histograms show clear diploid profiles (similar to the histograms shown in Chapter 2.2), not being observed any euploidy or aneuploidy aberration. Similarly to Cr^{3+}, plants exposed to Cr^{6+} concentrations did not induce aneuploidy or euploidy changes, nor cell cycle disturbances in either leaves or roots of lettuce exposed for 30 days, with regard to control organs.

Flow cytometric analysis allows determination of different events in the cell, including changes in the cell cycle, or alterations in the ploidy level (aneuploidy or euploidy), and even clastogenicity. From the present results, and similarly to other species, we found that neither Cr^{6+} nor Cr^{3+} induced changes in ploidy. For example, in pea plant it was observed that also high doses of Cr^{6+} did not induce ploidy anomalies (Rodriguez et al. 2011). Those authors found however, that higher Cr^{6+} doses in pea roots induced some changes in cell cycle dynamics (Rodriguez et al. 2011), while also inducing some point mutations (detected by microsatellites, Rodriguez et al. 2013) and clastogenicity (Rodriguez et al. 2011), not for the moment found in this lettuce cultivar.

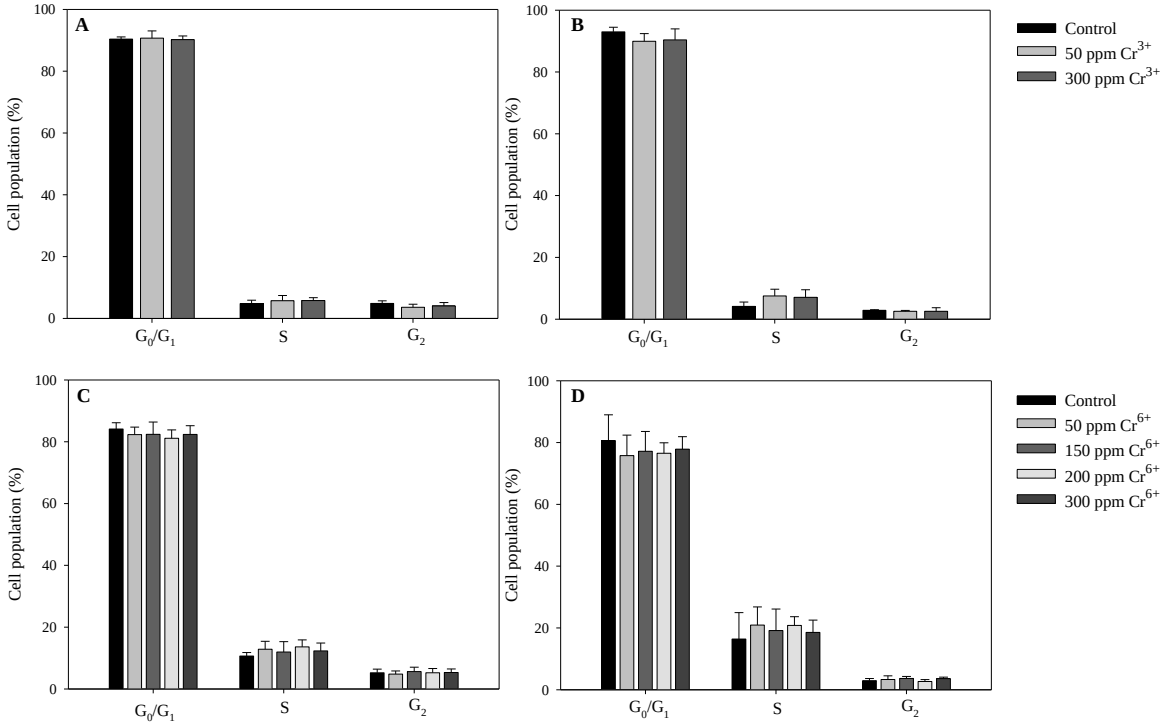

Figure 9. Cell cycle phases distribution in leaf and root cells from lettuce plants exposed to Cr^{3+} or Cr^{6+}, and control plants (n = 5). (A) Leaves of plants exposed to Cr^{3+}. (B) Roots of plants exposed to Cr^{3+}. (C) Leaves of plants exposed to Cr^{6+}. (D) Roots of plants exposed to Cr^{6+}. No significant differences were found between exposed and control plants ($p > 0.05$).

Mitotic aberrations and micronuclei

Regarding the analysis of the presence of mitotic aberrations and MN in root cells from lettuce it can be pointed that, no abnormal mitotic figures were observed in controls (Figure 10A), neither in any plants exposed to Cr^{3+}. Similarly, at the lowest dose of Cr^{6+}, 50 ppm, the metal did not induce visible abnormal mitotic figures. However, in the highest dose of Cr^{6+}, 300 ppm, it was possible to observe in roots the presence of putative abnormal mitotic figures, that may support abnormal disjunction of chromosomes, often associated with MN appearance (Figure 10B and C). Finally, these same roots also showed the formation of 3 ± 2 MN/200 cells (i.e., 15±10MN/1000 cells) (Figure 10D). However, more cytogenetic assays will be needed to confirm these putative abnormalities.

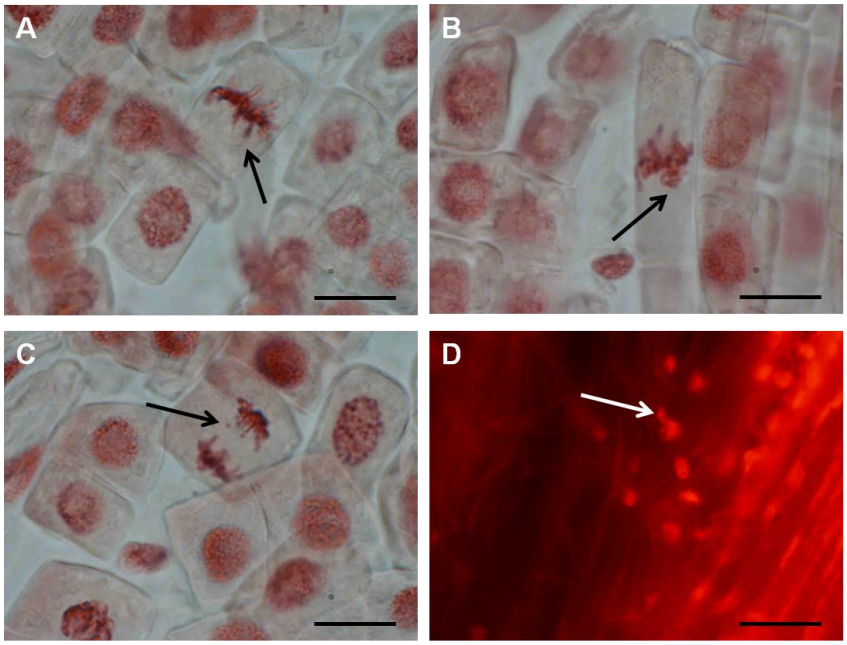

Figure 10. Mitotic aberrations and MN induced by 300 ppm Cr^{6+} in lettuce root cells. (A) Normal mitotic cell from control plants (metaphase). (B) Putative abnormal metaphase from an exposed plant. (C) Putative abnormal anaphase from an exposed plant showing some lagging chromosomes. (D) Cells from exposed plants showing the presence of a MN pointed by an arrow. (1000x; bar: 20 µm).

Other species were identified as having some genetic/mitotic sensitivity to Cr^{6+} as identified in *V. faba* with damages in mitotic index and chromosomal aberration (Chandra et al. 2004), as well as MN (Wang 1999). Also in *Tradescancia* sp. Knasmuller et al. (1998) identified MN formation in a Cr^{6+} dose-dependent manner. All these data support the results

obtained here, and that lettuce may be a good model species for this type of metal-related toxicity in mitotic disorders and MN formation.

Other species were identified as having some genetic sensitivity to Cr^{6+} as identified in *Brassica napus* (in doses similar to those used here for lettuce, which induced point mutations detected by AFLP, and DNA methylation) (Labra et al. 2004). Also Labra et al. (2003) detected DNA mutations by AFLP in *Arabidopsis taliana* induced by Cr^{6+}. So, in what concerns to lettuce, not only we demonstrate that Cr^{6+} induces genotoxicity in this species, using biomarkers also used for other species, but also that this may be an important species for genotoxicity studies.

DNA damage

The DNA damage was tested by the comet assay. Data showed that Cr^{6+} induced an increase of % tail DNA in leaves of lettuce subjected to 150 and 300 ppm Cr^{6+} for 30 days (Figure 11). However, in root cells exposed to the same Cr^{6+} doses, the exposure did not cause measureable DNA damage compared to the control (Figure 11).

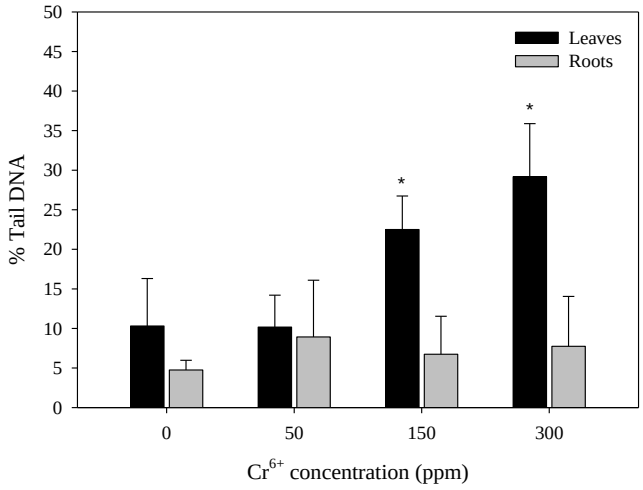

Figure 11. The average median % tail DNA of leaves and roots nuclei after 30 days of Cr^{6+} exposure of lettuce (n = 3). Symbol * represents significant difference relative to the control ($p < 0.05$).

These data can be explained by a possible existence of an adaptive mechanism in roots, with higher resistance of Cr in this organ (directly exposed to Cr) than in leaves, which may

be more sensitive to Cr exposure. For example, different mechanisms of accumulation and storage may be present in roots compared to leaves. The effect of Cr^{6+} on DNA damage was demonstrated in few studies, for example those of Koppen and Verschave (1996), who showed that $K_2Cr_2O_7$ (up to 10^{-3} M) induced DNA damage (using the comet assay) in *V. faba*. Cr^{6+} also induced DNA in other species as *P. sativum* (Rodriguez et al. 2011) and A. cepa (Patnaik et al. 2013). Similar results were already demonstrated in this thesis for Cr and other metals (e.g., Cd – Monteiro et al. 2012; see chapter 2.2).

The comet assay has been increasingly accepted as a simple, versatile and sensitive method to measure DSB/SSB and alkali-labile sites in cells under stress. However, as in mitotic disorders, further studies must proceed to confirm these results. Nevertheless, these data are in line with data of increased mitotic disorders and MN occurrence in the highest Cr^{6+} dose.

Antioxidant enzyme activities

Figure 12 shows how the antioxidant enzyme system in roots and leaves of lettuce was differently affected by Cr^{6+}. In general, under control conditions, the antioxidant enzyme system (APX, POX, GR, and SOD) is more expressed in leaves compared to roots. Antioxidant enzyme activities overall increased in Cr^{6+}-exposed plants compared to control ones at higher Cr^{6+} concentrations.

APX activity (Figure 12A) in control plants is about five times higher in leaves than roots. This enzyme activity showed a significant increase in leaves of plants exposed to Cr^{6+} concentrations above 150 ppm. In roots, APX activity decreased with the lowest Cr^{6+} concentration (50 ppm). At higher concentrations, and similar to that observed in leaves, there was an increase of APX activity in plants exposed to Cr^{6+} concentrations above 50 ppm, but the level of that increase in roots was lower than that observed in leaves. However, while the increase at the highest dose in leaves was twenty times higher than the values found for control, in roots this increase did not reach three times the value of the control. This result suggests that despite leaves uptake less Cr than roots, directly or indirectly, this exposure to Cr^{6+} increases the activity of APX in leaves.

POX (Figure 12B) was also more active in leaves than roots, under control conditions. This enzyme activity showed a hormetic response as POX was inhibited in leaves of plants exposed to 50-200 ppm Cr^{6+}, while the enzyme activity then increased at the highest Cr^{6+} dose (300 ppm), but it was not significantly different from the control. In roots despite of an initial slight decrease in the lowest dose, at the concentrations of 200 and 300 ppm Cr^{6+} the activity of POX increased substantially, suggesting that roots and leaves had for this enzyme a profile of a hormetic response to Cr^{6+} exposure.

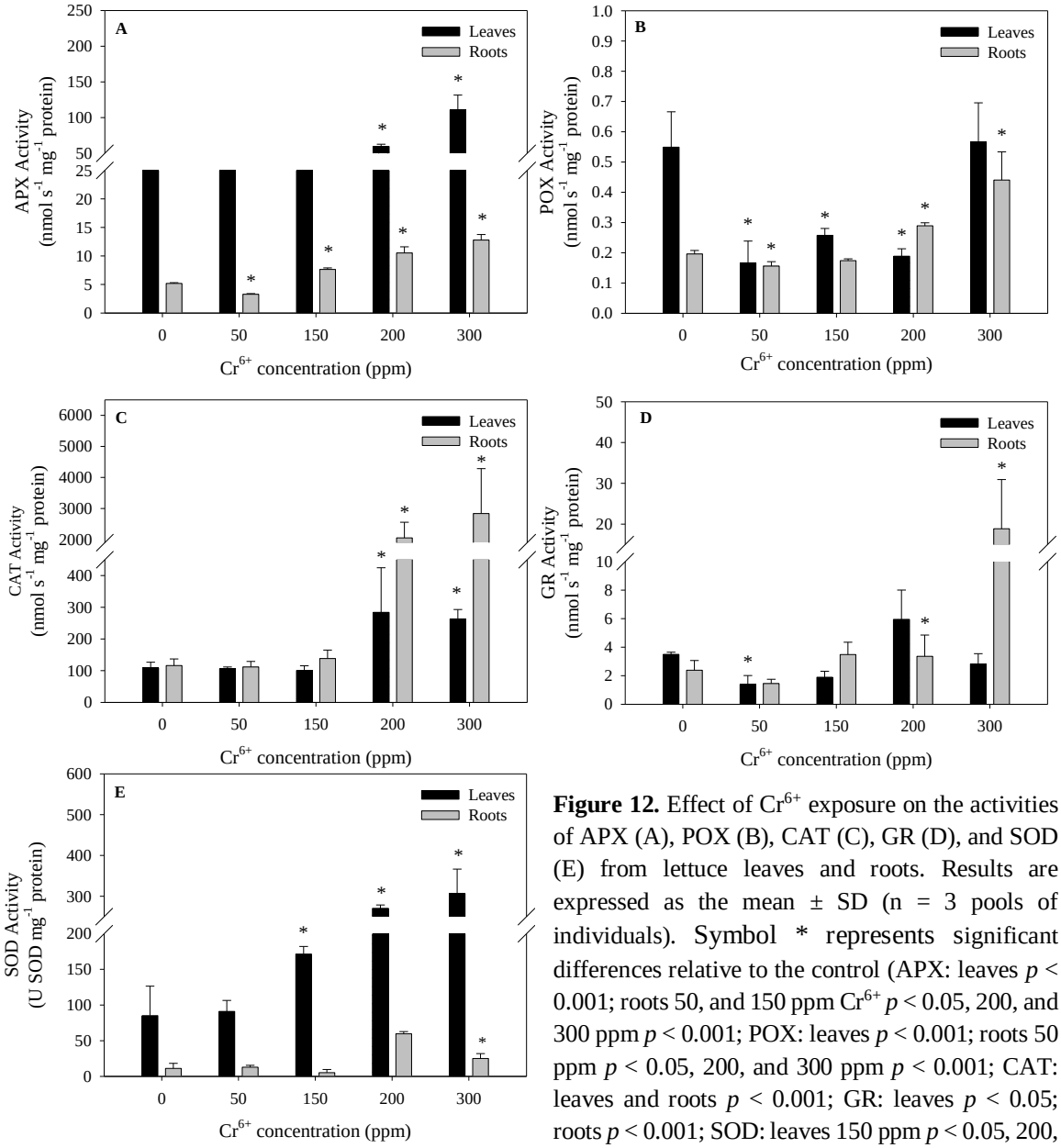

Figure 12. Effect of Cr^{6+} exposure on the activities of APX (A), POX (B), CAT (C), GR (D), and SOD (E) from lettuce leaves and roots. Results are expressed as the mean ± SD (n = 3 pools of individuals). Symbol * represents significant differences relative to the control (APX: leaves $p < 0.001$; roots 50, and 150 ppm Cr^{6+} $p < 0.05$, 200, and 300 ppm $p < 0.001$; POX: leaves $p < 0.001$; roots 50 ppm $p < 0.05$, 200, and 300 ppm $p < 0.001$; CAT: leaves and roots $p < 0.001$; GR: leaves $p < 0.05$; roots $p < 0.001$; SOD: leaves 150 ppm $p < 0.05$, 200, and 300 ppm $p < 0.001$; roots $p < 0.001$).

CAT activity (Figure 12C) increased in both leaves and roots of plants exposed to 200 and 300 ppm Cr^{6+}, and the incremental response was more evident in roots.

GR activity (Figure 12D) decreased in leaves of plants exposed to the lowest Cr^{6+} concentration (50 ppm), however in roots, GR activity increased in plants exposed to 200, and 300 ppm Cr^{6+}.

SOD activity (Figure 12E) showed a significant increase in both leaves and roots from plants exposed to Cr^{6+} concentrations above 50 ppm in leaves, and with 300 ppm Cr^{6+} in roots. The increase of SOD activity was far superior in leaves than in roots.

Data show that organs present different profiles of response to Cr^{6+} exposure. Briefly, most antioxidant enzymes in roots and leaves under moderate and/or high Cr-stress (> 50 ppm) seemed to be stimulated, meaning that different protective pathways may have been activated. In leaves POX and GR activities were repressed for the lowest Cr concentration and POX were still inhibited with the other Cr^{6+} doses. Such as in leaves, in roots there was the same profile of inhibition of activity only with the lowest Cr^{6+} concentration, not only in POX but also in APX. Although in leaves the overall antioxidant system was stimulated with Cr^{6+} at concentrations higher than 50 ppm, POX was inhibited and GR was not stimulated which may have been enough to lead to a hypothetic increase of ROS in leaves compared to roots, which may explain the DNA damage found in leaves and not in roots. However, more studies must be performed to verify this hypothesis.

It has been proposed by other authors that Cr-induced alteration of physiological activities in plants starts with malfunctioning of root physiology (e.g., Dhir et al. 2009), and may lead to impaired photosynthetic activities, disturbed water relations, or translocation of organic solutes (Panda 2007), and may also lead to point and gross mutations (Rodriguez et al. 2011; 2013). These processes may involve a first disturbance in the cell – oxidative stress. But the impact of oxidative stress on other events remains unclear. Wang et al. (2010) demonstrated that the uptake of Cr in excess induced oxidative stress by generation of ROS in levels that the cell cannot control. Plants under normal physiological status are able to balance internal ROS produced in different cellular compartments harboring electron transport chain (e.g., cell wall, apoplastic space, plasma membrane, chloroplast, mitochondria, etc). But the production of ROS beyond the capacity of cells may create

oxidative damage (Dhir et al. 2009). It was demonstrated for this and other species that Cr increased ROS and lipid peroxidation, a crucial consequence of ROS increase, which may have dramatic consequences on cell membrane.

The increase of peroxidase activity in plants exposed to Cr has been implicated as a detoxification of H_2O_2. Our results support previous earlier studies on upregulation of antioxidant enzymes under metal stress (Shanker et al. 2005), but this regulation is dependent on the organ. APX forms are present in cytosolic, chloroplastic, mitochondrial and other organelle environments and are reported to increase under various metal stresses (Hu et al. 2007), similarly to what was observed in roots, which supports an efficient defense system in roots to combat ROS formation, as SOD is the first line of ROS defense.

Conclusions

In conclusion, the effects that Cr^{3+} and Cr^{6+} induced in lettuce were shown, supporting the importance of the Cr valence in the toxicity of this metal. While Cr^{3+} was nontoxic to lettuce, Cr^{6+} showed to be toxic as it caused cytogenotoxicity (DNA damage, mitotic aberrations and MN) and oxidative stress. However, other relevant processes as cell cycle progress were not affected by the concentrations used. A distinct behavior between leaves and roots were also demonstrated, as despite leaves accumulate less Cr, some effects (namely DNA damage) were more dramatic in leaves. On the other hand some enzymes related with antioxidant system seemed to be inhibited or not stimulated by the stress in leaves. These data suggest that leaves had a more deficient antioxidant capacity than roots, but further studies will be needed to support this hypothesis.

References

Adki, V. S., Jadhav, J P., and Bapat, V. (2013) *Nopalea cochenillifera*, a potential chromium (VI) hyperaccumulator plant. *Environ. Sci. Pollut. Res. Int.* 20 (2), 1173–1180.

Agarwal, S., Sairam, R., Srivastava, G., and Meena, R. (2005) Changes in antioxidant enzymes activity and oxidative stress by abscisic acid and salicylic acid in wheat genotypes. *Biol. Planta.* 49 (4), 541−550.

Ali, M. B., Hahn, E.-J., and Paek, K.-Y. (2005) Effects of light intensities on antioxidant enzymes and malondialdehyde content during short-term acclimatization on micropropagated *Phalaenopsis* plantlet. *Environ. Exp. Bot.* 54, 109−120.

Apel, K., and Hirt, H. (2004) Reactive oxygen species: metabolism, oxidative stress, and signal transduction. *Annu. Rev. Plant Biol.* 55, 373–399.

Beers, R., and Sizer, I. (1952) A spectrophotometric method for measuring the breakdown of hydrogen peroxide by catalase. *J. Biol. Chem.* 195 (1), 133−140.

Bergmeyer, H. U. (1983) *Methods of enzymatic analysis: Vol. II, Samples, Reagents, Assessment of Results*, 3rd ed., p 268., Verlag Chemie, Weinheim, Germany.

Bradford, M. M. (1976) A rapid and sensitive method for the quantitation of microgram quantities of protein utilizing the principle of protein-dye binding. *Anal Biochem.*72, 248–254.

Brien, T. J. O., Brooks, B. R., and Patierno, S. R. (2005) Nucleotide excision repair functions in the removal of chromium-induced DNA damage in mammalian cells. *Mol. Cell. Biochem.* 279 (1), 85–95.

Chandra, S., Chauhan, L. K., Pande, P. N, Gupta, S. K. (2004) Cytogenetic effects of leachates from tannery solid waste on the somatic cells of *Vicia faba*. *Environ. Toxicol.* 19 (2), 129–934.

Dhir, B., Sharmila, P., Pardha, S. P., and Nasim, S. A (2009) Physiological and antioxidant responses of *Salvinia natans* exposed to chromium-rich wastewater. *Ecotoxicol. Environ. Saf.* 72 (6), 1790–1797.

Evers, F., and Bücking, K. (1976) Mineral analysis, In *Modern Methods in Forest Genetics*, Proceedings in Life Science, (Nitsche, J. P., Ed.) pp 165−188, Spriger-Verlag, Berlin, Germany.

Fenech, M. (2006) Cytokinesis-block micronucleus assay evolves into a “cytome” assay of chromosomal instability, mitotic dysfunction and cell death. *Mutat. Res.* 600 (1−2), 58−66.

Gardea-Torresdey, J. L., de la Rosa, G., Peralta-Videa, J. R., Montes, M., Cruz-Jimenez, G., and Cano-Aguilera, I. (2005) Differential uptake and transport of trivalent and hexavalent chromium by tumbleweed (*Salsola kali*). *Arch. Environ. Contam. Toxicol.* 48 (2), 225–232.

Gichner, T., Patková, Z., Száková, J., and Demnerová, K. (2004) Cadmium induces DNA damage in tobacco roots, but no DNA damage, somatic mutations or homologous recombination in tobacco leaves. *Mutat. Res.* 559 (1-2), 49−57.

Hu, C., Zhang, L., Hamilton, D., Zhou, W., Yang, T., and Zhu, D. (2007) Physiological responses induced by copper bioaccumulation in *Eichornia crassipes* (Mart.). *Hidrobiologia*. 579 (1), 211−218.

IARC (International Agency for Research on Cancer) (1990) Chromium, nickel and welding, *IARC monographs on the evaluation of carcinogenic risk of chemicals to humans*, Vol. 49, 49–214, International Agency for Research on Cancer, Lyon, France.

Knasmüller, S., Gottmann, E., Steinkellner, H., Fomin, A., Pickl, C., Paschke, A., Göd, R., and Kundi, M. (1998) Detection of genotoxic effects of heavy metal contaminated soils with plant bioassays. *Mutat. Res.* 420 (1-3), 37−48.

Koppen, G., and Verschaeve, L. (1996) The alkaline comet test on plant cells: a new genotoxicity test for DNA strand breaks in *Vicia faba* root cells. *Mutat. Res.* 360 (3), 193−200.

Labra, M., Di Fabio, T., Grassi, F., Regondi, G., Bracale, M., Vannini, C., Agradi, E. (2003) AFLP analyses as biomarker of exposure to organic and inorganic genotoxic substances in plants. *Chemosphere*. 52 (7), 1183–1188.

Labra, M., Grassi, F., Imazio, S., Di Fabio, T., Citterio, S., Sgorbati, S,, and Agradi. E. (2004) Genetic and DNA methylation changes induced by potassium dichromate in *Brassica napus*. *Chemosphere*. 54 (8), 1049–1058.

Loureiro, J., Rodriguez, E., Doležel., J., and Santos., C. (2007) Two new nuclear isolation buffers for plant DNA flow cytometry: a test with 37 species. *Ann. Bot.* 100 (4), 875-888.Maiti, S., Ghosh, N., Mandal, C., Das, K., and Dey, N. (2012) Responses of the maize plant to chromium stress with reference to antioxidation activity. *Braz. J. Plant Physiol.* 24 (3), 203–212.

Nakano, Y., and Asada, K. (1981) Hydrogen peroxide is scavenged by ascorbate specific-peroxidase in spinach chloroplasts. *Plant Cell Physiol.* 22 (5), 867−880.

O'Brien, T. R., Ceryak, S., and Patierno, S. R. (2003) Complexities of chromium carcinogenesis: role of cellular response, repair and recovery mechanisms. *Mutat. Res.-Fund. Mol. M.* 533 (1-2), 3–36.

OECD (Organization for Economic Co-operation and Development). (2006) OECD guidelines for the teseting ofchemicals. Terrestrial plant test: seedling emergence and seedling growth test. pp 208−221, OECD, Paris.

Oliveira, H. (2012) Chromium as an environmental pollutant: insights on induced plant toxicity. *J. Bot.* 2012, 375843, 8 pp.

Ozdener, Y., Aydin, B. K., Fatma, A. S., and Yürekli, F. (2011) Effect of hexavalent chromium on the growth and physiological and biochemical parameters on *Brassica oleracea* L. var. *acephala* DC. *Acta Biol. Hung.* 62 (4), 463–476.

Paiva, L. B., Gonçalves de Oliveira, J., Azevedo, R. A., Ribeiro, D. R., Gomes da Silva, M., and Vitória, A. P. (2009) Ecophysiological responses of water hyacinth exposed to Cr^{3+} and Cr^{6+}. *Environ. Exp. Bot.* 65 (2-3), 403–409.

Panda, S. K. (2007) Chromium-mediated oxidative stress and ultrastructural changes in root cells of developing rice seedlings. *J. Plant Physiol.* 164 (11), 1419–1428.

Panda, S. K., and Choudhury, S. (2005) Chromium stress in plants. *Braz. J. Plant Physiol.* 17 (1), 95–102.

Patnaik, A. R., Achary, V. M. M., and Panda, B.B. (2013) Chromium (VI)-induced hormesis and genotoxicity are mediated through oxidative stress in root cells of *Allium cepa* L. *Plant Growth Regul.* 71 (2), 157–170.

Pechova, A., and Pavlata, L. (2007) Chromium as an essential nutrient: a review. *Veterinarni Medicina.* 52, 2007 (1), 1–18.

Peralta-Videa, J. R., Lopez, M. L., Narayan, M., Saupe, G., and Gardea-Torresdey, J. (2009) The biochemistry of environmental heavy metal uptake by plants: implications for the food chain. *Int. J. Biochem. Cell Biol.* 41 (8-9), 1665–1677.

Rai, V. (2004) Effect of chromium accumulation on photosynthetic pigments, oxidative stress defense system, nitrate reduction, proline level and eugenol content of *Ocimum tenuiflorum* L. *Plant Sci*. 167 (5), 1159–1169.

Rodriguez, E., Azevedo, R., Fernandes, P., and Santos, C. (2011) Cr(VI) induces DNA damage, cell cycle arrest and polyploidization: a flow cytometric and comet assay study in *Pisum sativum*. *Chem. Res. Toxicol.* 24 (7), 1040–1047.

Rodriguez, E., Azevedo, R., Remédios, C., Almeida, T., Fernandes, P., and Santos, C. (2013) Exposure to Cr(VI) induces organ dependent MSI in two loci related with photophosphorylation and with glutamine metabolism. *J. Plant Physiol.* 170 (5), 534–538.

Rodriguez, E., Santos, C., Azevedo, R., Moutinho-Pereira, J., Correia, C., and Dias, M. C. (2012) Chromium (VI) induces toxicity at different photosynthetic levels in pea. *Plant Physiol. Biochem.* 53, 94–100.

Schützendübel, A., and Polle, A. (2002) Plant responses to abiotic stresses: heavy metal-induced oxidative stress and protection by mycorrhization. *J. Exp. Bot.* 53 (372), 1351–1365.

Scoccianti, V., Iacobucci, M., Paoletti, M. F., Fraternale, A., and Speranza, A. (2008) Species-dependent chromium accumulation, lipid peroxidation, and glutathione levels in germinating kiwifruit pollen under Cr(III) and Cr(VI) stress. *Chemosphere*. 73 (7), 1042–108.

Sgherri, C. L. M., Loggini, B., Puliga, S., and Navari-Izzo, F. (1994) Antioxidant system in Sporobolus stapfianus: changes in response to desiccation and rehydration. *Phytochemistry*. 35 (3), 561−565.

Shanker, A. K., Cervantes, C., Loza-Tavera, H., and Avudainayagam, S. (2005) Chromium toxicity in plants. *Environ. Int.* 31 (5), 739–753.

Shanker, A. K., and Pathmanabhan, G. (2004) Speciation dependant antioxidative response in roots and leaves of sorghum (*Sorghum bicolor* (L.) Moench cv CO 27) under Cr (III) and Cr (VI) stress. *Plant Soil.* 265 (1), 141–151.

Sharma, D. C., Sharma, C. P., and Tripathi, R. D. (2003) Phytotoxic lesions of chromium in maize. *Chemosphere*. 51 (1), 63–68.

Singh, H. P., Mahajan, P., Kaur, S., Batish, D. R., and Kohli, R. K. (2013) Chromium toxicity and tolerance in plants. *Environ. Chem. Lett.* 11 (3), 229-254.

Smirnoff, N. (1996) The function and metabolism of ascorbic acid in plants. *Ann. Bot.* 78 (6), 661–669.

Smirnoff, N. (2000) Ascorbate biosynthesis and function in photoprotection. *Philos. Trans. R. Soc. Lond. B Biol. Sci.* 355 (1402), 1455–1464.

Vajpayee, P., Tripathi, R. D., Rai, U. N., Ali, M. B., and Singh, S. N. (2000) Chromium (VI) accumulation reduces chlorophyll biosynthesis, nitrate reductase activity and protein content in *Nymphaea alba* L. *Plant Cell*. 41 (7), 1075–1082.

Vernay, P., Gauthier-Moussard, C., and Hitmi, A. (2007) Interaction of bioaccumulation of heavy metal chromium with water relation, mineral nutrition and photosynthesis in developed leaves of *Lolium perenne* L. *Chemosphere*. 68 (8), 1563–1575.

Wang, B. J., Sheu, H. M., Guo, Y. H., Lee, Y. H., Lai, C. S., Pan, M. H., and Wang, Y. J. (2010) Hexavalent chromium induced ROS formation Akt, Nf-kB and MAPK activation and TNF-α and IL-1α production in keratinocytes. *Toxicol. Lett.* 198 (2), 216–224.

Wang, H. (1999) Clastogenicity of chromium contaminated soil samples evaluated by *Vicia* root-micronucleus assay. *Mutat. Res.* 426 (2), 147–149.

Yu, X.-Z., Gu, J.-D., and Huang, S.-Z. (2007) Hexavalent chromium induced stress and metabolic responses in hybrid willows. *Ecotoxicology*. 16 (3), 299–309.

Zayed, A., Lytle, C. M., Qian, J.-H., and Terry, N. (1998) Chromium accumulation, translocation and chemical speciation in vegetable crops. *Planta*. 206 (2), 293–299.

Zayed, A. M., and Terry, N. (2003) Chromium in the environment: factors affecting biological remediation. *Plant Soil.* 249 (1), 139–156.

Zhitkovich, A. (2011) Chromium in drinking water: sources, metabolism, and cancer risks. *Chem. Res. Toxicol.* 24 (10), 1617–1629.

Zou, J., Chen, Q., Tang, S., Jin, X., Chen, K., and Zhang, T. (2009) Olaquindox-induced genotoxicity and oxidative DNA damage in human hepatoma G2 (HepG2) cells. *Mutat. Res.* 676 (1-2), 27–33.

Chapter 2.2 – Cadmium-induced cyto- and genotoxicity in lettuce

Cristina Monteiro, Conceição Santos, Sónia Pinho, Helena Oliveira, Tiago Pedrosa, Maria Celeste Dias

Department of Biology and CESAM, Laboratory of Biotechnology and Cytomics, University of Aveiro

Results presented in this chapter integrate paper published to international journal:

Monteiro, C., Santos, C., Pinho, S., Oliveira, H., Pedrosa, T., and Dias, M. C. (2012) Cadmium-induced cyto- and genotoxicity are organ-dependent in lettuce. *Chem. Res. Toxicol.* 25 (7), 1423–1434.

Abstract

Cadmium is a priority pollutant. Its mechanisms and effects within different plant organs remain unclear. Here, cyto- genotoxicity biomarkers were evaluated in roots and leaves after Cd exposure (0, 1, 10, and 50 μM) of the model crop *L. sativa* L. (cv. "Reine de Mai"). Overall, SOD and CAT activities were stimulated in leaves, where Cd accumulation was lower in comparison to that in roots. In roots, SOD and peroxidase (POX, APX) activities were stimulated. Moreover, in both organs GR was not affected by Cd. Overall, the H_2O_2 content increased in both organs, while TAA decreased in leaves and increased in roots with Cd concentrations. In both organs, lipid and protein oxidation rose with consequent increase of membrane permeability. Simultaneously, the comet assay showed that tail moment, tail length, and % tail DNA were maximum for 1 μM. For 10 μM, shorter tails were found suggesting induced Cd-DNA adducts that lead to DNA-DNA/DNA-protein crosslinks, and/or formation of longer DNA fragments, and/or impairment of DNA repair mechanisms, while at 50 μM, nucleoids sensitivity to the technique was evident. This result was consistent with the maximum MN frequency found for the 10 μM Cd dose in roots, suggesting that the surviving cells in this organ had an increase of mitotic catastrophe and that DNA repair systems for blocking cell cycle were dysfunctional. In lower Cd concentrations, root cells might have developed strategies to repair damaged DNA by blocking the cell cycle at specific checkpoints, thus avoiding mitotic catastrophe. Roots at 1 μM showed a cell cycle blockage trend at the G_2 checkpoint, while those at higher concentrations presented S phase delay. We finally discuss a general model of Cd-organ interaction covering these cyto- and genotoxic effects and the potential use of this cultivar in phytoremediation strategies.

Keywords

Cadmium, DNA damage, metal contamination, micronuclei, oxidative stress, plants

Introduction

Metal contamination of soil, water, and atmosphere is a worldwide problem due to the potential ecological and health impacts of contaminated products in plants (crops, in particular) and their transfer through the trophic chain (Nagajyoti et al. 2010). Cadmium naturally exists at low concentrations in the environment (0.04-0.32 μM) (Wagner 1993), but its main sources of contamination come from, e.g., mining, municipal, and industrial wastes, agricultural utilization of fertilizers, pesticides, and use of wastewater for irrigation (Nagajyoti et al. 2010). Cadmium is classified as Category 1 of human carcinogens (IARC 1993) and is in priority lists of hazardous substances/pollutants established by Environmental Protection Agency (2010) and European Commission (2001).

Plants are widely used as environmental bioindicators in toxicity assessment in terrestrial and aquatic environments (OECD 2006). However, the most common plant metal toxicity assays and endpoints are still focused on general parameters such as plant survival, germination, growth rates, and visual assessment (An 2004; OECD 2006). These general endpoints may result from more sensitive primary cytotoxic events, involving, e.g., oxidative stress, cell cycle blockage, or DNA damage, which can be analyzed in greater precision and detail.

Although Cd is an environmental threat, most mechanisms mediating its toxicity in plants are not fully understood (De Michele et al. 2009). Despite being a non-Fenton metal, Cd indirectly induced oxidative stress and ROS increment in plants (Azevedo et al. 2005b; Rodriguez-Serrano et al. 2006; De Michele et al. 2009; Monteiro et al. 2009b).

Cd-stressed cells activate mechanisms for ROS scavenging (Agrawal and Mishra 2009; DalCorso et al. 2010; Gill and Tuteja 2011). In sensitive cells unable to display efficient antioxidant capacity, peroxidation of macromolecules may occur. Lipid peroxidation is the most analyzed parameter in metal toxicity assays (Kovácik and Backor 2008; Agrawal and Mishra 2009), while Cd-induced protein oxidation has been far less explored (Romero-Puertas et al. 2002; Aravind et al. 2009).

A third class of macromolecules, nucleic acids (namely DNA), are also affected by ROS (Cooke et al. 2003), though its direct damage in DNA remains fuzzy in plant cells. DNA damage is considered an environmental marker of exposure to genotoxic agents (Dhawan et

al. 2009). Cd-induced point mutations in lettuce were age-dependent being the most sensitive seedling phase (Monteiro et al. 2009a), which also supports the previous findings of malformed embryos in *Arabidopsis* plants exposed to Cd (Ernst et al. 2008).

DNA damage and related genotoxic events have been assessed by several techniques: the occurrence of MN, also named mitotic catastrophe, is considered an effective method for cytogenotoxicity evaluation, being used to detect clastogenic and aneugenic effects of xenobiotics (Fenech 2006). Some authors, as Achary and Panda (2010), or Dhawan et al. (2009), proposed comet assay to assess DNA damage. Few plant species have been used for genotoxicity assessment by the comet assay and by MN assays, with *Allium* spp. (Souza et al. 2009), *V. faba* (Souguir et al. 2010), *Tradescantia* spp., and *N. tabacum* (Villarini et al. 2009) being the most used model species.

FCM is also a powerful tool as it assesses, in a single run, major mutations (aneuploidizations, euploidizations, and clastogenicity); nuclear DNA content; and cell cycle progression to infer cytostatic or mitogenic effects (Rayburn and Wetzel 2002; Monteiro et al. 2010; Rodriguez et al. 2011). Despite this huge potential, it has been mostly applied to animal cytogenotoxic studies (*in vivo* and *in vitro*) (e.g., Andersson et al. 2007; Oliveira et al. 2009) and rarely in plants (e.g., Monteiro et al. 2010; Rodriguez et al. 2011).

DNA damage may lead to cell cycle blockage, allowing its repair or preparation of the cell to die by apoptosis or necrosis (O'Connell and Cimprich 2005). Otherwise, when cell cycle proceeds with damaged DNA, MN may occur (Eriksson et al. 2007). Using *in vitro* synchronized tobacco plant cells, it was demonstrated that Cd differently affected G_0/G_1-S and G_2-M transitions (Kuthanova et al. 2008). Few studies explored putative Cd effects on cell cycle blockage in plant cells showing DNA damage.

The aim of this work is to clarify how moderate (1 µM) to high (10 and 50 µM) Cd concentrations induce cyto- and genotoxicity in plants. For that, primary responses of oxidative stress (antioxidant enzyme activities, TAA, H_2O_2 content, and macromolecules oxidation) are analyzed. Consequently, cell membrane permeability is analyzed. Simultaneously, Cd-induced DNA damage and resulting consequent interferences with cell cycle progression and/or mitotic catastrophe were evaluated by the comet assay, FCM, and MN assay. The Cd concentrations used can be found in moderately and highly contaminated

soils (Wagner 1993), and the comparison of all parameters will also allow us to design a functioning model integrating all data.

Environmental monitoring using species as crops should be of great importance to the risk assessment of crop health for consumption by humans or any other consumers. Therefore, our study was performed using *L. sativa* L., a valuable crop and one recommended for standard ISO toxicity tests (OECD 2006; Monteiro et al. 2009b).

Materials and methods

Plant culture and exposure to Cd

Seeds of *L. sativa* L. (cv. "Reine de Mai") were germinated in $Cd(NO_3)_2$ solutions: 0 (control), 1, 10, 50, and 100 µM. Germination rates and IC_{50} were determined. For other assays, only the concentrations up to 50 µM were used. After germination, plants were transferred to an aerated Hoagland hydroponic system (often used in greenhouse large-scale crop production, e.g., Cropking; Verti-gro). Plants were grown in a greenhouse, with a photon flux density of 200 $\mu molm^{-2}s^{-1}$, a photoperiod of 16 h:8 h (light/dark), and a temperature of 20 ± 2 ºC. After 28 days of exposure to Cd, leaves and roots of lettuce were harvested. Prior to estimating antioxidant enzyme activities, TAA, H_2O_2 content, lipid peroxidation and protein oxidation, the roots and leaves of a pool of plants (about 5-15 individuals per Cd concentration) were immersed in liquid nitrogen and kept at -80 ºC until analyzed. For the remaining parameters analyzed, the fresh organs were used.

Germination rate, plant growth, mortality, IC_{50}, and LC_{20} estimation

Germination rate was determined after exposure of lettuce seeds to Cd during 5 days. Mortality was calculated after 28 days of plants growth, and LC_{20} was determined. Also plant length was measured, and the corresponding IC_{50} was calculated using Sigma Plot 11.0 software (Systat Software Inc., Germany) with the four-parameter logistic function standard curve analysis for dose response.

Cadmium accumulation

Accumulation of elemental Cd was determined in plant leaves and roots. Plant roots were washed in a 0.5 mM $CaSO_4$ solution to remove Cd ions adsorbed to the tissue surface, then washed in water (Monteiro et al. 2010). These organs were dried to constant weight at 60 ºC. Then, dried material was treated according to Evers and Bücking (1976), and Cd content was analyzed by ICP-AES (Jobin Ivon JY70 Plus).

Soluble proteins and antioxidant enzyme activities

Frozen root and leaf samples were homogenized in 0.1 M potassium phosphate buffer (pH 7.5) containing 0.5 mM Na_2EDTA, 0.2% (v/v) Triton X-100, 2 mM DTT, and 1 mM PMSF as modified from Romero-Puertas et al. (2002) and with 1% (w/v) PVP (Ali et al. 2005). Homogenates were centrifuged twice in a refrigerated centrifuge at 8000*g* for 15 min. Supernatants obtained were used to assay activities of SOD (EC 1.15.1.1), CAT (EC 1.11.1.6), POX (EC 1.11.1.7), APX (EC 1.11.1.11), and GR (EC 1.6.4.2) and for soluble protein quantification. SOD was determined according to the method of Agarwal et al. (2005). One unit of SOD activity is the amount of enzyme required to cause a 50% inhibition on the rate of reduction of nitroblue tetrazolium. CAT activity was assayed as described by Beers and Sizer (1951). POX activity was determined according to Bergmeyer (1983). APX was extracted using the above-mentioned potassium phosphate buffer with 10 mM Asc (Almeselmani et al. 2006), and the enzyme activity was determined according to Nakano and Asada (1981). GR activity was determined according to Sgherri et al. (1994). Protein concentration was determined according to Bradford (1976).

Total antioxidant activity

TAA was determined with Antioxidant Assay Kit from Sigma-Aldrich (USA), catalog number CS0790. This assay is based on a colorimetric reaction that can be determined spectrophotometrically at 405 nm. The absorbance decrease reflects the increase of antioxidant activity (trolox, a water-soluble vitamin E analog, was used as a standard or control antioxidant).

Prior to analysis, frozen roots and leaves of lettuce were weighted (200 mg) and homogenized with proper assay 1x buffer and centrifuged twice at 15000*g* for 15 min at 4 ^{o}C.

The assay was prepared on a 96-well plate with 10µL of root and leaf samples, 20µL of myoglobin working solution, and 150µL of ABTS substrate working solution. After incubation, at RT during 5 min, 100 µL of STOP solution was added, and the absorbance was read with Synergy HT Bioteck, software Gen5 1.11.

Quantification of H_2O_2

To find out the amount of H_2O_2 production, the OxiSelectTM Hydrogen Peroxide/Peroxidase Assay Kit from Cell Biolabs, catalog number STA-344, was used. In the presence of HRP, the nonfluorescent ADHP reacts with H_2O_2 to produce highly fluorescent resorufin which can then be read with an excitation of 530-560 nm and an emission of 590 nm.

Homogenization of root and leaf samples (200 mg) was carried out with the kit's assay 1x buffer. Homogenates were centrifuged twice at 15000*g* for 15 min at 4 ^{o}C. The assay was performed on a 96-well fluorescent black microplate appropriate for fluorometric analysis, and readings were performed with Synergy HT Bioteck, software Gen5 1.11. The procedure was performed with 100 µL of root and leaf samples and 50 µL of ADHP/HRP working solution added to each well. After incubation at RT, protected from light during 30 min, the fluorescence was read.

Lipid peroxidation

MDA content was determined according to the modified protocol of Dhindsa and Matowe (1981): 0.5 g of frozen tissue was homogenized in 5 mL of 0.1% TCA. The homogenates were centrifuged for 5 min at 10000*g* and 4 ^{o}C. To 1 mL of supernatant was added 4 mL of 20% TCA containing 0.5% TBA. The mixture was heated at 95 ^{o}C for 30 min and then cooled on ice. After centrifugation at 10000*g* (4 ^{o}C), the absorbance of the

supernatant was read at 532 nm, and the nonspecific absorbance at 600 nm was subtracted. The MDA concentration was calculated using the $\varepsilon = 155\ mM^{-1}cm^{-1}$.

Protein oxidation

Proteins were extracted using the extraction phosphate buffer used for enzymes but also containing 1% (w/v) sulphate streptomycin to eliminate the interference of DNA carbonyls (Romero-Puertas et al. 2002). Protein oxidation was measured according to Hawkins et al. (2009). Protein carbonyls first reacted with 10 mM DNPH in 2.5 M HCl for 5 min. A blank without DNPH was used to quantify protein content of the sample. To all tubes 50% TCA was added and incubated at -20 ^{o}C, for at least 15 min. After centrifugation at 9000*g* and 4 ^{o}C for 15 min, pellets were washed with ice cold (1:1, v/v) ethanol/ethyl acetate. Pellets were centrifuged for 2 min at 9000*g* and then resuspended in 6 M guanidine-HCl. The absorbance was determined at 370 nm for DNPH tubes, and at 280 nm for tubes without DNPH. Standards of BSA were prepared and read at 280 nm.

Cell membrane permeability

Cell membrane permeability is a parameter of cell viability and was measured by electrolyte leakage assessment according to Lutts et al (1996). The leaves and roots were washed and immersed in deionized water. Then they were incubated overnight (25 ^{o}C, 85 rpm). Electrolyte leakage was determined by measuring conductance (µS) (Consort C830) before (L_0) and after (L_t) autoclaving (10 min, 121 ^{o}C) and by calculating the ratio L_0/L_t.

Comet assay

The comet assay was performed as described by Gichner et al. (2004) with slight modifications. Leaves and roots were sliced in cold 0.4 M Tris buffer (pH 7.5), and the isolated nucleoids were collected in the buffer. A mixture of 50 µL of the nucleoid suspension and 50 µL of 1% LMPA was spread on each slide with the 1% NMPA layer. The slides were immersed in an alkaline buffer (0.30 M NaOH and 1 mM EDTA, pH>13) for DNA unwinding (15 min) and electrophoresis at 0.74 V/cm and 300 mA for 30 min at 4 ^{o}C.

Slides were then neutralized with 0.4 M Tris buffer (pH 7.5) and washed with water. Nucleoids were stained with ethidium bromide and examined using a fluorescence microscope (Nikon Eclipse 80i) equipped with an excitation filter of 510-560 nm and a barrier filter of 590 nm. Images were captured with NIS-Elements F 3.00, SP7 software. The parameters % tail DNA and tail moment were calculated using image analysis software (CASP v1.2.2).

Micronuclei

Meristematic tissues (from roots and leaves) were collected from plants and stained with PI. Slide preparations were observed under 400x magnification using a fluorescence microscope (Nikon Eclipse 80i) with an excitation filter of 510-560 nm and a barrier filter of 590 nm. To calculate the frequency of MN, 1000 cells were scored from three plants, per Cd concentration. The criteria of Fenech (2007) for identifying MN were followed.

Flow cytometric analysis

Changes in cell cycle progression were evaluated in both roots and leaves by FCM, according to Rodriguez et al. (2011). Briefly, nucleus suspensions were obtained by fine chopping in WPB, containing 0.2 M Tris-HCl, 4 mM $MgCl_2$, 2 mM EDTA, 86 mM NaCl, 10 mM sodium metabisulfite, 1% PVP-10, 1% (v/v) Triton X-100, pH 7.5(Loureiro et al. 2007), and then filtered through a 55 µm nylon filter. To the nucleus suspensions, 50 µg/mL PI and 50 µg/mL RNase were added. About 2000-4000 nuclei (one replicate consisted of one individual in plant groups from the control, 1 µM and 10 µM Cd, and two individuals from plants exposed to 50 µM Cd) were analyzed per sample in a flow cytometer (EPICS-XL Coulter Electronics, USA) equipped with an argon laser (15 mW, 488 nm). The G_0/G_1 fluorescence peak of sample nuclei was adjusted to channel 200. The results were acquired using the SYSTEM II software (v. 3.0, Beckman Coulter®).

The nucleus populations in the phases G_0/G_1, S, and G_2 and changes in cell cycle progression were analyzed to assess Cd mitogenic/cytostatic effect. Changes in cell cycle dynamics were also expressed by the PRI [formerly named “proliferation index” by Sun et al. (2007)], which gives the percentage of cells that, in each population, were able to

overcome the R checkpoint (between G_0/G_1 and S phases). The equation to obtain the PRI is: PRI = (% S + % G_2)/(% G_0/G_1+ % S + % G_2).

Statistical analysis

Data were analyzed by one-way ANOVA ($p < 0.05$), followed by a Holm-Sidak test ($p < 0.05$) to evaluate the significance of differences in the parameters. When necessary, data were transformed to achieve normality and equality of variances. When these criteria were not verified, the non parametric test, Kruskal–Wallis one-way ANOVA by ranks, was done. All statistical analyses were performed using Sigma Plot 11.0 software (Systat Software Inc., Germany). The number of replicates and independent assays used for each parameter is provided in the corresponding figure or table.

Results

Germination rate, plant growth, mortality, IC_{50}, and LC_{20} estimation

After seed germination (5 days) in Cd solutions, the germination rate (Figure 13A) was calculated. A significant reduction in germination rate for all Cd concentrations (one-way ANOVA, $F_4 = 150.668$, $p < 0.001$; Holm-Sidak method, $p < 0.05$) was observed. After 28 days of exposure, general visible toxicity symptoms (Figure 14), like leaf chlorosis, were observed in all groups of exposed plants. Necrotic lesions were visible in older leaves at 10, 50, and 100 µM of Cd, being higher in the last two concentrations. Roots of treated plants (mostly for concentrations above 10 µM) were darker and shorter than those of control plants and had fewer lateral roots. Plant mortality was about 2.3% and 20% in plants exposed to 50 and 100 µM Cd, respectively. Growth inhibition from 10 µM to 100 µM (Figure 13B) (one-way ANOVA, $F_4 = 88.614$, $p < 0.001$; Holm-Sidak method, $p < 0.05$) was also observed. Therefore, the highest dose tested (100 µM) corresponds to the LC_{20} in this species. From the dose-response curve (Figure 13B) of lettuce length with Cd concentration, the IC_{50}, 20.667 ± 10.158 µM ($p > 0.05$), was estimated.

Cd accumulation

Cd accumulation in lettuce leaves and roots is presented in Figure 13C. In control plants, no detectable Cd content was found. Cd accumulation increased with Cd exposure in both organs (leaves, one-way ANOVA, $F_3 = 571.856$, $p < 0.001$; Holm-Sidak method, $p < 0.05$; roots, one-way ANOVA, $F_3 = 859.837$, $p < 0.001$; Holm-Sidak method, $p < 0.05$). Cd content in roots was approximately 2.5, 2.6, and 1.8 times greater than the Cd content in leaves of plants exposed to 1, 10, and 50 µM Cd, respectively.

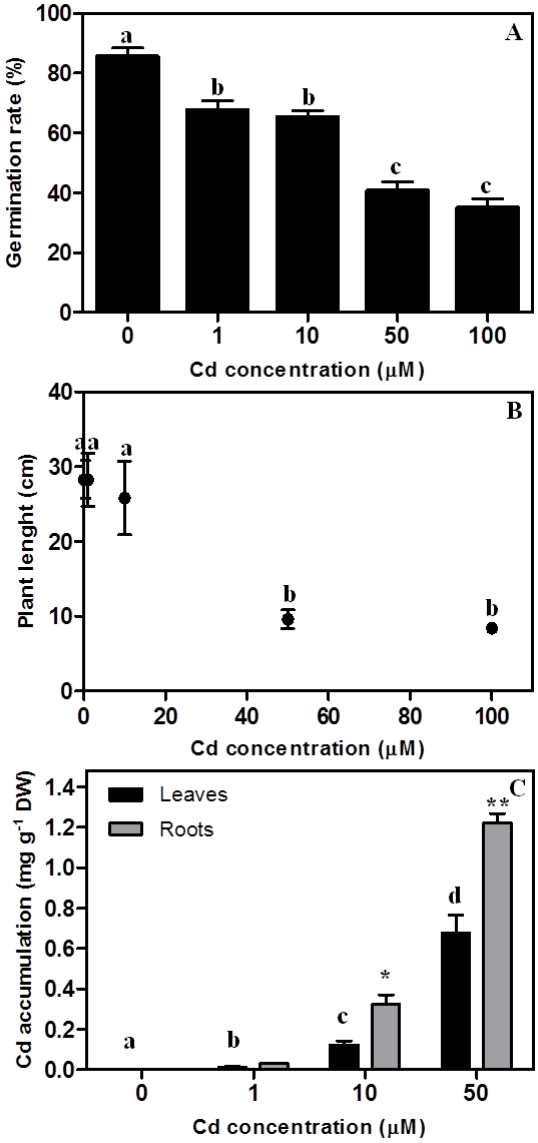

Figure 13. (A) Germination rate of lettuce seeds exposed to Cd during 5 days (three independent experiments, each one with up to 400 seeds). (B) Dose-response curve of plant length function of Cd concentration (n = 4). (C) Cd accumulation in roots and leaves of control and exposed lettuce (n = 3-5). Results are expressed as the mean ± SD. Different letters (for leaves) or number of asterisks (for roots) indicates significant differences between treatments at $p < 0.05$.

Figure 14. Lettuce plants after 28 days of Cd treatment. From left to right: control, 1, 10, and 50 µM Cd.

Antioxidant enzyme activities

The antioxidant enzyme system in roots and leaves was differently affected by Cd (Figure 15). In leaves, Cd generally increased SOD activity (one-way ANOVA, $F_3 = 21.994$, $p < 0.001$; Holm-Sidak method, $p < 0.05$) (Figure 15A) for concentrations of 10 and 50 µM, while CAT activity (Figure 15C) was only affected for the Cd dose of 10 µM (one-way ANOVA, $F_3 = 25.271$, $p < 0.001$; Holm-Sidak method, $p < 0.05$). Contrarily, POX activity (Figure 15E) tended to decrease, with increasing concentration of Cd, mostly at 50 µM (one-way ANOVA, $F_3 = 25.818$, $p < 0.001$; Holm-Sidak method, $p < 0.05$). Similarly, APX activity (Figure 15G) showed a general and significant decrease (one-way ANOVA, $F_3 = 14.258$, $p < 0.001$; Holm-Sidak method, $p < 0.05$) in plant leaves exposed to Cd, this effect being more evident at lower concentrations (1 and 10 µM). GR activity (Figure 15I) showed no significant differences in leaves exposed to Cd (one-way ANOVA, $F_3 = 1.630$, $p > 0.05$).

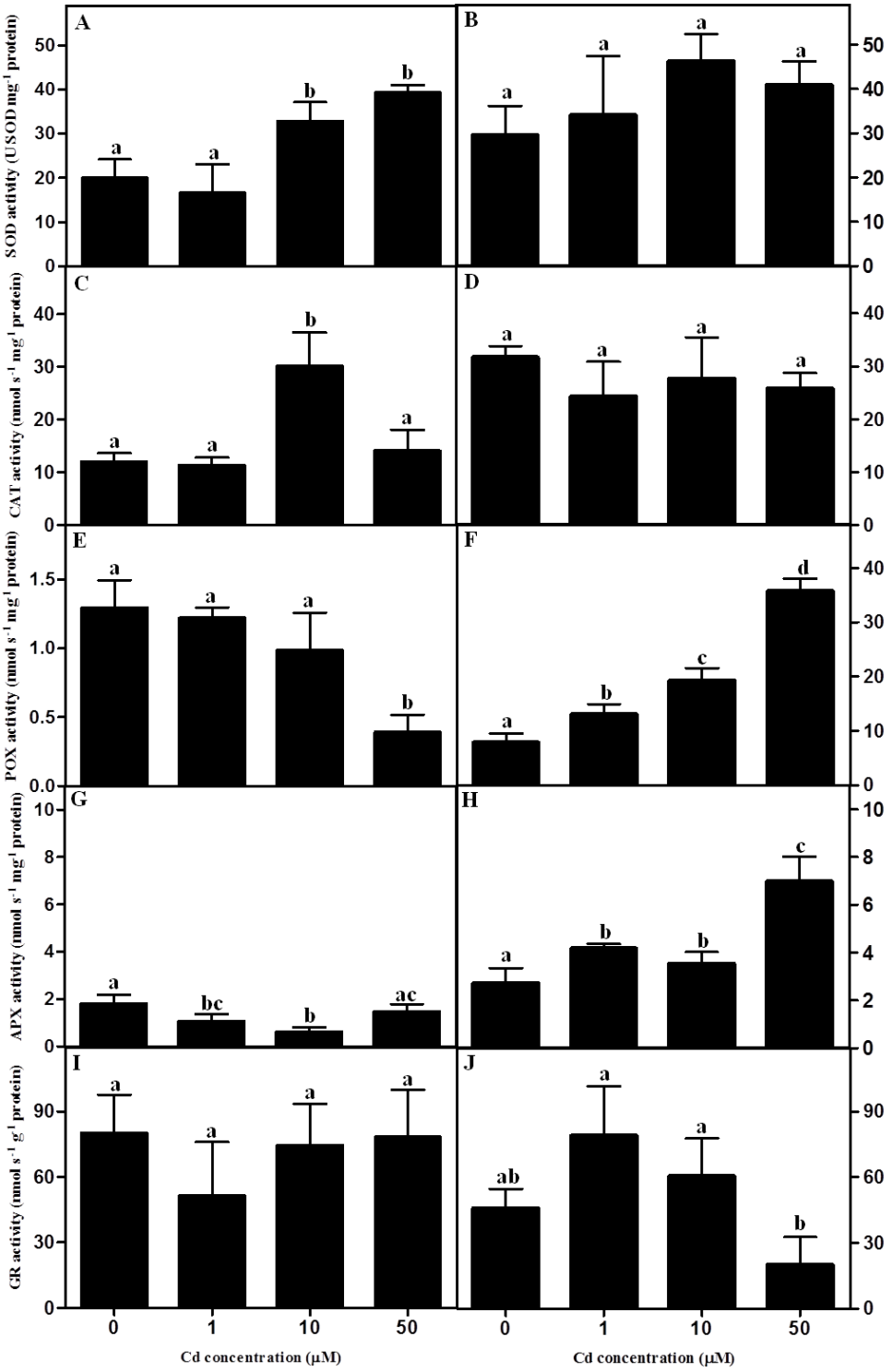

Figure 15. Effect of Cd accumulation on SOD, CAT, POX, APX, and GR activities in lettuce leaves (A, C, E, G, and I, respectively) and roots (B, D, F, H, and J, respectively), after 28 days of exposure. Results are expressed as the mean ± SD (n = 5). Different letters indicate significant differences between treatments at $p < 0.05$.

Compared to leaves, root antioxidant enzymes presented different responses to Cd: SOD (Figure 15B) also showed an increasing trend (one-way ANOVA, $F_3 = 3.006$, $p > 0.05$), although CAT activity (Figure 15D) showed no significant differences (one-way ANOVA, $F_3 = 1.783$, $p > 0.05$). POX activity (Figure 15F) increased exponentially with increasing Cd concentrations (one-way ANOVA, $F_3 = 175.514$, $p < 0.001$; Holm-Sidak method, $p < 0.05$). Compared with the control, roots exposed to all Cd doses showed a significant increase in APX activity (one-way ANOVA, $F_3 = 32.386$, $p < 0.001$; Holm-Sidak method, $p < 0.05$) (Figure 15H). Within Cd-exposed roots, GR activity (Figure 15J) was not significantly affected compared to the control, though the GR response has been significantly different among the concentrations 1, 10, and 50 µM Cd dose (one-way ANOVA, $F_3 = 9.404$, $p < 0.002$; Holm-Sidak method, $p < 0.05$).

Total antioxidant activity and H_2O_2 content

The TAA (Table 1) significantly decreased at 10 and 50 µM Cd in leaves compared to the control (one-way ANOVA, $F_3 = 62.107$, $p < 0.001$; Holm-Sidak method, $p < 0.05$). The decrease was 168.86 ± 0.24% and 122.58 ± 0.34% in 10 and 50 µM, respectively. In roots, a significant increase of TAA was observed for the same Cd concentrations: 17.84 ± 0.13% and 28.99 ± 0.08% in 10 and 50 µM, respectively (one-way ANOVA, $F_3 = 13.585$, $p < 0.001$; Holm-Sidak method, $p < 0.05$).

Table 1. Changes in the total antioxidant activity (TAA) in leaves and roots of lettuce exposed to Cd[a]

Total Antioxidant Activity (TAA)	Cd concentration (µM)		
	1	10	50
Leaves			
Decrease of TAA (% of control)	2.03 ± 0.25	168.86 ± 0.24*	122.58 ± 0.34*
Roots			
Increase of TAA (% of control)	1.73 ± 0.06	17.84 ± 0.13*	28.99 ± 0.08*

[a]Results are expressed as mean ± SD (n=5-6). Asterisks indicate significant differences between Cd treatments *vs* control at $p < 0.05$.

The content of H_2O_2 (Figure 16) was significantly enhanced at 10 and 50 µM Cd in leaves compared to the control (one-way ANOVA, $F_3 = 152.199$, $p < 0.001$; Holm-Sidak method, $p < 0.05$). In roots a significant increase of H_2O_2 was observed (one-way ANOVA, $F_3 = 6{,}061$, $p = 0.006$; Holm-Sidak method, $p < 0.05$) only at the highest Cd concentration.

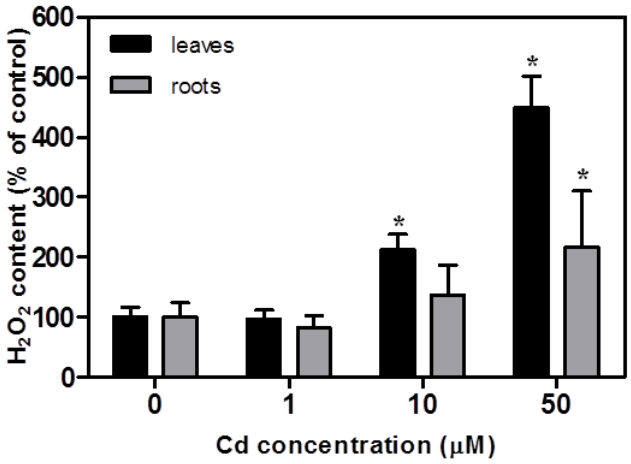

Figure 16. Cd effect on H_2O_2 production in lettuce leaves and roots (n = 3-6). Results are expressed as the mean ± SD. Asterisks indicate significant differences between treatments at $p < 0.05$.

Lipid and protein oxidation, and cell membrane permeability

Lipid peroxidation was measured in terms of MDA content. In leaves and roots, MDA generally increased, being significant for 10 µM in both organs and for 50 µM in roots (Table 2) (leaves, one-way ANOVA, $F_3 = 11.963$, $p < 0.001$; Holm-Sidak method, $p < 0.05$; roots, Kruskal-Wallis one-way ANOVA, $H = 10.941$, $df = 3$, $p = 0.012$; Tukey test, $p < 0.05$). However, in leaves exposed to 50 µM a significant decrease in MDA was found.

Protein carbonyls displayed a significant increase in their content in plants exposed to the highest Cd doses (10 and 50 µM Cd). This effect was observed in both leaves and roots, as can be seen in Table 2 (leaves, one-way ANOVA, $F_3 = 172.799$, $p < 0.001$; Holm-Sidak method, $p < 0.05$; roots, one-way ANOVA, $F_3 = 20.980$, $p < 0.001$; Holm-Sidak method, $p < 0.05$).

Cell membrane permeability was determined through measurement of electrolyte leakage and increased with Cd exposure in lettuce roots (Table 2). This increase was significant from the dose of 10 µM Cd (one-way ANOVA, $F_3 = 20.969$, $p < 0.001$; Holm-

Sidak method, $p < 0.05$), while in leaves there was a trend for an increase in electrolyte leakage in plants treated with 50 µM but not statistically significant (Kruskal-Wallis one-way ANOVA, H = 7.897, df = 3, $p = 0.048$; Tukey test, $p > 0.05$).

Table 2. Effect of Cd exposure on MDA content, carbonyl concentration and electrolyte leakage in leaves and roots[a]

	Cd concentration (µM)			
	0	1	10	50
		Leaves		
MDA content (nmol g^{-1} FW)	15.96 ± 2.75 a	18.07 ± 1.25 ab	24.18 ± 6.67 b	8.64 ± 1.18 c
Carbonyl concentration (nmol mg $protein^{-1}$)	2.96 ± 0.40 a	3.10 ± 0.29 a	4.89 ± 0.73 b	5.59 ± 0.75 c
Electrolyte leakage (%)	13.74 ± 1.16 a	15.24 ± 7.01 a	13.92 ± 2.55 a	44.82 ± 29.75 a
		Roots		
MDA content (nmol g^{-1} FW)	9.92 ± 0.07 a	10.66 ± 0.78 a	13.21 ± 2.68 b	13.34 ± 1.96 b
Carbonyl concentration (nmol mg $protein^{-1}$)	7.19 ± 1.19 a	7.23 ± 1.60 a	12.49 ± 1.05 b	13.15 ± 2.47 b
Electrolyte leakage (%)	17.08 ± 5.36 a	19.91 ± 7.14 a	29.97 ± 2.46 b	42.29 ± 3.71 b

[a]Results are expressed as mean ± SD (n=4-5). Different letters indicate significant differences between treatments at $p < 0.05$.

Comet assay and micronuclei

The data show a general increase in DNA damage in leaves and roots and of plants exposed to Cd. The % tail DNA, tail length, and tail moment, assessed by the comet assay, were used to evaluate DNA damage in roots and leaves exposed to Cd (Table 3).

In leaves, only for 1 µM Cd, DNA damage was found, produced by a significant increase of % tail DNA, tail length, and tail moment when compared to control (% tail DNA, one-way ANOVA, $F_2 = 25.508$, $p = 0.002$; Holm-Sidak method, $p < 0.05$; tail length, one-way ANOVA, $F_2 = 16.322$, $p = 0.006$; Holm-Sidak method, $p < 0.05$; tail moment, one-way ANOVA, $F_2 = 11.641$, $p = 0.013$; Holm-Sidak method, $p < 0.05$). In roots, however, DNA damage was detected at the Cd doses of 1 and 10 µM, as the % tail DNA was significantly

higher at these Cd concentrations compared to control (% tail DNA, one-way ANOVA, $F_2 = 42.830$, $p < 0.001$; Holm-Sidak method, $p < 0.05$; tail moment, one-way ANOVA, $F_2 = 6.381$, $p = 0.033$; Holm-Sidak method, $p < 0.05$). Also, at 50 µM nucleoids from both organs were consistently too degraded to be considered admissible for measurement (data not shown).

Table 3. Cd-Induced DNA damage by comet assay in leaves and roots after Cd exposure[a]

	Cd concentration (µM)			
	0	1	10	50
		Leaves		
% Tail DNA	9.11 ± 1.32 a	37.32 ± 7.69 b	11.42 ± 3.97 a	n.d.
Tail length	79.67 ± 18.82 a	243.00 ± 48.78 b	104.50 ± 37.48 a	n.d.
Tail moment	7.36 ± 2.63 a	97.89 ± 38.82 b	13.69 ± 10.08 a	n.d.
		Roots		
% Tail DNA	23.15 ± 4.02 a	54.00 ± 4.87 b	31.53 ± 1.84 c	n.d.
Tail length	208.83 ± 33.21 a	268.83 ± 77.20 a	243.00 ± 26.87 a	n.d.
Tail moment	47.98 ± 18.46 ab	148.09 ± 49.84 a	76.97 ± 5.37 b	n.d.

[a]Results are expressed as the median ± SD ((no slides) = 3). Different letters indicate significant differences between treatments at $p < 0.05$. n.d. (not detected) means that no comet was observed during microscope slide observation.

Figure 17 shows examples of comets found in roots of lettuce exposed to 0 (Figure 17A), 1 (Figure 17B), and 10 µM Cd (Figure 17C). In both leaves and roots, the maximum values of % tail DNA, tail length and tail moment were observed for 1 µM Cd.

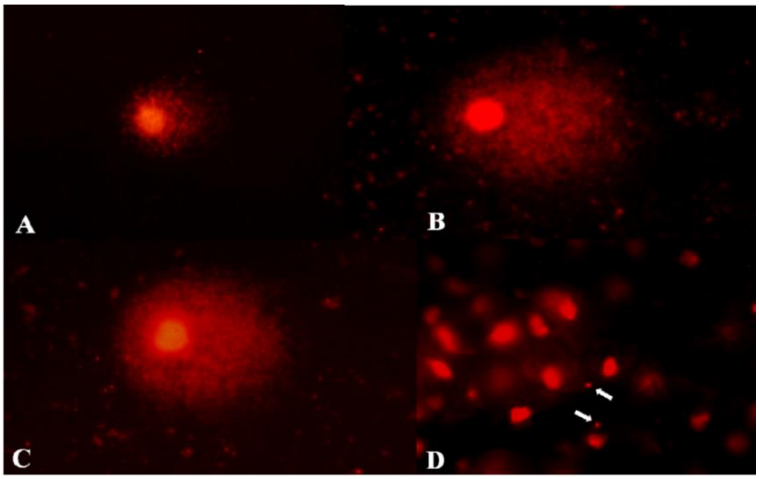

Figure 17. (A, B, and C) Comets from root cells of lettuce exposed to Cd for 28 days, observed under fluorescence microscopy (400×): A, 0µM; B, 1µM; C, 10µM; D, example of the observation of nuclei from root tips exposed to 50 µM Cd. White arrows indicate MN.

Cd induced MN (e.g., Figure 17D) formation in *L. sativa*, mostly in roots, as shown in Table 4. No MN were observed in leaves of control plants or those exposed to lower Cd concentrations (1 and 10 µM). In leaves of plants exposed to 50 µM Cd, there was a frequency of 2 MN per 1000 nuclei. No MN was found for control and 1 µM-exposed roots. At higher concentrations, MN appeared more frequently up to 82 MN per 1000 nuclei at 10 µM Cd, and 31 MN per 1000 nuclei at 50 µM (Table 4), but in this last concentration, the frequency of destroyed nuclei was higher than 50% (data not shown).

Table 4. Micronuclei (MN) frequency in leaves and roots of lettuce exposed to Cd[a]

MN (‰)	Cd concentration (µM)			
	0	1	10	50
Leaves	0	0	0	2
Roots	0	0	82	31[b]

[a]More than 50% of visualized cells/nuclei were highly degraded after the treatment. [b]Value represents ‰ for measurable nuclei.

Flow cytometric analysis

Nuclei from leaves and roots showed no statistical variation ($p > 0.05$) in both FS, a rough indicator of size (leaves, Kruskal-Wallis one-way ANOVA, H = 5.166, df = 3, $p > 0.05$; roots, one-way ANOVA, $F_3 = 1.644$, $p > 0.05$), and SS indicative of nuclei complexity/granularity (leaves, one-way ANOVA, $F_3 = 1.013$, $p > 0.05$; roots, one-way ANOVA, $F_3 = 1.697$, $p > 0.05$), independently of the Cd concentration tested (data not shown).

Control roots and leaves showed typical fluorescence histogram profiles with a main peak corresponding to nuclei 2*x* DNA at G_0/G_1 being the predominant nuclei population and a smaller peak with the double of FL corresponding to nuclei with 4*x* DNA (G_2) (see Figure 18A, B).

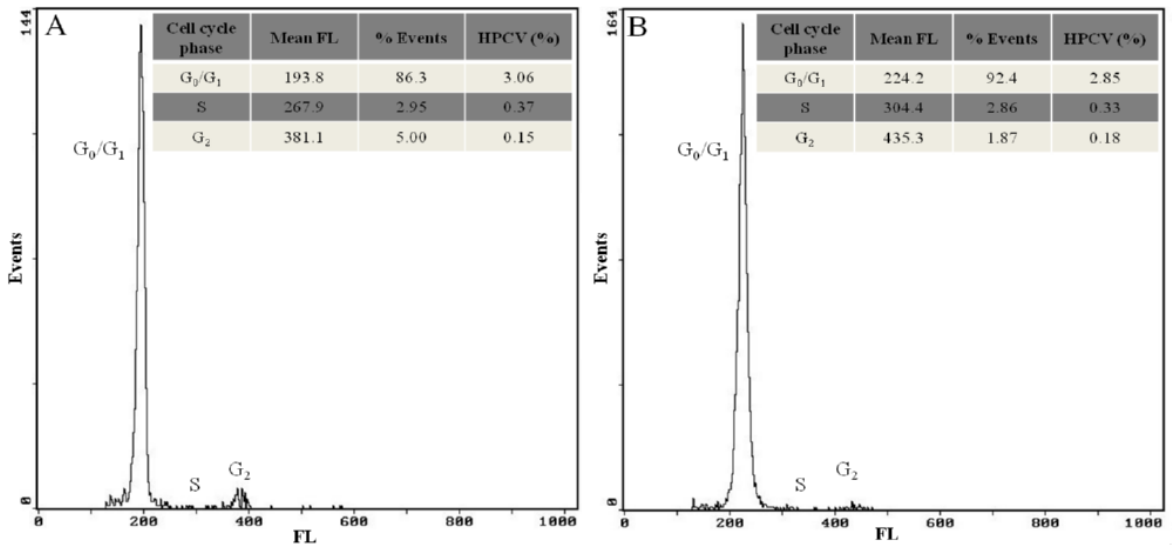

Figure 18. (A, B) Examples of histograms of relative FL for leaves (A) and roots (B) of control plants by the end of the experiment. The values are given as the mean position of the peak (mean FL), the percentage of nuclei (% events), and the HPCV of the G_0/G_1, S and G_2 peaks.

The HPCV of G_0/G_1, which is indicated as a measurement of quality of flow cytometric analysis for control samples, ranged from 3.85 ± 0.55 and 3.30 ± 0.30, in leaves and roots, respectively (Table 5). Despite the fact that no significant differences were found in the G_0/G_1 HPCV of leaves (one-way ANOVA, $F_3 = 1.582$, $p > 0.05$), in roots, the HPCV value at 10 µM Cd was higher than that in the control (one-way ANOVA, $F_3 = 7.687$, $p = 0.001$; Holm-Sidak method, $p < 0.05$).

Table 5. Half-Peak Coefficient of Variation (HPCV) of G_0/G_1 phase, cell cycle dynamics, and Post-R Index (PRI) in leaves and roots[a]

Cd concentration (µM)	HPCV	% G_0/G_1	% S	% G_2	PRI
Leaves					
0	3.85 ± 0.55	91.92 ± 0.67	4.70 ± 1.62	3.37 ± 1.03	0.08 ± 0.01
1	3.89 ± 0.58	90.80 ± 1.58	5.08 ± 2.24	4.12 ± 1.61	0.09 ± 0.02
10	3.63 ± 0.26	93.7 ± 1.95	3.73 ± 2.20	2.55 ± 0.49	0.06 ± 0.02
50	3.32 ± 0.54	93.20 ± 1.09	3.90 ± 3.10	2.88 ± 0.92	0.07 ± 0.03
Roots					
0	3.30 ± 0.30	92.65 ± 2.85	6.00 ± 2.26	1.37 ± 0.70	0.07 ± 0.03
1	3.41 ± 0.27	91.55 ± 2.87	6.03 ± 3.12	2.42 ± 0.38	0.08 ± 0.03
10	4.32 ± 0.67*	91.92 ± 2.52	6.65 ± 2.74	1.42 ± 1.07	0.08 ± 0.03
50	3.52 ± 0.17	89.30 ± 1.11	9.47 ± 1.38	1.22 ± 1.01	0.11 ± 0.03

[a]Results are expressed as the mean ± SD (n = 6). Asterisks indicate significant differences between treatments at $p < 0.05$.

Cell cycle transitions in leaves were only slightly affected by Cd. On the contrary Cd had cytostatic effects in root cells. Most evident effects were the blockage at G_2 phase in the lowest Cd concentration (1 µM), observed by an increase of cell percentage in G_2 phase; and delay of cell cycle at S phase in root cells at higher Cd concentrations observed by an increase of cell population in S phase. These blockages/delays contributed to the tendency of PRI increase along Cd concentration, in roots (Table 5).

Discussion

"Reine de Mai" is considered a Cd accumulator lettuce cultivar (Monteiro et al. 2009b), and its germination rate was decreased, supporting the fact that plantlet growing stage is most sensitive to Cd (Monteiro et al. 2010). As Cd led to growth inhibition after 28 days of exposure, IC_{50} was 20.667 ± 10.158 µM, although the wide range is due to the variability between plant individuals of lower Cd concentrations (1 and 10 µM). Plant death occurred at higher concentrations (50 and 100 µM), the estimated LD_{20} being approximately 100 µM. Moreover, this work demonstrates that some cyto- and genotoxic endpoints assessed here are sensitive to even lower doses (1 and 10 µM) and they are also organ dependent.

Cd^{2+} enters the cell probably by Fe^{2+}, Ca^{2+}, Cu^{2+} and Zn^{2+} transporters/channels (Clemens 2006), but in our experiments, Cd decreased Fe^{2+} accumulation in leaves (Monteiro et al. 2009b), which demonstrates that plants are under deficiency of this nutrient, and putative competition occurs between Cd and iron ions. Roots accumulated 2.5, 2.6 and 1.8 times more Cd than leaves in plants exposed to 1, 10, and 50 µM Cd, respectively. Even so, leaves accumulated significant levels of Cd per total plant matter, supporting the fact that lettuce may be considered a Cd-accumulator species as proposed by Monteiro et al. (2009b). The capacity of a species to accumulate a metal in its shoot is a general requisite for its use in phytoremediation strategies of contaminated sites. In a previous study, our group has shown that for the same experimental conditions and Cd concentration of 100 µM, lettuce plants accumulated less Cd per gram of DW than *T. caerulescens* but accumulated much more total Cd per plant due to its higher biomass (Monteiro et al. 2010). Therefore, for the same period of exposure and conditions, lettuce has the ability to remove higher amounts of this metal from contaminated soils than *Thlaspi sp*. The strategy of preferably using plants with large biomass instead of hyperaccumulators with very low biomass should deserve serious attention in phytoremediation studies at least while hyperaccumulators are not improved for higher biomass production.

Although not a Fenton-metal, Cd contributes to ROS increment, leading to oxidative stress that needs to be controlled, otherwise the cell enters into senescence and ultimately dies (Schröder et al. 2009). Within ROS, H_2O_2 acts as a second messenger to regulate the gene expression of some antioxidant enzymes in plant cells (Chen et al. 2010). The extremely high content of H_2O_2 in leaves exposed to 50 µM Cd may justify the decrease of

some of the antioxidant enzyme activities observed. In a previous screen of selectable biomarkers for Cd phytotoxicity our group has shown that high Cd concentrations (100 µM) affected some antioxidant enzymes and increased lipid peroxidation (Monteiro et al. 2009b). Therefore, these and other authors' data supported the antioxidant battery as potential reliable endpoint in surveying Cd phytotoxicity (Azevedo et al. 2005b; Monteiro et al. 2009b). However, there is heterogeneity in the responses of antioxidant enzymes to high and low concentrations of Cd (e.g., Azevedo et al. 2005b; Jin et al. 2008; Kovácik and Backor 2008; Qiu et al. 2008; Chen et al. 2010; Liu et al. 2011), and still no universal model was designed covering this Cd-oxidative stress relationship.

In this experiment, significant variations occurring in the antioxidant pathways used by leaves and roots are also shown: in general, the H_2O_2 generated by SOD is converted by CAT in leaves, the organ that accumulates less amounts of Cd. On the contrary, roots (where Cd is mostly accumulated) preferably use peroxidases pathways (POX and APX). Similarly, peroxidase was found to be the most important pathway for relief of oxidative stress in Cd stressed plants of *Matricaria chamomilla* (Kovácik and Backor 2008). In tobacco, it was found that roots present a larger number of peroxidase isoenzymes than leaves supporting different roles of these isoenzymes in plant organs (Lagrimini and Rothstein 1987). Moreover, according to Halušková et al. (2010), Cd differently activated the isoenzymes of peroxidase in barley roots. These authors hypothesized that the increases observed in peroxidase activities are associated with enhanced H_2O_2 production and lignification as a defense response. Similarly, we propose that the increase of POX and APX activities in Cd-stressed roots have both the roles of detoxification and contribution to increase cell wall lignification to prevent uncontrolled flux of Cd. Inhibition of CAT by an excessive H_2O_2 production consequent to Cd exposure may be a feasible explanation for no CAT activity alterations with Cd exposure in roots and a lower CAT activity in the highest Cd concentration in leaves (Aebi 1984).

In both roots and leaves, GR was not stimulated. In turn GSH, a major cell antioxidant molecule, is not regenerated, and an imbalance of the ratio GSH/GSSG occurs. The depletion of this antioxidant contributes to a decrease of TAA of cells to fight ROS. DalCorso et al. (2010) highlighted the fact that one mechanism that is thought to be involved in Cd sensing is the GSH/GSSG ratio and that glutathione may be involved in the differential expression

of SOD or GR. Currently, there are some contradictory results in what concerns GR activity in response to Cd (e.g., *Sedum alfredii* (Jin et al. 2008), alfalfa (Sobrino-Plata et al. 2009), *Solanum nigrum* (Deng et al. 2010), or *Tagetes patula* (Liu et al. 2011), which may be further explored.

This work demonstrates that roots and leaves have different antioxidant pathways to control excessive ROS. However, independently of the antioxidant pathway in the plant organ, it is important that the cells have an efficient TAA to balance the increase of ROS levels. The TAA decreased in 10 and 50 µM Cd exposed leaves, which is tuned with the increase of H_2O_2 levels and the consequent oxidative damages in proteins and lipids (H_2O_2 is hardly reactive with lipids and Cys) (Møller et al. 2007). Considering the high damages found in biomolecules, it should not be excluded that other ROS (besides H_2O_2) that also react with lipids and DNA (e.g., $^{\bullet}OH$**)** may have also increased (Møller et al. 2007).

On the contrary, in roots the TAA increased at 10 and 50 µM Cd. This suggests that despite being in direct contact with Cd, roots have a more efficient antioxidant capacity than leaves, which is also shown by the lower rates of biomolecule oxidation found in this organ. However, the effort to fight the increase of H_2O_2 accumulation was not enough to eliminate this ROS species and decrease the oxidative damages, mainly for higher Cd concentrations (10 and 50 µM).

The increase of lipid peroxidation and protein oxidation correlated with the increase of Cd in roots and leaves, confirming that when Cd concentrations exceed the detoxification capacity of the organ, uncontrolled oxidation of macromolecules occurs (Romero-Puertas et al. 2002; Monteiro et al. 2009b). Also the products of lipid peroxidation (e.g., MDA) can form conjugates with DNA and proteins (Møller et al. 2007) contributing to the high levels of damage observed in these molecules.

The loss of membrane integrity, a primary marker of loss of cell viability (Aly-Salama and Al-Mutawa 2009), is in accordance with the observed peroxidation of lipids and proteins and is consistent with the increase of cell senescence and death, as a consequence of exposure to Cd. However, the apparent decrease of MDA in leaves challenged by 50 µM Cd is explained by the abundance of necrotic regions in these leaves. On the contrary, roots showed no necrotic zones, but roots became light-brownish and ceased root elongation and

lateral root formation. Peroxidases regulate indoleacetic acid by catalyzing its oxidation and thus control processes regulated by this hormone such as cell elongation, cell division, and lateral root formation (Hiraga 2001).

The DNA degradation induced by Cd is evident by the comet assay, in both leaves and roots exposed to Cd. The shorter values of % tail DNA, tail length, and tail moment found in organs exposed to 10 µM can be explained by (a) Cd-DNA adduct formation that lead to DNA-DNA/DNA-protein cross-links (Hossain and Huq 2002; Valko et al. 2005); (b) and/or formation of longer DNA fragments; (c) and/or due to impairment of DNA repair mechanisms (Hartwig 2010), contributing to all the hypotheses regarding low DNA migration in electrophoresis. This particular DNA damage was also observed in experiments with Cd in *V. faba* (Koppen and Verschaeve 1996), and Pb in *Lupinus luteus* (Rucińska et al. 2004), and *N. tabacum* (Gichner et al. 2008). With 50 µM, nucleoids were too sensitive and were easily degraded during the comet procedure. Such an occurrence may be related to the high level of membranes degradation found in lettuce organs under this Cd concentration (observed by increases of membrane permeability and by protein and lipid oxidation). In these conditions, DNA may become more vulnerable to Cd exposure, and higher DNA damage would occur to such extent that it would not resist the preliminary procedure of nucleoids isolation in the comet assay. Similarly, when the DNA of *N. tabacum* and *A. cepa* was directly exposed to cadmium chloride and other mutagens, the measured DNA damage was higher than that when cells were treated with those chemicals (Bandyopadhyay and Mukherjee 2011).

According to Galbraith et al. (2001) and Loureiro et al. (2006), HPCV values of the G_0/G_1 peak from histograms of the cell cycle analysis are acceptable when below 5%, and this prerequisite was satisfied in our analyses.

In roots, Cd exposure led to an accumulation of cells in S and G_2 phases, mostly at the expense of cells in G_0/G_1. This trend of accumulation suggests that Cd induces cell cycle delay at the S phase and a blockage at G_2 checkpoint, slowing cell division. This indicates that either Cd leads to an increase of cells that pass the R-checkpoint (erroneously suggesting an increase of the "proliferation index" (as defined by Sun et al. (2007)) or the cells are delayed at S or blocked at G_2 phase, which seems most likely. Our group demonstrated, elsewhere, similar cell cycle delays in pea roots exposed to Cr(VI) (Rodriguez et al. 2011).

This trend of response may represent a cell strategy to cope with DNA damage, giving the cell extra time to repair the damage (O'Connell and Cimprich 2005) or activate an apoptosis-like program. However, some cells may continue proliferation without completing repair (Carballo et al. 2006). The S phase is particularly prone to DNA mutations accumulation increasing DNA's susceptibility to break. As a result of DNA damage and uncontrolled progress through G_2 checkpoint, entire or fragments of chromosomes may be lost during anaphase and resulting daughter cells will show cytogenetic abnormalities as MN. Because of Cd binding to sulphydryl groups of Cys (DalCorso et al. 2010), namely, in tubuline, microtubule production in G_2 phase may also have led to G_2 blockage in lettuce roots exposed to 1 µM. Then during mitosis, the mitotic spindle may become dysfunctional, consequently leading to spindle-related abnormalities as multipolar anaphases, chromosome aberrations, and/or mitotic catastrophe (only detected for 10 and 50 µM) (Seth et al. 2008). Similar to the work of Ünyayar et al. (2006), where other plant species were exposed to Cd, the MN formation in lettuce leaves and roots was increased in a non dose-dependent manner. Namely, 10 µM Cd led to a higher frequency of MN than 50 µM in roots, as observed in *A. sativum* and *V. faba* roots at the same Cd concentration, compared to higher doses. This high MN frequency at 10 µM may be related with the significant increment of HPCV of G_0/G_1, which some authors stated as an indicator of chromosome damage (Ünyayar et al. 2006). This way, the HPCV was not significantly higher at 50 µM when compared to the control, seeming to be less sensitive here than the MN assay to detect chromosome damages.

Conclusions

In conclusion, our data provide an overall perception of Cd cyto- and genotoxic effects in lettuce, depending on the organs, leaves and roots (see Figure 19). Here, the different antioxidant pathways used by roots and leaves are evidenced, in response to Cd. Overall, the H_2O_2 content increased in both organs, while the TAA decreased in leaves and increased in roots with Cd concentrations. Moreover, as consequence of ROS imbalances, in particular H_2O_2, lipids, and proteins were oxidized, membrane permeability increased, and cell viability was lost. Also, either directly or indirectly by ROS, Cd exposure also induced DNA damage. Data suggest that in roots, lower Cd concentrations led to cell cycle blockage at G_2 phase, allowing some DNA damage to be repaired, while some of the surviving cells exposed to 10 µM and mostly 50 µM do not seem to have an active G_2 checkpoint (despite of S phase delay), thus proceeding to mitosis and leading to micronucleated daughter cells.

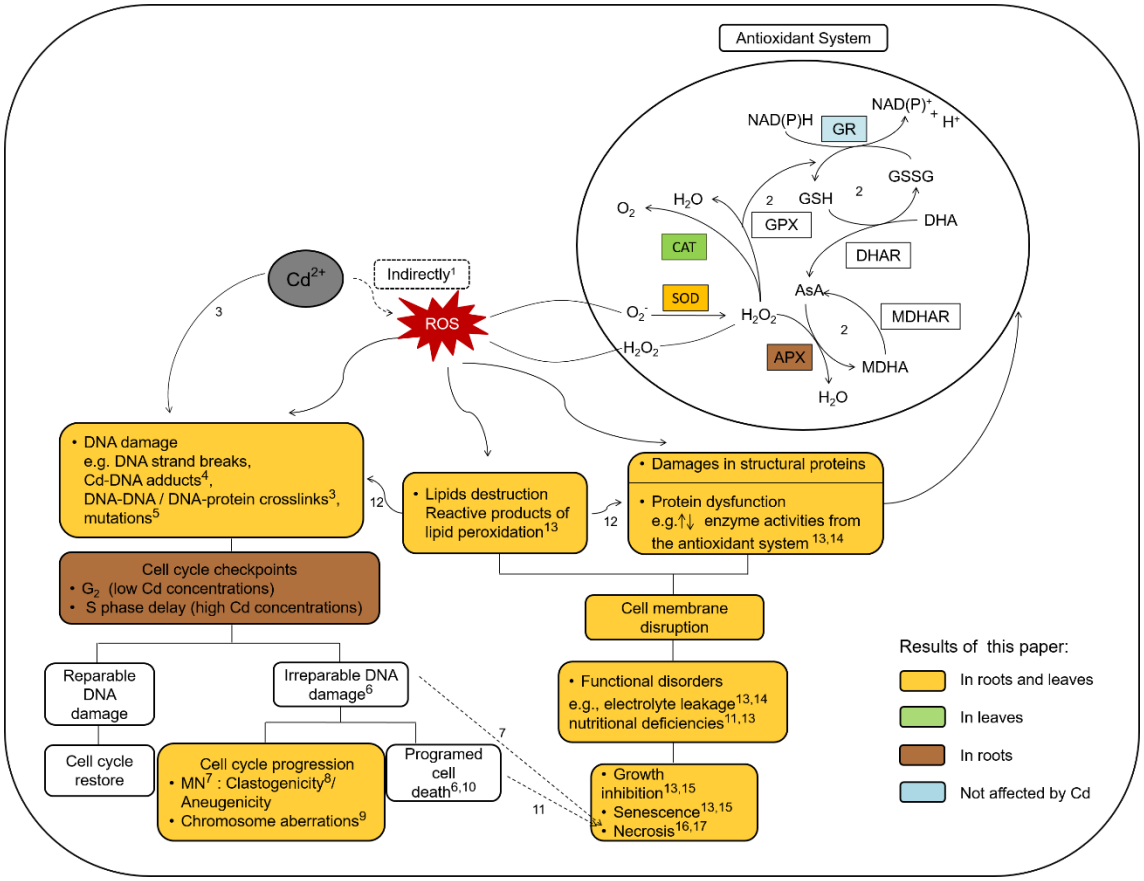

Figure 19. Overview of cyto- and genotoxic effects of Cd in lettuce leaves and roots. Despite being a non-Fenton metal, Cd increases ROS and stimulates SOD in both organs. In roots, the preferred pathway to remove H_2O_2 formed by SOD involves POX (not represented in this figure, as it represents all peroxidases in cells) and APX activities, while in leaves, the preferred pathway involves CAT. However, uncontrolled increase of ROS leads to oxidation of several macromolecules in the cell. First targets are lipids whose peroxidation alters structure and functionality; another group of sensitive macromolecules is protein, which can be oxidized (e.g., carbonylated), and consequently, its structure and functions may be affected. Both macromolecules are main constituents of membranes and their loss of structure reflects loss of integrity leading to increase of membrane permeability (a parameter for loss of cell viability). A third macromolecule affected by Cd (at least by the ROS induced) is DNA. This damage involves for example, point mutations (Monteiro et al. 2009a) and DNA strand breaks. DNA damage is an event that generally, may lead to cell cycle blockage (mostly delaying S phase and blocking at G_2 checkpoint, in lettuce roots). However, uncontrolled cell cycles may proceed and lead to abnormal mitosis leading, e.g., to MN formation. When DNA damage is too extensive, the cell may enter in programmed cell death.

White boxes indicate still unconfirmed data.

Numbers represent literature references: 1. Waisberg et al. (2003); 2. Gill and Tuteja (2011); 3. Hossain and Huq (2002); 4. Valko et al. (2005); 5. Monteiro et al. (2009b); 6. Hartwig (2010); 7. Fenech (2006); 8. Monteiro et al. (2010); 9. Seth et al. (2008); 10. Fojtová and Kovařík (2000); 11. Azevedo et al. (2005c); 12. Møller et al. (2007); 13. Monteiro et al. (2009a); 14. Azevedo et al. (2005b); 15. Azevedo et al. (2005a); 16. Schützendübel and Polle (2002); 17. Ortega-Villasante et al. (2005).

References

Achary, V. M. M., and Panda, B. B. (2010) Aluminium-induced DNA damage and adaptive response to genotoxic stress in plant cells are mediated through reactive oxygen intermediates. *Mutagen.* 25 (2), 201−209.

Aebi, H. (1984) Catalase *in vitro*. *Methods Enzymol.* 105, 121−126.

Agarwal, S., Sairam, R., Srivastava, G., and Meena, R. (2005) Changes in antioxidant enzymes activity and oxidative stress by abscisic acid and salicylic acid in wheat genotypes. *Biol. Planta.* 49 (4), 541−550.

Agrawal, S. B., and Mishra, S. (2009) Effects of supplemental ultraviolet-B irradiation and cadmium on growth, antioxidants and yield of *Pisum sativum* L. *Ecotoxicol. Environ. Saf.* 72 (2), 610−618.

Ali, M. B., Hahn, E.-J., and Paek, K.-Y. (2005) Effects of light intensities on antioxidant enzymes and malondialdehyde content during short-term acclimatization on micropropagated *Phalaenopsis* plantlet. *Environ. Exp. Bot.* 54 (2), 109−120.

Almeselmani, M., Deshmukh, P. S., Sairam, R. K., Kushwaha, S. R., and Singh, T. P. (2006) Protective role of antioxidant enzymes under high temperature stress. *Plant Sci.* 171 (3), 382−388.

An, Y.-J. (2004) Soil ecotoxicity assessment using cadmium sensitive plants. *Environ. Pollut.* 127 (1), 21−26.

Andersson, M. A., Grawé, K. V. P., Karlsson, O. M., Abramsson- Zetterberg, L. A. G., and Hellman, B. E. (2007) Evaluation of the potential genotoxicity of chromium picolinate in mammalian cells *in vivo* and *in vitro*. *Food Chem. Toxicol.* 45 (7), 1097−1106.

Aravind, P., Prasad, M. N. V., Malec, P., Aloszek, A., and Strzalka, K. (2009) Zinc protects *Ceratophyllum demersum* L. (free-floating hydrophyte) against reactive oxygen species induced by cadmium. *J. Trace Elem. Med. Biol.* 23 (1), 50−60.

Azevedo, H., Gomes, C., Pinto, G., Loureiro, S., and Santos, C. (2005a) Cadmium effects on sunflower growth and photosynthesis. *J. Plant Nutr.* 28 (12), 2211−2220.

Azevedo, H., Gomes, C., Pinto, G., and Santos, C. (2005b) Cadmium effects in sunflower: membrane permeability and changes in catalase and peroxidase activity in leaves and calluses. *J. Plant Nutr.* 28 (12), 2233−2244.

Azevedo, H., Gomes, C., Pinto, G., and Santos, C. (2005c) Cadmium effects in sunflower: nutrient imbalances in leaves and calluses. *J. Plant Nutr.* 28 (12), 2233−2241.

Bandyopadhyay, A., and Mukherjee, A. (2011) Sensitivity of *Allium* and *Nicotiana* in cellular and acellular comet assays to assess differential genotoxicity of direct and indirect acting mutagens. *Ecotoxicol. Environ. Saf.* 74 (4), 860−865.

Beers, R., and Sizer, I. (1952) A spectrophotometric method for measuring the breakdown of hydrogen peroxide by catalase. *J. Biol. Chem.* 195 (1), 133−140.

Bergmeyer, H. U. (1983) *Methods of enzymatic analysis: Vol. II, Samples, Reagents, Assessment of Results*, 3rd ed., p 268., Verlag Chemie, Weinheim, Germany.

Bradford, M. M. (1976) A rapid and sensitive method for the quantitation of microgram quantities of protein utilizing the principle of protein-dye binding. *Anal. Biochem.* 72, 248−254.

Carballo, J. A., Pincheira, J., and de la Torre, C. (2006) The G_2 checkpoint activated by DNA damage does not prevent genome instability in plant cells. *Biol. Res.* 39 (2), 331−340.

Chen, F., Wang, F., Wu, F., Mao, W., Zhang, G., and Zhou, M. (2010) Modulation of exogenous glutathione in antioxidant defense system against Cd stress in the two barley genotypes differing in Cd tolerance. *Plant Physiol. Biochem.* 48 (8), 663−672.

Clemens, S. (2006) Toxic metal accumulation, responses to exposure and mechanisms of tolerance in plants. *Biochimie*. 88 (11), 1707−1719.

Cooke, M., Evans, M., Dizdaroglu, M., and Lunec, J. (2003) Oxidative DNA damage: mechanisms, mutation, and disease. *FASEB J.* 17, 1195−1214.

DalCorso, G., Farinati, S., and Furini, A. (2010) Regulatory networks of cadmium stress in plants. *Plant Signal Behav.* 5 (6), 663−667.

Deng, X., Xia, Y., Hu, W., Zhang, H., and Shen, Z. (2010) Cadmium-induced oxidative damage and protective effects of N-acetyl-L-cysteine against cadmium toxicity in *Solanum nigrum* L. *J. Hazard Mater.* 180 (1−3), 722−729.

De Michele, R., Vurro, E., Rigo, C., Costa., A., Elviri, L., Di Valentin, M., Careri, M., Zottini, M., Sanità di Toppi, L., and Lo Schiavo, F. (2009) Nitric oxide is involved in cadmium-induced programmed cell death in arabidopsis suspension cultures. *Plant Physiol.* 150 (1), 217−228.

Dhawan, A., Bajpayee, M., and Parmar, D. (2009) Comet assay: a reliable tool for the assessment of DNA damage in different models. *Cell Biol. Toxicol.* 25 (1), 5−32.

Dhindsa, R. S., and Matowe, W. (1981) Drought tolerance in two mosses: correlated with enzymatic defense against lipid peroxidation. *J. Exp. Bot.* 32 (1), 79−91.

European Commission (2001) Decision 2455/2001/EC of the European Parliament and of the Council of 20 November 2001, establishing the list of priority substances in the field of water policy and amending Directive 2000/60/EC. *Off. J. Eur. Union.* O.J. L 331/4.

Environmental Protection Agency (2010) Priority Pollutants. Available from: http://water.epa.gov/scitech/methods/ cwa/pollutants.cfm) (accessed Dec, 2011).

Eriksson, D., Löfroth, P.-O., Johansson, L., Riklund, K. A., and Stigbrand, T. (2007) Cell cycle disturbances and mitotic catastrophes in HeLa Hep2 cells following 2.5 to 10 Gy of ionizing radiation. *Clin. Cancer Res.* 13 (18 Pt 2), 5501s−5508s.

Ernst, W. H., Krauss, G. J., Verkleij, J. A., and Wesenberg, D. (2008) Interaction of heavy metals with the sulphur metabolism in angiosperms from an ecological point of view. *Plant Cell Environ.* 31 (1), 123−143.

Evers, F., and Bücking, K. (1976) Mineral analysis, In *Modern Methods in Forest Genetics*, Proceedings in Life Science, (Nitsche, J. P., Ed.) pp 165−188, Spriger-Verlag, Berlin, Germany.

Fenech, M. (2006) Cytokinesis-block micronucleus assay evolves into a “cytome” assay of chromosomal instability, mitotic dysfunction and cell death. *Mutat. Res.* 600 (1−2), 58−66.

Fenech, M. (2007) Cytokinesis-block micronucleus cytome assay. *Nat. Protoc.* 2 (5), 1084−1104.

Fojtová, M., and Kovařík, A. (2000) Genotoxic effect of cadmium is associated with apoptotic changes in tobacco. *Plant, Cell Environ.* 23 (5), 531−537.

Galbraith, D. W., Lambert, G. M., Macas, J., and Doležel, J. (2002) Analysis of nuclear DNA content and ploidy in higher plants, In *Current Protocols in Cytometry* (Robinson, J. P., Darzynkiewicz, Z., Dean, P. N., Dressler, L. G., Rabinovitch, P. S., Stewart, C. V., Tanke, H. J., and Wheeless, L. L., Eds) pp 7.6.1−7.6.22, John Wiley & Sons, New York.

García-Medina, S., Razo-estrada, C., Galar-Martinez, M., Cortéz- Barberena, E., Gómez-oliván, L. M., Álvarez-González, I., and Madrigal- Bujaidar, E. (2011) Genotoxic and cytotoxic effects induced by aluminum in the lymphocytes of the common carp (*Cyprinus carpio*). *Comp. Biochem. Physiol.C Toxicol. Pharmacol.* 153 (1), 113−118.

Gichner, T., Patková, Z., Száková, J., and Demnerová, K. (2004) Cadmium induces DNA damage in tobacco roots, but no DNA damage, somatic mutations or homologous recombination in tobacco leaves. *Mutat. Res.* 559 (1-2), 49−57.

Gichner, T., Znidar, I., and Száková, J. (2008) Evaluation of DNA damage and mutagenicity induced by lead in tobacco plants. *Mutat. Res.* 652 (2), 186−190.

Gill, S. S., and Tuteja, N. (2011) Cadmium stress tolerance in crop plants: probing the role of sulfur. *Plant Signal Behav.* 6 (2), 215−222.

Halusková, L., Valentovicová, K., Huttová, J., Mistrík, I., and Tamás, L. (2010) Effect of heavy metals on root growth and peroxidase activity in barley root tip. *Acta Physiol. Plant.* 32 (1), 59−65.

Hartwig, A. (2010) Mechanisms in cadmium-induced carcinogenicity: recent insights. *Biometals.* 23 (5), 951−960.

Hawkins, C. L., Morgan, P. E., and Davies, M. J. (2009) Quantification of protein modification by oxidants. *Free Radical Biol. Med.* 46 (8), 965−988.

Hiraga, S., Sasaki, K., Ito, H., Ohashi, Y., and Matsui, H. (2001) A large family of class III plant peroxidases. *Plant Cell Physiol.* 42 (5), 462−468.

Hossain, Z., and Huq, F. (2002) Studies on the interaction between Cd^{2+} ions and nucleobases and nucleotides. *J. Inorg. Biochem.* 90 (3-4), 97−105.

IARC (International Agency for Research on Cancer) (1993) Beryllium, cadmium, mercury and exposures in the glass manufactur- ing industry, IARC Monographs on the Evaluation of Carcinogenic Risk of Chemicals to Humans, Vol. 58, p 444, International Agency for Research on Cancer, Lyon, France.

Jin, X, Yang, X., Islam, E., Liu, D., and Mahmood, Q. (2008) Effects of cadmium on ultrastructure and antioxidative defense system in hyperaccumulator and non-hyperaccumulator ecotypes of *Sedum alfredii* Hance. *J. Hazard. Mater.* 156 (1−3), 387−397.

Koppen, G., and Verschaeve, L. (1996) The alkaline comet test on plant cells: a new genotoxicity test for DNA strand breaks in *Vicia faba* root cells. *Mutat. Res.* 360 (3), 193−200.

Kovácik, J., and Backor, M. (2008) Oxidative status of *Matricaria chamomilla* plants related to cadmium and copper uptake. *Ecotoxicol.* 17 (6), 471−479.

Kuthanova, A., Fisher, L., Nick, P., and Opatrny, Z. (2008) Cell cycle phase-specific death response of tobacco BY-2 cell line to cadmium treatment. *Plant Cell Environ.* 31 (11), 1634−1643.

Lagrimini, L. M., and Rothstein, S. (1987) Tissue specificity of tobacco peroxidase isozymes and their induction by wounding and tobacco mosaic virus infection. *Plant Physiol.* 84 (2), 438−442.

Liu, Y. T., Chen, Z. S., and Hong, C. Y. (2011) Cadmium- induced physiological response and antioxidant enzyme changes in the novel cadmium accumulator *Tagetes patula*. *J. Hazard. Mater.* 189 (3), 724−731.

Loureiro, J., Rodriguez, E., Doležel., J., and Santos., C. (2006) Flow cytometric and microscopic analysis of the effect of tannic acid on plant nuclei and estimation of DNA content. *Ann. Bot.* 98 (3), 515−527.

Loureiro, J., Rodriguez, E., Doležel., J., and Santos., C. (2007) Two new nuclear isolation buffers for plant DNA flow cytometry: a test with 37 species. *Ann. Bot.* 100 (4), 875-888.

Lutts, S., Kinet, J. M., and Bouharmont, J. (1996) NaCl-induced senescence in leaves of rice (*Oryza sativa* L.) cultivars differing in salinity resistance. *Ann. Bot.* 78 (3), 389−398.

Møller, I. M., Jensen, P. E., and Hanson, A. (2007) Oxidative modifications to cellular components in plants. *Annu. Rev. Plant Biol.* 58, 459−481.

Monteiro, M. S., Lopes, T., Mann, R. M., Paiva, C., Soares, A. M. V. M., and Santos, C. (2009a) Microsatellite instability in *Lactuca sativa* chronically exposed to cadmium. *Mutat. Res.* 672 (2), 90−94.

Monteiro, M. S., Rodriguez, E., Loureiro, J., Mann, R. M., Soares, A. M. V. M., and Santos, C. (2010) Flow cytometric assessment of Cd genotoxicity in three plants with different metal accumulation and detoxification capacities. *Ecotoxicol. Environ. Saf.* 73 (6), 1231−1237.

Monteiro, M. S., Santos, C., Soares, A. M. V. M., and Mann, R. M. (2009b) Assessment of biomarkers of cadmium stress in lettuce. *Ecotoxicol. Environ. Saf.* 72 (3), 811−818.

Nagajyoti, P. C., Lee, K. D., and Sreekanth, T. V. M. (2010) Heavy metals, occurrence and toxicity for plants. *Environ. Chem. Lett.* 8 (3), 199−216.

Nakano, Y., and Asada, K. (1981) Hydrogen peroxide is scavenged by ascorbate specific-peroxidase in spinach chloroplasts. *Plant Cell Physiol.* 22 (5), 867−880.

O'Connell, M. J., and Cimprich, K. A. (2005) G_2 damage checkpoints: what is the turn-on? *J. Cell.Sci.* 118, 1−6.

OECD (Organization for Economic Co-operation and Development) (2006) Terrestrial plant test: seedling emergence and seedling growth test, pp 208−221, OECD, Paris.

Oliveira, H., Spanò, M., Santos, C., and Pereira, M. L. (2009) Adverse effects of cadmium exposure on mouse sperm. *Reprod. Toxicol.* 28 (4), 550−555.

Ortega-Villasante, C., Rellán-Alvarez, R., Del Campo, F. F., Carpena-Ruiz, R. O., and Hernández, L. E. (2005) Cellular damage induced by cadmium and mercury in *Medicago sativa*. *J. Exp. Bot.* 56 (418), 2239−2251.

Qiu, R.-L., Zhao, X., Tang, Y.-T., Yu, F.-M., and Hu, P.-J. (2008) Antioxidative response to Cd in a newly discovered cadmium hyperaccumulator, *Arabis paniculata*. F. *Chemosphere*.74 (1), 6−12.

Rayburn, A. L., and Wetzel, J. B. (2002) Flow cytometric analyses of intraplant nuclear DNA content variation induced by sticky chromosomes. *Cytometry*. 49 (1), 36−41.

Rodriguez, E., Azevedo, R., Fernandes, P., and Santos, C. (2011) Cr(VI) Induces DNA damage, cell cycle arrest and polyploidization: a flow cytometric and comet assay study in *Pisum sativum*. *Chem. Res. Toxicol.* 24 (7), 1040−1047.

Rodríguez-Serrano, M., Romero-Puertas, M. C., Zabalza, A., Corpas, F. J., Gómez, M., del Río, L. A., and Sandalio, L. M. (2006) Cadmium effect on oxidative metabolism of pea (*Pisum sativum* L.) roots. Imaging of reactive oxygen species and nitric oxide *in vivo*. *Plant Cell Environ.* 29 (8), 1532−1544.

Romero-Puertas, M. C., Palma, J. M., Gómez, M., del Río, L. A., and Sandalio, L. M. (2002) Cadmium causes the oxidative modification of proteins in pea plants. *Plant Cell Environ.* 25 (5), 677−686.

Rucińska, R., Sobkowiak, R., and Gwóźdź, E. A. (2004) Genotoxicity of lead in lupin root cells as evaluated by the comet assay. *Cell. Mol. Biol. Lett.* 9 (3), 519−528.

Salama, K. H. A., and Al-Mutawa, M. M. (2009) Glutathione- triggered mitigation in salt-induced alterations in plasmalemma of onion epidermal cells. *Int. J. Agric. Biol.* 11, 639−642

Schröder, P., Lyubenova, L., and Huber, C. (2009) Do heavy metals and metalloids influence the detoxification of organic xenobiotics in plants? *Environ. Sci. Pollut. Res.* 16 (7), 795−804.

Schützendübel, A., and Polle, A. (2002) Plant responses to abiotic stresses: heavy metal-induced oxidative stress and protection by mycorrhization. *J. Exp. Bot.* 53 (372), 1351−1365.

Seth, C. S., Misra, V., Chauhanb, L. K. S., and Singh, R. R. (2008) Genotoxicity of cadmium on root meristem cells of *Allium cepa*: cytogenetic and comet assay approach. *Ecotoxicol. Environ. Saf.* 71 (3), 711−716.

Sgherri, C. L. M., Loggini, B., Puliga, S., and Navari-Izzo, F. (1994) Antioxidant system in Sporobolus stapfianus: changes in response to desiccation and rehydration. *Phytochemistry*. 35 (3), 561−565.

Sobrino-Plata, J., Ortega-Villasante, C., Flores-Cáceres, M. F., Escobar, C., Del Campo, F. F., and Hernández, L. E. (2009) Differential alterations of antioxidant defenses as bioindicators of mercury and cadmium toxicity in alfalfa. *Chemosphere*. 77 (7), 946−954.

Souguir, D., Ferjani, E., Ledoigt, G., and Goupil, P. (2010) Sequential effects of cadmium on genotoxicity and lipoperoxidation in *Vicia faba* roots. *Ecotoxicol.* 20 (2), 329−336.

Souza, T. S., Hencklein, F. A., Angelis, D. F., Gonçalves, R. A., and Fontanetti, C. S. (2009) The *Allium cepa* bioassay to evaluate landfarming soil, before and after the addition of rice hulls to accelerate organic pollutants biodegradation. *Ecotoxicol. Environ. Saf.* 72 (5), 1363−1368.

Sun, J. Y., Yang, Y. S., Zhong, J., and Greenspan, D. C. (2007) The effect of the ionic products of Bioglass® dissolution on human osteoblasts growth cycle *in vitro*. *J. Tissue Eng. Regener. Med.* 1 (4), 281−286.

Ünyayar, S., Çelik, A., Çekiç, F. O., and Gözel, A. (2006) Cadmium-induced genotoxicity, cytotoxicity and lipid peroxidation in *Allium sativum* and *Vicia faba*. *Mutagenesis*. 21 (1), 77−81.

Valko, M., Morris, H., and Cronin, M. T. D. (2005) Metals, toxicity oxidative stress. *Curr. Med. Chem.* 12 (10), 1161−1208.

Villarini, M., Fatigoni, C., Dominici, L., Maestri, S., Ederli, L., Pasqualini, S., Monarca, S., and Moretti, M. (2009) Assessing the genotoxicity of urban air pollutants using two *in situ* plant bioassays. *Environ. Pollut.* 157 (12), 3354−3356.

Wagner, G. J. (1993) Accumulation of cadmium in crop plants and its consequences to human health. *Adv. Agron.* 51, 173−212.

Waisberg, M., Joseph, P., Hale, B., and Beyersmann, D. (2003) Molecular and cellular mechanisms of cadmium carcinogenesis. *Toxicology*. 192 (2-3), 95−117.

CHAPTER 3 – CHROMIUM AND CADMIUM CYTO- AND GENOTOXICITY IN HUMAN CELLS

Chapter 3.1 – Chromium-induced cyto- and genotoxicity in human osteoblasts

Cristina Monteiro, Helena Oliveira, Conceição Santos

Department of Biology and CESAM, Laboratory of Biotechnology and Cytomics, University of Aveiro

The results published in this chapter will be submitted to an international journal, with the title: Cr^{6+}-induced genotoxicity and cell cycle arrest at G_2 and S phases in human osteoblast cell line MG-63

Abstract

The main route of Cr^{6+} exposure is occupational and/or by ingestion of contaminated food/water, which justifies why cyto- and genotoxicity of Cr has been mostly evaluated in lung and intestinal cells *in vitro*. However, Cr may also allocate in bone tissues both by ingestion routes and/or due to the use of Cr containing prostheses. Chromium alloys are used in orthopedic prostheses and, as a result of wear and corrosion, Cr^{6+} is released from the prostheses and may affect bone tissue formation. The aim of this work was to evaluate the effects of clinically relevant concentrations of Cr^{6+} in human osteoblasts, by integrating genotoxicity results with possible changes in the cell cycle and cell viability. The human osteoblast cell line MG-63 was *in vitro* exposed to Cr^{6+} at concentrations ranging from 0.1 to 5 µM, for 24 and 48 h. The results pointed out a decrease of cell viability in a time- and dose-dependent manner. Related to decrease of cell viability, the cell cycle arrest and DNA damage were also found in cells exposed to Cr^{6+}. DNA damage induced by Cr^{6+} in MG-63 cells may be responsible for cell cycle arrest at G_2 or S phases observed by FCM, to allow the activation of mechanisms of DNA repair. However, abnormal cell division progression was also observed by the presence of chromosome breakage and/or loss, indicated by an increased formation of MN and NPBs identified in the CBMN assay. At the end of exposure times, 24 and 48 h, cell cycle arrest was evident, but after 29 h post-Cr^{6+} exposure (i.e. at the end of CBMN assay) Cr^{6+} did not show cytostatic effects and caused a great increase of cell death. Hence, these data suggest that throughout time after Cr^{6+} exposure, cells that had been arrested in the cell division with DNA damage may have followed cell death pathways, while some surviving ones still revealed DNA damage at chromosome level. In conclusion, Cr^{6+} induced cytotoxic and genotoxic effects in human bone cells *in vitro* at concentrations found in patients. Also, the early onset of genotoxic damage induced by Cr^{6+} at low concentrations immediately after 24 h of cell exposure alert to the relevance of periodic monitoring of humans exposed to Cr (e.g., ingestion, prosthesis) for genotoxicity diagnosis before clinical symptoms appear.

Keywords

Cell cycle arrest, DNA damage, hexavalent chromium, human osteoblasts, micronuclei

Introduction

Chromium is a metal present in several oxidation states in the environment and industry. They have been extensively used in chrome plating, wood preservation, leather tanning, and in the production of chromate, pigments and alloys. The most stable Cr forms are Cr^{3+} and Cr^{6+}, and unlike the metallic Cr and Cr^{3+}, the hexavalent form is considered human carcinogen (IARC 1990). Occupational exposure is the main route for long-term Cr^{6+} exposure and is highly related to lung cancer following inhalation of fumes (Keegan et al. 2008). Cr^{6+} may also be dispersed through the air, soil and water, leading to accumulation in humans by food and/or drinking water (IARC 1990). Moreover, many patients who need dental, hip or joint replacement are using orthopedic prostheses (Fu et al. 2008). These can be made of MoM materials, often stainless steel or Co-Cr alloys (Gunaratnam and Grant 2008). As a result of wear and corrosion, metal particles and ions are released from the prostheses to the local tissues and are disseminated throughout the body (Gunaratnam and Grant 2008; Campbell and Estey 2013). Therein metals develop local inflammatory reactions, tissue necrosis, lumps, nerve plasy, osteolysis and periprosthetic fracture resulting in aseptic loosening and pain, implant failure and need for revision surgery (Andrews et al. 2011; Campbell and Estey 2013). In rare cases these metals may be responsible for severe systemic symptoms as neurological impairment, cardiomiopathy, hypothyroidism, among other symptoms (Campbell and Estey 2013).

Epidemiological studies have been recording an increase of total Cr and other metals in biological samples (blood/serum/urine/synovial fluid) of patients using MoM prostheses. The mean blood concentration of Cr found in these patients is 14.7 µg L^{-1} (i.e. 0.28 µM), ranging from 1.24 to 123.2 µg L^{-1} (i.e. 0.02-2.37 µM) (Sidaginamale et al. 2013). Nevertheless, higher levels of Cr like 221 µg L^{-1} (i.e. 4.25 µM) can be found (Ikeda et al. 2010). Chromium ions are among the different metal ions released from prostheses surfaces, but which Cr species are released remains unclear (e.g., (Keegan et al. 2007; Andrews et al. 2011; Sidaginamale et al. 2013)). At first, Merritt and Brown (1995) concluded in their study that Cr^{6+} was released and preferentially taken by RBCs (rather than serum) where it is rapidly reduced to Cr^{3+}, while Cr^{3+} has a stronger affinity for serum, explaining the reason behind the fact that most of the Cr measured in patients was intracellular and in the state of Cr^{3+}. Later, Eiselstein and co-authors (2007) also discussed this issue, explaining that MoM prostheses form an oxide/hydroxide (i.e. $CrO_3/Cr(OH)_3$) barrier i*n vivo* which after generates

metal phosphate (i.e. $CrPO_4$), a Cr^{3+} ion found in periprosthetic tissues (Hart et al. 2010). At a first glance, only Cr^{3+} was released, but Eiselstein et al. (2007) took into account *in vivo* thermodynamic conditions, concluding that Cr^{6+} is potentially generated from the corrosion of implants.

In the extracellular environment part of Cr^{6+} is reduced to Cr^{3+} to prevent toxic effects, because Cr^{3+} has lower cell membrane permeability, entering slowly into the cell by diffusion or phagocytosis, and is less cytotoxic (Collins et al. 2010; Zhitkovich 2011). On the other hand, Cr^{6+} is rapidly taken up into the cells through sulphate and phosphate ion channels and is reduced to Cr^{5+}, Cr^{4+} and Cr^{3+} by reducing enzymes (e.g., NADPH cytochrome c reductase, GR) and non-enzymatic reductants (Afolaranmi et al. 2008). More than 95% of Cr^{6+} reduction is done by Asc, GSH and Cys, in a descending order. During Cr^{6+} reduction, ROS are generated in Fenton or Haber-Weiss reactions (Raghunathan et al. 2009). These ROS and intermediate forms of Cr can induce genetic damages, including Cr-DNA adducts, Cr-DNA crosslinks, Cr-DNA-protein crosslinks, DNA interstrand crosslinks, oxidative DNA damage, DNA DSB/SSB, and abasic sites (O'Brien et al. 2003). These damages in DNA trigger checkpoint mechanisms in the cell cycle to repair them. Irreparable damages are thought to lead to cytogenetic effects like aneuploidy, dicentric chromosomes, chromatid breaks and NPBs, and even cell death (O'Brien et al. 2003; Figgitt et al. 2010). Cytotoxic effects of Cr^{6+} on the viability and function of osteoblasts have been observed. Particularly, both short (3 days) and chronic exposure (13 days) to Cr^{6+} decreased proliferation of human osteoblasts and osteoclasts *in vitro* and inhibited osteoblast mineralization, therefore interfering with bone formation and absorption (Andrews et al. 2011). In another study, Cr^{6+} at concentrations found in patients with MoM prostheses inhibited protein, DNA and RNA synthesis and collagenase activity in rat calvarial osteoblasts (Ning et al. 2002). Using the same cell line other authors found that Cr^{6+} changed the expression of proteins involved in energy metabolism, stress signaling and proliferation (cytoskeletal proteins) (Raghunathan et al. 2010). Although genotoxic effects have been detected in several human cell types exposed to Cr^{6+}, such as epithelial cells from lung (A549 cell line) and colon (Caco-2 cell line) (Thompson et al. 2012), it is pertinent the evaluation of such effects in human osteoblasts as they are also targets of Cr^{6+}.

The aim of this work was to evaluate the effects of clinically relevant concentrations of Cr^{6+} in human osteoblasts, by integrating genotoxicity results with possible changes in the cell cycle and cell viability, and assess the usefulness of these markers as reliable endpoints in clinical assessments of Cr-induced toxicity in bone tissues.

Materials and methods

Cell culture

Human osteoblast cell line MG-63 was kindly provided by INEB – Instituto Nacional de Engenharia Biomédica, University of Porto, Portugal. MG-63 cell line was *in vitro* cultured in MEM-α medium without nucleosides, supplemented with 10% (v/v) FBS, 100 Units mL^{-1} penicillin/100 µg mL^{-1} streptomycin and 2.5 µg mL^{-1} fungizone (Life Technologies, Carlsbad, CA) at 37 °C, 5% CO_2, in humidified atmosphere. Cell confluence and morphology were daily observed using an inverted phase contrast microscope Nikon Eclipse TS100 (Japan). Cells were subcultured when confluence reached 80%, at a proportion of 1:9, using 0.25% trypsin/1 mM EDTA (Life Technologies, Carlsbad, CA). For metal exposure, cells were left 24 h for adhesion. Then, the medium was replaced by medium containing $K_2Cr_2O_7$ (Sigma-Aldrich, St. Louis, MO) at concentrations ranging from 0.1 to 5 µM. Culture media without $K_2Cr_2O_7$ served as control in each experiment. For the assessment of cell viability, MG-63 cells were cultured in the referred conditions for 24, and 48 h.

Cell viability

Cell viability was performed by the MTT assay according to Twentyman and Luscombe (1987) with slight modifications. Briefly, cells were seeded in a 96-well plate at $1x10^3$ cells/well, and after cell adhesion, they were exposed to Cr^{6+} as described above. At the end of the respective exposure time, 50 µL of MTT (Sigma-Aldrich, St. Louis, MO) solution (1 mg mL^{-1} in PBS pH 7.2, Life Technologies, Carlsbad, CA) were added to the medium and cells were then incubated for 4 h at 37 ºC, 5% CO_2, in darkness. The formed formazan crystals were solubilized with DMSO (Sigma-Aldrich, St. Louis, MO) and left on a shaking plate for 2 h at RT protected from light. Finally, the absorbance was read at 570 nm using a

microplate reader (Synergy™ HT Multi-Mode, BioTeK). Three independent assays were performed with four replicates per Cr^{6+} treatment.

Both the IC_{30} and IC_{50} of Cr^{6+} for cell viability of MG-63 cell line under the conditions tested were calculated using Sigma Plot 11.0 software (Systat Software Inc., Germany) with the four-parameter logistic function standard curve analysis for dose-response. The IC_{30} has been indicated by other authors (Tice et al. 2000) as a threshold concentration of cytotoxic effects to further analyze genotoxicity.

Cell cycle analysis

Cell cycle analysis was performed according to the method as previously described (Almeida et al. 2011) with slight modifications. Cells were plated in 6-well plates at $2x10^5$ cells/well. After Cr^{6+} treatment cells were trypsinized and centrifuged at 900*g* for 5 min at 4 ºC. Then, cells were washed with PBS pH 7.2, and resuspended in cold 85% ethanol for fixation and stored at -20 ºC.

At the time of analysis, cells were washed in PBS pH 7.2, and filtered through a 55 µm nylon mesh to eliminate large clusters. Then, for each sample 50 µg mL^{-1} RNase and 50 µg mL^{-1} PI (both from Sigma-Aldrich, St. Louis, MO) were added. Samples were then incubated for 20 min in the dark until analysis. The relative light scatter properties, SS and FS, as well as the relative FL of PI-stained nuclei were measured with a Coulter EPICS XL flow cytometer (Coulter Electronics, Hialeah, Florida, USA). The instrument was equipped with an air-cooled argon laser tuned at 15 mW and operating at 488 nm. Acquisitions were made using SYSTEM II software (v. 3.0, Beckman Coulter, USA). The amplification was adjusted so that the peak corresponding to cells in G_0/G_1 phase of cell cycle were positioned at channel 200. Four independent assays were performed, and for each sample, a minimum of 5000 events was recorded. Results were expressed as percentage of nuclei in G_0/G_1, S and G_2 phase of the cell cycle.

DNA damage

The comet assay was performed as previously described by Tice et al. (2000) with slight modifications. The cells were seeded in 6-well plates at $2x10^5$ cells/well. After Cr^{6+} exposure ending, the cells were harvested, and centrifuged at 300*g* for 4 min at 4 ºC, and washed with PBS pH 7.2. At this time, a sample of cells not treated with Cr^{6+} was exposed to 100 µM H_2O_2 (Sigma-Aldrich, St. Louis, MO) for 4 min at 4 ºC, consisting of a positive control for the comet assay. All the samples were centrifuged at 300*g* for 4 min at 4 ºC, and resuspended in PBS pH 7.2. A mixture of 50 µL of the cell suspension and 50 µL of 1% LMPA (Carl Roth GmbH + Co. KG, Karlsruhe, Germany) previously heated at 37 ºC was spread on each slide, previously covered with 1% NMPA (Fermentas, Carlsbad, CA). A coverslip was placed over the mixture and the agarose was allowed to solidify at 4 ºC for at least 10 min. Coverslips were removed and cells lysis was held for 2 h in a cold solution containing 2.5 M NaCl (Merck, Germany), 100 mM Na_2EDTA (Sigma-Aldrich, St. Louis, MO), 10mM Trizma Base (Sigma-Aldrich, St. Louis, MO), 0.2 M NaOH, pH 10 (Panreac, Barcelona, Spain), 1% Triton X-100, and 10% DMSO (both last reagents were bought from Sigma-Aldrich, St. Louis, MO). The slides were immersed in cold alkaline buffer (0.30 M NaOH and 1 mM Na_2EDTA, pH>13) for DNA unwinding (20 min), and electrophoresis at 0.74 V cm^{-1} and 300 mA for 30 min at 4 ºC. After that, slides were neutralized three times (5 min each) with 0.4 M Tris buffer pH 7.5 (Sigma-Aldrich, St. Louis, MO), and washed with distilled water. Nucleoids were stained with ethidium bromide (Sigma-Aldrich, St. Louis, MO) and examined using a fluorescence microscope (Nikon Eclipse 80i, Nikon, Tokyo, Japan) equipped with an ethidium bromide-compatible filter (excitation filter: 510-560 nm; dichroic mirror: 572; absorption filter: 590 nm). Fluorescence images of nucleoids were captured with a Digital Sight camera, software NIS-Elements F 3.00 SP7 (Nikon, Tokyo, Japan). The slides were analyzed by visual scoring of 50 comets per duplicate gel (i.e. 100 per slide). The comets were classified in five classes from 0 (undamaged, with no visible tail) to 4 (maximum damage, with most DNA in tail) (see results in Figure 23) and the total comet score was calculated and presented on a scale of 0-400 arbitrary units (Collins 2004).

CBMN assay

The CBMN assay was performed according to Fenech (2007) with some modifications. Briefly, approximately $1x10^5$ cells/well were seeded on coverslips inside 6-well plates. Cells were then treated with Cr^{6+} for 24 and 48 h, and after the exposure, cytochalasin B (Applichem, Darmstadt, Germany) at final concentration of 4 µg mL^{-1} was added to each well and incubated during 29 h. At the end of cytochalasin B treatment, cells were washed with cold PBS pH 7.2, and fixed with cold absolute methanol. Coverslips with the adherent cells were removed from the 6-well plates and left to dry in the dark until staining. The samples were stained with acridine orange (Merck, USA), a fluorochrome for nucleic acids that emits green fluorescence and orange fluorescence when binding to DNA and RNA, respectively. The cells were observed and analyzed under a fluorescence microscope Nikon Eclipse 80i (Nikon, Tokyo, Japan) equipped with an acridine orange-compatible filter (excitation filter: 450-490 nm; dichroic mirror: 505; absorption filter: 520 nm). Fluorescence images were captured with a Digital Sight camera, software NIS-Elements F 3.00 SP7 (Nikon, Tokyo, Japan). The samples from three independent biological replicates per Cr^{6+} treatment were scored for NDI, presence of NPBs and MN. The NDI provides a measure of viable cells' proliferative status and also enables the detection of cytostatic effects. It was calculated by scoring at least 500 cells for the presence of one, two, three or four nuclei. Nuclear division was not affected by the addition of cytochalasin B, but cytokinesis was arrested. The NDI formula is the following: NDI = (M1 + 2xM2 + 3xM3 +4xM4)/N, where M1 – M4 is the number of cells with 1-4 nuclei, and N is the total number of viable cells scored. NPBs and MN were scored in at least 1000 binucleated cells. MMS (Sigma-Aldrich, St. Louis, MO) treated cells were used as positive control at a final concentration of 20 µg mL^{-1}.

Statistical analysis

Three or four independent assays were performed for each analysis. All data were expressed as mean ± SD and were analyzed by one-way or two-way ANOVA, followed by a Holm-Sidak test to evaluate the significance of differences in the parameters. When necessary, data were transformed to achieve normality and equality of variances. When

justified, Pearson correlation was performed and the respective correlation coefficient was presented as *r*. The level of statistic significance was set at $p < 0.05$.

All the statistical analyses were performed with SigmaPlot Version 11.0 for Windows.

Results

Cell viability

After Cr^{6+} exposure the cell viability in terms of mitochondrial activity is represented by the dose-response curves shown in Figure 20. It was observed a dose-and time-dependent relationship at every time of exposure, where it is evident a significant inhibition of cell viability.

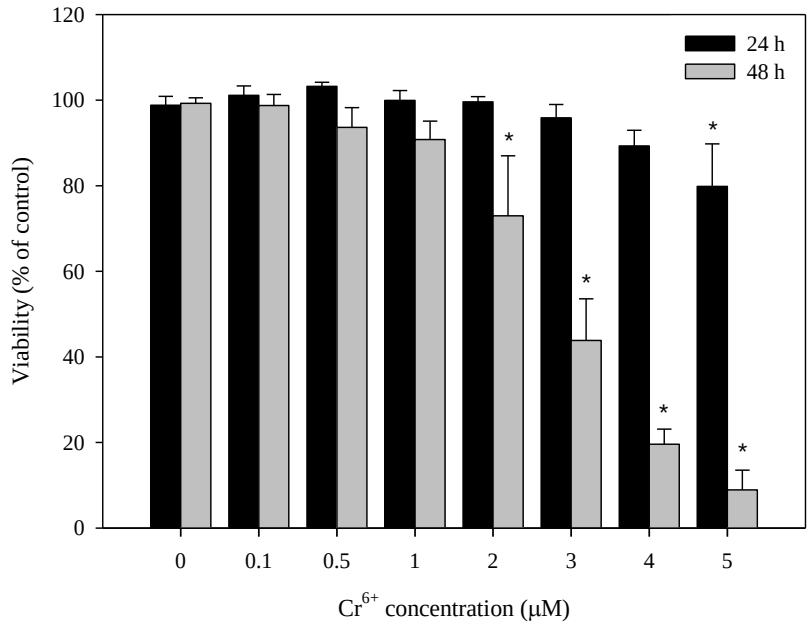

Figure 20. Cr^{6+} effects on MG-63 cell viability after 24, and 48 h of exposure. Symbol * represents significant difference relative to the control ($p < 0.001$).

After 24 h of Cr^{6+} exposure cell viability decreased to 80% at the highest dose (5 µM) and no cytotoxic effects were detected at lower doses. With 48 h of exposure cell viability decreased at a higher extent than with 24 h, specifically in the populations exposed to concentrations above 1 µM. The decrease of cell viability after 48 h became very high with

the increase of Cr^{6+} concentrations allowing the quantification of IC_{30} and IC_{50} that are 1.9 and 3.1 µM Cr^{6+}, respectively. Based on the results, and on literature recommendations, the concentrations under IC_{30} were chosen for further assays, i.e. 0.1-5 µM, and 0.1-1 µM Cr^{6+} were used in the assays of 24 and 48 h of exposure, respectively.

Cell growth and morphology of MG-63 cells after exposure to Cr^{6+} for 24 and 48h were observed by phase-contrast microscopy. Figure 21 shows representative images of control cells (Figure 21A, and D) and cells exposed to 2 (Figure 21B, and E), and 5 µM Cr^{6+} (Figure 21C, and F) after 24 and 48 h. After both times of exposure, the cell confluence began to decrease with 2 µM Cr^{6+}. At 24 h of exposure it was not observed cell death in any group of exposed-cells. After 48 h, cell death continuously increased from the Cr^{6+} concentration of 3 µM, represented by round, swollen and detached cells, also some cell debris and cells with blebs.

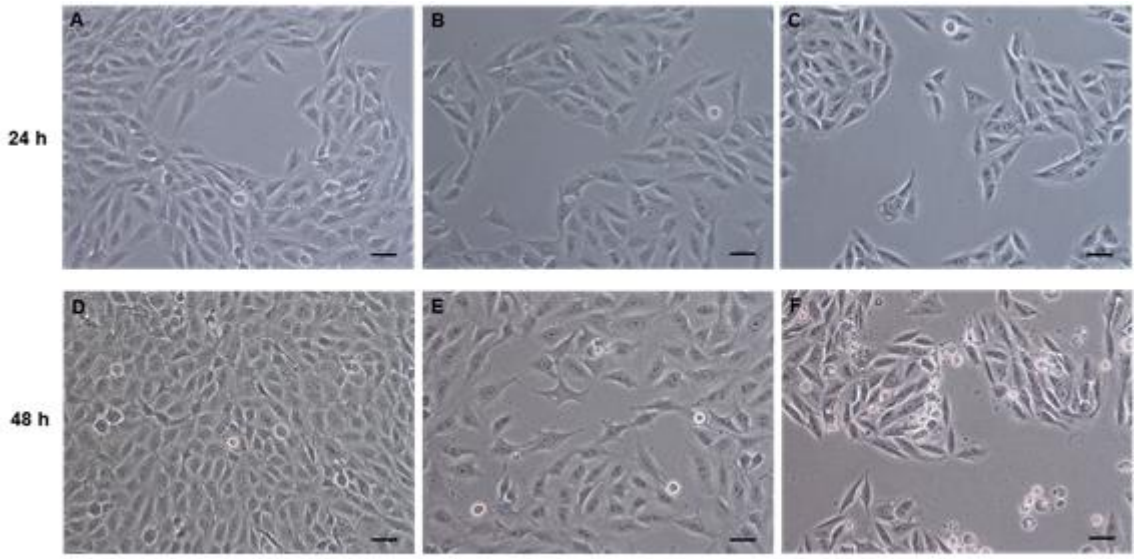

Figure 21. MG-63 cells observed under an inverted phase-contrast microscope, after Cr^{6+} exposure for 24 (A-C), and 48 h (D-F) (100x; bar: 50 µm). (A, D) Control. (B, E) 2 µM Cr^{6+}. (C, F) 5 µM Cr^{6+}.

Cell cycle analysis

By analyzing the profiles of histograms from control and exposed-cells, some cell cycle changes can be pointed out. There were significant effects on the cell cycle in all groups of

Cr^{6+}-exposed cells after 24 h of exposure (Figure 22A) and for concentrations above 0.1 µM Cr^{6+} after the 48 h (Figure 22B), with accumulation of cells at G_2 phase, as well as decrease of the population at G_0/G_1 phase. Cells also accumulated at S phase when subjected to 5 µM Cr^{6+} for 24 h.

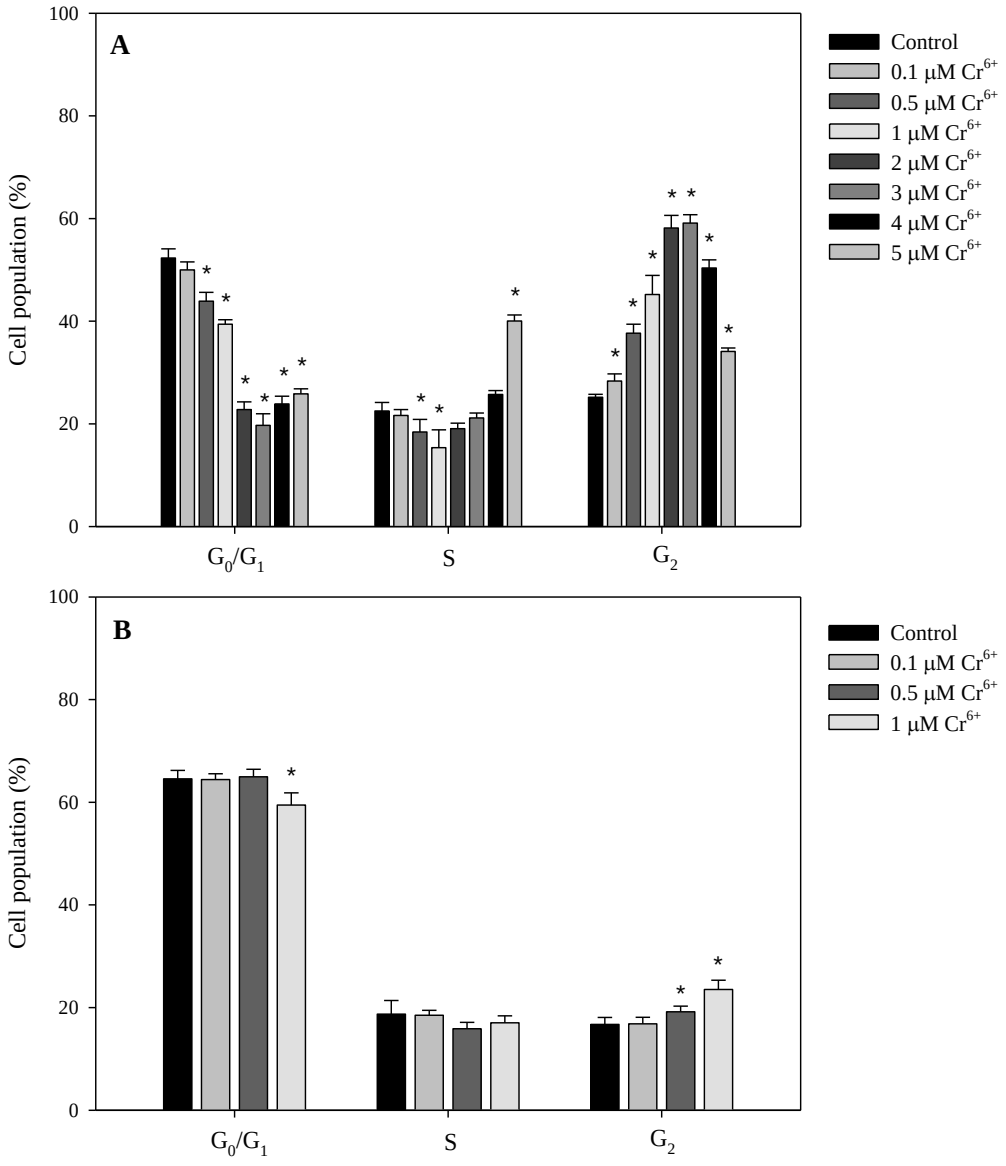

Figure 22. Effect of Cr^{6+} on cell cycle progression of MG-63 cell line. Percentage of cells in the cell cycle phases G_0/G_1, S and G_2 after 24 (A) and 48 h (B). Symbol * represents significant difference relative to the control ($p < 0.05$).

DNA damage

After visual scoring analysis of nucleoids (see Figure 23) observed in the comet assay, it was detected a time- and dose-dependent increase of DNA damage in cells exposed to Cr^{6+} concentrations above 0.5 µM for 24 h, and all concentrations applied for 48 h (Figure 24).

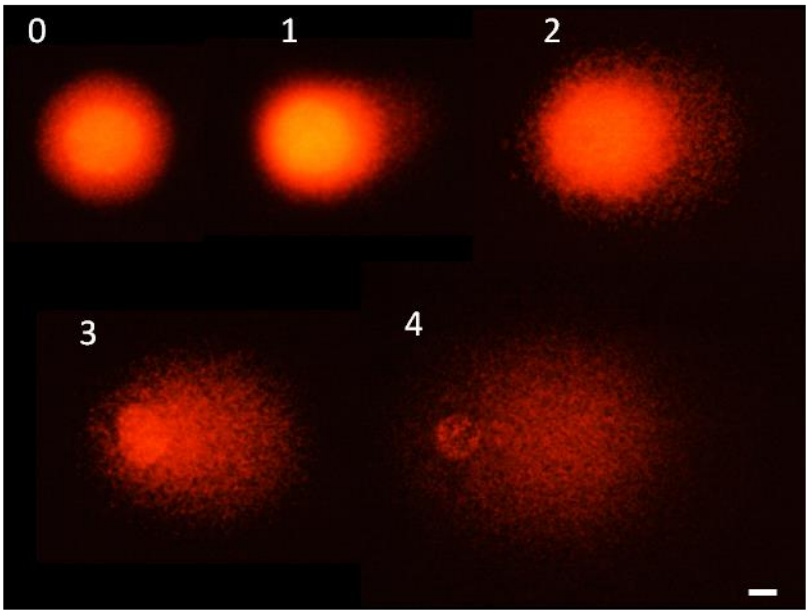

Figure 23. Images of nucleoids from MG-63 cells visualized under fluorescence microscopy (400x; bar: 10 µm). The nucleoids are representative of classes 0-4 as used in visual scoring. Comets of classes 0-3 were present in cells exposed to Cr^{6+} and positive control (H_2O_2). Comets of class 4 were only present in positive control cells.

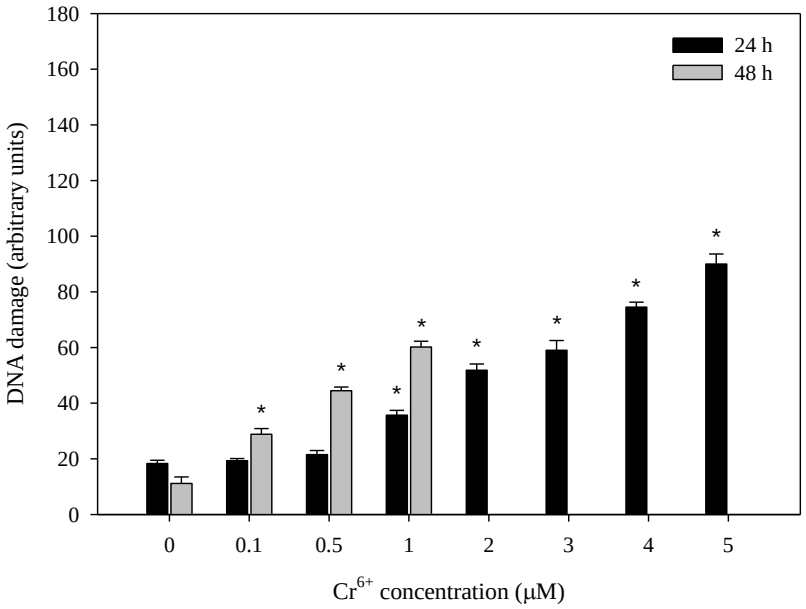

Figure 24. DNA damage induced to MG-63 cells after Cr^{6+} exposure for 24 h and 48 h. Symbol * represents significant difference relative to the control ($p < 0.001$).

According to the comet's classification, all groups subjected to Cr^{6+} exposure as well as the negative control had nucleoids of class 0 (undamaged DNA) and class 1 (Figure 25). At both times of exposure, the increase of DNA damage was mainly due to the increasing number of nucleoids of class 1. Moreover, with increasing Cr^{6+} concentrations other comet classes had appeared, indicating higher levels of DNA damage though at a relatively low percentage of cells. In particular, at 24 h of exposure nucleoids of class 2 were present in cells exposed to 4 (1.5%) and 5 µM (1.8%) Cr^{6+}, and class 3 ones only appeared in cells exposed to 5 µM (2.2%) (Figure 25A). The highly measurable level of DNA damage, i.e. nucleoids of class 4, was not detected at 24 h of exposure. After 48 h (Figure 25B) comets of class 2 began to appear with 0.5 µM and all the following concentrations. Nucleoids of class 2 were present in cells exposed to 0.5 and 1 µM for 48 h, with an incidence of 2.0% and 1.3%, respectively. Comets of classes 3 and 4 were not detected in cells exposed to 0.1-1 µM Cr^{6+} for 48 h.

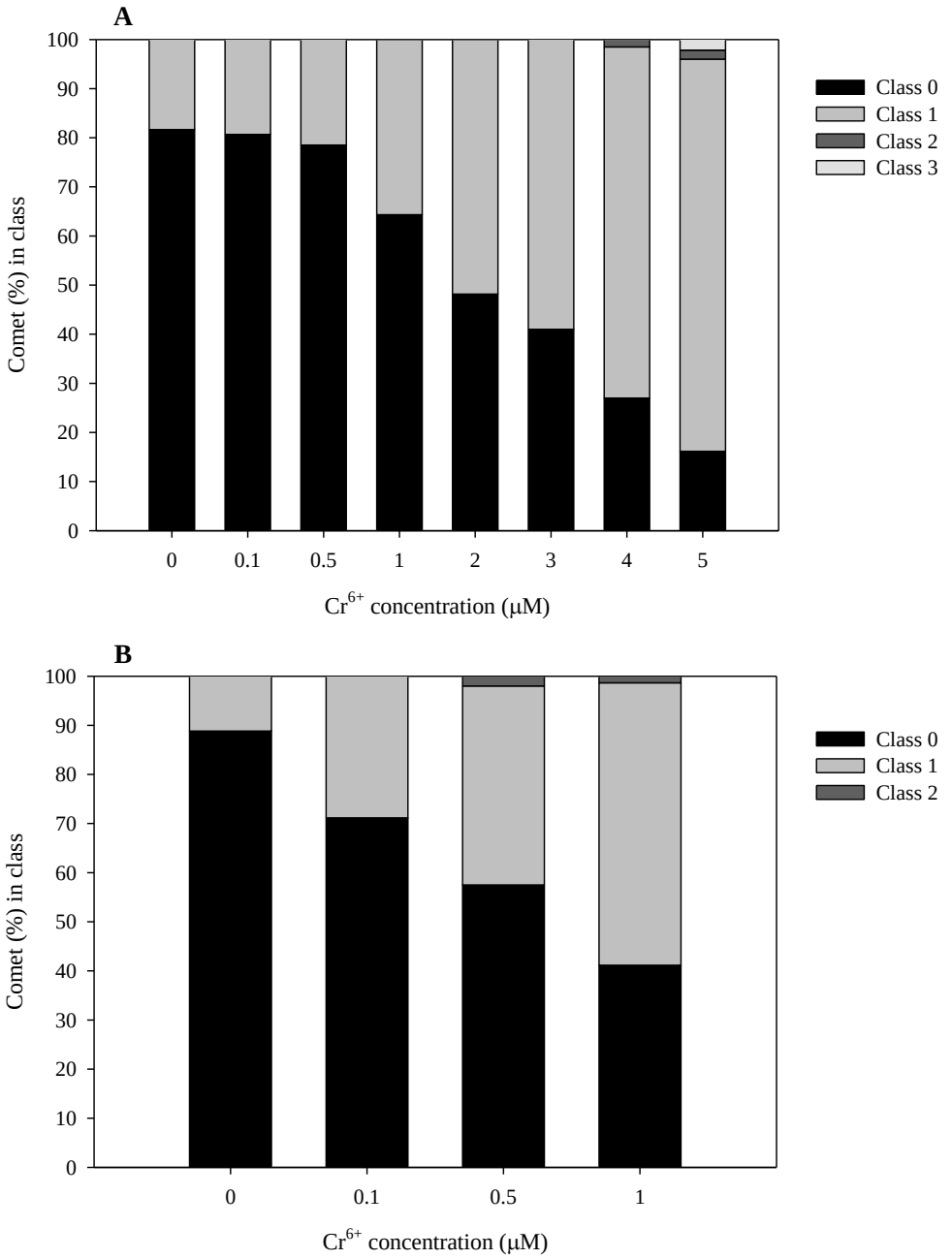

Figure 25. Classes of DNA damage induced to MG-63 cells after Cr^{6+} exposure for 24 h (A) and 48 h (B).

CBMN assay

The CBMN assay enabled to score MN, NPBs and evaluate cytostasis by the calculation of NDI on MG-63 cells exposed to Cr^{6+} (Figure 26).

After the times of Cr^{6+} exposure cells were submitted to cyto-B for 29 h and, after that, it was observed extensive cell death, predominance of mononucleated (M1) cells, very low

frequency of binucleated cells (M2) and lack of multinucleated cells (M3 and M4) in groups submitted to concentrations above 1 µM (data not shown). In this case, slides were unsatisfactory for analysis. This way, CBMN endpoints were scored only in cells exposed to up to 1 µM Cr^{6+}.

Cr^{6+} induced an increasing number of MN (Figure 26A) from the lowest Cr^{6+} dose (0.1 µM) to 1 µM for 24 h of exposure. After 48 h of exposure, the MN frequency increased in cells submitted to the Cr^{6+} dose of 1 µM.

Regarding the formation of NPBs (Figure 26B), their levels increased in cells exposed to 1 µM Cr^{6+} for 24 h. However when cells were submitted to Cr^{6+} for 48 h, the frequency of NPBs remained the same as compared to the control. Also, Figure 26C shows that NDI was not affected by Cr^{6+}.

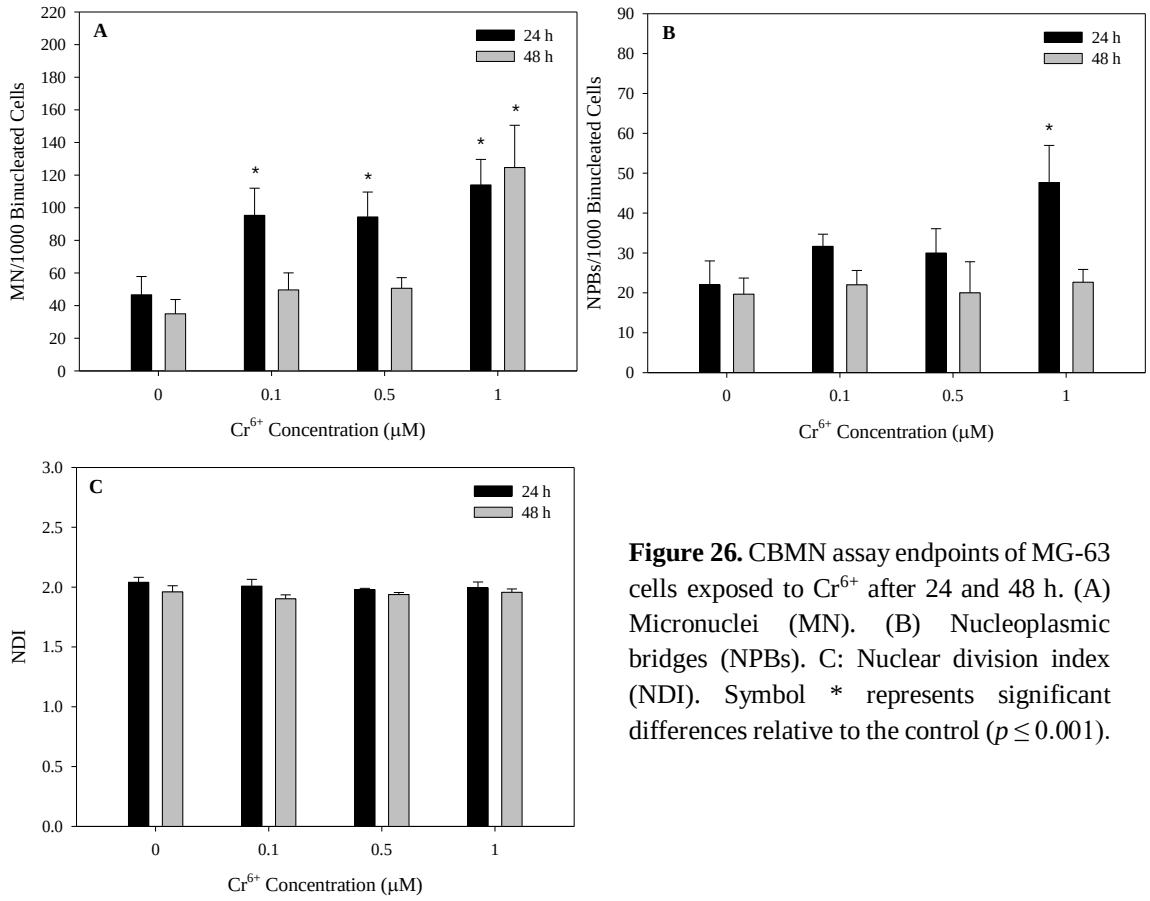

Figure 26. CBMN assay endpoints of MG-63 cells exposed to Cr^{6+} after 24 and 48 h. (A) Micronuclei (MN). (B) Nucleoplasmic bridges (NPBs). C: Nuclear division index (NDI). Symbol * represents significant differences relative to the control ($p \leq 0.001$).

Discussion

Accumulation of Cr in human tissues may have different causes, such as occupational, dietary, or Cr release from Cr-containing prostheses. Particularly, in this last case, as Cr^{6+} is thought to be released from MoM prostheses and cause bone injuries, in this work the human osteoblast cell line MG-63 was exposed to clinically relevant Cr^{6+} concentrations (from 0.1 to 5 µM) for 24 and 48 h to assess cytotoxic and genotoxic effects of Cr^{6+}. The cell viability measured in terms of mitochondrial reduction of MTT decreased in a time- and dose-dependent manner in Cr^{6+}-exposed cells, more clearly from 48 h of exposure. In addition, Cr^{6+} induced cell death when cells were treated for 48 h. Previously, other authors (Fu et al. 2007, 2008) exposed MG-63 and FFC cell lines to higher Cr^{6+} concentrations (5-20 µM) and observed a decrease of cell viability after 24 h, which however was measured using other parameters like morphological and ultrastructural changes such as swollen mitochondria, dilatation of RER and presence of large vacuoles in the cytoplasm of exposed cells, and also irregular shaped nuclei in FFC cells. Another osteoblast cell line, Saos-2, showed similar levels of Cr^{6+}-induced cytotoxicity compared to that observed in MG-63 cells in our study, i.e. those cells showed an IC_{50} of 2.2 µM CrO_3 after 72 h of exposure (Andrews et al. 2011), a value just slightly higher than that of MG-63. This little difference might be due to different reasons: $K_2Cr_2O_7$ used in the present work is more water-soluble than CrO_3, thus it may enters more easily into the cells and causing more cytotoxicity (Levis and Majone 1981). On the other hand, the influence of the culture medium has to be considered, as in this work MG-63 cells were cultured in complete MEM-α medium containing Asc, unlike the medium used for Saos-2 (DMEM) in the study of Andrews et al. (2011). In general, culture media is severely Asc deficient, so the cellular metabolism and cytotoxic effects may be distorted in such conditions (Reynolds and Zhitkovich 2007). Therefore, in the present study it was used a cell culture medium containing 250 µM Asc to create similar conditions to those physiological and also because Asc is the main and faster Cr^{6+} reducer (Wong et al. 2013). Otherwise, in cell culture medium without Asc the first Cr^{6+} reducer would be glutathione (Wong et al. 2013). The justification for exceeding normal maximum Asc concentrations in plasma, 100 µM (Levine et al. 2011), is that Asc is not stable in cell culture medium (Michels and Frei 2013).

Comparing again the differences between the sensitivity of the cell lines MG-63 and Saos-2, it can also be due to heterogeneity of cellular responses between cell lines usually

observed in toxicity assays. For example, other authors (Angle et al. 1993) showed that the osteoblast cell line HOS TE 85 when exposed to Pb showed stronger inhibition of cell proliferation than the other cell line ROS 17.28 cell line. However, when exposed to Cd ROS 17.28 was more sensitive than HOS TE 85. Therefore, considering the heterogeneous data available on Cr toxicity in osteoblasts (obtained for different cell lines, exposure conditions, etc.), and also taking into account that bone cells are sites of metal accumulation, including Cr, it would be interesting to perform a systematic comparative cytotoxic study with a large battery of osteoblast cell lines, and/or, eventually, extend this type of study to other metals.

Besides heterogeneous responses found among cells lines of the same tissue, also different sensitivities were demonstrated between cells of different tissues. For example, in this study, the viability of MG-63 cell line decreased to around 80% when exposed to the highest dose (5 µM) of Cr^{6+} for 24 h. In another study, for the same time period of exposure, it was found that macrophages showed a high decrease of viability and presented an IC_{50} of 2.48 µM Cr^{6+} (Lalaouni et al. 2007). Therefore, apparently MG-63 cells used in the present work seem to be more resistant than these macrophages used by Lalaouni et al. (2007), but the influence of different conditions must be carefully considered. Raghunathan et al. (2009) used similar conditions of culture (only different culture media due to particular growth requirements of each cell line)/exposure to compare the responses of monocytes *vs* osteoblasts after exposure to Cr^{6+} concentrations ranging 0.05-0.5 µM for 4 weeks and demonstrated that osteoblasts were more resilient, with higher levels of GSH and GR activity and expression. These authors suggested that these increases might be involved in the adaptation of cells to chronic exposure by reducing Cr^{6+} to Cr^{3+} and by scavenging ROS, leading to higher cell viability of osteoblasts (Raghunathan et al. 2009).

After 24 h of exposure of MG-63 cells to Cr^{6+} there was a decrease in cell growth (confluence) without observable cell death under phase-contrast microscopy. This seems to be related to cell cycle arrest detected by FCM, although G_2 arrest was detected at lower Cr^{6+} concentrations that did not yet lead to a visible decrease in cell confluence. Depending on the cell line or exposure conditions (Cr^{6+} concentration/exposure time), Cr^{6+} can disrupt cell cycle progression at different cell cycle phases, and thus there is not a standard response. At both times of exposure, 24 and 48 h, Cr^{6+} led to cell cycle arrest at G_2 phase (24 h: ≥ 0.1 µM; 48 h: ≥ 0.5 µM), and at 24 h the cell cycle also delayed at S phase (5 µM). MG-63 cell line

is p53-deficient, which might justify the accumulation of cells at G_2 and S phases, instead of G_0/G_1. Also in other p53-mutated cells (U937 cell line), 10 and 20 µM Cr^{6+} for 24 h induced G_2 arrest, as well as nuclear morphologic changes and DNA fragmentation related to apoptosis induced via G_2 arrest (Hayashi et al. 2004). However, in p53 wild type cell lines cells were able to block cell cycle at G_2 or S phase after Cr^{6+} exposure. For example, A549 cells arrested at G_2 when subjected to 1-25 µM Cr^{6+} for 24 h, which was associated with the generation of $^{\cdot}OH$ produced by H_2O_2 and Cr^{6+} reductive intermediates (i.e. Cr^{5+} and Cr^{4+}) (Zhang et al. 2001). Moreover, Cr^{6+} exposure in human colorectal adenocarcinoma cells (DLD1 cell line) was responsible for cell cycle delay at S phase, also resulting from ROS production (Sun et al. 2012). It was also shown that Cr^{6+} reduction and ROS generation induced DNA oxidative damage (8-OHdG) and increased γ-H2AX, a sensitive indicator of DNA DSB, in Caco-2 cells (Thompson et al. 2012). Therefore, Cr^{6+}-induced DNA damage may be responsible for cell cycle delay, as observed in MG-63 cells in the present study through the positive correlation between the increasing DNA damage and cell population at S phase after 24 h of Cr^{6+} exposure ($r = 0.714$; $p = 0.0465$). A similar integration of data involving the evaluation of DNA damage and cell cycle in other cell types showed that Cr^{6+} induced DNA DSB in normal human dermal fibroblasts (Ha et al. 2004) and HeLa cells (Wakeman et al. 2004), as well as Cr-DNA, DNA-DNA, and DNA-protein crosslinks in normal human lung cells (LL 24 cell cline) (Xu et al. 1996). In those works the authors concluded that the observed DNA damage may activate S phase checkpoint, resulting in decreased DNA synthesis by inhibition of DNA polymerase, and delay in S phase of the cell cycle.

The DNA damage observed in MG-63 cells under the tested conditions of this work was mostly detected as comets of class 1, although the level of DNA damage was rising with increasing Cr^{6+} concentrations and with time of exposure, also explaining the increase of cell populations at G_2 and S phases. While cells arrest or delay their cell cycle they activate mechanisms of DNA repair and enhances apoptosis (Chiu et al. 2010). Direct induction of DNA damage by Cr^{6+}, either by forming Cr-DNA adducts or by ROS formation during Cr^{6+} reduction, or induction of DNA damage via DNA repair pathway (Thompson et al. 2012) may be followed by chromosome breakage and/or loss.

In previous researches using non-osteoblasts, treatments with $K_2Cr_2O_7$ for 24-30 h induced chromosome breaks as well as aneuploidy after a short post-exposure time of 24-30 h (Güerci et al. 2000; Seoane et al. 2002; Figgitt et al. 2010). Furthermore, after larger post-exposure times, 2-15 days, evidence of aneuploid cells in human primary foreskin fibroblasts (BJ cell line) exposed to K_2CrO_4 was demonstrated (Figgitt et al. 2010). Using the same cell line, Glaviano et al. (2006) showed that an exposure with $K_2Cr_2O_7$ for 24 h also led to clastogenic/aneugenic effects (MN formation) after 24 h post-exposure. Even after 30 days post-exposure, MN were still present and NPBs showed up in these cells. The results of the CBMN assay in present work with MG-63 cells allowed the detection of putative DNA damage (MN and NPBs) and cytostasis (NDI) some time (29 h) after a complete cell cycle following Cr^{6+} exposure. MN and NPBs formation was higher after 24 h than 48 h of Cr^{6+} exposure. Unexpectedly, despite the observed cell cycle arrest detected by FCM, the CBMN assay showed no detectable cytostatic effects induced by Cr^{6+}. After 29 h post-Cr^{6+} exposure the level of cell death increased a lot, such a way that in the assay of 24 h of exposure every exposed-cell groups contained a population of dead cells and for concentrations above 1 µM most cells were mononucleated or dead (data not shown). Hence in the course of time after Cr^{6+} exposure, data support that cells that were arrested with DNA damage may have followed cell death pathways, and surviving ones were still revealing DNA damage at chromosome level. Corroborating this hypothesis, Pearson correlations showed positive correlation between G_2 cell population (48 h: $r = 0.957$, $p = 0.0428$) and MN formation. Moreover, DNA damage (24 h: $r = -0.894$, $p = 0.00272$; 48 h: $r = -0.955$, $p = 0.0452$), and cell cycle arrest at G_2 (48 h: $r = -0.953$, $p = 0.0469$) or delay at S (24 h: $r = -0.926$, $p = 0.000953$) induced by Cr^{6+} were also correlated with decrease of cell viability.

Conclusions

In conclusion, the results of the present study show for the first time that Cr^{6+}, at concentrations equivalent to those that may be found in humans, induced genotoxicity in human bone cells *in vitro*. DNA damage induced by Cr^{6+} has led to cell cycle arrest at G_2 and delay at S phase, also contributing to an increase of structural and/or numerical chromosome aberrations. This sequence of events contributed to decreasing cell viability. Moreover, even before cell viability had decreased, DNA damage and cell cycle alterations were already occurring in cells subjected to low concentrations of Cr^{6+} and after 24 h of exposure. These results also alert to the relevance of periodic monitoring of humans at high risk of Cr-exposure, for genotoxicity diagnosis. This is particularly relevant for patients with implantation of Cr-containing prostheses before clinical symptoms appear.

References

Afolaranmi, G. A., Tettey, J., Meek, R. M. D., and Grant, M. H. (2008) Release of chromium from orthopaedic arthroplasties. *Open Orthop. J.* 2, 10–18.

Almeida, T., Leite Ferreira, B. J. M., Loureiro, J., Correia, R. N., and Santos, C. (2011) Preliminary evaluation of the in vitro cytotoxicity of PMMA-co-EHA bone cement. *Mater. Sci. Eng: C*, 31 (3), 658–662.

Andrews, R. E., Shah, K. M., Wilkinson, J. M., and Gartland, A. (2011) Effects of cobalt and chromium ions at clinically equivalent concentrations after metal-on-metal hip replacement on human osteoblasts and osteoclasts: implications for skeletal health. *Bone*. 49 (4), 717–723.

Angle, C. R., Thomas, D. J., and Swanson, S. A. (1993) Osteotoxicity of cadmium and lead in HOS TE 85 and ROS 17/2.8 cells: relation to metallothionein induction and mitochondrial binding. *Biometals*. 6 (3), 179–184.

Campbell, J. R., and Estey, M. P. (2013) Metal release from hip prostheses: cobalt and chromium toxicity and the role of the clinical laboratory. *Clin. Chem. Lab. Med.* 51 (1), 213–220.

Chiu, A., Shi, X. L., Lee, W. K. P., Hill, R., Wakeman, T. P., Katz, A., Xu, B., Dalal, N. S., Robertson, J. D., Chen, C., Chiu, N., and Donehower, L. (2010) Review of chromium (VI) apoptosis, cell-cycle-arrest, and carcinogenesis. *J. Environ. Sci. Health C Environ. Carcinog. Ecotoxicol. Rev.* 28 (3), 188–230.

Collins, A. R. (2004) The comet assay for DNA damage and repair: principles, applications, and limitations. *Mol. Biotecnol.* 26 (3), 249-261.

Collins, B. J., Stout, M. D., Levine, K. E., Kissling, G. E., Melnick, R. L., Fennell, T. R., Walden, R., Abdo, K., Pritchard, J. B., Fernando, R. A., Burka, L. T., and Hooth, M. J. (2010) Exposure to hexavalent chromium resulted in significantly higher tissue chromium burden compared with trivalent chromium following similar oral doses to male F344/N rats and female B6C3F1 mice. *Toxicol. Sci.* 118 (2), 368–379.

Eiselstein, L. E., Proctor, D. M., and Flowers, T. C. (2007) Trivalent and hexavalent chromium issues in medical implants. *Mater. Sci. Forum*. 539-543, 698–703.

Fenech, M. (2007) Cytokinesis-block micronucleus cytome assay. *Nat. Protoc.* 2 (5), 1084–1104.

Figgitt, M., Newson, R., Leslie, I. J., Fisher, J., Ingham, E., and Case, C. P. (2010) The genotoxicity of physiological concentrations of chromium (Cr(III) and Cr(VI)) and cobalt (Co(II)): an *in vitro* study. *Mutat. Res.* 688 (1-2), 53–61.

Fu, J., Liang, X., Chen, Y., Tang, L., Zhang, Q., and Dong, Q. (2008) Oxidative stress as a component of chromium-induced cytotoxicity in rat calvarial osteoblasts. *Cell. Biol. Toxicol.* 24 (3), 201–212.

Fu, J., Liang, X., Chen, Y., Zhang, Q., Tang, L., and Zhang, N. (2007) Effect of chromium ion and antioxidant N-acetyl-cysteine on morphology of human osteoblast-like MG63 cell line. *Journal of Sichuan University. Medical Science Edition.* 38 (3), 459–462.

Glaviano, A., Nayak, V., Cabuy, E., Baird, D. M., Yin, Z., Newson, R., Ladon, D., Rubio, M. A., Slijepcevic, P., Lying, F., Mothersill, C., and Case, C. P. (2006) Effects of hTERT on metal ion-induced genomic instability. *Oncogene*. 25 (24), 3424–3435.

Güerci, A., Seoane, A., and Dulout, F. N. (2000) Aneugenic effects of some metal compounds assessed by chromosome counting in MRC-5 human cells. *Mutat. Res.* 469 (1), 35–40.

Gunaratnam, M., and Grant, M. H. (2008) Cr (VI) inhibits DNA, RNA and protein syntheses in hepatocytes: involvement of glutathione reductase, reduced glutathione and DT-diaphorase. *Toxicol. In Vitro*. 22 (4), 879–886.

Ha, L., Ceryak, S., and Patierno, S. R. (2004) Generation of S phase-dependent DNA double-strand breaks by Cr(VI) exposure: involvement of ATM in Cr(VI) induction of γ-H2AX. *Carcinogenesis*. 25 (11), 2265–2274.

Hart, A. J., Quinn, P. D., Sampson, B., Sandison, A., Atkinson, K. D., Skinner, J. A., Powell, J. J., and Mosselmans, J. F. W. (2010) The chemical form of metallic debris in tissues surrounding metal-on-metal hips with unexplained failure. *Acta Biomater.* 6 (11), 4439–4446.

Hayashi, Y., Kondo, T., Zhao, Q.-L., Ogawa, R., Cui, Z.-G., Feril, L. B., Teranishi, H., and Kasuya, M. (2004) Signal transduction of p53-independent apoptotic pathway induced by hexavalent chromium in U937 cells. *Toxicol. Appl. Pharmacol.* 197 (2), 96–106.

IARC (International Agency for Research on Cancer) (1990) Chromium, Nickel and Welding, *IARC Monographs on the Evaluation of Carcinogenic Risk of Chemicals to Humans*, Vol. 49, 49–214, International Agency for Research on Cancer, Lyon, France.

Ikeda, T., Takahashi, K., Kabata, T., Sakagoshi, D., Tomita, K., and Yamada, M. (2010) Polyneuropathy caused by cobalt-chromium metallosis after total hip replacement. *Muscle Nerve*. 42 (1), 140–143.

Keegan, G. M., Learmonth, I. D., and Case, C. P. (2007) Orthopaedic metals and their potential toxicity in the arthroplasty patient: a review of current knowledge and future strategies. *J. Bone Joint Surg. Br.* 89 (5), 567–573.

Keegan, G. M., Learmonth, I. D., and Case, C. P (2008) A systematic comparison of the actual, potential, and theoretical health effects of cobalt and chromium exposures from industry and surgical implants. *Crit. Rev. Toxicol.* 38 (8), 645–674.

Lalaouni, A., Henderson, C., Kupper, C., and Grant, M. H. (2007) The interaction of chromium (VI) with macrophages: depletion of glutathione and inhibition of glutathione reductase. *Toxicology*. 236 (1-2), 76–81.

Levine, M., Padayatty, S. J., and Espey, M. G. (2011) Vitamin C: a concentration-function approach yields pharmacology and therapeutic discoveries. *Adv. Nutr.* 2 (2), 78–88.

Levis, A. G., and Majone, F. (1981) Cytotoxic and clastogenic effects of soluble and insoluble compounds containing hexavalent and trivalent chromium. *Br. J. Cancer*. 44 (2), 219–235.

Merritt, K., and Brown, S. A. (1995) Release of hexavalent chromium from corrosion of stainless steel and cobalt-chromium alloys. *J. Biomed. Mater. Res.* 29 (5), 627–633.

Michels, A. J., and Frei, B. (2013) Myths, artifacts, and fatal flaws: identifying limitations and opportunities in vitamin C research. *Nutrients*. 5 (12), 5161–592.

Ning, J., Henderson, C., and Grant, M. H. (2002) The cytotoxicity of chromium in osteoblasts: effects on macromolecular synthesis. *J. Mater. Sci. Mater. Med.* 13 (1), 47–52.

O'Brien, T., Ceryak, S., and Patierno, S. R. (2003) Complexities of chromium carcinogenesis: role of cellular response, repair and recovery mechanisms. *Mutat. Res.* 533 (1-2), 3–36.

Raghunathan, V. K., Grant, M. H., and Ellis, E. M. (2010) Changes in protein expression associated with chronic *in vitro* exposure of hexavalent chromium to osteoblasts and monocytes: a proteomic approach. *J. Biomed. Mater. Res. A*. 92 (2), 615–625.

Raghunathan, V. K., Tettey, J. N. A., Ellis, E. M., and Grant, M. H. (2009) Comparative chronic *in vitro* toxicity of hexavalent chromium to osteoblasts and monocytes. *Mater. Res. A*. 88 (2), 543–550.

Reynolds, M., and Zhitkovich, A. (2007) Cellular vitamin C increases chromate toxicity via a death program requiring mismatch repair but not p53. *Carcinogenesis*. 28 (7), 1613–1620.

Seoane, A. I., Güerci, A. M., and Dulout, F. N. (2002) Malsegregation as a possible mechanism of aneuploidy induction by metal salts in MRC-5 human cells. *Environ. Mol. Mutagen.* 40 (3), 200–206.

Sidaginamale, R. P., Joyce, T. J., Lord, J. K., Jefferson, R., Blain, P. G., Nargol, A. V. F., and Langton, D. J. (2013) Blood metal ion testing is an effective screening tool to identify poorly performing metal-on-metal bearing surfaces. *Bone Joint Res.* 2 (5), 84–95.

Sun, L., Wang, X., Yao, H., Li, W., Son, Y.-O., Luo, J., Liu, J., and Zhang, Z. (2012) Reactive oxygen species mediate Cr(VI)-induced S phase arrest through p53 in human colon cancer cells. *J. Environ. Pathol. Toxicol. Oncol.* 31 (2), 95–107.

Thompson, C. M., Fedorov, Y., Brown, D. D., Suh, M., Proctor, D. M., Kuriakose, L., Haws, L. C., Harris, M. A. (2012) Assessment of Cr(VI)-induced cytotoxicity and genotoxicity using high content analysis. *PloS One*. 7 (8), e42720.

Tice, R. R., Agurell, E., Anderson, D., Burlinson, B., Hartmann, A., Kobayashi, H., Miyamae, Y., Rojas, E., Ryu, J.-C., and Sasaki, Y. F. (2000) Single cell gel/comet assay: guidelines for *in vitro* and *in vivo* genetic toxicology testing. *Environ. Mol. Mutagen.* 35 (3), 206–221.

Twentyman, P. R., and Luscombe, M. (1987) A study of some variables in a tetrazolium dye (MTT) based assay for cell growth and chemosensitivity. *Br. J. Cancer.* 56 (3), 279–285.

Wakeman, T. P., Kim, W.-J., Callens, S., Chiu, A., Brown, K. D., and Xu, B. (2004) The ATM-SMC1 pathway is essential for activation of the chromium(VI)-induced S-phase checkpoint. *Mutat. Res.* 554 (1-2), 241–251.

Wong, V., Armknecht, S., and Zhitkovich, A. (2013) Metabolism of Cr(VI) by ascorbate but not glutathione is a low oxidant-generating process. *J. Trace Elem. Med. Biol.* 26 (2-3), 192–196.

Xu, J., Bubley, G. J., Detrick, B., Blankenship, L. J., and Patierno, S. R. (1996) Chromium(VI) treatment of normal human lung cells results in guanine-specific DNA polymerase arrest, DNA-DNA cross-links and S-phase blockade of cell cycle. *Carcinogenesis*. 17 (7), 1511–1517.

Zhang, Z., Leonard, S. S., Wang, S., Vallyathan, V., Castranova, V., Shi, X. (2001) Cr (VI) induces cell growth arrest through hydrogen peroxide-mediated reactions. *Mol. Cell. Biochem.* 222 (1-2), 77–83.

Zhitkovich, A. (2011) Chromium in drinking water: sources, metabolism, and cancer risks. *Chem. Res. Toxicol.* 24 (10), 1617–1629.

Chapter 3.2 – Cadmium-induced cyto- and genotoxicity in human osteoblasts

Helena Oliveira, Cristina Monteiro, Francisco Pinho, Sónia Pinho, José Miguel Pimenta Ferreira de Oliveira, Conceição Santos

Department of Biology and CESAM, Laboratory of Biotechnology and Cytomics, University of Aveiro

Results presented in this chapter integrate paper published to international journal.

Oliveira, H., Monteiro, C., Pinho, F., Pinho, S., Ferreira de Oliveira, J. M. P., and Santos, C. (2014) Cadmium-induced genotoxicity in human osteoblast-like cells. *Mutat. Res. Genet. Toxicol. Environ. Mutagen.* 775-776, 38–47.

Abstract

Cadmium is a widespread heavy metal used in numerous industrial processes. Cadmium exerts toxicological effects mostly in kidney and liver. Bone is also an important target of Cd, however, the cellular mechanisms of Cd toxicological effects in the bone cells are still poorly understood. Therefore, the present work aimed to investigate the putative cytotoxic and genotoxic effects of Cd to human bone cells. For that, cells of the MG-63 cell line were exposed to 20 and 50 µM Cd for 24 and 48h. Results showed a dose-dependent increase in Cd accumulation in cells and a decrease in cell viability, especially after 48h. Cell cycle analysis showed a delay at S phase concomitant with a decrease in cells at G_0/G_1 phase. After 24h, Cd treatment downregulated the expression of *CHEK1*, *CHEK2* and *CDK2* genes and upregulated the expression of *CCNE1* gene. After 48h, the expression of *ATM* and *CCNB1* genes were downregulated. Also, a 3.3 fold increase on the expression of gene *CCNE1* was detected. Both Cd doses induced DNA fragmentation at 48h, while an increase in MN and NPBs together with an increase in the percentage of apoptotic/necrotic cells was detected for both time periods. Overall, our results demonstrate the cytotoxicity and genotoxicity of Cd in human bone cells. Also, the CBMN assay parameters (MN, NPBs and the percentage of cells under apoptosis or necrosis) together with the cell cycle appear as the most sensitive to Cd cyto- and genotoxicity, being early affected even with the lowest Cd dose. Therefore, these cyto-/genotoxic techniques may be selected for early detection of Cd-induced toxicity.

Keywords

Cadmium, cell cycle, cytotoxicity, DNA damage, genotoxicity, micronuclei

Introduction

Cadmium is a widespread metal used in several industrial processes as smelting, battery manufacturing, pigment and plastic production and also in alloys, solders and electroplating (Waisberg et al. 2003; Faroon et al. 2012). One of the main sources of exposure to Cd is tobacco smoking, mostly due to tobacco plant hyperaccumulating characteristics and contamination of the soils where tobacco plants grow (Faroon et al. 2012). Moreover, apart from being a widespread metal, Cd presents a biological half-life of 20-40 years in humans (Robards et al. 1991). Recently, Thévenod and Lee (2013) reported that chronic exposure to low Cd^{2+} doses emerged as a "*previously underestimated significant health hazard for ~10 % of the general population that increases morbidity and mortality*".

Cadmium absorbed in the body accumulates mainly in the liver and kidney and its toxicological effects are observed mostly in lungs, prostate and belly (IARC 1993). Also, the bone tissue was reported as an important target of Cd toxicity. Itai-itai disease was the most severe case of mass Cd intoxication documented and originated from industrial contamination in Jinzu river basin. Among other symptoms, this disease was characterized by osteomalacia and osteoporosis due to Cd accumulation in bone (Nordberg 2009). Cadmium appears to alter skeletal processes by decreasing the accumulation of bone mass during skeletal growth and influencing bone metabolism and maturity causing osteopenia in rats (Brzóska and Moniuszko-Jakoniuk 2004). In mice, Cd has been shown to stimulate the formation and activity of osteoclasts, the cells responsible of bone resorption (Battacharyya et al. 1988). Therefore, Cd can stimulate bone resorption and inhibit bone formation leading to bone loss. Moreover, in animals exposed to Cd bone demineralization began shortly after the start of Cd exposure and before the beginning of kidney damage (Wang and Battacharyya 1993; Wilson and Battacharyya 1997), indicating that Cd directly affects bone metabolism. Also, Ogoshi et al. (1992) reported that Cd at 100 ng/g DW in bone decreased the strength of rat femurs. These studies indicate that Cd may affect bone metabolism directly, however, the mechanisms by which Cd disrupts bone function are not fully understood.

Cadmium is not a nutrient and therefore it is unlikely to have specific dedicated transport mechanisms for cellular uptake. Studies of Lévesque et al. (2008) in osteoblast cell line MG-63 showed that Cd may enter the cell via Ca and Mg channels to enter cells and suggest that the effect of Cd in bone metabolism may be enhanced under low Ca/Mg levels.

Recently, Thévenod and Lee (2013) reviewed the cellular signaling cascades elicited by Cd and described that after acute Cd exposure, the levels of Ca and ROS increase, acting as second messenger systems in the cell. Other cell signaling mechanisms (including upstream signaling pathways for apoptosis *vs* upstream signaling pathways for cell survival) were also described (Thévenod and Lee 2013).

Cadmium does not catalyze Fenton-type reactions, however it is known to induce oxidative stress indirectly through interference in antioxidative balance by inhibition of antioxidant enzyme activities and depletion of enzymatic/non-enzymatic antioxidants such as GSH (Risso-de Faverney et al. 2001; Smith et al. 2009; Cuypers et al. 2010; Nemmiche et al. 2011, 2012). For what is known in bone cells, Brzóska et al. (2011) showed that Cd disturbs oxidative status of rat bone, contributing to damage of this tissue. It has been also hypothesized that Cd might induce oxidative stress damage in osteoblasts through the decrease of the expression of RUNX2 mRNA leading to apoptosis (Smith et al. 2009). There are also evidences that Cd does not interact directly with DNA (Valverde et al. 2001), moreover some authors consider it as "*weakly genotoxic*" ((Bertin and Averbeck 2006), for a review). However, the oxidative stress generated in Cd-exposed cells may originate DNA strand breaks, chromosomal aberration, MN occurrence and generation of 8-OHdG in several types of mammalian cells (Mikhailova et al. 1997; Filipic and Hei 2004; Nemmiche et al. 2012; Pereira et al. 2013). Wang et al. (2013) found that rats exposed to chronic low doses of Cd showed persistent damage in kidney with increased cell proliferation and decrease in global DNA methylation. Also, Cd exposure increased the occurrence of MN in polychromatic erythrocytes in rats (Celik et al. 2005) and in fish models (zebrafish) (Cambier et al. 2010). Finally, humans occupationally exposed to Cd showed increased levels of chromosomal aberrations and sister chromatid exchanges (Abrahim et al. 2007). These authors highlighted the reliability of cytogenetic techniques in the detection of Cd-induced mutagenicity (Abrahim et al. 2007). Cadmium has also been shown to interfere with genomic stability by inhibiting a number of DNA repair enzymes. In fact, Cd inhibits several systems such as NER, BER (Hartwig 2013), MMR and NHEJ, the major DSB repair pathway (Viau et al. 2008). Also, our previous work proved that Cd exposure induces microsatellite instability in mice testis (Oliveira et al. 2012).

In this context, the aim of the present study was to: (a) give an updated overview of the genotoxic and cytotoxic effects of Cd in human osteoblast cell line MG-63 using several biomarkers; (b) select the most sensitive and reliable biomarkers considering the importance of using cytogenetic techniques as a sensitive and effective means for detection of Cd-induced genotoxicity/mutagenicity.

Materials and methods

Cell culture

Human osteoblast cell line MG-63 was kindly provided by INEB – Instituto Nacional de Engenharia Biomédica, University of Porto, Portugal. MG-63 cell line was cultured *in vitro* cultured in MEM-α without nucleosides, supplemented with 10% (v/v) FBS, 100 Units mL^{-1} penicillin/100 µg mL^{-1} streptomycin and 2.5 µg mL^{-1} fungizone, (all medium components from Life Technologies, Carlsbad, CA, USA) at 37ºC, 5% CO_2, in a humidified atmosphere. Cell confluence and morphology were daily observed under an inverted phase contrast microscope Nikon Eclipse TS100 (Japan). Cells were subcultured when confluence reached 80% using 0.25% trypsin/1 mM EDTA (Life Technologies, Carlsbad, CA, USA). For metal exposure, cells were left 24 h for adhesion and after that medium was replaced with fresh medium containing $CdCl_2$ (Sigma-Aldrich, St. Louis, MO, USA) at concentrations of 20 and 50 µM (selected based on MTT results). Culture medium without $CdCl_2$ served as control in each experiment. MG-63 cells were cultured in the referred conditions for 24 h and 48 h.

Cell viability

Cell viability was performed by the MTT assay according to Twentyman and Luscombe (1987) with slight modifications. Briefly, cells were seeded in a 96-well plate at $1x10^3$ cells/well and, after cell adhesion, they were exposed to Cd from 5 to 150 µM. At the end of each exposure time, 50 µL of MTT (Sigma-Aldrich, St. Louis, MO) solution (1 mg mL^{-1} in PBS pH 7.2) were added to the medium and cells were incubated for 4 h at 37 ºC, 5% CO_2, in darkness. The formed formazan crystals were solubilized with DMSO (Sigma-Aldrich, St. Louis, MO) and left on a shaking plate for 2 h at RT protected from light. The absorbance

was read at 570 nm using the microplate reader Synergy™ HT Multi-Mode (BioTeK®, Winooski, VT, USA). The IC_{30} and IC_{50} of Cd for cell viability of MG-63 cell line under the conditions tested was calculated using Sigma Plot 11.0 software (Systat Software Inc., Germany) with the four-parameter logistic function standard curve analysis for dose-response.

For 24 h of exposure, the IC_{30} and IC_{50} of Cd for cell viability of MG-63 cells are 68 µM, and 91 µM, respectively. For 48 h of exposure, the IC_{30} and IC_{50} are 54, and 91 µM, respectively. The IC_{30} has been indicated by Tice et al. (2000) as a threshold concentration of cytotoxic effects to further analyze genotoxicity. Therefore, concentrations below that value should be used. Based on the results, two doses under IC_{30} were chosen for further assays: 20 and 50 µM Cd.

Cadmium quantification

Cells ($1.5x10^6$) were cultured in 100 mm dishes and exposed to Cd as described above. After Cd treatment, cells were washed and scraped in cold PBS at pH 7.2. Then, cell suspensions were harvested and centrifuged at 1000*g* for 10 min at 4ºC and the pellets were resuspended in 300 µL of cold ultrapure water. Then, samples were homogenized by sonication for 30 s, intermittently. From these samples, 50 µL were retrieved for total protein quantification by the Bradford (1976) method. For Cd quantification, 200 µL of concentrated HNO_3 (65% (v/v)) (Panreac, Barcelona, Spain) were added to 200 µL of remaining sample. Each sample was vortexed and placed in a water bath for 2h at 80ºC and then transferred to 60ºC overnight. Finally, the three independent biological replicates per Cd treatment samples were diluted with ultra pure water to yield 4% HNO_3 final concentration and stored at RT until Cd analysis by ICP-OES in a Jobin Yvon Activa M. Spectrometer (Horiba scientific Inc, NJ, USA). The detection limit was 2 µg L^{-1}. Cd contents were expressed as µg mg^{-1}protein.

Cell cycle analysis

Cell cycle analysis was performed according to the method described by Almeida et al. (2011) with slight modifications. Cells were seeded in 6-well plates with an initial density

of $5x10^5$ cells. After Cd treatment cells were trypsinized and centrifuged at 600*g* for 10 min at 4 ºC. Then, cells were washed with PBS pH 7.2, and resuspended in cold 85% ethanol for fixation and stored at -20 ºC.

For cell cycle analysis, fixed cells were washed in PBS pH 7.2, and filtered through a 55 µm nylon mesh to eliminate large clusters. Then, for each sample 50 µg mL^{-1} RNase and 50 µg mL^{-1} PI (both from Sigma-Aldrich, St. Louis, MO, USA) were added. Samples were then incubated for 20 min at RT in the obscurity until analysis. The relative light scatter properties, SS and FS, as well as the relative FL of PI-stained nuclei were measured with a Beckman Coulter EPICS XL flow cytometer (Coulter Electronics, Hialeah, Florida, USA). The instrument was equipped with an air-cooled argon-ion laser tuned at 15 mW and operating at 488 nm. Acquisitions were made using SYSTEM II^{TM} software (v. 3.0, Beckman Coulter, USA). The amplification was adjusted so that the peak corresponding to cells in G_0/G_1 phase of cell cycle was positioned at channel 200. For each sample, a minimum of 5000 events were recorded. Cell cycle analysis was performed using the FlowJo software **(**Tree Star Inc., Ashland, Oregon, USA). Results were expressed as percentage of nuclei in G_0/G_1, S and G_2 phases of the cell cycle.

Gene expression of cell cycle related proteins and DNA damage checkpoints

The web interface Primer3 (Rozen and Skaletsky 2000) was used for the design of gene-specific primer pairs (Table 6), which were confirmed for genome single hits by the UCSC In-Silico PCR Genome Browser (Kent et al. 2002). RNA was extracted using the Trizol method from MG-63 control and exposed to 50 µM Cd cells for 24 and 48 h. Phase-Lock Gel Heavy tubes (5 Prime 3 Prime, Inc., Boulder, CO-USA) were used for phase separation. The aqueous phase was mixed with 1 vol 70% ethanol and RNA was purified using RNeasy Mini Kit columns (Qiagen, Hilden, Germany). For cDNA synthesis, 2 µg total RNA were pre-incubated with DNase I (Sigma-Aldrich, St. Louis, MO-USA) and reverse-transcribed with 1 mM Oligo dT18, using the Omniscript RT Kit (Qiagen, Hilden, Germany). The cDNA samples were prediluted in ultrapure MilliQ water (1:20). The final individual qPCR reactions contained iQ SYBR Green Supermix (BioRad, Hercules, CA-USA), 1.5 µM each gene-specific primer and 1:4 (v/v) prediluted cDNA (1:20). At least three qPCR technical replicates were performed per sample from each of two independent biological replicates.

Average PCR efficiencies and cycle thresholds were determined from the fluorescence data using the algorithm Real-Time PCR Miner (Zhao and Fernald 2005). Gene expression relative to control cells was normalized with the *GAPDH* reference gene and calculated from the average efficiencies and cycle thresholds using the Pfaffl (2001) method.

Table 6. Oligonucleotide primer sequences used for qPCR

Gene	Forward primer (5'-3')	Reverse primer (5'-3')
ATM	GTTTGTATGGCTGTGGTGGA	AGACGGAAAGAATATGGCAGAG
CHEK1	CCCGCACAGGTCTTTCCTT	CGTGTCATTCTTTTGACCAACC
CHEK2	CACAGCTCTACCCCAGGTTC	CACAACACAGCAGCACACAC
CDC25A	GTTTGACTCCCCTTCCCTGT	GGGCCTTCTCTGGATTAGTTG
CDK2	ACCTCCCCTGGATGAAGATG	AGATGGGGTACTGGCTTGGT
CCNB1	GCTGAAAATAAGGCGAAGATCAA	ACCAATGTCCCCAAGAGCTG
CCNE1	CAGCCTTGGGACAATAATGC	GAGGCTTGCACGTTGAGTTT
GAPDH	ACACCCACTCCTCCACCTTT	TACTCCTTGGAGGCCATGTG

Indirect immunofluorescence of microtubules

Cytoskeletal components from MG-63 cells exposed to Cd were visualized through indirect immunofluorescence staining the heterodimer α-tubulin (one of the subunits of microtubules) and the F-actin (the major constituent of microfilaments). Cells were seeded on glass coverslips at $2.5x10^4$ cells/well, and Cd treatment was done as described above. For α-tubulin staining, the method was performed according to Schrader et al. (1998) with some modifications. Cells were washed with PBS, pH 7.4, fixed and permeabilized with ice-cold methanol for 30 min. After blocking with 2% BSA, cells were washed in PBS and then incubated for 1h at RT with the primary antibody monoclonal anti α-tubulin (Sigma-Aldrich, St. Louis, MO, USA), at 1:100 in PBS pH 7.4 (Sigma-Aldrich, St. Louis, MO, USA). After extensive washing in PBS, cells were incubated with fluorescently labeled secondary antibody donkey anti-mouse DαM-TRITC (Jackson ImmunoResearch Europe), at 1:300 in

PBS. For F-actin staining, cells were washed with PBS pH 7.4, fixed with 4% paraformaldehyde (Sigma-Aldrich, St. Louis, MO) (pH 7.4) for 20 min at RT, and then permeabilized with 0.2% Triton X-100 (Sigma-Aldrich, St. Louis, MO) for 10 min (Schrader et al. 1998). After blocking, cells were incubated during 20 min with rhodamine phalloidin (Molecular Probes, Thermo Fisher Scientific Inc., Waltham, MA, USA) diluted in PBS pH 7.4 (Zimmerhackl et al. 1998). Samples were examined using the Nikon Eclipse 80i microscope (Nikon, Tokyo, Japan) equipped with a PlanApo 100X objective and images were captured with a Digital Sight camera, software NIS-Elements F 3.00 SP7 (Nikon, Tokyo, Japan). Each sample was analyzed in duplicate.

DNA damage

The comet assay was performed as described by Tice et al. (2000) with slight modifications. Cells were seeded in 6-well plates at $2x10^5$ cells/well and exposed to Cd as described above. After Cd exposure, cells were harvested and washed with PBS pH 7.2. For positive control, cells were exposed to 100 µM H_2O_2 for 4 min at 4 ºC. A mixture of 50 µL of the cell suspension and 50 µL of 1% LMPA (Carl Roth GmbH + Co. KG, Karlsruhe, Germany) previously heated at 37 ºC was spread on each slide, pre-coated with 1% NMPA (Fermentas, Thermo Fisher Scientific Inc., Waltham, MA, USA). A coverslip was then placed over the mixture and the agarose was allowed to solidify at 4 ºC for 10 min. Coverslips were removed and cell lysis was held for 2 h in a solution containing 2.5 M NaCl, 100 mM EDTA, 10mM Trizma Base, 0.2 M NaOH, (pH 10), 1% Triton X-100 and 10% DMSO at 4ºC. Then slides were collected and placed in cold alkaline buffer (0.3 M NaOH and 1 mM Na_2EDTA, pH>13) for DNA unwinding (20 min) Electrophoresis was conducted at 0.74 V cm^{-1} and 300 mA for 30 min at 4 ºC. After that, slides were neutralized with 0.4 M Tris buffer pH 7.5, and washed with distilled water. Nucleoids were stained with ethidium bromide (Sigma-Aldrich, St. Louis, MO) and observed using the fluorescence microscope Nikon Eclipse 80i (Nikon, Tokyo, Japan) equipped with an ethidium bromide-compatible filter (excitation filter: 510-560 nm; dichroic mirror: 572; absorption filter: 590 nm). Fluorescence images of each nucleoid were captured with a Digital Sight camera, software NIS-Elements F 3.00 SP7 (Nikon, Tokyo, Japan). The parameters % tail DNA was calculated using image analysis software (CASPLab v1.2.2). For each sample, two gels were screened and 50-100 randomly visualized nucleoids were assayed.

CBMN assay

The CBMN assay was performed according to Fenech (2007) with few modifications. Briefly, approximately $1x10^5$ cells/well were seeded on coverslips inside 6-well plates. Cells were then exposed to Cd as described. After 24 and 48 h of Cd exposure, cytochalasin B (Applichem, Darmstadt, Germany) at concentration of 4 µg mL^{-1} was added to each well and incubated for 29 h. At the end of cytochalasin B treatment, cells were washed with cold PBS pH 7.2, and fixed with cold absolute methanol. Coverslips were air dried and stained with acridine orange (Merck, USA). Cells were observed and analyzed using the fluorescence microscope Nikon Eclipse 80i (Nikon, Tokyo, Japan) equipped with an acridine orange-compatible filter (excitation filter: 450-490 nm; dichroic mirror: 505; absorption filter: 520 nm). Fluorescence images were captured with a Digital Sight camera, software NIS-Elements F 3.00 SP7 (Nikon, Tokyo, Japan). Samples from three independent biological replicates per Cd treatment were scored for NDI, presence of NPBs, MN, and cells under apoptosis and necrosis. NDI provides a measure of viable cells' proliferative status and also enables the detection of cytostatic effects. It was calculated by scoring at least 500 cells for the presence of one, two, three or four nuclei. NPBs and MN were scored in at least 1000 binucleated cells. MMS (Sigma-Aldrich, St. Louis, MO) treated cells were used as positive control at a final concentration of 20 µg mL^{-1}. The apoptosis and necrosis assessment was conducted on the slides by scoring at least 500 cells.

Statistical analysis

Three independent assays were performed for each analysis. The qPCR data was expressed as mean ± SE, and the remaining data expressed as mean ± SD. Data were analyzed by two-way ANOVA, followed by a Holm-Sidak test to evaluate the significance of differences between the different conditions. When necessary, data were transformed to achieve normality and equality of variances. When justified, Pearson correlation was performed and the respective correlation coefficient was presented as *r*. The level of statistical significance was set at $p<0.05$. All statistical analyses were performed with SigmaPlot Version 11.0 for Windows.

Results

General cell characterization and viability

Microscopic observations of cell cultures show that Cd exposure decreased cell confluence and increased the number of cells in suspension (Figure 27). In this figure there are representative images of control cells (Figure 27A and D) and cells exposed to 20 (Figure 27B and E), and 50 µM Cd (Figure 27C and F), after 24 h and 48 h of exposure. Overall, the adherent cells were oval to spindle-shaped, resembling fibroblasts. At both times of exposure, adherent cells were decreasing with the increase of Cd concentrations, with greater incidence with 50 µM Cd. In the meantime, the cell death continuously increased from the Cd concentration of 20 µM, represented by round, swollen and detached cells, also some cell debris and cells with blebs. These facts were more pronounced after 48 h of Cd exposure than after the 24 h.

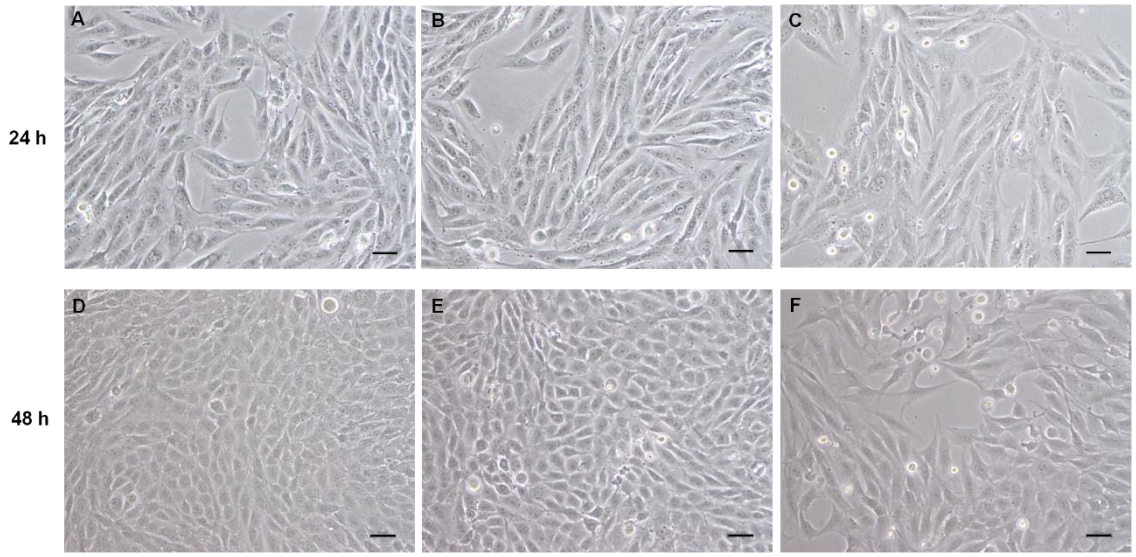

Figure 27. MG-63 cells observed using an inverted phase-contrast microscope, after Cd exposure for 24 (A-C) and 48 h (D-F). (A, D): Control; (B, E), 20 µM Cd; (C, F), 50 µM Cd (100x; bar: 50 µm).

The MTT assay was used to assess cell viability of MG-63 cells after Cd treatment. At both times of Cd exposure, 24 and 48 h, the dose-response curve of cell viability (see Figure 28) shows a dose-dependent relationship, where it is evident a significant inhibition of cell viability for Cd concentrations above 45 and 30 µM at 24 and 48 h, respectively.

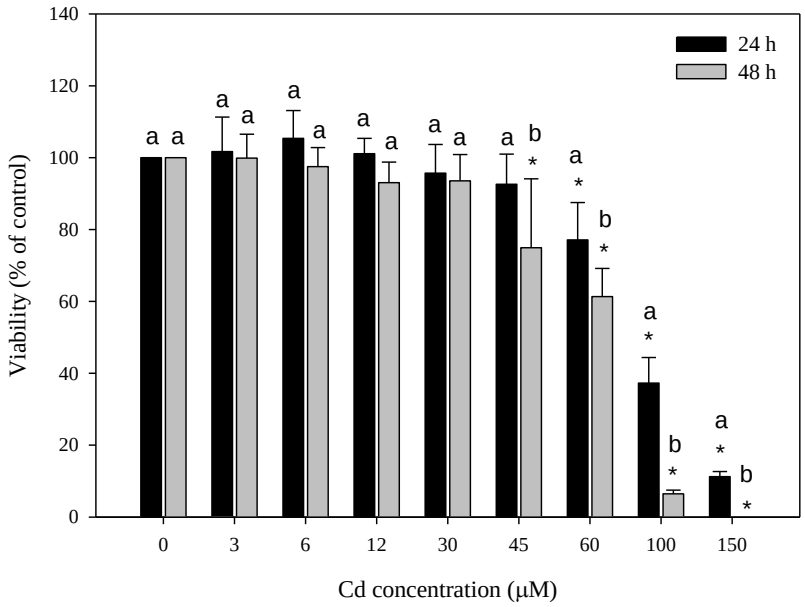

Figure 28. Cd effects on MG-63 cell viability for both times of exposure, 24 and 48 h. Symbol ∗ represents significant difference between Cd concentrations and the respective control for 24 and 48h ($p < 0.001$). Different letters represent significant difference between times of exposure for the same Cd concentration ($p < 0.05$).

The four-parameter logistic function standard curve analysis for dose-response allowed the calculation, by interpolation, of cell viability for cells exposed to 20 and 50 μM Cd. For the 24 h exposure to 50 μM dose, the viability decreased approximately 13% comparatively to the control. As for the 48 h exposure, the viability decreased 3% and 27% to 20 μM and 50 μM, respectively.

Cadmium quantification

Figure 29 shows Cd accumulation in MG-63 cells. Control cells showed levels of Cd lower than the detection limit (2 μg L^{-1}). Concerning Cd-exposed cells for all doses and exposure periods there was a significant increase ($p<0.001$) in Cd accumulation in a dose-dependent manner (r = 0.954, p = 0.045 and r = 0.952, p = 0.048 for 24 and 48 h respectively).

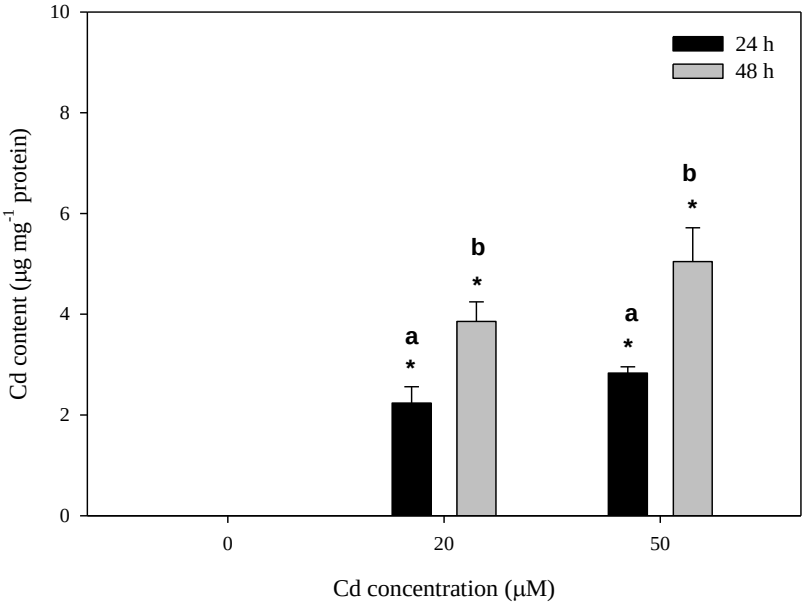

Figure 29. Intracellular Cd content in MG-63 cells after 24 and 48 h of exposure to $CdCl_2$. Symbol * represents significant difference between Cd concentrations and the respective control for 24 and 48 h of exposure (p < 0.001). Different letters represent significant difference between times of exposure for the same Cd concentration (p < 0.001).

Cell cycle analysis

Cell cycle analysis by FCM both at 24 and 48h of Cd exposure showed a decrease in the percentage of cells in G_0/G_1 phase and an S phase delay, observed by an increase of the percentage of cells in S phase (Figure 30). Cell population in G_2 phase also showed a tendency to an increase with Cd dose, but differences did not reach statistical significance ($p > 0.05$).

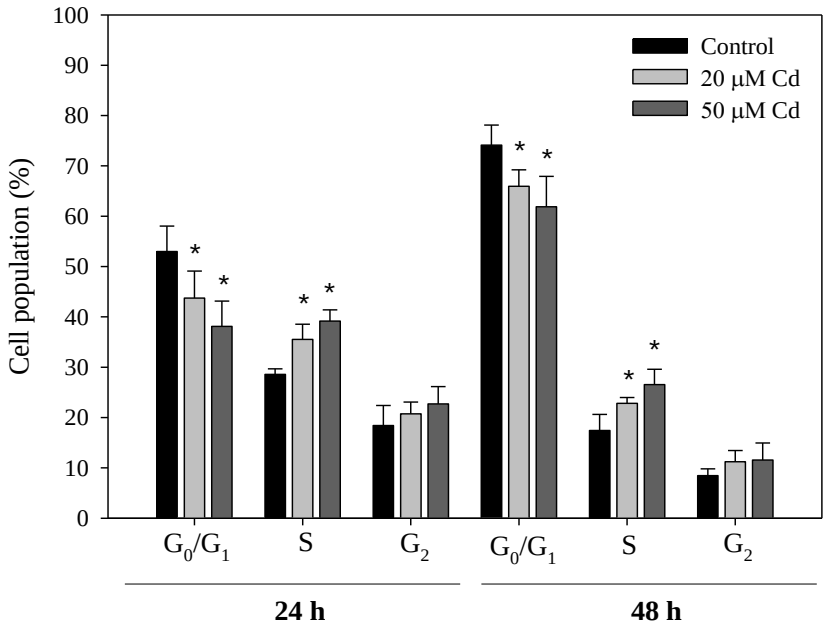

Figure 30. Effect of Cd on cell cycle progression of MG-63 cell line: percentage of cells in the cell cycle phases G_0/G_1, S and G_2 after 24 h and 48 h of exposure. Symbol * represents significant difference between Cd concentrations and the respective control for 24 and 48 h of exposure ($p < 0.05$).

Expression of genes related to the cell cycle proteins and DNA damage checkpoints

In general, the expression levels of the selected genes were affected by the exposure of MG-63 cells to 50 µM Cd, compared to the control group (Figure 31). At both times of Cd treatment, *CCNE1* was overexpressed by 2.1- and 3.4-fold, at 24 and 48 h, respectively, although it was not significant for the 48 h of exposure.

After 24h (Figure 31A) Cd at 50 µM significantly downregulated the expression of *CHEK1*, and *CHEK2* by 0.4-fold, and *CDK2* by 0.3-fold. The expression of *CHEK2* was reversed over the time, becoming upregulated by 1.3-fold after 48 h (Figure 31B). Moreover, at this time of Cd exposure, *ATM* and *CCNB1* were downregulated by 0.2- and 0.4-fold, respectively. The expression of *CDC25A* was unchanged by 50 µM Cd in both time periods.

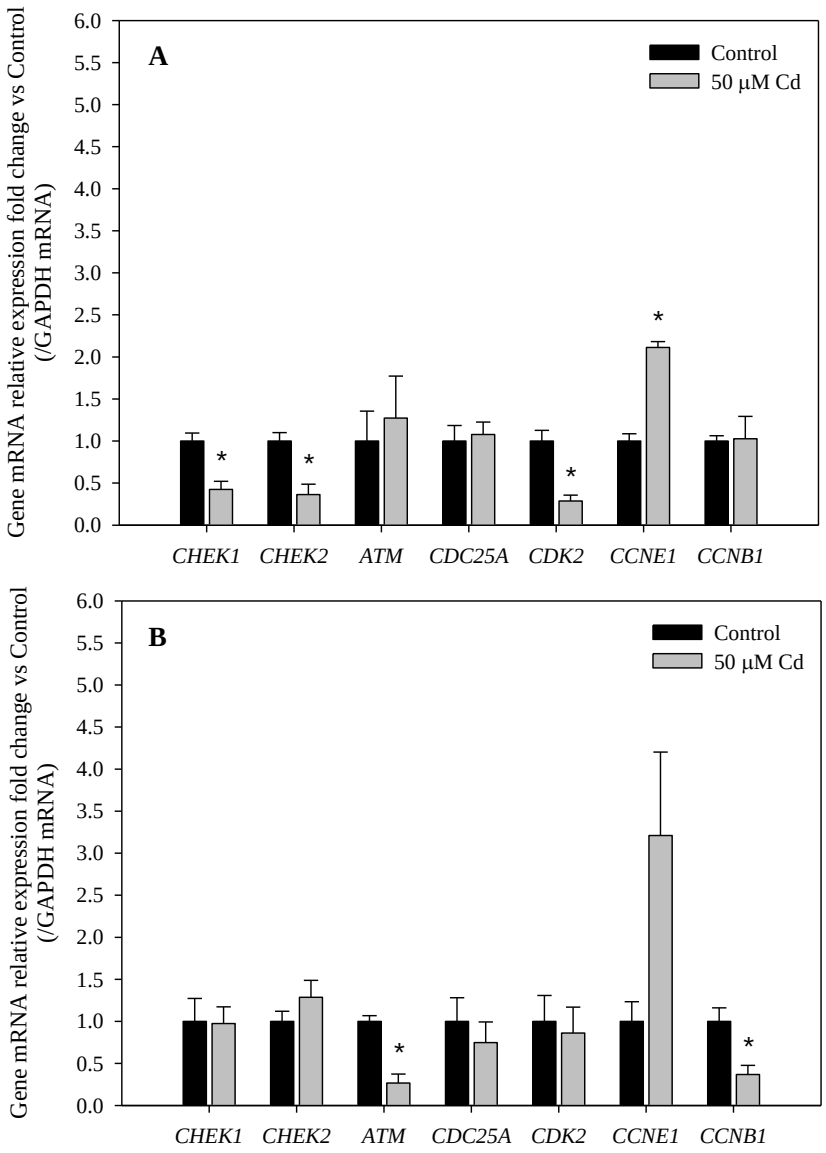

Figure 31. Relative expression of genes related to the cell cycle and DNA damage checkpoints for MG-63 cells treated with 50 μM Cd after 24 (A) and 48 h (B). Symbol * represents significant difference between Cd concentrations and the respective control for 24 and 48 h of exposure ($p < 0.05$).

Cytoskeletal organization

Figure 32 shows the effect of Cd on cytoskeletal organization at the level of both α -tubulin (Figure 32A) and F-actin (Figure 32B). These images show that Cd induced slight change on α -tubulin polymerization. Also, minimal effects were detected in the actin filaments of cells exposed to the doses of Cd tested for both periods. However, for the dose of 65 µM, a more evident degree of disruption of actin filaments was observed (data not shown).

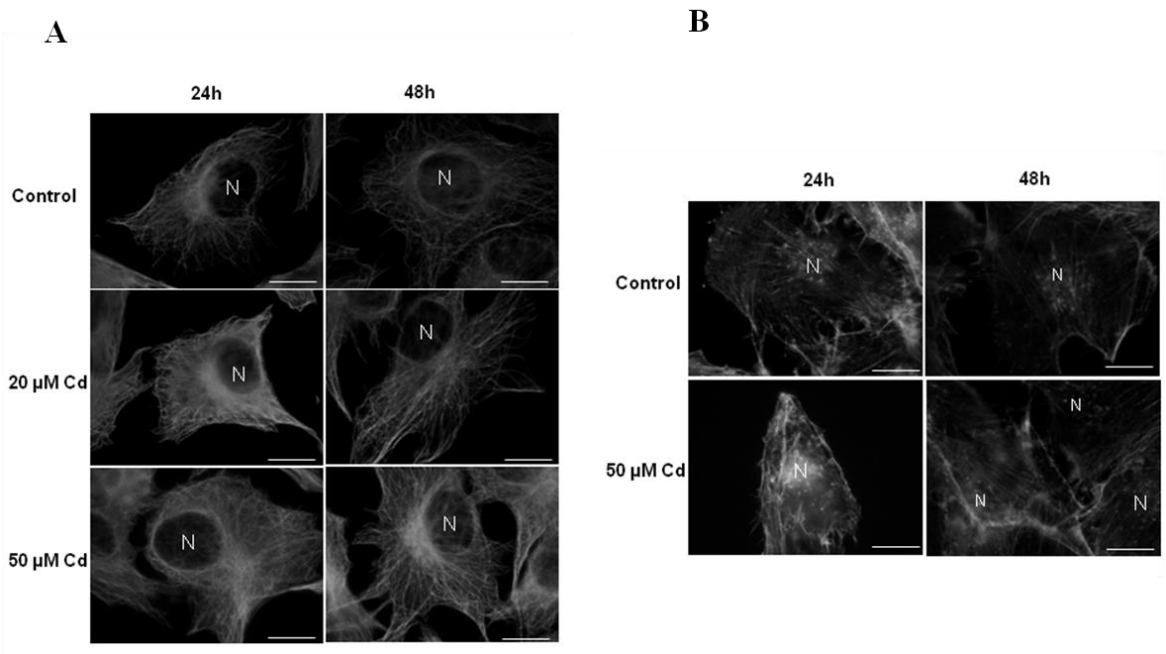

Figure 32. Effect of Cd in distribution of α-tubulin and F-actin cytoskeleton observed by fluorescence microscopy using α-tubulin antibody (A), or rhodamine phalloidin to selectively stain F-actin (B) (1000x; bar: 20 µm). N (Nucleus).

DNA damage

Comet assay was performed in order to detect DNA damage. Figure 33A-C shows representative nucleoids from the control and Cd-treated cells for 48 h observed by fluorescence microscopy. Figure 33D represents the amount of fragmented DNA, given by the % tail DNA. As can be seen in this figure DNA fragmentation increased significantly by exposure to both Cd doses at 48h, contrarily to what was found at 24h, where no statistically significant change was detected. The comet images obtained, as seen in the examples of Figure 33A-C, show that the dose of 20 µM generated a higher percentage of DNA in the tail than the dose of 50 µM.

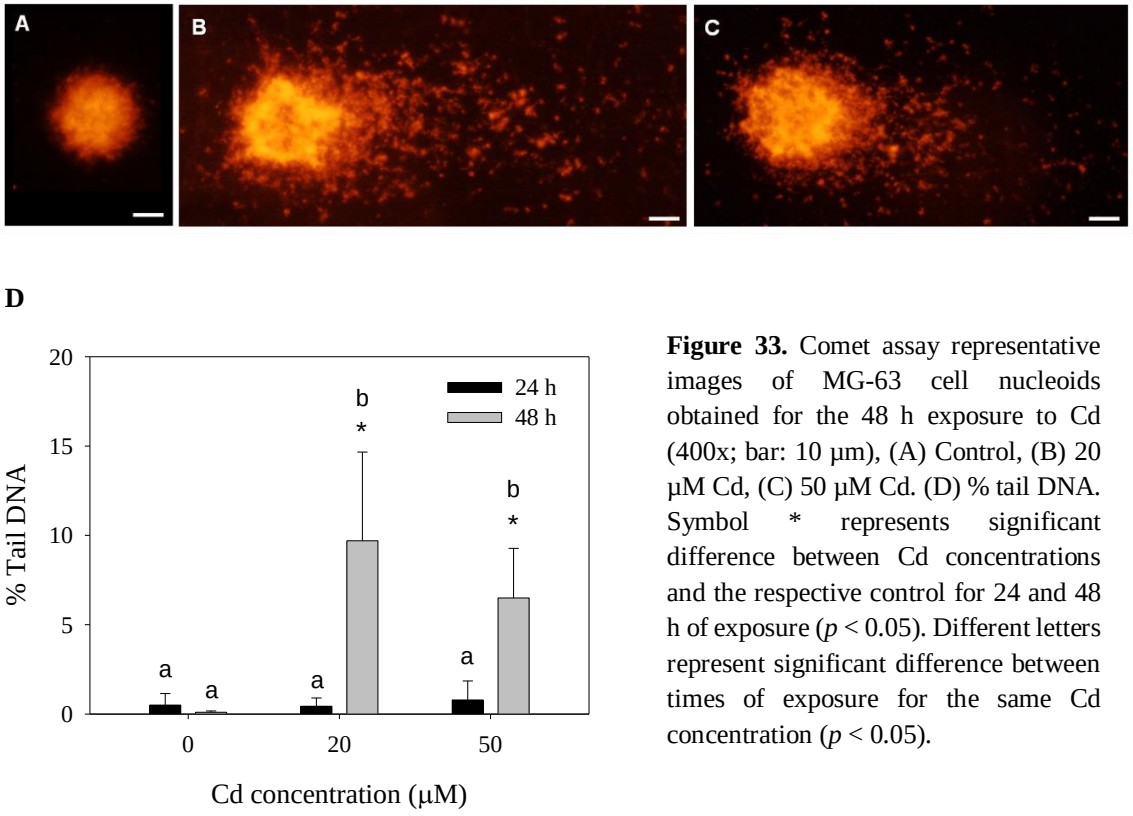

Figure 33. Comet assay representative images of MG-63 cell nucleoids obtained for the 48 h exposure to Cd (400x; bar: 10 µm), (A) Control, (B) 20 µM Cd, (C) 50 µM Cd. (D) % tail DNA. Symbol * represents significant difference between Cd concentrations and the respective control for 24 and 48 h of exposure ($p < 0.05$). Different letters represent significant difference between times of exposure for the same Cd concentration ($p < 0.05$).

CBMN assay

The CBMN assay was used to measure DNA damage (MN and NPBs), cytostasis (the proportion of mono-, bi-, and multi-nucleated cells; NDI) and cytotoxicity (necrotic and apoptotic cells) on MG-63 cells exposed to Cd (Figure 34).

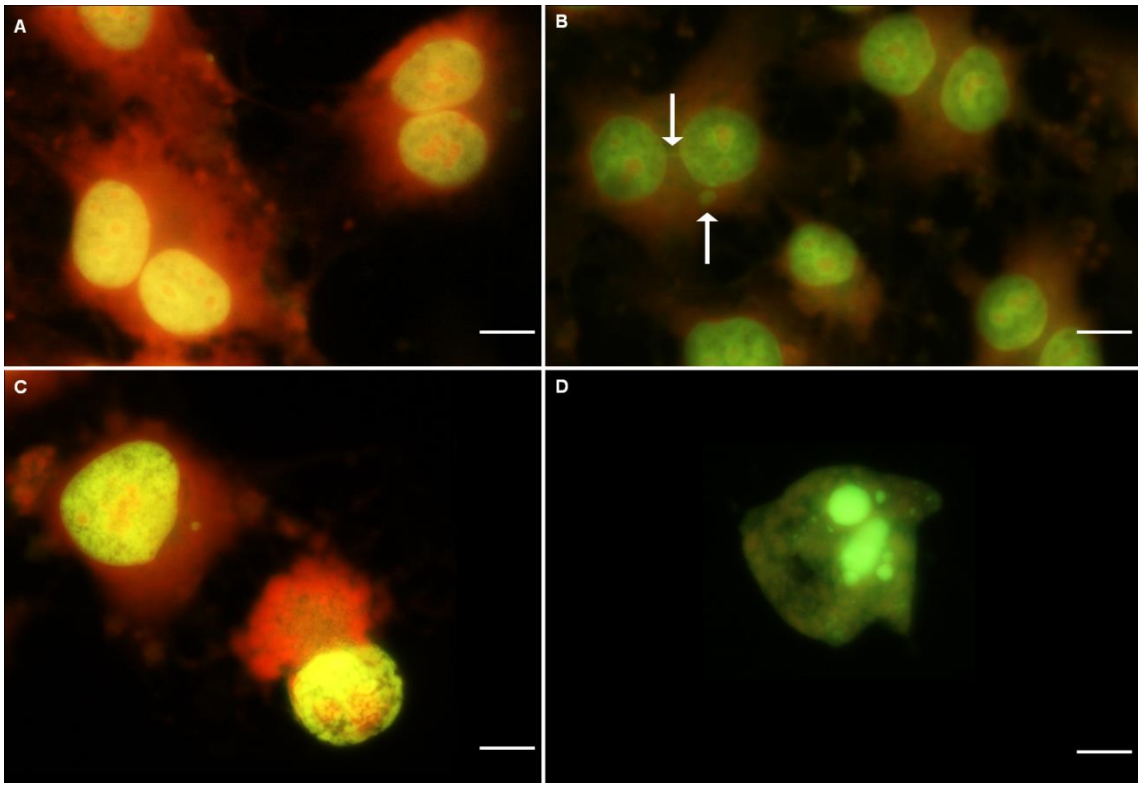

Figure 34. Representative images observed under fluorescence microscopy of MG-63 cells after Cd exposure and cytokinesis block with cytochalasin-B (400x; bar: 10 µm). (A) Binucleated cells from control sample. (B) Binucleated cell with MN pointed by upwards arrow, and NPB pointed by downwards arrow. (C) Necrotic cell. (D) Apoptotic cell.

Cd exposure induced dose-dependent increase in the percentage of MN at 24h (Figure 35A). Irrespective of the conditions tested, Cd exposure significantly increased MN frequency (Figure 35A). For 24h exposure, Cd increased MN frequency in a dose-dependent manner. For 48h exposure, however, MN frequency did not increase from 20 µM to 50 µM Cd.

The presence of NPBs also increased with Cd treatment at both time periods, except for 50 µM Cd at 48h, and being dose-dependent at 24h. However, for the dose of 50 µM Cd the frequency of NPBs was lower at 48h than at 24h (Figure 35B).

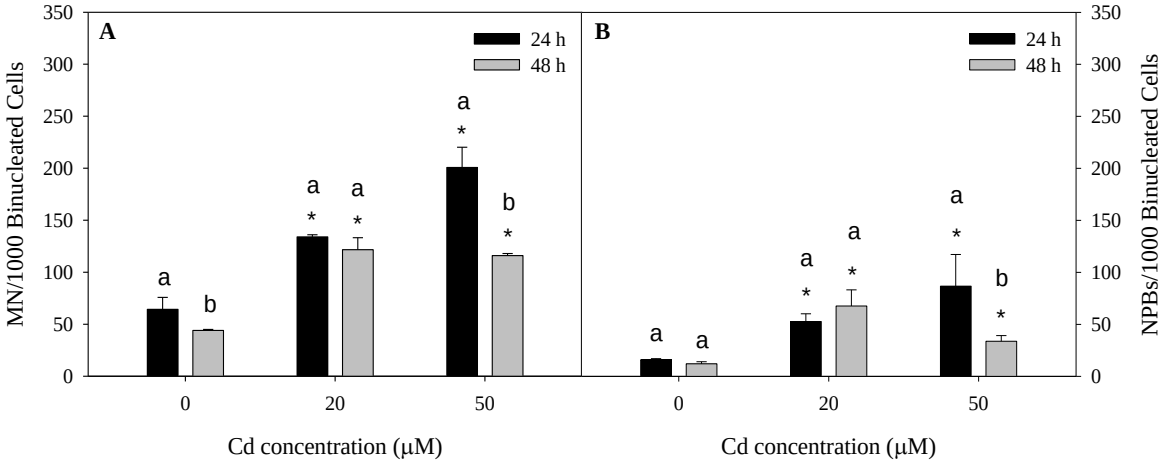

Figure 35. CBMN assay endpoints: formation of MN (A) and NPBs (B) in MG-63 cells treated with Cd for 24 and 48 h. Symbol * represents significant difference between Cd concentrations and the respective control for 24 and 48 h of exposure ($p < 0.001$). Different letters represent significant difference between times of exposure for the same Cd concentration ($p < 0.001$).

Table 7 shows the pattern of distribution of the number of nuclei per cell from 1 to 4 (M1 to M4, respectively). After both 24 and 48h there was an increase with Cd exposure in the percentage of mononucleated cells and simultaneously a decrease in the percentage of binucleated cells was detected. The frequency of multinucleated cells increased after 48 h of exposure, in particular the trinucleated cells with the Cd concentration of 50 μM, and the tetranucleated cells in a dose-dependent manner. At 24 h of Cd treatment there were not significant differences in the frequency of multinucleated cells.

Table 7. CBMN assay endpoints of MG-63 cells treated with Cd after 24 and 48h: pattern of distribution of the number of nuclei per cell from 1 to 4 (M1 to M4, respectively) and NDI [a]

	[Cd] (μM)	M1 (%)	M2 (%)	M3 (%)	M4 (%)	NDI
24 h	0	4.56 ± 0.52	91.13 ± 0.65	2.44 ± 0.21	2.06 ± 0.54	2.02 ± 0.01
	20	9.41 ± 0.67*	86.68 ± 0.89*	2.59 ± 0.22	1.99 ± 0.22	1.98 ± 0.01
	50	11.27 ± 1.40*	84.46 ± 1.02*	2.85 ± 0.88	2.00 ± 0.54	1.97 ± 0.03
48 h	0	3.96 ± 0.86	94.85 ± 1.07	1.06 ± 0.11	0.93 ± 0.31	2.01 ± 0.03
	20	7.54 ± 1.53*	88.95 ± 0.23*	1.57 ± 1.15	1.82 ± 0.33*	1.98 ± 0.04
	50	10.05 ± 1.87*	85.64 ± 2.29*	2.53 ± 0.24*	2.29 ± 0.22*	1.99 ± 0.04

[a]M1 – mononucleated cells; M2 – binucleated cells; M3 – trinucleated cells; M4 – tetranucleated cells. Symbol * represents significant difference relative to the control ($p < 0.05$).

Concerning the rate of cells under apoptosis and necrosis, Cd induced a significant increase in the percentage of apoptotic/necrotic cells as can be observed in Figure 36. Considering apoptosis, for the dose of 50 µM Cd there was a decrease on the rate of apoptosis at 48h of exposure, comparatively to 24h (Figure 36A). A positive correlation between Cd dose and the percentage of cells under necrosis ($r = 1$; $p = 0.016$) was found at 24h. At 48h there was an increase in the levels of necrosis for both doses, however, for 50 µM Cd there was a decrease comparatively to 24h (Figure 36B). Also, the number of cells under necrosis was lower than the observed for 20 µM Cd.

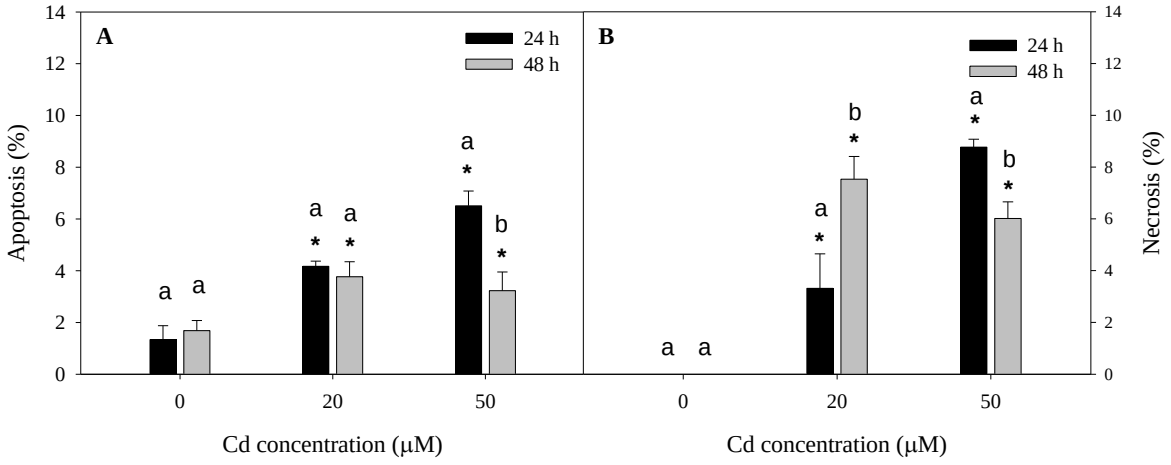

Figure 36. CBMN assay endpoints: percentage of cells under apoptosis (A) and necrosis (B) of MG-63 cell line treated with Cd for 24 and 48 h. Symbol * represents significant difference between Cd concentrations and the respective control for 24 and 48 h of exposure ($p < 0.001$). Different letters represent significant difference between times of exposure for the same Cd concentration ($p < 0.001$).

Discussion

Cytotoxic effects of Cd on human osteoblasts have been demonstrated, namely on Saos-2 (Coonse et al. 2007), and MG-63 (Lévesque et al. 2008) and also in mouse osteoblast cell lines as MC3T3-E1 cells (Martineau et al. 2010). Adherent MG-63 cells appear oval to spindle-shaped with fibroblast-like morphology and with increasing Cd concentration in culture medium cell detachment from the culture surface also increases and cells appear floating and round shaped. E-cadherin is a member of the cadherin family of Ca-dependent adhesion molecules. As Cd competes for Ca, E-cadherins are targets of Cd toxicity resulting in loss of cell-cell adhesion. The results of Prozialeck (2000) in osteoblast ROS17/28 cell

line show that Cd at low concentration (5 µM Cd for 2 h) induces cell separation and retraction from each other.

Given that MTT is reduced by mitochondrial enzymes, MTT assay measures metabolic activity of cells indicating, therefore, the cell viability and proliferation. Under the tested *in vitro* conditions, results showed that Cd affected viability of the human MG-63 cells in a time- and dose-dependent manner following a 24 h and 48 h exposure. Lévesque and co-workers (2008) characterized Cd accumulation in human osteoblast cell line MG-63 and found a decrease in cell viability upon Cd exposure to 100 µM of Cd after 3 h and a LC_{50} value of 18 µM after 24 h. In our results, the dose of 20 µM of Cd did not reduce significantly cell viability at the same period. Differences may be attributed to the presence of BSA in the culture medium, which was absent in the experiments of Lévesque et al. (2008). In fact, the presence of BSA was demonstrated to decrease Cd toxicity in this cell line (Lévesque et al. 2008) and also in Saos-2 cells (Smith et al. 2009). These authors also found a decrease in cell viability of more than 50% in Saos-2 cells exposed to 50 µM Cd for 48 h, however, after 24 h viability decreased less than 25% for the same dose (Smith et al. 2009).

Cellular signal cascades elicited by Cd are characterized by a high number of interactions e.g., between the ER stress-associated unfolded protein response, the ubiquitin-proteasome system, apoptosis, autophagy, and the cell cycle as previously reviewed (Thévenod and Lee 2013). In this respect, regulation of the cell cycle plays an eminent role in the cell's response to DNA damage induced by DNA damaging agents such as toxic metals. In this study, cell cycle analysis showed that Cd exposure induced a decrease ($p < 0.05$) in the percentage of cells in G_0/G_1 and an increase ($p < 0.05$) in the percentage of cells in S phase for both periods of analysis, suggesting a delay in S phase. This profile was associated with an increase of the levels of *CCNE1* transcript levels for cells exposed to 50 µM of Cd in both periods of analysis. *CCNE1* encodes for CCNE1 which accumulates at G_1/S boundary and is degraded as cell progresses to S phase. One of the main functions of CCNE1 is to activate CDK2 in the transition from G_1/S phase. In this context, Natrajan et al. (2012) found that *CCNE1* RNAi-mediated silencing led to G_1 arrest. Moreover, CCNB1 involved in G_2/M phase transition was found significantly underexpressed for the 48 h exposure period. G_1 phase transition and accumulation in S phase could therefore be explained by the large *CCNE1*/*CCNB1*expression ratio observed in this study.

Previous studies in the literature indicate that Cd activates cell cycle control in several types of cells. However, the degree of this disturbance varies with the treatment (time and dose of Cd exposure) and cell type. In fact, most studies in cell types other than osteoblasts refer that Cd induces cell cycle arrest at G_2/M phase. For instance, Yang and co-workers (2004) in Chinese hamster ovary cells exposed to 1 µM Cd for 8 h found an arrest at G_2/M phase, while cells exposed to 4 µM Cd arrested at S phase after 4 h. These authors also found that G_2/M arrest mainly occurred when cells were exposed to the narrow range of Cd (0.8 to 2 µM Cd) (Yang et al. 2004). Xie and Shaikh (2006) also found a time and concentration dependent increase of cells in G_2/M phase of cell cycle in rat kidney epithelial cells. However, in *Xenopus* kidney epithelial cells, Cd at 0.4 mM for 24 h was found to arrest cells at G_1 phase of cell cycle (Bjerregaard 2007).

Cao and co-workers (2007) evaluated the role of p53 in Cd-induced response in human fibroblasts and found that in p53-expressing cells, Cd inhibited DNA synthesis and arrested cells at G_2 phase, however in cells with defective p53, DNA synthesis was not affected and significantly less cells accumulated at G_2 and also no inhibition of mitosis was detected. Moreover, these authors found that p53-deffective cells were more resistant to Cd comparatively to normal cells (Cao et al. 2007). MG-63 cells are p53 deficient (Masuda et al. 1987; Diller et al. 1990; Chandar et al. 1992) and therefore the increase in S phase upon Cd exposure in MG-63 cells might be related with the p53 deficiency of this cell line. However, this effect seems to be not straightforward, since findings of Bork and co-workers (2010) revealed that in p53-deficient kidney tubular cells, an arrest at G_2/M phase of cell cycle was detected upon exposure to 100 µM Cd for 6 h. In cells with wild type p53, Cd is known to disrupt p53 native conformation, impairing p53 dependent response to DNA damage (Méplan et al. 1999). For instance, exposure to 20 mM Cd was found to suppress the p53-dependent cell cycle arrest in G_1 and G_2/M phases of cell cycle induced by γ-irradiation (Méplan et al. 1999). Nevertheless, Cao et al. (2007) found similar patterns of DNA degradation assessed by the comet assay in both normal and p53-defective cells.

The comet assay is an electrophoretic test, usually used in genotoxicity assessment detecting DNA strand breaks and alkali-labile sites in individual cells. Exposure to 20 and 50 µM Cd for a 24 h period did not result in DNA strand breaks detectable by the comet assay. This suggests that the cytotoxic effect observed at 50 µM Cd for 24 h exposure is

probably not due to induction of DNA strand breaks. After 48 h of exposure, an increase ($p < 0.05$) in the % of tail DNA was observed for both Cd doses. The level of DNA damage detected at 48 h for cells exposed to 50 µM Cd was lower than that detected for cells exposed to 20 µM Cd, however differences did not reach statistical significance ($p > 0.05$). Similar profiles were found by Risso-de Faverney et al. (2001) in rainbow trout hepatocytes exposed to Cd, who also found higher levels of DNA fragmentation in cells exposed to 2 µM rather than 10 µM of Cd. This decrease in DNA damage detected by the comet assay with increasing Cd concentration could be due to a high level DNA fragmentation and subsequent loss of the small fragments during electrophoresis (Olive et al. 1993). Our previous studies have shown that Cd is able to induce DNA fragmentation in sperm cells and microsatellite instability *in vivo* in testis of mice exposed to low doses of Cd (Oliveira et al. 2009, 2012). Cd both in the forms of $CdCl_2$ and $CdSO_4$ salt at low concentrations (4 µM) and short time exposure (2 h) was able to induce DNA damage in MRC-5 fibroblasts (Mourón et al. 2004). Yu and co-workers (2007) found that Cd induced a dose-dependent DNA damage assessed by the comet assay in hepatocytes of rats exposed to 5, 10, and 20 µmol kg^{-1}.

As Cd is not able to interact directly with DNA as shown by Valverde et al. (2001), Cd induced DNA damages are suggested to be caused by indirect interactions with DNA, as for instance through enhancement of ROS formation that can induce oxidative damage to macromolecules such as DNA (Mikhailova et al. 1997). In HaCat cells exposed to Cd at concentrations up to 100 µM for 24 and 48 h, Nzegue et al. (2008) were not able to detect DNA damages assessed by the comet assay, but they were able to prove the formation of 8-OHdG, a form of oxidation of guanine in DNA, indicating the reduced ability to repair DNA oxidative damage. Banfalvi and co-workers (2000) found increased levels of the oxidative DNA damage product, 8-OHdG, in CHO-K1 cells upon exposure to Cd, which varied with the cell cycle phase, being higher in early S phase and gradually declined as damaged cells progressed through the cell cycle.

Cadmium also interferes with DNA repair mechanisms as studies have shown that proteins involved in DNA repair systems, mostly in BER, NER and MMR, are sensitive to Cd (Dally and Hartwig 1997; Jin et al. 2003; Giaginis et al. 2006). As repair mechanisms are compromised upon Cd exposure, induced DNA lesions will persist and originate strand breaks that will result in DNA migration observed in the comet assay.

Our results showed that Cd induced an increase in the NPBs occurrence. NPBs occur when centromers of dicentric chromosomes are pulled to opposite poles during anaphase and are a result of DNA misrepair of strand breaks in DNA or telomere end fusions (Fenech 2007). Confirming that, a positive correlation between the comets tail moment (data not shown) and the number of NPBs was found at 24 h (r = 0.999; p = 0.030). Maes et al. (2012) also found an increase of NPBs in the human hepatocyte cell line C3A, upon Cd exposure. NDI, which characterizes the rate of cell division, decreased at 24 h of Cd exposure for the dose of 50 µM, but was unchanged for the 48 h period. A negative correlation was found between NDI and the number of cells in S phase (r = 0.999; p = 0.0262), suggesting that S phase delay is associated with Cd-induced cytostasis. Also, a positive correlation between the number of monucleated cells and the number of cells in S phase was detected at both time periods (r = 0.997; p = 0.046, for 24 h and r = 1; p = 0.002 for 48 h). On the other hand, a negative correlation was detected between the number of cells in S phase and the number of binucleated cells (r = -1; p = 0.007, for 24 h and r = -0.998; p = 0.035, for 48 h).

The frequency of cells with MN is a key indicator of the extent of DNA damage. In our work an increase in the frequency of MN occurrence was observed in both Cd doses, however literature results on Cd-induced MN formation are controversial. Some studies show increase in MN formation due to Cd exposure, as for instance that of Fatur and co-workers (2002) who detected Cd-induced DNA damage and MN formation in HepG2 cells at non-cytotoxic doses and the studies of Pereira et al. (2013) who found MN induction in ZF4 embryonic cells exposed to Cd. Also, *in vivo* studies have shown that in rats exposed to 0.5 mg $kg^{-1}day^{-1}$ for 8 and 12 weeks there was an increase in MN formation in peripheral blood lymphocytes (Bao et al. 2012). The presence of MN at 24 h was correlated positively with the presence of NPBs and with the number of cells in G_2 phase of cell cycle (r = 1; p = 0.005 and r = 1; p = 0.019, respectively). The levels of apoptosis and necrosis microscopically assessed by the CBMN assay also increased with Cd dose, however and for the latter a time-dependent effect was not observed. Also, apoptosis assessed by the annexin V assay also showed a similar trend of increase upon Cd exposure by both concentrations (data not shown). At 24 h the percentage of cells under apoptosis correlated positively with the presence of MN and NPBs (r=0.999; p=0.0226 and r=0.999; p=0.0229, respectively) and with the number of cells in G_2 phase of cell cycle (r = 1; p = 0.007). On other hand, apoptosis was negatively correlated with NDI at 48 h (r = 0.999; p = 0.033).

Microtubules are core intervenients during chromosomal segregation, and their functional accuracy is crucial for keeping the normal karyotypes in the progeny. Moreover, in response to DNA damage, several mechanisms in cells are activated to stop, decline or/and repair the injuries. Although in various studies, cell cycle arrest and cytoskeletal disruption have been positively associated with DNA damage, other studies refer that cytoskeletal disruption contributes but is not essential for induction of apoptosis (Liu and Templeton 2010). Numerous mechanisms are involved to mediate cell cycle arrest, e.g., the ATM-CHEK2 and ATR-CHEK1 pathways and cyclins (Smith et al. 2010). In our studies with MG-63 cells, Cd in the concentrations and periods of exposure tested induced minimal changes in both α-tubulin and F-actin. The role of Cd on cytoskeleton proteins remains unclear. On one hand, Cd is known to cause selective disruption of F-actin in other cell types as for instance, mouse mesangial cells (Wang et al. 1996) and rat mesangial cells (Wang et al. 1996; Apostolova et al. 2006) and smooth muscle (Apostolova et al. 2006). Specifically, it was found that Cd causes loss of phalloidin-stainable F-actin (Apostolova et al. 2006). Liu and Templeton (2010) examined the effect of the actin cytoskeleton on apoptosis induced by Cd in mouse mesangial cells and found that cytoskeletal disruption is a downstream event in Cd-induced cell death by both apoptosis and apoptotic-like mechanisms. On the other hand, Cd treated sponge *Clathrina clathrus* cells showed marked enhancement of α-tubulin acetylation and detyrosination supporting that Cd ions stabilize microtubules (Ledda et al. 2013). Moreover, increased expressions of α-tubulin in Cd-treated cells were reported for *Anopheles gambiae* mosquito (Mirejiet al. 2010), while recently Bhom (2014) demonstrated that Cd affected the kinesin-microtubule motility generating system in neuronal cells, which may contribute to the development of neuronal disorders. To our knowledge no studies in literature have related Cd with α-tubulin filament disruption in cells.

Conclusions

In conclusion this work shows the cyto- and genotoxic effects of Cd in bone cells. Cadmium affected cell cycle at both time periods even at sub-toxic doses by decreasing the % of cells in G_0/G_1 and delaying S phase, shown by an accumulation of cells in this phase, along with changes in the expression of cell cycle related genes. An increase in MN and NPBs together with an increase in the percentage of cells under apoptosis/necrosis was detected for both Cd doses at both time periods. However, an increase in DNA fragmentation was observed for both doses, but only significant for the 48 h time period. From our results,

the CBMN assay parameters (MN, NPBs and the percentage of cells under apoptosis or necrosis) together with the cell cycle appear as the most sensitive to Cd-induced cyto- and genotoxicity, being early affected even at sub-toxic doses. Lastly, some of the selected biomarkers discussed here may be used as reliable endpoints to detect early toxic effects of Cd to human bone cells.

References

Abrahim, K. S., Abdel-Gawad, N. B., Mahmoud, A. M., El-Gowaily, M. M., Emara, A. M., and Hwaihy, M. M. (2011) Genotoxic effect of occupational exposure to cadmium. *Toxicol. Ind. Health.* 27 (2), 173–179.

Faroon, O., Ashizawa, A., Wright, S., Tucker, P., Jenkins, K., Ingerman, L., and Rudisill, C. (2012) Toxicological profile for cadmium. Atlanta (GA). Agency for Toxic Substances and Disease Registry (US). Available from: http://www.ncbi.nlm.nih.gov/books/NBK158838/ (accessed Jan, 2013)

Almeida, T., Leite Ferreira, B. J. M., Loureiro, J., Correia, R. N., and Santos, C. (2011) Preliminary evaluation of the *in vitro* cytotoxicity of PMMA-co-EHA bone cement. *Mater. Sci. Eng. C.* 31 (3), 658–662.

Apostolova, M. D., Christova, T., Templeton, D. M. (2006) Involvement of gelsolin in cadmium-induced disruption of the mesangial cell cytoskeleton. *Toxicol. Sci.* 89 (2), 465–474.

Banfalvi, G., Littlefield, N., Hass, B., Mikhailova, M., Csuka, I., Szepessy, E., and Chou, M. W. (2000) Effect of cadmium on the relationship between replicative and repair DNA synthesis in synchronized CHO cells. *Eur. J. Biochem.* 267 (22), 6580–6585.

Bao, Y., Chen, H., Hu, Y., Bai, Y., Zhou, M., Xu, A., and Shao, C. (2012) Combination effects of chronic cadmium exposure and gamma-irradiation on the genotoxicity and cytotoxicity of peripheral blood lymphocytes and bone marrow cells in rats. *Mutat. Res.* 743 (1-2), 67–74.

Bertin, G., and Averbeck, D. (2006) Cadmium: cellular effects, modifications of biomolecules, modulation of DNA repair and genotoxic consequences (a review). *Biochimie*. 88 (11), 1549–1559.

Bhattacharyya, M. H., Whelton, B. D., Stern, P. H., and Peterson, D. P. (1988) Cadmium accelerates bone loss in ovariectomised mice and fetal rat limb bones in culture. *Proc. Natl. Acad. Sci.* U.S.A. 85 (22), 8761–8765.

Bjerregaard, H. F. (2007) Effects of cadmium on differentiation and cell cycle progression in cultured Xenopus kidney distal epithelial (A6) cells. *Altern. Lab. Anim.* 35 (3), 343–348.

Böhm, K. J. (2014) Kinesin-dependent motility generation as target mechanism of cadmium intoxication. *Toxicol. Lett.* 224 (3), 356–361.

Bork, U., Lee, W. K., Kuchler, A., Dittmar, T., and Thévenod, F. (2010) Cadmium-induced DNA damage triggers G_2/M arrest via chk1/2 and cdc2 in p53-deficient kidney proximal tubule cells. *Am. J. Physiol. Renal Physiol.* 298 (2), F255–F265.

Bradford, M. M. (1976). A rapid and sensitive method for the quantitation of microgram quantities of protein utilizing the principle of protein-dye binding. *Anal. Biochem.* 72, 248–254.

Brzóska, M. M., and Moniuszko-Jakoniuk, J. (2004) Low-level lifetime exposure to cadmium decreases skeletal mineralization and enhances bone loss in aged rats. *Bone*. 35 (5), 1180–1191.

Brzóska, M. M., Rogalska, J., and Kupraszewicz, E. (2011) The involvement of oxidative stress in the mechanisms of damaging cadmium action in bone tissue: a study in a rat model of moderate and relatively high human exposure. *Toxicol. Appl. Pharmacol.* 250 (3), 327–335.

Cambier, S., Gonzalez, P., Durrieu, G., and Bourdineaud, J.-P. (2010) Cadmium-induced genotoxicity in zebrafish at environmentally relevant doses. *Ecotoxicol. Environ. Saf.* 73 (3), 312–319.

Cao, F., Zhou, T., Simpson, D., Zhou, Y., Boyer, J., Chen, B., Jin, T., Cordeiro- Stone, M., and Kaufmann, W. (2007) p53-Dependent but ATM-independent inhibition of DNA synthesis and G_2 arrest in cadmium-treated human fibroblasts. *Toxicol. Appl. Pharmacol.* 218 (2), 174–185.

Celik, A., U. Çömelekoğlu, and Yalin, S. (2005) A study on the investigation of cadmium chloride genotoxicity in rat bone marrow using micronucleus test and chromosome aberration analysis. *Toxicol. Ind. Health.* 21 (9), 243–248.

Chandar, N., Billig, B., McMaster, J., Novak, J. (1992) Inactivation of p53 gene in human and murine osteosarcoma cells. *Br. J. Cancer*. 65 (2), 208–214.

Coonse, K. G., Coonts, A. J., Morrison, E. V., and Heggland, S. J. (2007) Cadmium induces apoptosis in the human osteoblast-like cell line Saos-2. *J. Toxicol. Environ. Health A.* 70 (7), 575–581.

Cuypers, A., Plusquin, M., Remans, T., Jozefczak, M., Keunen, E., Gielen, H., Opdenakker, K., Nair, A. R., Munters, E., Artois, T. J., Nawrot, T., Vangronsveld, J., and Smeets, K. (2010) Cadmium stress: an oxidative challenge. *Biometals.* 23 (5), 927–940.

Dally, H., and Hartwig, A. (1997) Induction and repair inhibition of oxidative DNA damage by nickel(II) and cadmium(II) in mammalian cells. *Carcinogenesis*. 18 (5), 1021–1026.

Diller, L., Kassel, J., Nelson, C. E., Gryka, M. A., Litwak, G., Gebhardt, M., Bressac, B., Ozturk, M., Baker, S. J., and Vogelstein, B. (1990) p53 functions as a cell cycle control point in osteosarcoma. *Mol. Cell. Biol.* 10 (11), 5772–5781.

Fatur, T., Tusek, M., Falnoga, I., Scancar, J., Lah, T. T., and Filipic, M. (2002) DNA damage and metallothionein synthesis in human hepatoma cells (HepG2) exposed to cadmium. *Food Chem. Toxicol.* 40 (8), 1069–1076.

Fenech, M. (2007) Cytokinesis-block micronucleus cytome assay. *Nat. Protoc.* 2 (5), 1084–1104.

Filipic, M., and Hei, T. K. (2004) Mutagenicity of cadmium in mammalian cells: implication of oxidative DNA damage. *Mutat. Res.* 546 (1-2), 81–91.

Giaginis, C., Gatzidou, E., and Theocharis, S. (2006) DNA repair systems as targets of cadmium toxicity. *Toxicol. Appl. Pharmacol.* 213 (3), 282–290.

Hartwig, A. (2013) Cadmium and cancer. *Met. Ions Life Sci.* 11, 491–507.

IARC (International Agency for Research on Cancer) (1993) Beryllium, cadmium, mercury and exposures in the glass manufactur- ing industry, *IARC Monographs on the Evaluation of Carcinogenic Risk of Chemicals to Humans*, Vol. 58, pp. 119–146, International Agency for Research on Cancer, Lyon, France.

Jin, Y. H., Clark, A. B., Slebos, R. J., Al-Refai, H., Taylor, J. A., and Kunkel, T. A. (2003) Cadmium is a mutagen that acts by inhibiting mismatch repair. *Nat. Genet.* 34 (3), 326–329.

Kent, W. J., Sugnet, C. W., Furey, T. S., Roskin, K. M., Pringle, T. H., Zahler, A. M., and Haussler, D. (2002) The human genome browser at UCSC. *Genome Res.* 12 (6), 996–1006. http://genome.ucsc.edu/cgi-bin/hgPcr (accessed Dec, 2012).

Ledda, F. D., Ramoino, P., Ravera, S., Perino, E., Bianchini, P., Diaspro, A., Gallus, L., Pronzato, R., and Manconi, R. (2013) Tubulin posttranslational modifications induced by cadmium in the sponge *Clathrina clathrus*. *Aquat. Toxicol.* 140–141, 98–105.

Lévesque, M., Martineau, C., Jumarie, C., and Moreau, R. (2008) Characterization of cadmium uptake and cytotoxicity in human osteoblast-like MG-63 cells. *Toxicol. Appl. Pharmacol.* 231 (3), 308–317.

Liu, Y., and Templeton, D. M. (2010) Role of the cytoskeleton in Cd^{2+}-induced death of mouse mesangial cells. *Can. J. Physiol. Pharmacol.* 88 (3), 341–352.

Maes, A., Anthonissen, R., and Verschaeve, L. (2012) Testing chemical agents with the cytokinesis-block micronucleus cytome assay. *Folia Biol. (Praha)*. 58 (5), 215–220.

Martineau, C., Abed, E., Médina, G., Jomphe, L.-A., Mantha, M., Jumarie, C., and Moreau, R. (2010) Involvement of transient receptor potential melastatin-related 7 (TRPM7) channels in cadmium uptake and cytotoxicity in MC3T3-E1 osteoblasts. *Toxicol. Lett.* 199 (3), 357–363.

Masuda, H., Miller, C., Koeffler, H. P., Battifora, H., and Cline, M. J. (1987) Rearrangement of the p53 gene in human osteogenic sarcomas. *Proc. Natl. Acad. Sci. USA.* 84 (21), 7716–7719.

Méplan, C., Mann, K., and Hainaut, P. (1999) Cadmium induces conformational modifications of wild-type p53 and suppresses p53 response to DNA damage in cultured cells. *J. Biol. Chem.* 274 (44), 31663–31670.

Mikhailova, M. V., Littlefield, N. A., Hass, B. S., Poirier, L. A., and Chou, M. W. (1997) Cadmium-induced 8-hydroxydeoxyguanosine formation, DNA strand breaks and antioxidant enzyme activities in lymphoblastoid cells. *Cancer Lett.* 115 (2), 141–148.

Mireji, P. O., Keating, J., Hassanali, A., Impoinvil, D. E., Mbogo, C. M., Muturi, M. N., Nyambaka, H., Kenya, E. U., Githure, J. I., and Beier, J. C. (2010) Expression of metallothionein and α-tubulin in heavy metal-tolerant *Anopheles gambiae* sensu stricto (Diptera: Culicidae). *Ecotoxicol. Environ. Saf.* 73 (1), 46–50.

Mourón, S. A., Grillo, C. A., Dulout, F. N., Golijow, C. D. (2004) A comparative investigation of DNA strand breaks, sister chromatid exchanges and K-*ras* gene mutations induced by cadmium salts in cultured human cells. *Mutat. Res.* 568 (2), 221–231.

Natrajan, R., Mackay, A., Wilkerson, P. M., Lambros, M. B., Wetterskog, D., Arnedos, M., Shiu, K.-K., Geyer, F. C., Langerød, A., Kreike, B., Reyal, F., Horlings, H. M., van de Vijver, M. J., Palacios, J., Weigelt, B., and Reis-Filho, J. S. (2012) Functional characterization of the 19q12 amplicon in grade III breast cancers. *Breast Cancer Res.* 14 (2), R53.

Nemmiche, S., Chabane-Sari, D., Kadri, M., and Guiraud, P. (2011) Cadmium chloride-induced oxidative stress and DNA damage in the human Jurkat T cell line is not linked to intracellular trace elements depletion. *Toxicol. In Vitro.* 25 (1), 191–198.

Nemmiche, S., Chabane-Sari, D., Kadri, M., and Guiraud, P. (2012) Cadmium-induced apoptosis in the BJAB human B cell line: involvement of PKC/ERK1/2/JNK signaling pathways in HO-1 expression. *Toxicology*. 300 (3), 103–111.

Nordberg, G. F. (2009) Historical perspectives on cadmium toxicology. *Toxicol. Appl. Pharmacol.* 238 (3), 192–200.

Nzengue, Y., Steiman, R., Garrel, C., Lefèbvre, E., and Guiraud, P. (2008) Oxidative stress and DNA damage induced by cadmium in the human keratinocyte HaCaT cell line: role of glutathione in the resistance to cadmium. *Toxicology*. 243 (1-2), 193–206.

Ogoshi, K., Nanzai, Y., and Moriyama, T. (1992) Decrease in bone strength of cadmium-treated young and old rats. *Arch. Toxicol.* 66 (5), 315–320.

Olive, P. L., Frazer, G., and Banáth, J. P. (1993) Radiation-induced apoptosis measured in TK6 human B lymphoblast cells using the comet assay. *Radiat. Res.* 136 (1), 130–136.

Oliveira, H., Lopes, T., Almeida, T., Pereira, M. L., and Santos, C. (2012) Cadmium-induced genetic instability in mice testis. *Hum. Exp. Toxicol.* 31 (12), 1228–1236.

Oliveira, H., Spanò, M., Santos, C., and Pereira, M. L. (2009) Adverse effects of cadmium exposure on mouse sperm. *Reprod. Toxicol.* 28 (4), 550–555.

Pereira, S., Cavalie, I., Camilleri, V., Gilbin, R., and Adam-Guillermin, C. (2013) Comparative genotoxicity of aluminium and cadmium in embryonic zebrafish cells. *Mutat. Res.* 750 (1-2), 19–26.

Pfaffl, M. W. (2001) A new mathematical model for relative quantification in real-time RT-PCR. *Nucleic Acids Res.* 29 (9), e45.

Prozialeck, W. C. (2000) Evidence that E-cadherin may be a target for cadmium toxicity in epithelial cells. *Toxicol. Appl. Pharmacol.* 164 (3), 231–249.

Risso-de Faverney, C., A. Devaux, Lafaurie, M., Girard, J. P., Bailly, B., and Rahmani, R. (2001) Cadmium induces apoptosis and genotoxicity in rainbow trout hepatocytes through generation of reactive oxygen species. *Aquat. Toxicol.* 53 (1), 65–76.

Robards, K., and Worsfold, P. (1991) Cadmium: toxicology and analysis, a review. *Analyst*. 116 (6), 549–568.

Rozen, S., and Skaletsky, H. (2000) Primer3 on the WWW for general users and for biologist programmers. *Methods Mol. Biol.* 132, 365–386.

Schrader, M., Krieglstein, K., and Fahimi, H. D. (1998) Tubular peroxisomes in HepG2 cells: selective induction by growth factors and arachidonic acid. *Eur. J. Cell Biol.* 75 (2), 87–96.

Smith, S. S., Reyes, J. R., Arbon, K. S., Harvey, W. A., Hunt, L. M., and Heggland, S. J. (2009) Cadmium-induced decrease in RUNX2 mRNA expression and recovery by the antioxidant N-acetylcysteine (NAC) in the human osteoblast-like cell line, Saos-2. *Toxicol. In Vitro*. 23 (1), 60–66.

Smith, J., Tho, L. M., Xu, N., and Gillespie, D. A. (2010) The ATM-Chk2 and ATR-Chk1 pathways in DNA damage signaling and cancer. *Adv. Cancer Res.* 108, 73-112.

Thévenod, F., and Lee, W.-K. (2013) Cadmium and cellular signaling cascades: interactions between cell death and survival pathways. *Arch. Toxicol.* 87 (10), 1743–1786.

Tice, R. R., Agurell, E., Anderson, D., Burlinson, B., Hartmann, A., Kobayashi, H., Miyamae, Y., Rojas, E., Ryu, J.-C., and Sasaki, Y. F. (2000) Single cell gel/comet assay: guidelines for in vitro and in vivo genetic toxicology testing. *Environ. Mol. Mutagen.* 35 (3), 206–221.

Twentyman, P. R., and Luscombe, M. (1987) A study of some variables in a tetrazolium dye (MTT) based assay for cell growth and chemosensitivity. *Br. J. Cancer.* 56 (3), 279–285.

Valverde, M., Trejo, C., and Rojas, E. (2001) Is the capacity of lead acetate and cadmium chloride to induce genotoxic damage due to direct DNA-metal interaction? *Mutagenesis*. 16 (3), 265–270.

Viau, M., Gastaldo, J., Bencokova, Z., Joubert, A., and Foray, N. (2008) Cadmium inhibits non-homologous end-joining and over-activates the MRE11-dependent repair pathway. *Mutat. Res.* 654 (1), 13–21.

Waisberg, M., Joseph, P., Hale, B., and Beyersmann, D. (2003) Molecular and cellular mechanisms of cadmium carcinogenesis. *Toxicology*. 192 (2-3), 95–117.

Wang, B., Luo, Q., Shao, C., Li, X., Li, F., Liu, Y., Sun, L., Li, Y., and Cai, L. (2013) The late and persistent pathogenic effects of cadmium at very low levels on the kidney of rats. *Dose-Response*. 11 (1), 60–81.

Wang, C. H., and Bhattacharyya, M. H. (1993) Effect of cadmium on bone calcium and 45Ca in nonpregnant mice on a calcium-deficient diet: evidence of direct effect of cadmium on bone. *Toxicol. Appl. Pharmacol.* 120 (2), 228–239.

Wang, Z., Chin, T. A., and Templeton, D. M. (1996) Calcium-independent effects of cadmium on actin assembly in mesangial and vascular smooth muscle cells. *Cell Motil. Cytoskelet.* 33 (3), 208–222.

Wilson, A. K., and Bhattacharyya, M. H. (1997) Effects of cadmium on bone: an in vivo model for the early response. *Toxicol. Appl. Pharmacol.* 145 (1), 68–73.

Xie, J., and Shaikh, Z. A. (2006) Cadmium-induced apoptosis in rat kidney epithelial cells involves decrease in nuclear factor-kappa B activity. *Toxicol. Sci.* 91 (1), 299–308.

Yang, P. M., Chiu, S. J., Lin, K. A., and Lin, L. Y. (2004) Effect of cadmium on cell cycle progression in Chinese hamster ovary cells. *Chem. Biol. Interact.* 149 (2-3), 125–136.

Yu, R. A., He, L. F., and Chen, X. M. (2007) Effects of cadmium on hepatocellular DNA damage, proto-oncogene expression and apoptosis in rats. *Biomed. Environ. Sci.* 20 (2), 146–153.

Zhao, S., and Fernald, R. D. (2005) Comprehensive algorithm for quantitative real-time poly-merase chain reaction. *J. Comput. Biol.* 12 (8), 1047–1064.

Zimmerhackl, L. B., Momm, F., Wiegele, G., and Brandis, M. (1998) Cadmium is more toxic to LLC-PK1 cells than to MDCK cells acting on the cadherin–catenin complex. *Am. J. Physiol.* 275 (1), F143–F153.

Chapter 3.3 – Cadmium-induced mitochondrial dysfunction and oxidative stress in human osteoblasts

Cristina Monteiro[1], Francisco Pinho[1], Tiago Pedrosa[1], José Miguel Pimenta Ferreira de Oliveira[1], Helena Oliveira[1], Francisco Peixoto[2], Conceição Santos[1]

[1] Department of Biology and CESAM, Laboratory of Biotechnology and Cytomics, University of Aveiro

[2] Department of Biology and Environment, CITAB, School of Life and Environmental Sciences, University of Trás-os-Montes e Alto Douro

Results published in this chapter will be submitted to an international journal, with the title: Cadmium-induced mitochondrial dysfunction and oxidative stress in human osteoblast cell line MG-63

Abstract

Cadmium is a highly toxic environmental pollutant, and Human exposure occurs mainly in workplaces where Cd is used in the manufacture and also from cigarette smoke or eating Cd-contaminated food. Cd accumulation and toxicity have been mostly determined (*in vivo*/*in vitro*) in e.g., kidney, liver, bones, lung, testis, and prostate. Few studies have been addressed Cd toxicity in osteoblasts, concretely on oxidative stress. Moreover, mitochondrial function had not yet been approached in bone cells. Therefore, this work focused on the evaluation of the effects of Cd in human osteoblasts by analyzing the mitochondrial energy processing and putative associations with oxidative stress. Mitochondria are an intensive source of ROS becoming a target itself. It has been verified that Cd induces ROS further increasing oxidative insult in many organs and cell lines. To assess the influence of Cd exposure on mitochondrial function and oxidative stress in osteoblasts, MG-63 cell line was exposed to Cd (up to 65 μM) for 24 and 48h. Intracellular ROS and antioxidant defense mechanisms (TAA, and gene expression of antioxidant enzymes) were analyzed, as well as the resulting protein oxidation, and lipid peroxidation. Furthermore, Cd effects on mitochondrial function were evaluated by analyzing the activity of enzymes involved in mitochondrial respiration, $\Delta\Psi m$, mitochondrial morphology and adenylate energy charge. In Cd-exposed osteoblasts, results indicate an increase of oxidative stress, together with lipid and protein oxidation. Gene expression of antioxidant enzymes showed that GR was down-regulated compared to control cells. Mitochondrial function was affected by decrease of $\Delta\Psi m$, and inhibition of mitochondrial respiratory chain enzymes, and citrate synthase. Moreover, the energetic status of cells was also diminished by Cd exposure. In conclusion, Cd induced mitochondrial dysfunction that seems to be related with oxidative stress in human osteoblasts.

Keywords

Antioxidant defenses, cadmium, human osteoblasts, mitochondrial dysfunction, ROS,

Introduction

Humans are exposed to Cd mainly through ingestion of water and food crops grown in Cd-contaminated soils, or by inhalation of cigarette smoke, and fumes/dusts from industries (Mead 2010; Xu et al. 2013). Due to its broad accumulation in several tissues, chronic exposure to Cd may lead to different pathologies, like neurological diseases, infertility, diabetes, cancer, and mostly to renal and bone injuries like osteoporosis and osteomalacia (Oliveira et al. 2009; Nair et al. 2013).

In a previous study on Cd toxicity in human osteoblasts (see Chapter 3.2, and Oliveira et al. 2014), our group demonstrated that Cd induced cytotoxicity in the MG-63 cell line, with observed increases of DNA damage and MN formation, cell cycle delay and cell death (apoptosis and necrosis) (Oliveira et al. 2014). It is known that Cd exposure may lead to increase of oxidative stress in the cell, i.e. an increasing imbalance between ROS production *vs* antioxidant defense mechanisms (Patra et al. 2011). A proposed mechanism supports that although Cd does not produce ROS, it replaces Fenton-active metals, Fe and Cu, and these may become available to the generation of ROS such as $^{\bullet}O_2^-$, $^{\bullet}OH$ and H_2O_2 (Arroyo et al. 2012). Additionally, Cd has high affinity for thiol groups of proteins and GSH, a major antioxidant, thus decreasing the antioxidant potential of the cell and contributing to increasing levels of ROS (Arroyo et al. 2012). In order to decrease this ROS production and to maintain the GSH/GSSG ratio at a high level, antioxidant enzymes like CAT, GPx, GR, SOD are required, but their activity has been shown to be inhibited by Cd both in human cells (see for review: Waisberg et al. 2003; Patra et al. 2011) and plants (e.g., Azevedo et al. 2005; Monteiro et al. 2009; Monteiro et al. 2012, see Chapter 2.2). On the other hand, in some experiments, long periods of exposure to Cd stimulated the activity of antioxidant enzymes possibly as a result of an adaptive response (Thévenod and Lee 2013).

Mitochondria are responsible for several cell functions (e.g., energy processing, apoptosis, oxidative stress). Mitochondria were identified as key targets of Cd toxicity in *in vivo* studies (e.g., liver, brain and heart of guinea pigs (Wang et al. 2004)), and in *in vitro* cultures (e.g., vero cells (Murugavel et al. 2007), rat hepatoma cells (Belyaeva et al. 2008), human hepatoma cells and rat glioma cells (Yang et al. 2004)). Also, it was observed that Cd induced ROS formation and inhibited the electron transfer chain in isolated mitochondria (Wang et al. 2004) and hepatoma cells (Belyaeva et al. 2006).

Finally, since mitochondria are a source of intensive ROS generation due to mitochondrial respiratory chain and, simultaneously, become targets of that ROS, mitochondria may become dysfunctional and lead to energy decline, oxidative stress and apoptosis (Desagher and Martinou 2000). However, to our knowledge, and despite Cd particularly accumulates in bone tissues, only one study focused on Cd-induced oxidative stress in osteoblasts (Saos-2 cell line) (Smith et al. 2009). In these cells, Smith and co-authors (2009) showed that when Saos-2 cells were exposed to 10 µM $CdCl_2$, it was measured an increase of oxidative stress by the observed decrease of GSH levels, and increase of ROS formation and lipid peroxidation (Smith et al. 2009). Therefore, our study is the first one regarding a comprehensive screening of Cd effects on osteoblast mitochondrial function and oxidative stress.

The present study aimed to evaluate the effects of Cd in the MG-63 cell line by analyzing oxidative stress and mitochondrial function responses. For that, intracellular ROS and antioxidant defense mechanisms (TAA, and gene expression of antioxidant enzymes) were analyzed, as well as the resulting protein and lipid oxidation. Furthermore, the effects on mitochondrial function and energetic status were evaluated by analyzing the activity of enzymes involved in mitochondrial respiration, $\Delta\Psi m$, mitochondrial morphology and adenylate energy charge.

Materials and methods

Cell culture

Human osteoblast cell line MG-63 was kindly provided by INEB – Instituto Nacional de Engenharia Biomédica, University of Porto, Portugal. MG-63 cell line was *in vitro* cultured in MEM-α medium without nucleosides, supplemented with 10% (v/v) FBS, 100 Units mL^{-1} penicillin/100 µg mL^{-1} streptomycin and 2.5 µg mL^{-1} fungizone (Life Technologies, Carlsbad, CA) at 37 °C, 5% CO_2, in humidified atmosphere. Cell confluence and morphology were daily observed under an inverted phase contrast microscope Nikon Eclipse TS100 (Japan). Cells were subcultured when confluence reached 80%, at a proportion of 1:9, using 0.25% trypsin/1 mM EDTA (Life Technologies, Carlsbad, CA). For metal exposure, cells were left 24 h for adhesion. Then, the medium was replaced by medium containing $CdCl_2$ (Sigma-Aldrich, St. Louis, MO) at final concentrations of 20, 50 and 65

µM. Culture media without $CdCl_2$ served as control in each experiment. MG-63 cells were cultured in the referred conditions for 24, and 48 h.

Protein quantification

Total protein was quantified by the method of Bradford (1976). In brief, 250 µL of Bradford Reagent (Sigma-Aldrich, St. Louis, MO) were added to 5 µL of sample that was previously measured to each well of a 96-well plate. The plate was incubated with shaking at RT and in the dark for 10 min. The absorbance was read at 595 nm using a microplate reader (Synergy™ HT Multi-Mode, BioTeK). A standard curve of BSA (Sigma-Aldrich, St. Louis, MO) was used to calculate the unknown concentrations.

Intracellular adenine nucleotides

Quantification of adenine nucleotides was used to assess the energetic status of cells, that is indicated by the equation of adenylate energy charge (EC) = ([ATP] + ½ [ADP]) / ([ATP] + [ADP] + [AMP]) (Atkinson 1968). To quantify adenine nucleotides, $1.5x10^6$ cells were plated in 100 mm dishes and exposed to Cd for 24 h, and 48 h. After Cd treatment, cells were washed and scraped in cold PBS pH 7.2. Cell suspension was centrifuged at 1000*g* for 10 min, at 4 ºC. The pellet was then resuspended in 350 µL of cold PBS pH 7.2 and samples were frozen with liquid nitrogen and stored at -80 ºC until protein quantification and the extraction of adenine nucleotides. The extraction procedure was performed according to Ryll and Wagner (1991), with some modifications. For this, 200 µL of KOH 0.5 M were added to each cell suspension and samples were vigorously vortexed intermittently for 5 min, at 4 ºC to minimize the degradation of nucleotides. After alkaline incubation, samples rested on ice for 5 min and were diluted with 300 µL of ultra pure water. Then, a centrifugation was done at 16000*g* for 15 min at 4 ºC, the pH of supernatants was adjusted to 6.5 with a saturated solution of KH_2PO_4, and samples were stored at -80 ºC until chromatographic analysis. Adenine nucleotides were identified and quantified by HPLC following the method described by Stocchi et al. (1985) with modifications. An UltiMate 3000 Column Compartment Dionex (Model TCC-3200) equipped with a PDA 100 Dionex, and an ACE 5 C18 reversed phase column (250×4.6 mm×5 µm) with a precolumn were

used, and the column oven temperature was set at 25 ºC. The flow rate was 0.7 mL min^{-1} and the elution was performed using a solvent system comprising solvent A (1.2% methanol in KH_2PO_4 0.1 M, pH 6.5) and solvent B (20% methanol in KH_2PO_4 0.1 M, pH 6.5): 100% of solvent A for 14 min to elute adenine nucleotides, followed by 3 min of a linear gradient to 100% of solvent B, maintaining at 100% for 3 min to elute other compounds from the sample in order to clean the column. This was followed by 2 min of a linear gradient to 100% of solvent A, maintaining at 100% for 7 min to reequilibrate the column to the next run. At the beginning of each day the column was equilibrated with 50% of each solvent for 5 min, and 30 min of 100% solvent A. After that a blank was run. The injection volume was 35 µL. The PDA detector was set in the range of 200-600 nm for spectral and purity analysis of sample and standard peaks, and the wavelength of 260 nm was used to detect adenine nucleotides. The compounds were identified based on their retention time of commercial standards of ATP (>99% HPLC, Sigma-Aldrich, St. Louis, MO), ADP (98% HPLC, Sigma-Aldrich, St. Louis, MO) and AMP (>99% HPLC, Sigma-Aldrich, St. Louis, MO) and by comparison with the UV-spectrum. Successive dilutions of a mix of adenine nucleotides were used to make a standard curve. In addition, co-elution of each single standard with samples confirmed the identification of the correspondent peak in the sample chromatogram. Moreover, to optimize sample chromatograms, all the samples were trypsinized (0.08% trypsin) for 3 h at 4 ºC before runs, thus decreasing the interference of proteins and peptides during elution and preventing column clogging. Also, after each day the column was inverted and cleaned by running 50% methanol/50% water (up to 1 ml min^{-1}) for 30 min, at 35 ºC. Chromeleon Software (version 6.80 DU12a Build 3599, Dionex Corporation) allowed chromatogram analyses, with identification of peaks and their integration.

Mitochondria isolation

Mitochondria were isolated from cells cultured (initial density of $10x10^6$ cells) in 150 mm Petri dishes and exposed to Cd for 24, and 48 h and also in the absence of Cd (control group). Cells were washed and scraped in cold PBS pH 7.2. Cell suspension was centrifuged at 2000*g* for 15 min, at 4 ºC. The pellet was resuspended in 5 mL of sucrose buffer (0.25 M sucrose, 0.2 mM EGTA, 0.1% BSA and 5 mM HEPES, pH 7.4) and incubated on ice for 5 min (Peixoto et al. 2008). Cells were then homogenized with a 5 ml syringe fitted with 25 G

(10 times, approximately 90 % of cell disruption confirmed by microscopy observation of homogenized) (Xiao et al. 2012). The homogenates were centrifuged at 1800*g* for 15 min at 4 ºC, and the resulting supernatants were centrifuged at 15550*g* for 30 min at 4 ºC (according to Xiao et al. 2012), with adjustments on centrifugation speed and time. Then, the mitochondrial pellet was washed in 1.5 mL of sucrose buffer pH 7.2 without BSA and EGTA (i.e. 0.25 M sucrose and 5 mM HEPES, pH 7.2) and, finally, resuspended in 150 µL of the same buffer (Peixoto et al. 2008). The samples were frozen with liquid nitrogen and stored at -80 ºC until protein quantification and measurement of mitochondrial enzyme activities.

Mitochondrial respiratory chain enzymes and citrate synthase activities

Spectrophotometric assays were used to measure the activity of two components of the electron transfer chain using a microplate reader (Synergy™ HT Multi-Mode, BioTeK). Complex I (NADH:ubiquinone oxireductase) and complex IV (cytochrome c oxidase) activities were assessed following the method described by Kiebish et al. (2013), with minor modifications. Complex I specific activity was determined by measuring the oxidation of NADH at 340 nm (ε = 6.22 $mM^{-1}cm^{-1}$). The assay was performed at 30 ºC in buffer 35.5 mM potassium phosphate (pH 7.4) containing 2 mM KCN, 5 mM $MgCl_2$, 2.5 mg mL^{-1} BSA, supplemented with 100 µM decylubiquinone as electron acceptor and 30 µM antimycin to block electron transport downstream from complex I. After 2 min the reaction was initiated by adding 0.3 mM NADH and enzyme activity was measured for 5 min. Complex I activity was inhibited with 25 µM rotenone. Complex IV specific activity was determined by measuring the oxidation of reduced cytochrome c at 550 nm (ε = 21.84 $mM^{-1}cm^{-1}$). The assay was performed at 30 ºC in buffer 9 mM Tris-HCl (pH 7.0) containing 108 mM KCl. After 2 min the reaction was initiated by adding 11 µM reduced cytochrome c and enzyme activity was measured for 3 min. Complex IV activity was inhibited with 2.75 mM KCN.

Citrate synthase specific activity was spectrophotometrically measured according to Srere (1969), with minor modifications. Citrate synthase catalyzes the reaction between acetyl-CoA and oxaloacetate to originate citric acid, and resulting in the formation of CoA-SH. The thiol group reacts with the DTNB to form TNB, a yellow compound. The assay was performed at 30 ºC in buffer 160 mM Tris-HCl (pH 7.0), containing 0.1% Triton X-100, 0.13 mM DTNB, 0.33 mM acetyl-CoA and 0.9 mM oxaloacetate. After 2 min the reaction

was initiated by adding mitochondrial enzyme and activity was measured for 3 min. Citrate synthase specific activity was determined by measuring the decrease in the concentration of DTNB at 412 nm (ε = 13.6 $mM^{-1}cm^{-1}$).

Mitochondrial membrane potential

$\Delta\Psi m$ was assessed by FCM following the method described by Barros et al. (2013). Firstly, 1.5×10^5 cells were seeded in a 6-well plate and, after cell adhesion, they were exposed to Cd as described above. At the end of the respective exposure time, cells were washed with PBS pH 7.2 and incubated with 5µg mL^{-1} Rho123 (Sigma-Aldrich, St. Louis, MO) for 30 min, at 37 ºC. The cells were washed with PBS pH 7.2, trypsinized and centrifuged at 800g for 5 min, at 4 ºC. From the centrifugation step, the following procedures were performed at 4 ºC. The cell pellet was washed with 1 mL of PBS pH 7.2 containing 1% BSA, and resuspended in 500 µL of PBS pH 7.2 containing 1% BSA and 5µg mL^{-1} PI (Sigma-Aldrich, St. Louis, MO). The samples were analyzed by FCM using a Coulter EPICS XL flow cytometer (Coulter Electronics, Hialeah, Florida, USA) and at least 10000 events were analyzed. Data was acquired using the SYSTEM II (v. 2.5) software. FCM data was analyzed by FlowJo software (Tree Star Inc., Ashland, OR). The loss of $\Delta\Psi m$ was visualized as indicated by the reduction of Rho123 FL.

Fluorescence microscopy of mitochondria

Mitochondria morphology was visualized by fluorescence microscopy. Cells were seeded on glass coverslips placed in 12-well plates at $2.5x10^4$ cells/well, and Cd treatment was done as described above. Cells were washed with PBS pH 7.4, fixed with 4% paraformaldehyde (Sigma-Aldrich, St. Louis, MO) in PBS pH 7.4 (pH 7.4) for 20 min at RT, and permeabilized with 0.2% Triton X-100 (Sigma-Aldrich, St. Louis, MO) for 10 min (Schrader et al. 1998). After blocking with 2% BSA, cells were washed in PBS pH 7.4 and then incubated for 1 h at RT with the primary antibody (mouse monoclonal antibody α-TOM20, 1:200 dilution, was purchased from BD Biosciences, USA) diluted in PBS pH 7.4 (Wang et al. 2009). After extensive washing in PBS pH 7.4, cells were incubated with secondary antibody donkey anti-mouse (DαM-TRITC, 1:100 dilution, was purchased from

Sigma-Aldrich, St. Louis, MO) diluted in PBS pH 7.4. Samples were examined using the Nikon Eclipse 80i microscope (Nikon, Tokyo, Japan) equipped with a PlanApo 100x objective; a TRITC-compatible filter (excitation filter: 543/22 nm; dicroic mirror: 562 nm; and emission filter: 593/40 nm). Fluorescence images were acquired with a Digital Sight camera, software NIS-Elements F 3.00 SP7 (Nikon, Tokyo, Japan). Usually two coverslips per preparation and two to three independent experiments were performed, with mitochondria observation and classification in filamentous, intermediate and fragmented.

Intracellular ROS

The generation of intracellular ROS was measured by FCM according to Ferreira de Oliveira et al. (2014), using the fluorogenic probe $DCFH_2$-DA (Sigma-Aldrich, St. Louis, MO-USA). This probe enters the cells and is deacetylated by cellular esterases producing non-fluorescent $DCFH_2$ and diacetate. In the cytosol $DCFH_2$ is quickly oxidized to fluorescent DCF by intracellular ROS.

Cells were plated in 6-well plates at a density of $150x10^3$ cells/well. After 24 and 48 h of Cd exposure, cells were washed with PBS pH 7.2 (Gibco by Life Technologies) and cells were incubated for 30 min, at 37 °C in the dark with serum-free MEM-α containing 10 µM $DCFH_2$-DA. Cells were trypsinized and collected in 1 mL of cold MEM-α to be analyzed. Acquisitions were made using a Coulter EPICS XL flow cytometer (Coulter Electronics, Hialeah, Florida, USA) and the MFI of DCF was analyzed with FlowJo software (Tree Star Inc., Ashland, OR). For each sample, the number of events reached at least 10000.

Total antioxidant activity

TAA was determined with Antioxidant Assay Kit (Sigma-Aldrich, St. Louis, US-MO). Cells were plated in 100 mm Petri dishes at a density of $1.5x10^6$ cells. After times of Cd treatment, cells were washed with PBS pH 7.2, scraped on ice and centrifuged at 1000*g* for 10 min at 4 ºC. It was added 300 µL of assay 1x buffer (from the assay kit) to the pellet, and samples were sonicated intermittently for 30 s on ice. Homogenized samples were centrifuged at 12000*g* for 15 min at 4 ºC. Supernatants were stored at -80 ºC until subsequent analysis.

The assay was prepared on a 96-well plate with 15 µL of sample, 20 µL myoglobin working solution and 150 µL of ABTS substrate working solution. After incubation, at RT during 30 min, 100 µL of STOP solution was added and the absorbance was read at 405 nm in a microplate reader (Synergy™ HT Multi-Mode, BioTeK). The absorbance decrease reflects the increase of antioxidant activity. Trolox, a water-soluble vitamin E analog, was used as a standard or control antioxidant and the results were normalized by protein concentration.

Protein oxidation

Protein oxidation was measured using Protein Carbonyl Colorimetric Assay Kit (Cayman Chemical Company, USA). For that, cells were seeded in 150 mm Petri dishes at an initial density of approximately $10x10^6$ cells. After cell exposure to Cd for 24 and 48 h, cells were washed and scraped in cold PBS pH 7.2. Cell suspension was centrifuged at 1000*g* for 5 min, at 4 ºC. The pellet was resuspended in 50 mM phosphate buffer pH 6.7 containing 1 mM EDTA and samples were sonicated intermittently for 30 s on ice. Homogenized samples were centrifuged at 10000*g* for 15 min at 4 ºC. The supernatants were incubated for 15 min at 4 ºC with 1% sulphate streptomycin to eliminate nucleic acids detected by a ratio of absorbance of $A_{280\ nm}/A_{260\ nm}$ less than 1. Posterior steps of the procedure were performed following the kit instructions. Absorbance measurements of DNPH tubes (370 nm) and tubes without DNPH (280 nm) were carried out using a microplate reader (Synergy™ HT Multi-Mode, BioTeK). A standard curve of BSA was used to calculate protein concentration, and carbonyl content was expressed in nmol $protein^{-1}$.

Lipid peroxidation

Lipid peroxidation was measured by fluorimetric TBARS assay. Cells were seeded in 150 mm Petri dishes at an initial density of approximately $10x10^6$ cells. After cell exposure to Cd, according to Ahmad et al. (2012), cells were washed twice and scraped in cold 400 mM Tris-HCl pH 7.3. An aliquot of cell suspension (200 µL) was mixed with 800 µL of color reagent solution containing 0.4% (w/v) TBA, 0.5% (w/v) SDS, 5% (v/v) acetic acid, pH 3.5 and incubated for 60 min at 95 ºC. Mixtures were immediately incubated on ice for

10 min to stop the reaction and then centrifuged at 1600*g* for 10 minutes at 4 ^{o}C. Samples were left at RT for 30 min and fluorescence of supernatants was read at an excitation wavelength of 528 nm and an emission wavelength of 550 nm, using a microplate reader (Synergy™ HT Multi-Mode, BioTeK). TBARS concentration was normalized by protein concentration.

Gene expression of antioxidant enzymes

RNA extraction and qPCRGene expression was analyzed by qPCR. The forward and reverse primers for the selected genes were designed using Primer3 (Rozen and Skaletsky 2000) and are listed in Table 8. Primer specificity was confirmed using the In-Silico PCR UCSC Genome Browser (Kent et al. 2002).

Table 8. Oligonucleotide primer sequences used for qPCR (obtained from Rozen and Skaletsky (2000))

1. Gene	Forward primer (5'-3')	Reverse primer (5'-3')
CAT	TGAACTGTCCCTACCGTGCT	TATTGGATGCTGTGCTCCAG
GPX1	CGGGACTACACCCAGATGAA	TCTCTTCGTTCTTGGCGTTC
GSR	GATCCCAAGCCCACAATAGA	TCGCTGGTTATTCCTAAGCTG
SOD1	GGTGTGGCCGATGTGTCTAT	TTCCAGCGTTTCCTGTCTTT
SOD2	CCCTGGAACCTCACATCAAC	CTGAAGAGCTATCTGGGCTGTAA
GAPDH	ACACCCACTCCTCCACCTTT	TACTCCTTGGAGGCCATGTG

Cells ($1.5x10^6$) were plated in 100 mm dishes and exposed to 50 µM Cd for 24 h. After Cd treatment, cells were washed twice in cold PBS pH 7.2 and 1 mL TRIzol® reagent (Life Technologies, Saint Louis, MO, USA) was added for cell lysing, and RNA extraction and preservation. Samples were incubated for 5 min at RT, 200 µL of chloroform were added, vortexed for 10 s, and incubated for 2 min at RT. Phase separation was achieved by centrifugation at 12000*g* for 5 min at 4 °C in Phase-Lock Gel Heavy tubes (5 Prime Inc., Boulder, CO, USA). To the aqueous phase 1 volume of 70% ethanol was added and RNA was further purified using RNeasy Mini Kit columns (Qiagen, Hilden, Germany) following the manufacturer's recommendations. The total RNA was quantified and checked for its purity by spectrophotometry, determining the absorbance ratios $A_{260/280}$ and $A_{260/260}$ (Nanodrop Spectrophotometer ND-1000®, Thermo Fisher Scientific, Wilmington, DE, USA).

cDNA synthesis was carried out after incubation of 2 µg of total RNA with DNase I (Sigma-Aldrich, St. Louis, MO-USA). RNA was reverse-transcribed using the Omniscript RT Kit (Qiagen, Hilden, Germany), and cDNA samples were diluted in MilliQ water (1:15).

The final individual qPCR reactions contained iQ SYBR Green Supermix (BioRad, Hercules, CA-USA), 1.5 µM each primer and 1:4 (v/v) prediluted cDNA (1:15). Two qPCR technical replicates were performed per sample from each of three independent biological replicates. The qPCR program, in the iQ5 Bio-Rad thermal cycler, included 1 min of

denaturation at 95 °C, followed by 60 cycles of denaturation at 94 °C for 5 s, annealing at 58 °C for 15 s, and extension at 72 °C for 15 s. After qPCR, a melting temperature program was performed. Mean PCR efficiencies and cycle thresholds were determined from the fluorescence data using the algorithm Real-Time PCR Miner (Zhao and Fernald 2005). Gene expression relative to control cells and normalized with the *GAPDH* reference gene was calculated from the mean efficiencies and cycle thresholds using the Pfaffl (2001) method.

Statistical analysis

At least three independent assays were performed for each analysis. The qPCR data was expressed as mean ± SE, while the remaining data was expressed as mean ± SD. The qPCR data were analyzed by one-way ANOVA, followed by a Holm-Sidak test, while the remaining data were analyzed by two-way ANOVA to evaluate the significance of differences in the parameters. When necessary, data were transformed to achieve normality and equality of variances. The level of statistic significance was set at $p < 0.05$. All the statistical analyses were performed with SigmaPlot Version 11.0 for Windows.

Results

Cell energetic status and activity of mitochondrial respiratory chain enzymes and citrate synthase

Cadmium did not affect the energetic status of cells exposed to Cd for 24 h, but after 48h, all Cd concentrations induced a decrease of adenylate energy charge in MG-63 cells (Figure 37A). Thus, the activity of some enzymes involved in mitochondrial respiration was analyzed to find if these checkpoints were disrupted by Cd. Also citrate synthase activity was measured, as this enzyme is the first intervenient of the TCA cycle which regulates energy generation in mitochondrial respiration.

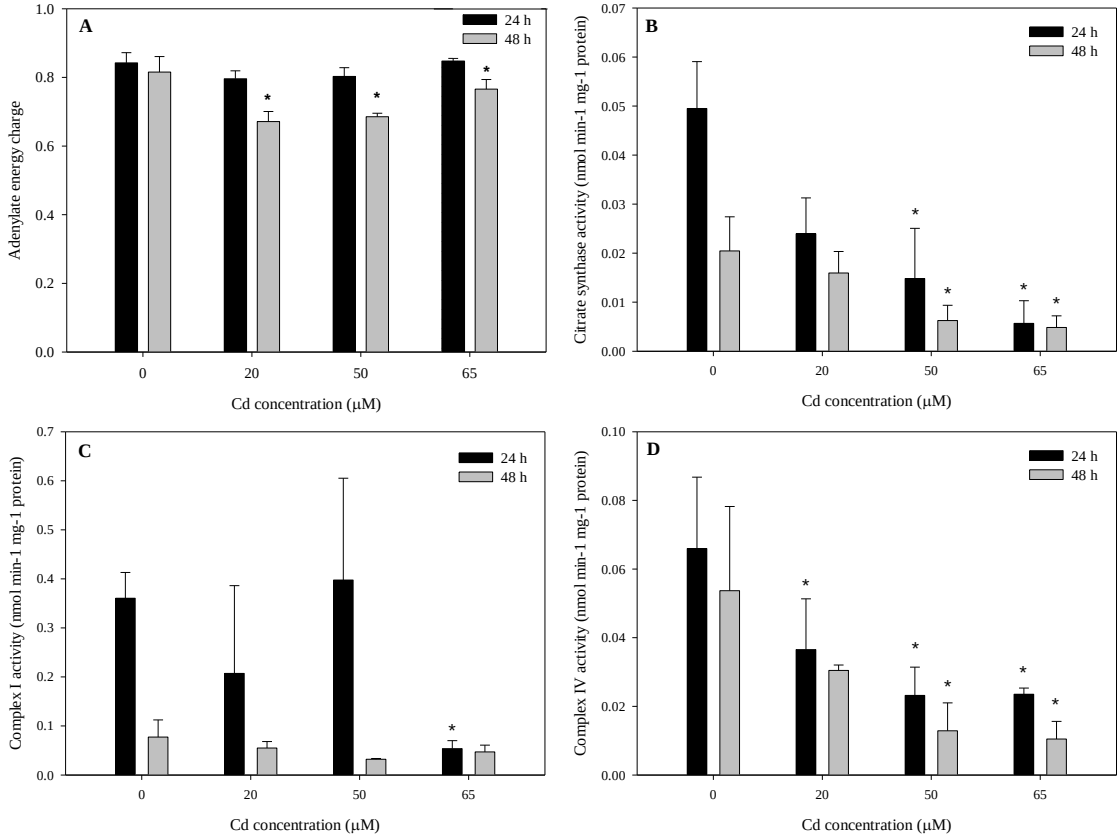

Figure 37. Effects of Cd on the cell energetic status (A) and activity of citrate synthase (B), and mitochondrial respiratory chain enzymes, complex I (C) and complex IV (D) Symbol * represents significant difference relative to the control (adenylate energy charge: $p < 0.05$; citrate synthase $p < 0.05$; complex I: $p < 0.001$; complex IV: $p < 0.05$).

Concerning citrate synthase, Figure 37B shows that Cd induced a decrease of its activity in cells exposed to 50 and 65 µM after 24, and 48 h. Regarding the mitochondrial respiratory chain, complexes I and IV were also analyzed, and Figure 37C shows that complex I activity of MG-63 cells was significantly inhibited with 65 µM Cd after 24 h of exposure, compared to the control group. This inhibition was reverted after 48 h, with complex I activity of Cd-exposed cells having values similar to those of control cells. Moreover, complex IV activity (Figure 37D) showed a dose- and time-dependent inhibition with Cd.

Mitochondrial membrane potential and morphology

The cytograms from control and exposed-cells after Rho123 (a fluorescent dye for ΔΨm) incubation indicated that the profile of the cell population positive for Rho123 was changed with Cd exposure. So, Figure 38 shows that Cd decreased ΔΨm in cells subjected to 65 µM after both times of exposure, compared to control cells, and the effect was a little more pronounced after 48 h.

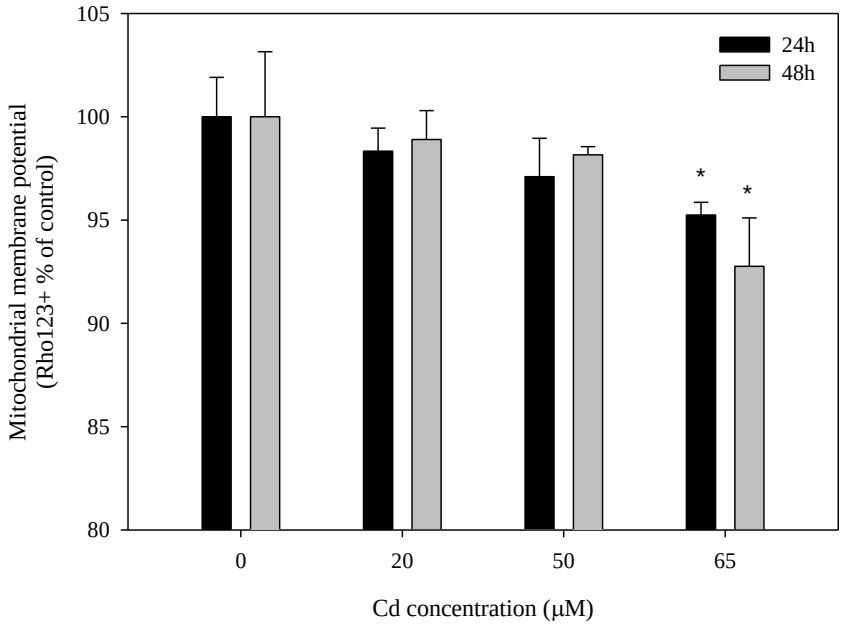

Figure 38. Effects of Cd in ΔΨm of MG-63 cells after 24 and 48 h of exposure. Symbol * represents significant difference relative to the control ($p < 0.001$).

Figure 39 shows how mitochondria morphology was changed by Cd. After 24 h, although control cells presented variability in mitochondrial morphology, showing filamentous, as well as fragmented and intermediate mitochondria, it was observed that at higher Cd concentrations (≥ 50 µM) there was an increase of fragmented mitochondria. After 48 h, mitochondrial morphology of Cd-exposed cells was similar to that of control ones, though mitochondria swelling was observed in some cells exposed to 50 and 65 µM Cd.

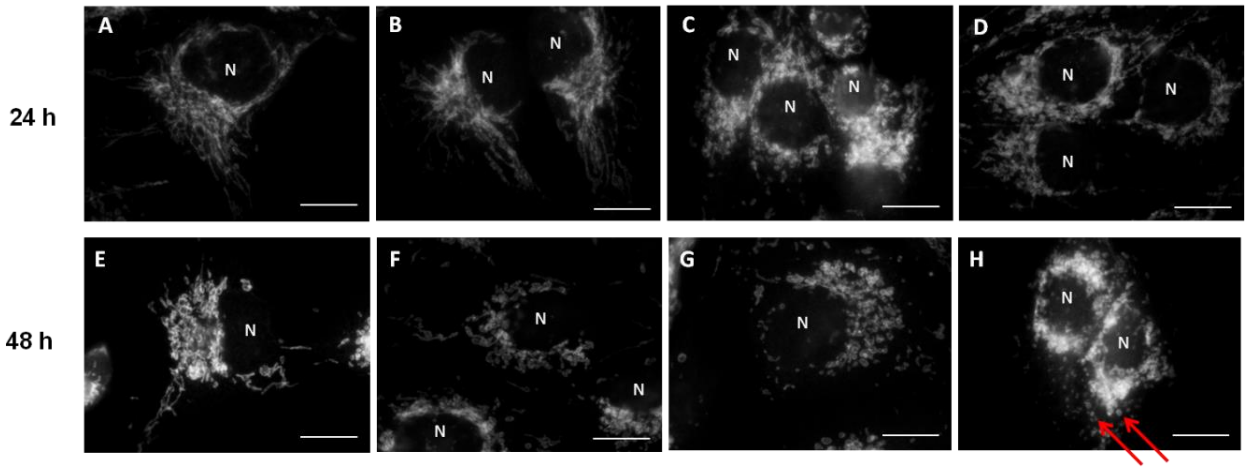

Figure 39. Effects of Cd in mitochondrial morphology of MG-63 cells, after 24, and 48 h of exposure, observed under fluorescence microscopy. Mitochondria of MG-63 cells stained by indirect immunofluorescence using antibodies against the outer membrane protein TOM20 involved in protein transport (1000x; bar: 20 µm). Control cells (A and E), 20 µM (B and F), 50 µM (C and G), and 65 µM Cd (D and H). Arrows in figure H indicate swelling of mitochondria. N – nucleus.

Intracellular ROS and total antioxidant activity

Cadmium induced an accumulation of ROS in cells exposed to 65 µM after 24 and 48 h of exposure (Figure 40A). The TAA levels were not significantly different between control and exposed-cells, neither after 24 h nor 48 h of Cd exposure (Figure 40B). However, TAA of MG-63 cells tended to decrease with 50 µM Cd after 24 h, and tended to increase with Cd concentrations after 48 h.

In Figure 40C it is presented the ratio between TAA and ROS showing the antioxidant capacity of cells *vs* ROS formation. Considering the behavior as function of Cd doses, after 24 h, there was a decrease of the ratio TAA/ROS in a dose-dependent manner. After 48 h,

cells showed different behavior: those exposed to 20 µM Cd showed a higher ratio, while cells exposed to higher doses had lower TAA/ROS ratios. Considering the responses regarding the period of exposure, the TAA/ROS ratio after 48 h was higher than after 24 h, for cells exposed to 20 and 50 µM Cd. Contrarily, cells exposed to 65 µM Cd showed a decrease of this ratio after 48 h.

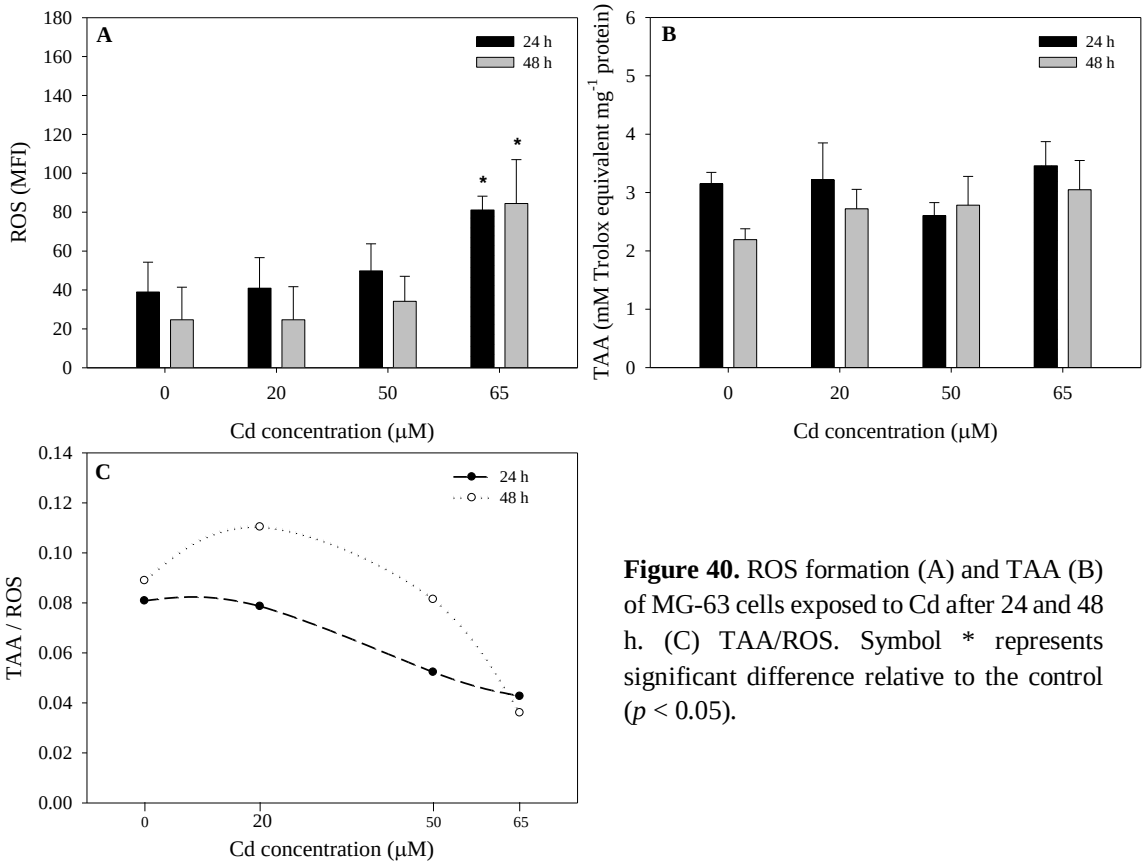

Figure 40. ROS formation (A) and TAA (B) of MG-63 cells exposed to Cd after 24 and 48 h. (C) TAA/ROS. Symbol * represents significant difference relative to the control ($p < 0.05$).

Protein oxidation and lipid peroxidation

Protein carbonyl levels increased in a dose-dependent manner in cells exposed to Cd for 48 h, but not in those ones exposed for 24 h. (Figure 41A). Regarding lipid peroxidation, after 24 h, TBARS content decreased in a dose-dependent manner and significantly for concentrations higher than 20 µM (Figure 41B). After 48 h, the same pattern was observed, but at the highest concentration, 65 µM, Cd induced a very high level of lipid peroxidation.

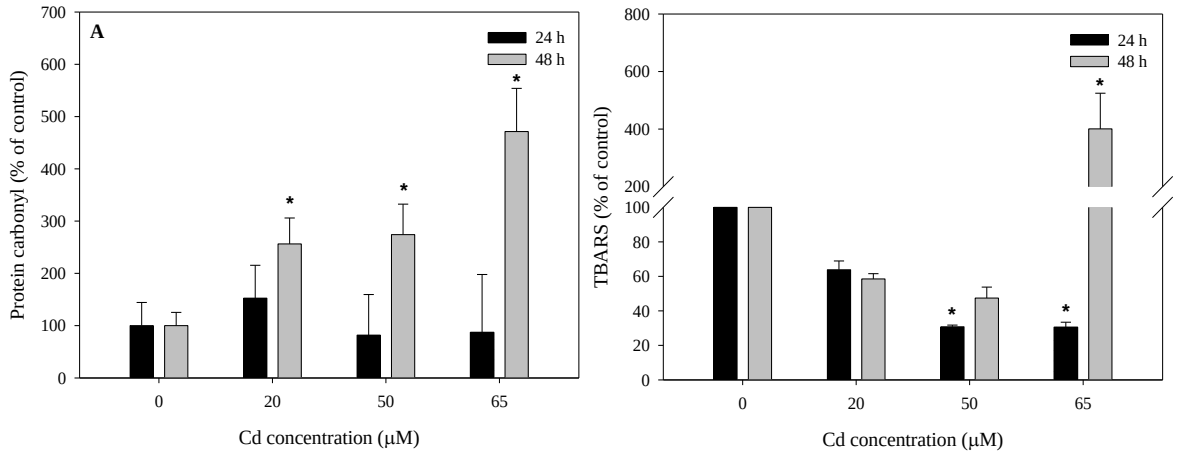

Figure 41. Protein oxidation and lipid peroxidation levels on MG-63 submitted to Cd for 24 and 48 h. (A) Protein carbonyl content. (B) TBARS content. Symbol * represents significant difference relative to the control ($p < 0.05$).

Gene expression of antioxidant enzymes

Among the analyzed genes of antioxidant enzymes, *GSR* gene expression was decreased to approximately ¼ in cells exposed to 50 µM for 24 h, compared to the control (Figure 42). The relative gene expression of *CAT*, *GPX1*, *SOD1* and *SOD2* was not significantly affected by Cd when cells were exposed for 24 h.

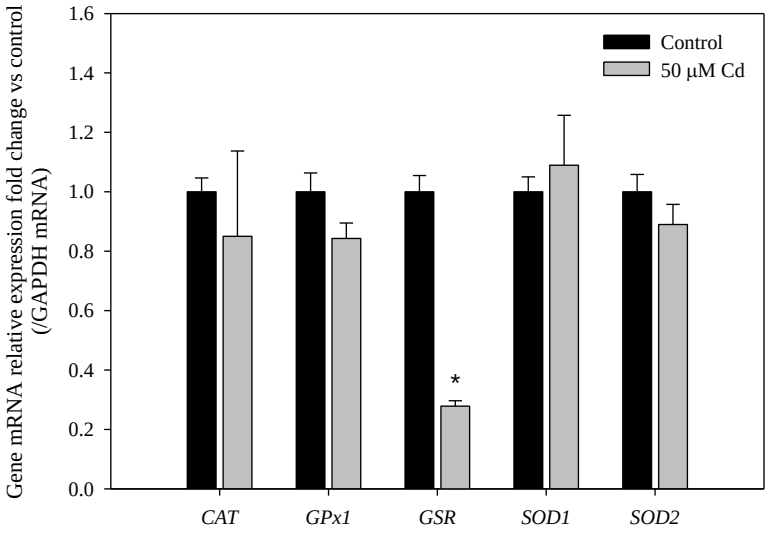

Figure 42. Relative gene expression of antioxidant enzymes: CAT, GPx, GR, and two SOD isoforms (SOD1 and SOD2). Symbol * represents significant difference relative to the control ($p \leq 0.001$).

Discussion

This is the first comprehensive study on the effects of Cd in human osteoblasts, involving changes at the levels of both oxidative stress and mitochondrial function. In general, disturbances were more severe when high Cd concentrations and longer exposure time were applied.

Regarding mitochondrial energetic function, it is evident that with time, Cd decreased the capacity of the mitochondria to maintain an energetic balance ([ATP] + ½ [ADP]) / ([ATP] + [ADP] + [AMP]), which suggests a dysfunction in the regulation of adenylate energy charge in MG-63 cells. Several authors have been proposed the assessment of adenylate energy charge that has a critical role in regulating catabolic and anabolic pathways. Several authors, therefore, highlight the importance of using this parameter in toxicological

studies, because of its importance in metabolic regulation (e.g., Matsui et al. 1994). As stated by Matsui et al. (1994) instead of measuring the amount of ATP, adenylate energy charge evaluates the changes of the energy metabolism in cells and evaluates the inhibitory effect of the stress condition (Matsui et al. 1994).

Our data also show that complexes I and IV were negatively affected, especially complex IV, which can be related to the increase of mitochondrial ROS in Cd-exposed cells, since inhibition of complex IV enhances the production of ROS from certain upstream sites in the electron transport chain (Chen et al. 2003). Toxicity assays using other cell/tissues showed impairment of mitochondrial complexes I, II, III and IV by Cd and other metals (e.g., Belyaeva et al. 2011; 2012; Adiele et al. 2012, Liu et al. 2013; Liu et al. 2014) suggesting a decreased function of ATP formation. Despite we cannot directly assume a decrease of ATP, the combined decrease of activity of complexes I and IV, and the decrease of adenylate energy charge, support that Cd leads to a decrease of mitochondrial function leading to biochemical disorders that may also influence ATP formation and, potentially, culminating to apoptotic pathways.

Together with the negative effects on the mitochondrial electron transport chain (complex I and IV) and adenylate energy charge, the impact of Cd on the activity of citrate synthase (the first intervenient of the TCA cycle, which regulates energy generation in mitochondrial respiration) was also evaluated. Citrate synthase has shown to be highly sensitive to Cd in oysters (Ivanina et al. 2008). The inhibition of citrate synthase by Cd in osteoblasts suggests an accumulation of citrate and, consequently, the glycolytic pathway is possibly inhibited at the phosphofructokinase level and, therefore, the energy obtained via this pathway may also be limited.

The data provided above was also supported by the observed negative effects of Cd on $\Delta\Psi m$, which could result from increased mitochondrial permeability transition pore opening, leading to release of pro-apoptotic factors and consequently to apoptotic processes (e.g., Ly et al. 2003). Recently we have found that Cd also induced apoptosis in these MG-63 cells, supporting these data (Oliveira et al. 2014, see Chapter 3.1). Supporting this severe dysfunction observed in osteoblasts mitochondria and energy processing, we also demonstrate that Cd exposure for 24 h increases morphological changes, as those observed by the increase of fragmented mitochondria. These mitochondrial morphological changes

may lead to mitochondrial damage through altering the matrix content and, therefore, contributing to altered ΔΨm, and inhibition of the respiratory electron chain as reported in a research of Xu et al. (2013) using human normal liver cells (L02 cell line) and rat liver tissue exposed to Cd. It was already shown that Cd can lead to mitochondrial swelling, for example, in both kidney (Kobroob et al. 2012) and liver (Zhang et al. 2011) of rats. In MG-63 cells data showed that the highest used Cd doses (50 and 65 μM) increased the mitochondrial swelling after 48 h of Cd exposure, also explaining the observed decrease of ΔΨm induced by Cd. However, no other mitochondrial morphological changes were observed in Cd-exposed cells at this time of exposure.

In summary, it is evident that Cd induced severe functional and morphological changes in some critical functions of the cell, leading for example to the impairment of the electron transport chain, TCA cycle, and consequently to lower adenylate energy charge, and simultaneously it stimulates mitochondrial depolarization, which could be related to the induction of apoptosis evidenced by us in a previous work (Oliveira et al. 2014; see Chapter 3.1).

As stated above, mitochondria are intimately related with oxidative stress, and this is highly dependent on the intracellular levels of ROS *vs* the capacity of the cell to increase the total antioxidant status. Regarding TAA/ROS ratio, data demonstrate that Cd induced an accumulation of ROS while the TAA tended to decrease (particularly for higher doses). Moreover, when cells were exposed to low Cd doses (20 μM), there was a response of defense to scavenge the increase of ROS after 48 h of exposure, with an observed increase of TAA. Also the gene expression analysis demonstrates that, among the different transcripts of antioxidant enzymes tested, only *GSR* gene expression was significantly decreased after 48 h of Cd exposure. Despite no evidence is provided on the negative effects on other enzymes, the impairment of GSR can be sufficient to disrupt GSH redox cycling leading to a decrease in GSH with a concomitant increase in GSSG. GSH among other relevant functions on cell (e.g., immune system and detoxification system) is the most important endogenous antioxidant, and also plays a crucial role in the regulation of protein function through thiol modification (e.g., Morgan 2014; Nair et al. 2014). The observed increase of oxidation of macromolecules found in the present study for lipids and proteins support the increase of membrane damage previously found in these MG-63 cells (Oliveira et al. 2014;

see Chapter 3.1). Deregulated oxidative stress often leads to oxidation of macromolecules, with particular evidence in lipids, proteins and/or nucleic acids. Despite Cd is not a Fenton metal, it is evident in MG-63 cells that the doses studied led (mostly after 48h) to increased oxidation of proteins and lipids. Considering that lipids and proteins are major constituents of membranes, it should be hypothesized that membranes may ultimately be affected with loose of permeability (membrane permeability was measured by the flow cytometer using PI that enters only in cells with damaged membrane).

Conclusions

In conclusion, this is the first study on the effect of Cd on mitochondrial function and induction of oxidative stress in human osteoblasts. We demonstrate that Cd leads to severe impairments in electron flux transport and in TCA, as well as a deficient adenylate energy charge, together with a decrease in $\Delta\Psi m$ and mitochondria morphological abnormalities. Simultaneously, Cd increased cell oxidative stress, with evident decrease in the transcripts of related enzyme (GR) and with severe consequences at the oxidation of lipids and proteins. All these data demonstrate that Cd induced severe mitochondrial dysfunction related to oxidative stress in human osteoblasts.

References

Adiele, R. C. Don Stevens, D., and Kamunde, C. (2012) Differential inhibition of electron transport chain enzyme complexes by cadmium and calcium in isolated rainbow trout (*Oncorhynchus mykiss*) hepatic mitochondria. *Toxicol. Sci.* 127 (1), 110–119.

Ahmad, I., Khan, M. I., Patil, G., and Chauhan, L. K. S. (2012) Evaluation of cytotoxic, genotoxic and inflammatory responses of micro- and nano-particles of granite on human lung fibroblast cell IMR-90. *Toxicol. Lett.* 208 (3), 300–307.

Arroyo, V. S., Flores, K. M., Ortiz, L. B., Gómez-Quiroz, L. E., and Gutiérrez-Ruiz, M. C. (2012) Liver and cadmium toxicity. *J. Drug Metab. Toxicol.* S5, 001.

Atkinson, D. E. (1968) The energy charge of the adenylate pool as a regulatory parameter: interaction with feedback modifiers. *Biochemistry*. 7 (11), 4030–4034.

Azevedo, H., Gomes, C., Pinto, G., and Santos, C. (2005) Cadmium effects in sunflower: membrane permeability and changes in catalase and peroxidase activity in leaves and calluses. *J. Plant Nutr.* 28 (12), 2233–2241.

Barros, S., Mencia, N., Rodríguez, L., Oleaga, C., Santos, C., Noé, V., and Ciudad, C. J. (2013) The redox state of cytochrome c modulates resistance to methotrexate in human MCF7 breast cancer cells. *PLoS One*. 8 (5), e63276.

Belyaeva, E. A., Dymkowska, D., Wieckowski, M. R., and Wojtczak, L. (2008) Mitochondria as an important target in heavy metal toxicity in rat hepatoma AS-30D cells. *Toxicol. Appl. Pharmacol.* 231 (1), 34–42.

Belyaeva, E. A., Dymkowska, D., Wieckowski, M. R., and Wojtczak, L. (2006) Reactive oxygen species produced by the mitochondrial respiratory chain are involved in Cd^{2+}-induced injury of rat ascites hepatoma AS-30D cells. *Biochim. Biophys. Acta.* 1757 (12), 1568–1574.

Belyaeva, E. A., Korotkov S. M., and Saris, N.-E. L. (2011) *In vitro* modulation of heavy metal-induced rat liver mitochondria dysfunction: a comparison of copper and mercury with cadmium. *J. Trace Elem. Med. Biol.* 25, Suppl 1, S63–S73.

Belyaeva, E. A., Sokolova, T. V., Emelyanova, L. V., and Zakharova, I. O. (2012) Mitochondrial electron transport chain in heavy metal-induced neurotoxicity: effects of cadmium, mercury, and copper. *Scientific World Journal*. 2012, 136063.

Bradford, M. M. (1976) A rapid and sensitive method for the quantitation of microgram quantities of protein utilizing the principle of protein-dye binding. *Anal Biochem.*72, 248–254.

Chen, Q., Vazquez, E. J., Moghaddas, S., Hoppel, C. L., and Lesnef-Sky, E. J. (2003) Production of reactive oxygen species by mitochondria: central role of complex III. *J. Biol. Chem.* 278 (38), 36027–36031.

Desagher, S., and Martinou, J. C. (2000) Mitochondria as the central control point of apoptosis. *Trends Cell Biol.* 10 (9), 369–377.

Ferreira de Oliveira, J. M. P., Costa, M., Pedrosa, T., Pinto, Pedro, Remédios, C., Oliveira, H., Pimentel, F., Almeida, L., and Santos, C. (2014) Sulforaphane induces oxidative stress and death by p53-independent mechanism: implication of impaired glutathione recycling. *PLoS One*. 9 (3), e92980.

Ivanina, A. V., Habinck, E., and Sokolova, I. M. (2008) Differential sensitivity to cadmium of key mitochondrial enzymes in the eastern oyster, *Crassostrea virginica* Gmelin (Bivalvia: Ostreidae). *Comp. Biochem. Physiol. C Toxicol. Pharmacol.* 148 (1), 72–79.

Kent, W. J., Sugnet, C. W., Furey, T. S., Roskin, K. M., Pringle, T. H., Zahler, A. M., and Haussler, D. (2002) The human genome browser at UCSC. *Genome Res.* 12 (6), 996–1006. http://genome.ucsc.edu/cgi-bin/hgPcr (accessed Dec, 2012).

Kiebish, M. A., Yang, K., Liu, X., Mancuso, D. J., Guan, S., Zhao, Z., Sims, H. F., Cerqua, R., Cade, W. T., Han, X., and Gross, R. W. (2013) Dysfunctional cardiac mitochondrial bioenergetic, lipidomic, and signaling in a murine model of Barth syndrome. *J. Lipid Res.* 54 (5), 1312–1325.

Kobroob, A., Chattipakorn, N., and Wongmekiat, O. (2012) Caffeic acid phenethyl ester ameliorates cadmium-induced kidney mitochondrial injury. *Chem. Biol. Interact.* 200 (1), 21–27.

Liu, S., Xu, F. P., Yang, Z. J. Li, M., Min, Y. H., and Li, S. (2014) Cadmium-induced injury and the ameliorative effects of selenium on chicken splenic lymphocytes: mechanisms of oxidative stress and apoptosis. *Biol. Trace Elem. Res.* 160 (3), 340–351.

Liu, Y., Barber, D. S., Zhang, P., and Liu, B. (2013) Complex II of the mitochondrial respiratory chain is the key mediator of divalent manganese-induced hydrogen peroxide production in microglia. *Toxicol. Sci.* 132 (2), 298–306.

Ly, J. D., Grubb, D. R., and Lawen, A. (2003) The mitochondrial potential (deltapsi(m)) in apoptosis; an update. *Apoptosis*. 8 (2), 115–128.

Matsui, Y., Kitade, H., Kamiya, T., Kanemaki, T., Hiramatsu, Y., Okumura, T., and Kamiyama, Y. (1994) Adenylate energy charge of rat and human cultured hepatocytes. *In Vitro Cell. Dev. Biol.* 30A (9), 609–661.

Mead, M. N. (2010) Cadmium confusion: do consumers need protection? *Environ. Health Perspect.* 118 (12), A528–A534.

Monteiro, C., Santos, C., Pinho, S., Oliveira, H., Pedrosa, T., and Dias, M. C. (2012) Cadmium-induced cyto- and genotoxicity are organ-dependent in lettuce. *Chem. Res. Toxicol.* 25 (7), 1423–1434.

Monteiro, M. S., Santos, C., Soares, M. V. M., and Mann, R. M. (2009) Assessment of biomarkers of cadmium stress in lettuce. *Ecotoxicol. Environ. Saf.* 72 (3), 811–818.

Morgan, B. (2014) Reassessing cellular glutathione homoeostasis: novel insights revealed by genetically encoded redox probes. *Biochem. Soc.Trans.* 42 (4), 979–984.

Murugavel, P., Pari, L., Sitasawad, S. L., Kumar, S., and Kumar, S. (2007) Cadmium induced mitochondrial injury and apoptosis in vero cells: protective effect of diallyl tetrasufide from garlic. *Int. J. Biochem. Cell Biol.* 39 (1), 161–170.

Nair, A. R., DeGheselle, O., Smeets, K., Van Kerkhove, E., and Cuypers, A. (2013) Cadmium-induced pathologies: where is the oxidative balance lost (or not)? *Int. J. Mol. Sci.* 14 (3), 6116–6143.

Nair, A. R., Lee, W. K., Smeets, K., Swennen, Q., Sanchez, A., Thévenod, F., and Cuypers, A. (2014) Glutathione and mitochondria determine acute defense responses and adaptive processes in cadmium-induced oxidative stress and toxicity of the kidney. *Arch. Toxicol.* [Epub ahead of print].

Oliveira, H., Monteiro, C., Pinho, F., Pinho, S., Ferreira de Oliveira, J. M. P., and Santos, C. (2014) Cadmium-induced genotoxicity in human osteoblast-like cells. *Mutat. Res. Toxicol. Environ. Mutagen.* 775-776, 38–47.

Oliveira, H., Spanò, M., Santos, C., and Pereira, M. de L. (2009) Adverse effects of cadmium exposure on mouse sperm. *Reprod. Toxicol.* 28 (4), 550–555.

Patra, R. C., Rautray, A. K., and Swarup, D. (2011) Oxidative stress in lead and cadmium toxicity and its amelioration. *Vet. Med. Int.*, 457327.

Peixoto, F., Martins, F., Amaral, C., Gomes-Laranjo, J., Almeida, J., and Palmeira, C. M. Evaluation of olive oil mill wastewater toxicity on the mitochondrial bioenergetics after treatment with *Candida oleophila*. *Ecotoxicol. Environ. Saf.* 70 (2), 266–275.

Pfaffl, M. W. (2001) A new mathematical model for relative quantification in real-time RT-PCR. *Nucleic Acids Res.* 29 (9), e45.

Rozen, S., and Skaletsky, H. (2000) Primer3 on the WWW for general users and for biologist programmers. *Methods Mol. Biol.* 132, 365–386.

Ryll, T, and Wagner, R. (1991) Improved ion-pair high-performance liquid chromatographic method for the quantification of a wide variety of nucleotides and sugar-nucleotides in animal cells. *J. Chromatogr.*570 (1), 77–88.

Schrader, M., Reuber, B. E., Morrell, J. C., Jimenez-Sanchez, G., Obie, C., Stroh, T. A., Valle, D., Schroer, T. A., and Gould, S. J. (1998) Expression of PEX11beta mediates peroxisome proliferation in the absence of extracellular stimuli. *J. Biol. Chem.* 273 (45), 29607–29614.

Smith, S. S., Reyes, J. R., Arbon, K. S., Harvey, W. A., Hunt, L. M., and Heggland, S. J. (2009) Cadmium-induced decrease in RUNX2 mRNA expression and recovery by the antioxidant N-acetylcysteine (NAC) in the human osteoblast-like cell line, Saos-2. *Toxicol. In Vitro.* 23 (1), 60–66.

Srere, P. A. (1969) Citrate Synthase. *Methods Enzymol.* 13, 3–11.

Stocchi, V., Cucchiarini, L., Magnani, M., Chiarantini, L., Palma, P., and Crescentini, G. (1985) Simultaneous extraction and reverse-phase high-performance liquid

chromatographic determination of adenine and pyridine nucleotides in human red blood cells. *Anal Biochem*. 146 (1), 118–124.

Thévenod, F., and Lee, W.-K. (2013) Cadmium and cellular signaling cascades: interactions between cell death and survival pathways. *Arch. Toxicol.* 87 (10), 1743–1786.

Waisberg, M., Joseph, P., Hale, B., and Beyersmann, D. (2003) Molecular and cellular mechanisms of cadmium carcinogenesis. *Toxicology*. 192 (2-3), 95–117.

Wang, Y., Fang, J., Leonard, S. S., and Rao, K. M. K. (2004) Cadmium inhibits the electron transfer chain and induces reactive oxygen species. *Free Radic. Biol. Med.* 36 (11), 1434–1443.

Wang, H., Lim, P. J., Karbowski, M., and Monteiro, M. J. (2009) Effects of overexpression of huntingtin proteins on mitochondrial integrity. *Hum. Mol. Genet.* 18 (4), 737–752.

Xiao, F., Feng, X., Zeng, M., Guan, L., Hu, Q., and Zhong, C. (2012) Hexavalent chromium induces energy metabolism disturbance and p53-dependent cell cycle arrest via reactive oxygen species in L-02 hepatocytes. *Mol. Cell Biochem.* 371 (1-2), 65–76.

Xu, S., Pi, H., Chen, Y., Zhang, N., Guo, P., Lu, Y., He, M., Xie, J., Zhong, M., Zhang, Y., Yu, Z., and Zhou, Z. (2013) Cadmium induced Drp1-dependent mitochondrial fragmentation by disturbing calcium homeostasis in its hepatotoxicity. *Cell Death Dis.* 4 (3), e540.

Yang, M. S., Yu, L. C., and Gupta, R. C. (2004) Analysis of changes in energy and redox states in HepG2 hepatoma and C6 glioma cells upon exposure to cadmium. *Toxicology*. 201 (1-3), 105–113.

Zhang, Y., Li, J. H., Liu, X. R., Jiang, F. L., Tian, F. F., and Liu, Y. (2011) Spectroscopic and microscopic studies on the mechanisms of mitochondrial toxicity induced by different concentrations of cadmium. *J. Membr. Biol.* 241 (1), 39–49.

Zhao, S., and Fernald, R. D. (2005) Comprehensive algorithm for quantitative real-time polymerase chain reaction. *J. Comput. Biol.* 12 (8), 1047–1064.

CHAPTER 4 – GENERAL CONCLUSIONS AND FUTURE PERSPECTIVES

General conclusions and future perspectives

The cyto- and genotoxicity of Cr and Cd salts are raising environmental concerns, with demonstrated effects in different taxa including plants and animals, with some described effects being common to all biological models. The cyto- and genotoxicity of these salts were evaluated in lettuce and in human cells (osteoblast) using diverse biomarkers of susceptibility related to metal uptake and cyto- and genotoxicity, being transversal to both biological models and metals used in general.

In lettuce, all the metal forms tested, Cr^{3+}/Cr^{6+} in Chapter 2.1, and Cd^{2+} in Chapter 2.2 were accumulated mostly in roots compared to the level of metals measured in leaves. In addition, lettuce organs accumulated more Cr when exposed to Cr^{6+} than when treated with Cr^{3+}, however the rate of Cr translocation from roots to leaves was similar in both exposure conditions.

Cr^{3+} did not cause cytotoxicity in lettuce while Cr^{6+} was found to be toxic and reduced plant growth. Cr^{6+} also induced cytogenotoxic effects in roots including formation of MN and mitotic aberrations, which were not observed in any plants exposed to Cr^{3+}. Cr^{6+} also induced DNA damage at high concentrations (150 and 300 ppm) in leaves though not in roots, which can putatively be related to the inhibition of POX activity. The inhibition of this enzyme may have been enough to lead to a hypothetic increase of ROS in leaves compared to roots, which are known to have major impact in DNA integrity. However, to confirm the hypothesis of oxidative DNA damage, ROS quantification and comet assay with specific enzyme to detect 8-OHdG should be done in the future. Despite no toxicity was observed in lettuce plants exposed to Cr^{3+}, it would be important to consider the assessment of DNA damage (including oxidative injuries), ROS content, and antioxidant enzyme activities in these plants. Some putative causes of the observed decrease of growth in Cr^{6+}-exposed plants migh involve deficiencies in carbon metabolism which has already been proved by our group (Dias et al. 2015, unpublished data). In that study the decrease of plant growth at the end of 15 days of exposure can be related to lower CO_2 photosynthetic rate due to lower activity of Rubisco since Cr is able to substitute Mg (Dias et al. 2015, unpublished data).

The evaluation of Cr^{3+}/Cr^{6+} and Cd-induced toxicity is not directly comparable, so we cannot conclude which metal, Cr or Cd, is in fact more toxic to lettuce. Different cultivars were used (i.e., *L. sativa* L. cv. “Povoa” and *L. sativa* L. cv. “Reine de Mai”), thus, different

sensitivity to metals might be in place. Moreover, different conditions of exposure were used namely hydroponic culture in the assay with Cd, and plant growth in soil with Cr, which can lead to plants having different bioavailability levels of these metals. Plant growth in soil represents a closer condition to the reality of lettuce produced in polluted agriculture fields, and thus Cr bioavailability may be diminished by organic matter able to chelate or reduce metals, and other soil factors mentioned in the General Introduction (Chapter 1). However, in another test performed by our group exposing lettuce to the same Cr^{6+} concentrations but using hydroponic culture, almost all plants from the assay were dead within one week of exposure, while in the assay using soil plant death was not observed after 30 days of exposure. Furthermore, hydroponic culture was also used in lettuce production in our research (see Chapter 2.2) to provide an exposure without interferences on metal (Cd) bioavailability. It would be interesting to study the effects of Cr^{3+}/Cr^{6+} at lower concentrations in lettuce cultured in hydroponics and also the level of cyto- and genotoxicity of Cd in lettuce grown in soil to see the main differences in the response of lettuce to each metal, depending on the method of culture. In these studies the bioconcentration factor should also be assessed to analyze how much metal is absorbed by the plant in comparison to the remaining in the culture medium (soil/solution).

Cadmium was toxic to lettuce, reducing plant growth and germination rate. Moreover, this metal induced cyto- and genotoxic effects. Exposure of plants to Cd led to oxidative stress more in leaves than in roots, but cells from both organs were similarly affected compared to control regarding the observed increased levels of oxidative damage in lipids and proteins with consequent loss of membrane integrity. Indirectly by ROS increase and/or by Cd-DNA adducts formation and/or impairment of DNA repair mechanisms, Cd induced DNA damage more in leaves than in roots compared to the control. Despite of the tendency for cell cycle delay at S phase or arrest at G_2 in root cells to activate DNA repair mechanisms, these could be deregulated, leading to MN formation (in addition to the DNA damage).

As stated above, the toxicity of these two metals is transversal to biological models. In particular, by environmental and/or occupational exposure, by using prosthesis, or even by ingestion of contaminated water and/or food, humans are critical targets of Cr and Cd accumulation and toxicity.

In human osteoblasts *in vitro* (MG-63 cell line) both Cr^{6+} (Chapter 3.1) and Cd (Chapters 3.2 and 3.3) induced cyto- and genotoxicity in a dose- and time-dependent manner. Just after a short period of time (24 h) and at low doses, Cr^{6+} and Cd decreased cell viability and induced DNA damage that may be responsible for the observed cell cycle arrest at G_2 (in Cr^{6+}-exposed cells) or S phases (in Cr^{6+} and Cd-exposed cells). While cells arrest or delay their cell cycle, they activate mechanisms of DNA repair. However, this may be followed by chromosome breakage and/or loss shown in the assays by an increase of MN and NPBs formation. Otherwise, cells may follow death pathways (observed in both Cr^{6+} and Cd-exposed cells), apoptosis and/or necrosis. In the case of Cd, this research allowed to conclude that mitochondria of osteoblasts became dysfunctional mainly at the highest tested dose, since mitochondria are a source of intensive ROS generation and, simultaneously, become targets of that ROS, leading to energy decline, oxidative stress, lipid peroxidation and protein oxidation. As Cr^{6+} is known to induce oxidative stress this should be evaluated in the future, as well as mitochondrial function, energetic status and apoptosis.

Cyto- and genotoxicity of Cd were also reflected at the gene expression level, thus it would be also interesting to analyze e.g., the expression of genes involved in cell cycle arrest at G_2 in Cr^{6+}-exposed osteoblasts, and to complement and allow a better understanding of the signaling pathways, quantification of phosphorylated/non-phosphorylated proteins by western blotting would be interesting to perform.

Additionally to MG-63 cell line used in the assays, other osteoblastic cell lines from humans or other animals should be used in the assessment of Cd/Cr toxicity: e.g., hFOB, human immortalized osteoblastic cell line; MC3T3-E1, mouse immortalized osteoblastic cell line. Other *in vitro* assays could be done like clonogenic assay in order to assess the survival at the end of a recovery period after an exposure; longer and repeated exposures with low concentrations of metals in normal osteoblastic cell lines to analyze carginogenic processes (e.g., migration, DNA damage, MN).

Finaly, it should be mentioned that in both metals and both biological models further studies should be done particularly regarding: quantification of Cd/Cr-DNA adducts, quantification of DNA crosslinks, measure of DNA repair (by comet assay). In plants, it would be beneficial also to evaluate mitochondrial function. Finally, for an open gap to be fullfilled and another thesis to be born it would be interesting to consider the evaluation of

trophic transfer of Cd/Cr from lettuce to other living organism, feeding e.g., rats with lettuce contaminated with each metal and observe short and long term consequences to this organism.